Insubria University
Department of Science and High Technology

Integrated multidisciplinary approaches to investigate geochemical anomalies in waters

By Gilberto Binda

Dissertation submitted for the degree of Philosophiae Doctor (PhD)
in Chemical and Environmental Sciences

Supervisor: Prof. Andrea Pozzi

Contents

Abstract

Water is a fundamental need for human and environmental benefits, and its inorganic quality is a mandatory standard. Potentially Toxic Elements (PTEs), due to their high toxicity and persistence need to be carefully evaluated to maintain good water standards. And consequently, in the case of possibly alarming concentration, the causes need to be clarified, to evaluate possible remediation techniques.

Natural phenomena which mainly affect water quality are: water-rock interaction, mineral dissolution (both influenced by the lithological setting), residence time of groundwater, flow paths and mixing among different water bodies, adsorption on sediments. Anthropic emissions, also affecting inorganic quality of waters in different ways, include different kind of industries: from smelting, to mining, electronics and impurities of other compound (i.e., herbicides).

These elements could directly dissolve in waters from their source areas, but also cases of long range transport could happen, and they can be observed even in remote areas. Moreover, natural or anthropic occurring phenomena (i.e., mining, erosion) could enhance the weathering and dissolution of PTEs in water causing anomalies.

Therefore, to evaluate causes of anomalous concentrations is important to establish the natural (or background) concentrations of PTEs in water, and this application needs univocal and generally accepted methods. Used methods in literature include: multivariate statistical methods, geostatistics, geochemical markers. These methods, anyway, often are limited or require good a-priori knowledge about chemical features and minerals dissolution mechanisms, and can fail in the evaluation of geochemical anomalies.

Also, dynamicity of water environment, causing high temporal heterogeneity, limits the applicability of most of the statistical approaches already standardly applied to more stable environmental compartments (i.e., soils and sediments).

To clearly evaluate the background values and its anomalies, integrated multidisciplinary approaches are needed, coupling chemical, hydrogeological and statistical tools, especially in dynamic environments as water bodies.

In this dissertation, I would highlight the importance of applying multidisciplinary approaches to clearly evaluate geochemical anomalies in waters, and understand their causes, naturally or anthropically induced, through the presentation of different case studies. They include the analyses of two areas (an Alpine catchment and a series of springs with different water sources in Central Italy).

In more detail, natural background is evaluated, and then natural or anthropic source of PTEs is discussed in a mountainous water catchment in the central Alps. In this case, after the failure of single-way approaches, a multidisciplinary integrated approach is presented including: multivariate statistics, temporal trend evaluation and multiple compartment analyses. Through this approach, 11 PTEs (Cr, Mn, Fe, Co, Ni, Cu, Zn, As, Ag, Cd and Pb) sources are identified. Anomalously high concentration of natural occurring Ni was observed, and Zn, Cd, Ag were observed as anthropically enriched. Elements showing controversial trends with the different approaches are: Cu, As and Pb. Also, anomalous presence of As was observed in a spring, with a high concentration in sediment too, as an index of geochemical anomaly.

In the same Alpine catchment two secondary projects dealing with geochemical anomalies will be included: the evaluation of Ni anomalous speciation aiming to understand the possible mechanisms of dissolution causing high concentration in waters through sulfides oxidation, and the application of the geochemical anomalies as marker to validate groundwater flow modeling through discrete fracture networks, which preliminary results suggest a communication of the two basins composing the analyzed watershed.

Another application includes the evaluation of the hydrogeochemical anomalies caused by a seismic sequence in Central Italy. Different chemical parameters (including major ions, PTEs and water and carbon isotope ratios) are evaluated along a seismic sequence which struck Central Italy in 2016-2017, and compared to pre-earthquake available chemical values to observe the possible anomalies, and then the temporal trends and the changed variables are used to conceptualize the mechanism causing anomalies. Water samples were collected in karst springs, starting few days after the first mainshock. Obtained data were compared with pre-earthquake concentrations. Then, observing variables changes, using a multivariate statistical approach and observing response timing the possible cause of geochemical anomalies is investigated.

We observe a transient increase immediately after the first mainshocks of different trace metals, not typically dissolving in carbonate aquifers (i.e., Pb, Ni, Cu, Mn), which come back to pre-earthquake values after 2-3 months after the first shocks, and do not show peculiar responses after the following shocks. Also, most of major ions and water isotopes did not show significant changes, as elements typically markers of deep fluids (Li, B).

This response suggest that main driver of elements dissolution was permeability increase after the earthquake shaking effect of the aquifer, causing the fast movement of deep pores and fractures water, with high rock-water interaction and a great presence of dissolved ions. Also, the opening of new fractures could exposed fresh rock, enhancing PTEs dissolution.

The collection of these case studies highlights the need of a complete, integrated, and multidisciplinary approach to deal with geochemical data. In fact, a multidisciplinary knowledge is necessary to understand all the processes governing leaching, dissolution and transport of PTEs. Then, single-way approaches are highlighted as easy failing in the case studies shows along my dissertation. This approach still requires a good knowledge of analyzed area lithology and a good data set of chemical variables, but could fit as a first step to create leaching and transport models.

1 Introduction

1.1 The importance of water quality monitoring

Water is a fundamental need for human and environmental benefits, and its quality and availability are a major issue in environmental sciences. Thus, ground and surface water quality need to be monitored and maintained. Adverse effects for the environment should be minimized, and increasing pollution trends have to be identified and reversed, as reported also from regulatory levels (Hinsby et al., 2008).

Potentially toxic elements (PTEs; i.e., Cd, Pb, Ni, Cu, Cr) are among the most crucial water quality parameters that define the overall status of a water resource, because their increase in concentration can compromise water quality for human and ecosystem health because of their toxicity for many organisms and persistence in the environment (Devic et al., 2014; Dung et al., 2013; Kierczak et al., 2008).

Therefore, different management of legislation impose threshold limits for values for drinking water and ecological quality.

PTEs in the environment are continuously redistributed in hydrological/hydrochemical as well as biological cycles and pathways. Human activities, however, affected the distribution and concentration levels of PTEs. Man, in fact, has influenced the environment since the onset of his civilization (Galuszka, 2007) and pollution of soil and surface waters due to metal releases from point sources and diffuse sources have been reported in numerous cases (Förstner and Wittmann, 1979; Ledin et al., 1989).

But, also natural conditions hazardous concentrations of PTEs can be reached in water. Therefore, the evaluation of the natural load of inorganic compounds (often defined as “natural background” or “geochemical background”) requires a deep knowledge of aquifer features and the bedrock geochemistry. Also, natural events can cause anomalous increase in concentrations of potentially harmful elements and should be considered as well for human and ecosystems risk assessment.

Therefore, evaluate the sources of PTEs contaminations in water bodies results a difficult operation, due to: the high dynamicity of this environmental compartment, the complex systems of PTEs natural release, and the high spatial variance of PTEs sourcing rocks. So,

understand sources and the impact of human emissions in environment need to be improved, in order to improve risk assessment for possible harmful PTEs concentrations.

1.2 Natural and anthropic sources of PTEs in waters

Natural phenomena which mainly affect water quality are: water-rock interaction, mineral dissolution (both influenced by the lithological setting), residence time of groundwater, flow paths and mixing among different water bodies, adsorption on sediments (Busico et al., 2018; Schneider et al., 2017).

Anthropic emission affects inorganic quality of waters in different ways, and different types of industries could cause emission of toxic metals (from smelting to mining to electronics and impurities of other compound; i.e., herbicides); the effect can be direct for solid emissions or dissolved metals from wastes, but they can be observed even in remote areas.

There is evidence that small amounts of elements have been transported on intercontinental scales to remote regions and deposited (for example, in ice sheets and glaciers) after being released into the atmosphere due to human activity (Gabrielli et al., 2008; Schneider et al., 2017). But similarly, also large masses of natural materials are released into the atmosphere and globally transported from volcanic eruptions and dust from desert windstorms (Nriagu, 1989).

Sometimes, in natural conditions, elements concentration in water can already be so high to be considered dangerous also for human health. These anomalous natural values indicate the need to understand the natural (or geochemical) background concentrations. This step, in fact, is preliminary to the evaluation of anthropic impact caused by emissions, which become harder to investigate with a high geochemical load of the elements.

Moreover, events (both naturally or anthropogenically caused) can change or enhance the dissolution of metals. For example, natural catastrophic events (flooding, earthquakes) can enhance natural dissolution, and even cause anomalies and increase of PTEs in waters. But also anthropic factors can enhance weathering and metals mobilization in waters chemically (i.e., acid rains , acid drainage) and mechanically (i.e., mining activities) (Runnells et al., 1992); also changes in land use of the catchment areas can alter water-rock interaction (Schneider et al., 2017). Figure 1.1 indexes in a scheme the main natural and anthropic PTEs sources in watersheds.

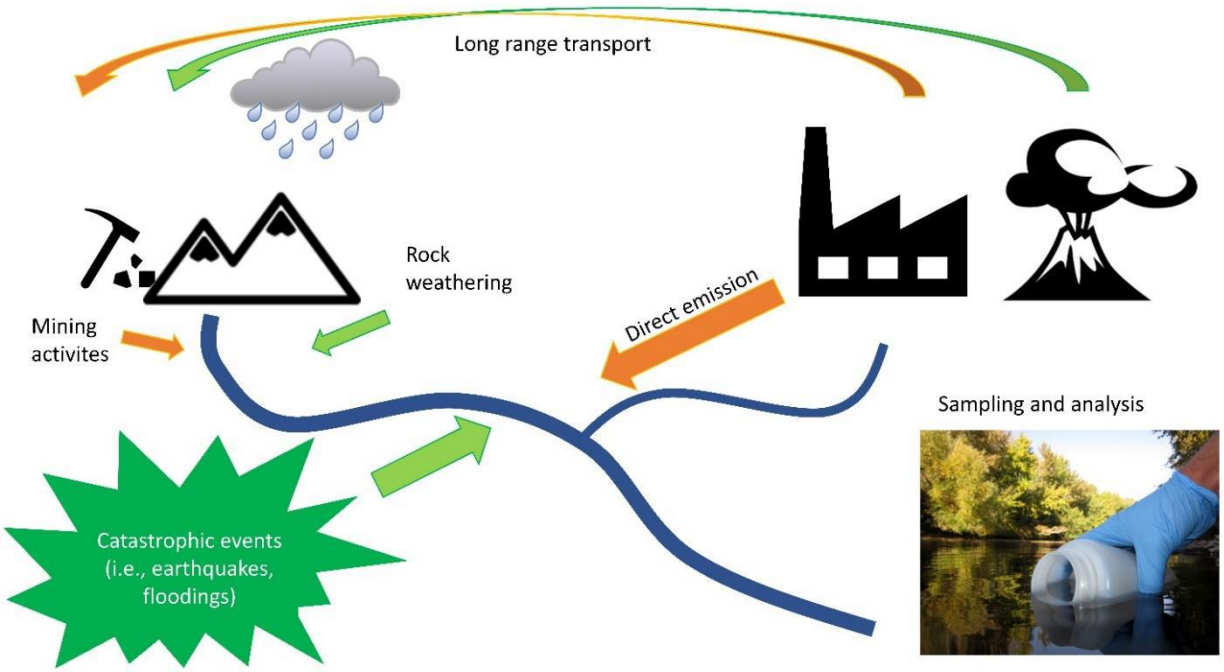

Figure 1.1: example of mixed sources of Potentially Toxic Elements in waters.

1.3 The concept of geochemical (or natural) background in waters

"By definition, an anomaly is a deviation from the norm. A geochemical anomaly, more specifically, is a departure from the geochemical patterns that are normal for a given area or geochemical landscape" (Rose et al., 1979). Therefore, an anomalous value represents a concentration above the level considered as the natural background. Thus, background values are necessary to be established in function of different environmental conditions.

The concept of geochemical background was introduced in explorative geochemistry to differentiate between normal element concentrations and anomalies, which might be indicative of an ore occurrence. This term was then applied in environmental geochemistry to indicate a natural value for a given medium not impacted by anthropogenic activities (Reimann and Garrett, 2005).

The establishment of background concentrations in the surface environment allows to distinct contaminated or polluted areas from unpolluted ones, and enables modeling of the anthropogenic influence on the mobilization, migration, and deposition/uptake of substances in the environment (Galuszka, 2007). This approach is usually applied in geochemical mapping for surface or water sediments, but can be applied in water science for environmental analyses

(Flem et al., 2018). The geochemical background evaluation, therefore, results a fundamental step to assess quality in ground and surface waters, and to infer possible anthropic impacts as well. This environmental compartment is in fact dynamic and present big seasonal changes, driven for example by climatic data. First studies in this field, therefore, were applied in soils and sediment, more stable environmental compartments (Galuszka, 2007; Reimann and Garrett, 2005). Academic interest is anyway increasing regarding the evaluation of background concentrations in waters, which would be the preliminary observation to understand possible geochemical anomalies or anthropic emissions.

However, the lack of a clear definition or agreement on its use is observable from the different published studies. Since the meaning of this term is crucial and important to understand natural or anthropic origin of elements in waters, it is correct to put some effort both into a clear and unmistakable definition and into the necessary methods to obtain the respective information (Matschullat et al., 2000).

Different authors agree regarding the fact that natural background levels are a range of values rather than single values with concentration ranging of several orders of magnitude, depending on aquifer type and location of the aquifer (Hinsby et al., 2008).

There are, however, few studies of the composition of truly 'undisturbed' groundwaters, and 'normal' background levels of trace elements in various groundwaters from various geological environments cannot generally be assessed. Moreover, with long range transport of pollutants, even the most remote settings present pollution of anthropically-derived trace metals. Thus, generally is difficult to distinguish between from anthropogenic sources (including sample contamination) and background levels originating from natural sources for PTEs (Ledin et al., 1989).

Therefore, with an unclear unique interpretation of what is the “real” background concentration, became challenging to assess the risk for environment, especially where concentration consider as natural, are already at the threshold for human and environmental risk.

Geochemists, with their knowledge of elements variability on Earth, have the important task to provide data and maps on, and explain the concept of, background variations of elements to regulators and the public. Then, the establishment of reliable background concentrations

of elements in soils and waters become a fundamental issue in environmental sciences (Reimann and Garrett, 2005).

1.4 PTEs natural anomalies and their causes: examples

Different geological settings can lead to the release even in water environment of relatively high load of metals in watersheds, causing a high geochemical background. Therefore, even naturally sourced elevated element concentrations can genuinely pose a risk to human health. One example is natural high concentrations of As in drinking water wells in India and Bangladesh (Figure 1.2; Gaus et al., 2003). As present hazardous presence in water also in the central Alps, with concentrations in springs up to 230 µg/L (Peña Reyes et al., 2015).

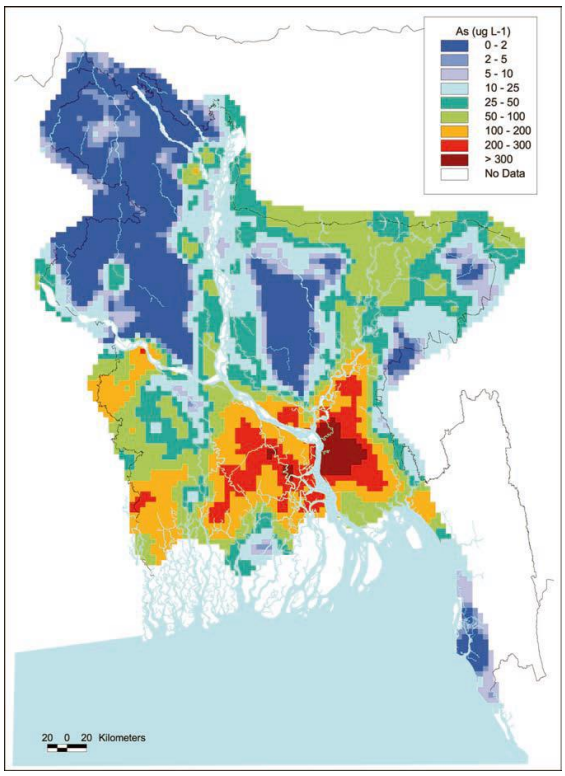

Figure 1.2: Distribution of As concentration (in micrograms per liter) in Bangladesh groundwaters (from Gaus et al.,2003).

Another example is presented by soils derived from mafic rocks, causing high releases of Ni and Cr (Binda et al., 2018; Kierczak et al., 2008; Tassi et al., 2018). In these soils special plant communities adapted to live with high metals concentrations and a unique ecosystem has developed that relies on the unusual environment for its existence. Ecotoxicological experiments could cause incompatibility problems using biota exotic to these peculiar environments, without a natural adapting.

Another example is represented by a general high concentration of F in water of a Brazilian aquifer in São Paulo, reaching concentration higher than 10 mg/L, when World Health Organization (WHO) limit is 1.5mg/L, and explained as a fluorite source from deep water circulation in the crystalline rock basement with ancient hydrothermal activity (Martins et al., 2018).

Therefore, anomalously high geochemical backgrounds concentration can lead to concerning concentrations for human health in waters without the observation of pollution sources (Binda et al., 2018; Dung et al., 2013).

Also, catastrophic natural events (i.e., earthquakes, eruptions, floodings) can change dissolution patterns and causing directly emissions of PTEs in water.

Earthquakes, for example, trigger changes the water chemistry of surroundings aquifers too. Hydrogeochemical responses to earthquakes are, in fact, reported worldwide (Bella et al., 1998; Ingebritsen and Manga, 2014; Woith et al., 2013). Earthquake can directly cause the emission of deep fluids richer in trace elements and even cause major dissolution after increasing in permeability, or ease the dissolution of metals (i.e., increasing CO_2 dissolved, causing therefore higher dissolution of elements). While the mechanism in different cases are still partly unclear, seeming to be hardly dependent from the type of aquifer involved and the bedrock lithology, the evidences show clearly that these events can cause changes in water flow and chemical features as well. Also, some authors try to analyze possible precursory chemical signal (changes in elements, temperature, dissolved gases) of earthquakes, possibly due to rock stress and fracturing, or upwelling of deep fluids or gases (Hartmann and Levy, 2005; Silver and Wakita, 1996).

Floodings can also be the cause of the release of PTEs from natural source in waters. As an example, Brown et al. (2014) reported the increase of metals (Ni, Fe, Pb, Cu) after floodings and high precipitation events in northern Florida (USA). Storms, in fact, trigger changes hydraulic gradients between rivers and adjacent aquifers. River water displaces groundwater in the conduit into the aquifer, then organic matter transported into the aquifer during river intrusion drives carbonate dissolution, alters redox state, and impacts trace metal mobility, impacting groundwater and surface water quality.

Cameron et al. (2002) report geochemical anomalies in sediment deposits above fracture zones in the gravels. They explain that during earthquakes in this seismically active region there was pumping of saline basement waters up the faults and fracture zones, entraining mineralized groundwaters from the deposits. After surface flooding and evaporation, elements were redistributed. Sampling shows that surface-active cations, such as Cu, were adsorbed and retained in the top few centimeters of soil. Anomalies may have formed by repeated episodes of seismically induced flooding.

Moreover, aquifer mixing can sometimes cause the dissolution in water of PTEs: for example, Morelli et al. (2017) showed how the increasing of water with higher concentration of Cl (simulating high-salinity groundwaters intrusion) could enhance the mobility of As.

Therefore, anomalously high concentrations of PTEs in the catchment bedrock cause an enrichment in concentration in watersheds, and thus cause issue for environmental and human risk, even without an anthropogenic contamination, and even natural sources should be considered as possibly harmful for human health in peculiar settings.

1.5 Data analyses to evaluate geochemical background and its anomalies

The determination of a geochemical background (and then anomalies) requires the ability to sample, work and quantitatively analyze the medium of interest without losses or contamination of the analyte.

Because of the extreme variability of analytes within the individual environmental spheres and compartments, a geochemical background can only be derived for a defined spatial setting. This determination requires the proof of relative homogeneity and thus comparability of the investigated matrix within the investigated space. This homogeneity is identical with a certain similarity mainly of climatological, lithological and pedological characteristics (Matschullat et al., 2000). In general, there are geochemical and statistical methods.

1.5.1 Geochemical methods

Geochemical methods are based on the analysis on any of the upper crust averages, as well as record with compartment not impacted by human activities (archives such as lacustrine and marine sediments, overbank and river sediments, cave sediments, etc.). The determined values, thus, represent hypothetical baseline concentrations without consideration of the natural variability. These methods depend upon a-priori knowledge and can easily present

subjective decision criteria, as assuming what is considerable as completely natural or not contaminated. This determination requires also wide knowledge about the geochemical behavior of PTEs under the prevailing environmental conditions. Also, is hard to find and collect an "archival" material that has not undergone chemical changes, deposition or generally alteration. Environmental materials are part of a "living" system in an overall biogeochemical cycle, with rarely maintenance of unaltered conditions. In different cases authors just use as background concentration samples collected upvalley from pollutions sources (Kara et al., 2017), otherwise old fractions were obtained as natural background from ice or sediment cores (von Gunten et al., 1997).

Also, isotopic analyses can help in understanding natural or anthropogenic sources of PTEs in waters. For instance, Castorina et al. (2013) used Fe and Sr isotopic fingerprinting to help them in the evaluation of human impact and geochemical sources of Fe contaminations in waters of a phreatic aquifer in northern Italy. Pb isotopic analysis are often used as marker for source evaluation (natural or anthropic) of this element (Renberg et al., 2002), and a study also report a geochemical anomaly prior to an earthquake in the Pyrenees (Poitrasson et al., 1999).

1.5.2 Statistical methods

Other approaches (more used in literature) include the application of statistical approaches to assess background concentration (Arpine and Gayane, 2016; Matschullat et al., 2000; Reimann and Garrett, 2005; Runnells et al., 1992).

To select better methods to deal with geochemical data, the basic properties of geochemical data sets need to be identified and understood. These include:

- Spatially dependence of data (the closer two sample sites, the higher the probability that the samples show comparable analytical results—however, all classical statistical tests assume independent samples);
- Different natural processes influencing the measured analytical value (i.e., climate conditions, pH, redox potential, organic matter and vegetation cover). For most statistical tests, it is necessary that the samples come from the same distribution—this is not possible if different processes influence different samples;

- Precision of geochemical data, like much natural science data, is crucial: these data often contain uncertainty unavoidably introduced at the time of sampling, sample preparation and analyses.

It should be pointed out, however, that the data often do not comply with the formal requirements of parametric statistics, but need non-parametric methods, like most environmental data. This requirement seems to contrast with the above-stated assumption that the natural element distribution may be described via a normal or log-normal distribution (Reimann et al., 2005). Thus, assumption of data normality, independence, or identical distribution as in different statistical test, easily fail using geochemical data; do better-suited tools for the treatment of geochemical data exist? (Reimann et al., 2005)

Generally, in literature, three main approaches are used to establish the background concentrations of PTEs in environmental compartments: analysis of data distribution (exploration data analysis), multivariate statistical techniques, and geostatistical approaches. Figure 1.3 synthetizes the most used methods in environmental geochemistry for background value evaluations.

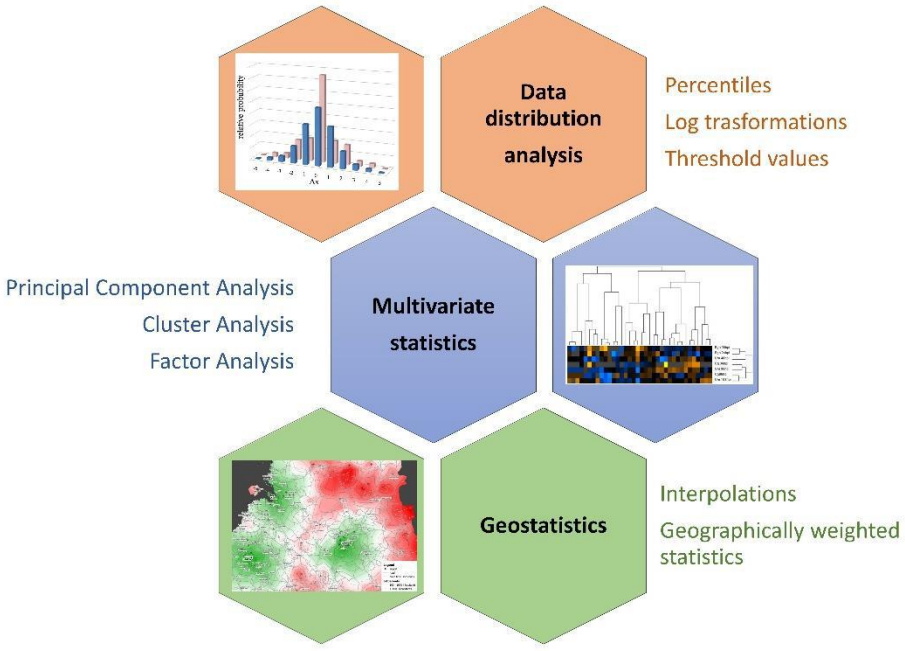

Figure 1.3: main statistical methods used to evaluate geochemical background values.

Analysis of data distribution

The analysis of distribution could be a useful approach for legislation: in fact, it could be useful to understand threshold limits and to consider a site possibly endangered, but it is not easy to separate the natural or anthropic source of contamination. Also, could easily fail in local setting where geochemical background values are already possibly dangerous for human and environmental health.

Analysis of the background range is often limited, especially for the analysis of surface water catchments, to the evaluation of data distribution of concentrations inside the considerate "unpolluted" areas, and removing the 90 or 95% of the distribution, and observing possible bi-modal distribution (Arpine and Gayane, 2016; Hinsby et al., 2008; Peña Reyes et al., 2015; Reimann et al., 2005).

Most statistical tests are only helpful to remove so-called outliers, and thus to reduce the original data set to a "clean" data collective. From this reduced data set, which is being addressed as anthropogenically undisturbed, the essential descriptive statistical parameters can be calculated. The only communication of any mean value without its standard deviation is of little use and may only be used in comparison with geochemical methods. It makes sense, however, to show concentration ranges (e.g. the normal range of a sample as defined by the mean ± 2 SD; ca. 95% of the samples) or upper values (threshold level; i.e., the 95^{th} or 97^{th} percentile). Only this type of data includes sufficient information about the natural scatter of the background. This approach requires anyway a careful estimation of which elements could come from an anthropic source (Matschullat et al., 2000).

Hinsby et al. (2008) proposed a methodology to evaluate background concentrations in groundwater, suggesting the use of 90^{th} or 97.7^{th} percentiles of analyzed PTEs concentrations as the natural background level depending on the amount and quality of data. (97.7^{th} percentile with large amounts of data, ca. >60 data points; 90^{th} for smaller datasets).

This approach requires anyway strict rules:

- exclusion of samples presenting: incorrect ion balance (exceeding 10%), unknown depth or unknown aquifer type.
- exclusion and separation of salinized or thermal aquifers ([Na]+[Cl] > 1000 mg/L);

- conversion of time series at each monitoring point to median values (assuring that long time series do not bias results and that all sampling sites contribute equally to the natural background).
- Exclusion of data in monitoring points presenting NO_3 concentrations above 10 mg/L, and directly considered to be polluted. Hence, screens with NO_3 concentrations less than or equal to 10 mg/L are used as a proxy for groundwater with a natural composition and remains in the dataset for further analysis and estimation of the natural background level as the 90th or 97.7th percentile.

Anyway, this approach requires a preliminary knowledge of aquifers type and the exclusion of different samples basing on these assumptions.

Multivariate statistics

To clearly define the ongoing hydrogeochemical processes within aquifers, large data sets and advanced methodologies are required. Due to the high complexity of environmental systems, evaluation of geochemical background, their anomalies, and anthropic emissions assessments need powerful data analyses tools. Multivariate statistics helps to preliminary understand relationships and similarities between variables, or to understand factors driving element source in environmental compartments. The analysis of these phenomena in water, with his dynamic environment remarks the need of multivariate statistical techniques.

Multivariate statistical analysis, such as: the factor analysis (FA), the principal component analysis (PCA) and cluster analysis (CA), are widely used in hydrogeological sciences to understand processes driving elements dissolution and their source in aquifers (Busico et al., 2018; Gabrielli et al., 2008; Kramer, 1998; Ou et al., 2012; Vaselli et al., 1997; Zhou et al., 2008).

Multivariate statistical procedures can sometimes discriminate between elemental patterns of natural and anthropogenic origin that can be used to estimate pre-anthropogenic element levels. (Reimann and Garrett, 2005).

Nonetheless, this approach requires large datasets, usually requires high data transformations to obtain a normal distribution (i.e., logarithmic transformations) and needs anyway an a-priori assumption of terrigenous or anthropic-derived elements (Zhou et al., 2008). Also,

preliminary data treatment can include changes which need to be gradually described and observed before preparing multivariate statistics applications.

Geostatistical techniques

Geostatistical techniques are often used in geochemical mapping and environmental geochemistry, and this strategy is already used to treat data from geochemical surveys of soils and sediments. The analysis of spatial heterogeneities and correlations helps to understand anomalous concentrations (also called hot-spots) of PTEs in the environment. Main geostatistical approaches to evaluate background concentrations and localize anomalies are: spatial interpolation techniques, indexes for spatial outliers and spatial correlations of variables (Yuan et al., 2018; Zhang et al., 2008) and geographically weighted statistics and regressions (Ling et al., 2018; Sarma, 2010).

Nonetheless, this strategy is often limited for water analysis (especially in rivers) due to the high variability of this environment. Some authors used anyway geostatistical tools to evaluate spatial trends of PTEs in confined aquifers (i.e., Dalla Libera et al., 2017) or in lakes (Ou et al., 2012).

1.6 Application of geochemical background and anomalies in freshwaters studies

So far, I reported different examples of geochemical anomalous concentrations in waters, and the main methods used in literature for the estimation of geochemical background. But the main connections between water sciences and the geochemical background evaluations approaches are missing. This is mainly because in most of the presented study, anomalously high concentrations even from natural sources were only reported, and the causes are not often well discussed. Also, few studies try to discriminate the different sources of PTEs, especially when the geochemical background already present concentrations which are possibly harmful for human and environmental health.

The lack is caused by big variance in space and time of water bodies. In fact, while soils and sediment often present a real record for inorganic and organic pollutants and therefore a sink, water can easily change concentrations in time and space for trace elements, and the dissolution conditions can change too.

1.6.1 Limits of the most used techniques

For example, temporal variations are often underestimate or not considered at all, but in a dynamic environment as the water it is fundamental to understand the timing response to climate factors, or for example, to understand the timing effect after catastrophic events, or for example, after drainage loss or anthropic emissions.

Nonetheless, another helpful tool to understand geochemical anomalies include the analysis of time trends and seasonal changes, as well as other dynamics that can influence water bodies (i.e., water levels, flow), especially for little catchments or aquifer mainly alimented by snow or ice melting, or other seasonally driven effect as rain seasons or tidal oscillations.

Dynamics of water environments, also, cause problems for the application of spatial distribution can be helpful as, with the high spatial heterogeneity distribution of springs make the application of geostatistics harder than in other environmental compartments (i.e., soils) or different water bodies (i.e., lakes (Ou et al., 2012); confined aquifers (Dalla Libera et al., 2017; Gaus et al., 2003)).

1.6.2 Integrated multidisciplinary approaches as a winning strategy

Generally, the analysis of ground and surface waters joins different disciplines of geology and chemistry. Thus, in environmental analysis and especially focusing with a dynamic and mutant compartment as water, is necessary to use multidisciplinary approaches. So, develop integrated multidisciplinary approaches could be the winning strategy to understand geochemical background and its anomalies.

So, this single approach requires anyway a good knowledge of lithology and of pollutants point emissions, and could not be enough complete without other data processing methods.

Clearly, the bedrock geology, which could be analyzed through the collection of solid samples (i.e., sediments) would influence the water quality in case of geochemical anomalies and anomalous background values, and the evaluation of the easily leachable species will be necessary to understand mechanism causing PTEs dissolution in water and migration.

Processes governing the occurrence of metals in both sediment and water need to be studied to understand the mobility, reactivity and consequently, the availability of toxic trace elements (de Vallejuelo et al., 2014). Therefore, the geochemical background evaluation often includes the analysis of other compartments to understand the geochemically available

elements, and the kinetics of dissolution causing the mobilization of PTEs in ground and surface waters.

Also, a complete observation of the main trends of PTEs in waters (both spatial and/or temporal) and strong multivariate statistical tools to process the data can be useful tools in obtaining sources of PTEs and their anomalies in waters.

The necessary steps to make to understand geochemical anomalies and their mechanisms are synthetized in Figure 1.4.

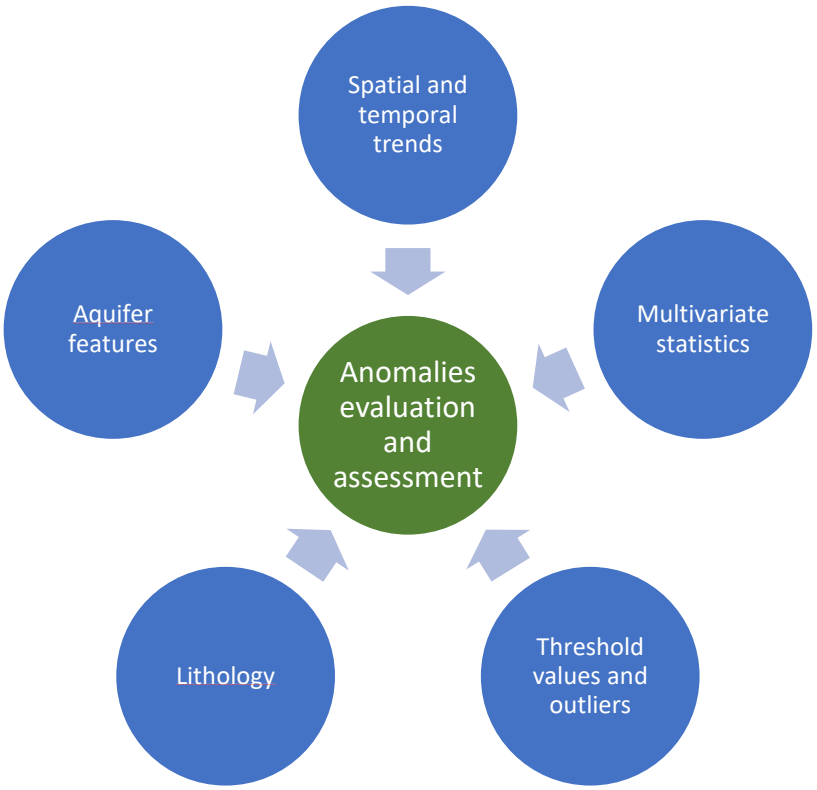

Figure 1.4:foundamentals step for the comprehension of geochemical anomalies.

Negative aspects of integrated approaches application include: the big quantity of samples and analysis required to understand the effect of temporal and spatial variations, the multidisciplinary aspects of water analysis, and therefore the requirements of big multidisciplinary team to achieve a good comprehension of geochemical anomalies. Nonetheless, the application of integrated approaches could give better results when single-way approaches would easily fail.

Thus, integrated multidisciplinary approaches can be the best way to understand and right interpret geochemical anomalies, especially in water compartment, where single approaches can easily fail in understanding metal sources and dissolution dynamics.

1.7 Aim and scope of the dissertation

Through this dissertation, I will present different environmental case studies with innovative approaches aiming to understand the natural background of elements and their anomalies with different final aims, as the evaluation of possible anthropic emissions in a remote area, and the analysis of mechanisms inducing anomalies after a catastrophic event (an earthquake sequence). Geochemical anomalies will be also used as markers to understand groundwater flow. In all the case studies, the application of integrated multidisciplinary approaches will show their high applicability in geochemical background and anomalies evaluations in water science.

Thus, the dissertation will be organized as follows:

- the evaluation of geochemical background and pollution assessment in an Alpine study area (the Ventina valley) will be proposed, thanks to a multidisciplinary integrated approach;
- a project of geochemical anomalies induced by the 2016-2017 seismic sequence in Central Italy will be presented, trying to understand the mechanisms causing the changes through the temporal analysis of chemical anomalies;
- secondary projects in the same study area will be discussed, which include:
    - the understanding of the chemical phase causing anomalously high Ni concentration in the Ventina valley;
    - a project aiming to understand deeper fractured groundwater flow, and the validation of model was done through geochemical markers.

2 Integrated multidisciplinary approach to evaluate PTEs sources in an area with high geochemical background

2.1 Introduction

Source apportionment for PTEs in waters is an issue of high concern in environmental research, legislation and decision making.

Strategies relying on single analytical approaches or statistical analysis usually tend to overlook spatial or temporal trends or, conversely, assume the invariability of some of the variables, as will be discussed below. Therefore, an integrated approach is proposed, composed by analytical and statistical data analysis, which integrates chemical analysis in water and solid samples with the evaluation of main spatial and temporal trends and correlations of variables.

Generally, the first step in source apportionment of PTEs is the geochemical background evaluation (i.e., the natural load), including possible anomalies (Dung et al., 2013). This will then be used to evaluate anthropic emissions, by subtracting the natural load from the total one.

Several studies focused on sources apportionment in soils and sediments (Gong et al., 2010; Hinsby et al., 2008; Jiang et al., 2017; Liang et al., 2017; Pelica et al., 2018; Sollitto et al., 2010; Zhang et al., 2008), nevertheless only few works tried to identify metal sources from surface waters analysis (Muhammad et al., 2011; Su et al., 2011).The main reason resides in the fast and variable dynamics of this environmental compartment, with seasonal changes and complex temporal trends. Therefore, despite different standard European methodologies are diffuse to evaluate geochemical background in soil and sediments (Ander et al., 2013; Reimann et al., 2018), for surface waters a generally accepted and standardized methodology to assess geogenic background values for metals does not exist (Schneider et al., 2017), and some authors (i.e., Galuszka, 2007) consider impossible to evaluate the geochemical background for waters.

The high dynamicity of surface water limits also the applications of spatial trends analysis as tool to understand sources of elements in this compartment: even though geostatistical methods are often used to recognize spatial trends for assessment in soils and sediments

(Albanese et al., 2007; de Vallejuelo et al., 2014; Zhang et al., 2008), still applying this approach to waters is generally more complicated (e. g., Dalla Libera et al., 2017 in ground waters; Ou et al., 2012 in lakes).

Moreover, in remote settings, where point sources of pollutants emissions are not present, medium- and long-range transport of metals can mark anthropic source of metals, which can be deposed through hydrometeors and dry depositions (Dossi et al., 2007; Gabrielli et al., 2008; Shah et al., 2012). This effect makes more difficult to establish possible sources of pollutant especially with high geochemical background of PTEs.

All these factors require a careful evaluation to successfully identify and measure metals and metalloids sources. Thus, even in simple-structured and apparently unpolluted basins, the understanding of the main drivers of elements concentration in waters is subordinate to the characterization of natural background and to the analysis of spatial and temporal trends.

In this study, an integrated approach including the quantification of different potentially toxic elements in different environmental compartment, the application of multivariate statistical analysis, and the observation of spatial and temporal trends is proposed, aimed to understand the geochemical background of PTEs and to assume possible anthropic contributions. The described approach will be then applied to a case study in a remote high mountain catchment in the Italian central Alps.

2.2 Proposed approach for source apportionment of trace elements in waters

I present an integrated approach, particularly suitable to understand sources of metals in water catchments, including a three-steps investigation strategy, parallelly performed on water and solid sample analysis, and then combined in data analysis (Figure 2.1):

- sampling and analysis: a prepared sampling design, collection, and chemical analysis of samples;
- data treatment: data treatment with careful observation of seasonal trends and clustering of variables;
- output evaluation: data output interpretation and source apportionment in waters.

In the following, I will describe assumptions and procedures for each step of the investigation.

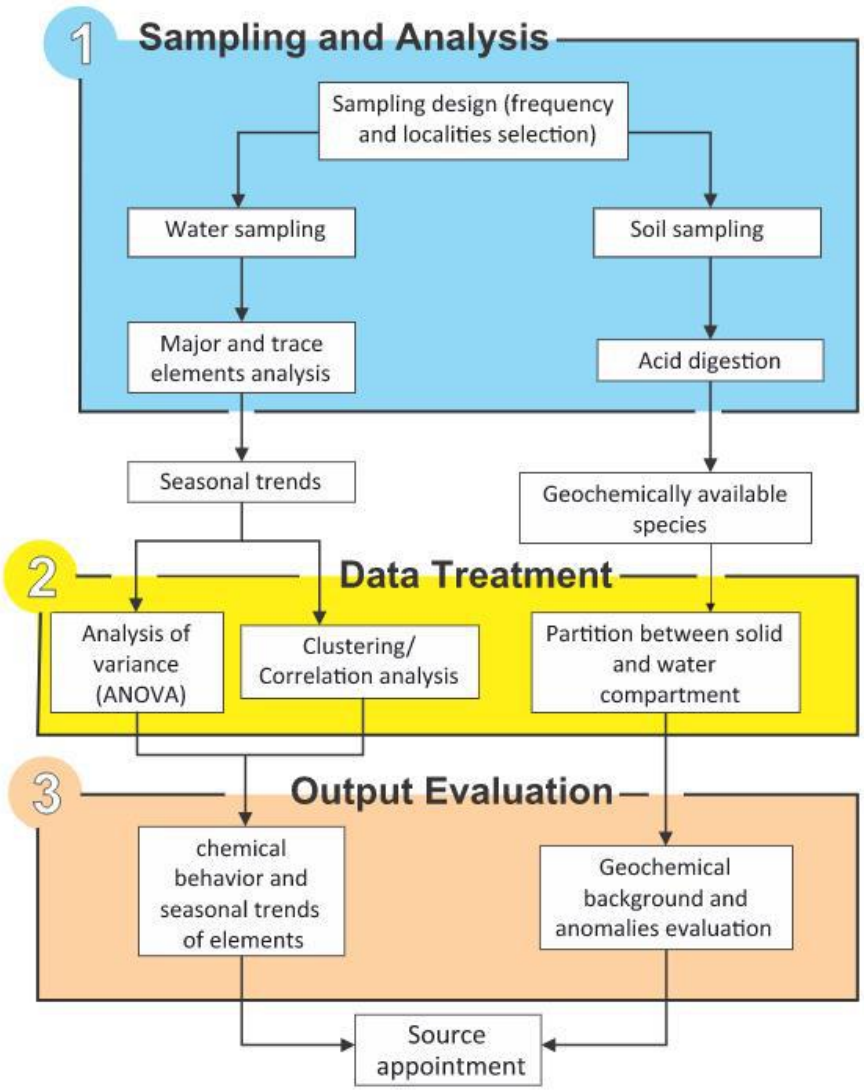

Figure 2.1: workflow of the proposed method to evaluate PTEs source.

2.2.1 Step 1: Sampling and Analysis

First step includes: sampling design, collection, and analysis for waters and solid (soils and sediment) samples. We assume that the bedrock geochemistry (at least regarding main mineral components) and water flow and source are already known. Thus, the sampling of water samples should be made with an adequate design aiming to understand water from different sources in areas presenting different bedrock lithology, and covering main temporal and seasonal changes; the analysis should include the quantification of major ions (to have a preliminary idea of main dissolutions conditions) and trace elements. The analysis of solid

samples is fundamental to evaluate the geochemical load available for dissolution: sampling design for this kind of samples should be made mainly in function of the distribution of lithologies, and analysis should include acid digestions to understand the total geochemical metal load (Filgueiras et al., 2002; Pueyo et al., 2008).

2.2.2 Step 2: Data treatment

Second step includes data statistical processing, and I propose to: analyze temporal trends in waters, focusing on seasonal analysis and clustering of variables, and then to evaluate concentrations ratios between the water samples and the solid ones to clarify if the PTEs derived mainly from geochemical source in the bedrock or from other sources. The assumptions are: the main natural source for PTEs in water would be rock weathering, that sediments generally maintain a good marker of rock geochemistry, and that temporal changes in sediments could be negligible.

In more detail, temporal trends should be analyzed in water, to monitor how main climatic seasonal conditions (i.e., dry or wet season, tidal changes, snow/ice melting (Hindshaw et al., 2011) act on dissolution and/or transport of PTEs. Then, observed trends should be confirmed: analysis of variance (ANOVA) would be a useful tool to compare seasonal changes with inter-annual variability, and so to understand the significance of these changes informing us if climatic factors favor the dissolution from water/rock interaction or the enrichment from atmospheric deposition.

Then, a clustering analysis of variables (through multivariate statistics; i.e., Cluster Analysis, Principal Component Analysis) should be performed to observe how clustering of variables changes in the different seasons (or observed periods) and which variables follow precise seasonal trends. Therefore, Cluster Analysis and PCA are useful method to classify similarities between variables, showing distances (for cluster analysis) or correlations (for PCA) among them. In this way, variables can be classified in groups, but the interpretation of the anthropic or naturally-derived elements is not preliminary assumed, and is only evaluated afterward through the entire approach. Water data should be then compared with the bedrock-derived samples ones (sediments, soils), to quantify if the geochemically available species could be dissolved after water/rock interactions. Then, observing the ratio between dissolved and

geochemically available elements will have clearer idea about the geochemical background of the elements.

2.2.3 Step 3: Output evaluation

Third step would aim to finally understand the sources of trace elements in waters through the combination of different approaches outputs. Clustering of variables and observed similar trends is assumed to indicate the same source for PTEs in waters. Therefore, observing specific seasonal trends and clustering of variables, we could group PTEs presenting the same source, and then combining the geochemically available metals we could quantify if the available chemical species could dissolve from bedrock, or if we have an enrichment coming from anthropic emissions.

2.3 Integrated approach application: a high mountain catchment

High mountain sites are excellent field laboratories to separate geochemical background from anthropic emissions: watersheds are relatively simple-structured, climatic factors directly control the hydrology, the underlying geology mainly influence the hydrochemistry (e. g., Fortner et al., 2011; Hindshaw et al., 2011; Lecomte et al., 2008), and the limited soil development, with typically low concentrations of organic matter, reduce possible disturbance in metals dissolution (Tranter, 2003). These areas, typically far from direct human impact, do not present local spot emissions of trace elements; the only anthropogenic sources are usually represented by atmospheric long-range transport and deposition (Gabrielli et al., 2008; Loska and Wiechuła, 2003).

The experimental area chosen to set up this approach will include a little catchment in the Italian Alps presenting a high geochemical background of PTEs, caused by the bedrock lithology (Binda et al., 2018).

2.4 Study area

2.4.1 Geographic setting

The study area is located in the Ventina valley (Central Alps, Northern Italy, Figure 2.2), encompassing an area of ca. 4 km^2, and with an elevation drop from 2450 to 1960 m a.s.l. A cold and temperate climate characterizes the region, with a mean annual temperature of 2 °C

and precipitations of 1123 mm (data from Lombardia Regional Environmental Protection Agency, weather forecast section, www2.arpalombardia.it/siti/arpalombardia/meteo).

The study area is located about 100 km far north from Milan and the northern fringe of the Po plain, which represents a highly urbanized area and the main source of different emissions reaching the site (Finardi et al., 2014); considering the remote setting of the study area, the precipitation in the area would be the only possible anthropogenic enrichment of metals due to urban emissions (Dossi et al., 2007). Most of the precipitation come from the south, accordingly with the mesoscale atmospheric circulation in central Alps (Ambrosetti et al., 1998), therefore emissions from the relatively close urbanized area could come from this direction.

The study area includes two hydrological basins: i) the Ventina glacier basin, where an ice tongue actively supplies the Ventina river and ii) the adjacent Pirola lake basin, collecting contributions by atmospheric precipitations and periglacial landforms (i.e., melting of rock glaciers and snowfields).

The Ventina river flows from south to north into a glacio-fluvial plain (i.e., sandur), ca. 700 m long and 200 m wide (Figure 2.2); further down-valley in the NW part of the study area the water is collected into a single stream channel. These river features, originating from differences in discharge flow from glacier during the year, typically support braided river systems with highly erodible bed and channel coarse sediments (Carrivick and Russell, 2007).

2.4.2 Geological and geomorphological setting

Two different metamorphic terrains, whose emplacement is the result of a complex tectonic history during alpine collision, crop out in the study area: the Margna nappe, to the north, and the Suretta nappe, to the south (Coward and Dietrich, 1989; Schmid et al., 2004), separated by an E-W trending subvertical fault (Pirola fault, Figure 2.2).

Margna nappe lithologies are represented by metagabbros and paragneiss. The metagabbros present foliated or lenticular texture, and the most abundant minerals are plagioclase, (i.e., albite; $NaAlSi_3O_8$ and anortite; $CaAl_2Si_2O_8$) and pyroxenes (i.e., diopside; $CaMgSi_2O_6$); small lenses of hornblende ($Ca_2(Mg,Fe,Al)_5\ (Al,Si)_8O_{22}(OH)_2$), are included (Trommsdorff et al., 2007). Accessory minerals are prehnite ($Ca_2Al_2Si_3O_{10}(OH)_2$), natrolite ($Na_2[Al_2Si_3O_{10}]\cdot 2(H_2O)$) and sfalerite (ZnS) (Bedogné et al., 1993). To the NE, albitic and chloritic paragneiss crops out,

(Bonsignore et al., 1971). Main minerals included are plagioclase ((Na,Ca)(Si,Al)4O8), biotite ($K(Mg,Fe)_3[AlSi_3O_{10}(OH,F)_2$) and quartz ($SiO_2$) (Bedogné et al., 1993). Also, As bearing minerals as realgar (As_4S_4) are present especially in the fault area (Bedogné et al., 1993). Geochemical studies made on Margna nappe rocks samples report possibly concerning concentrations of: Fe, Zn, Mn, Co, As (Burkhard, 1989; Muntener et al., 2000).

The Suretta nappe lithologies outcropping south of the Pirola fault, along the Ventina valley, include ultramaphic rocks (i.e. serpentinites). These are hydrothermally altered metamorphic rocks derived from igneous Mg- Fe rich protholith (i.e. peridotite).

The major minerals are antigorite ($(Mg,Fe)_3Si_2O_5(OH)_4$) both as aggregate and in big sheets, chlorites, pyroxenes and olivine ($(Mg,Fe)_2SiO_4$). Magnetite (FeO x Fe_2O_3) is often present in serpentinites as lens or grains (Bonsignore et al., 1971), this mineral can contain also Cr_2O_3 , up to ca. 10,8% in wt. Serpentinites present accessory minerals containing significant amount of heavy metals, such as Ni and Cr and Cu: Taenite (Ni, Fe), pentlandite ((Fe,Ni)9S8), calcocite (Cu_2S) digenite (Cu_9S_5) and galena (PbS) (Bedogné et al., 1993; Kierczak et al., 2007; Morrison et al., 2015). Therefore Fe, Ni, Cr, Cu Co and Mn are PTEs presenting high load in these rocks, as also was observed in other studies collecting rock samples in proximity of the study area (Bloise et al., 2016; Cavallo, 2018).

In proximity of the glacier terminus, lenses of ophicarbonates are present (Bedogné et al., 1993). This zone consists of a 10 to 400 m wide tabular volume that strikes ca. NW-SE and is exposed approximately 6 km within the Malenco ultramafic body (Bonsignore et al., 1971; Trommsdorff and Evans, 1977). These rocks exhibit a prevalently brecciated texture containing fragments of serpentinite, embedded in a fine- to medium-grained white matrix of predominantly calcitic ($CaCO_3$) composition (Pozzorini and FruhGreen, 1996).

Following this brief description of study-area geological framework, it is possible to estimate expected principal metals both in water and sediment samples (Table 2.1).

Geological unit	**Expected PTEs (ordered by concentrations)**
Margna nappe	Fe, As, Zn, Co, Mn
Suretta nappe	Fe, Ni, Cr, Cu, Co, Mn

Table 2.1: expected metals in the analyzed samples from the different geological units in the study area.

In order to correctly interpret the source of metals and metalloids in water from water-rock interaction, it is important to consider the typical sediment present in the glacial and periglacial forms typical on high mountain sites (i.e. glacial *diamicton* or *till*). These sediments present low permeability due to its dominant silty-to-clayey grain size, and are often subject to interaction with glaciofluvial activity, which can promote metals mobility (Evans, 2013; Tranter, 2003).

Different moraines (i.e., frontal and lateral glacial deposits) are present in the study area: more recent moraines (i.e., ascribable to the Little Ice Age; XIV -mid IXX Cent. AD; Matthews and Briffa, 2005) in the Ventina glacier forefield (Trommsdorff et al., 2007), and older lateral moraines (from the Last Glacial Maximum; 26.5 – 20 ka BP; Clark et al., 2009) at higher elevation (Trommsdorff et al., 2007). These forms can enhance metals release through the low permeability and long residence time of water in their bodies.

2.5 Material and methods

2.5.1 Water sampling and analysis

Water samples were obtained monthly, during four sampling campaign in 2014, three samplings in 2015 and three in 2016. A total of 150 water samples were collected in all sampling campaigns. Samples were collected only during the melting season (early summer to early fall), because of the thick snow cover during winter and spring, with scarce water from snow melting in springs and a high avalanche risk.

Water samples were collected at 21 localities (Figure 2.2) and included water from different surface and underground sources (Table 2.2).

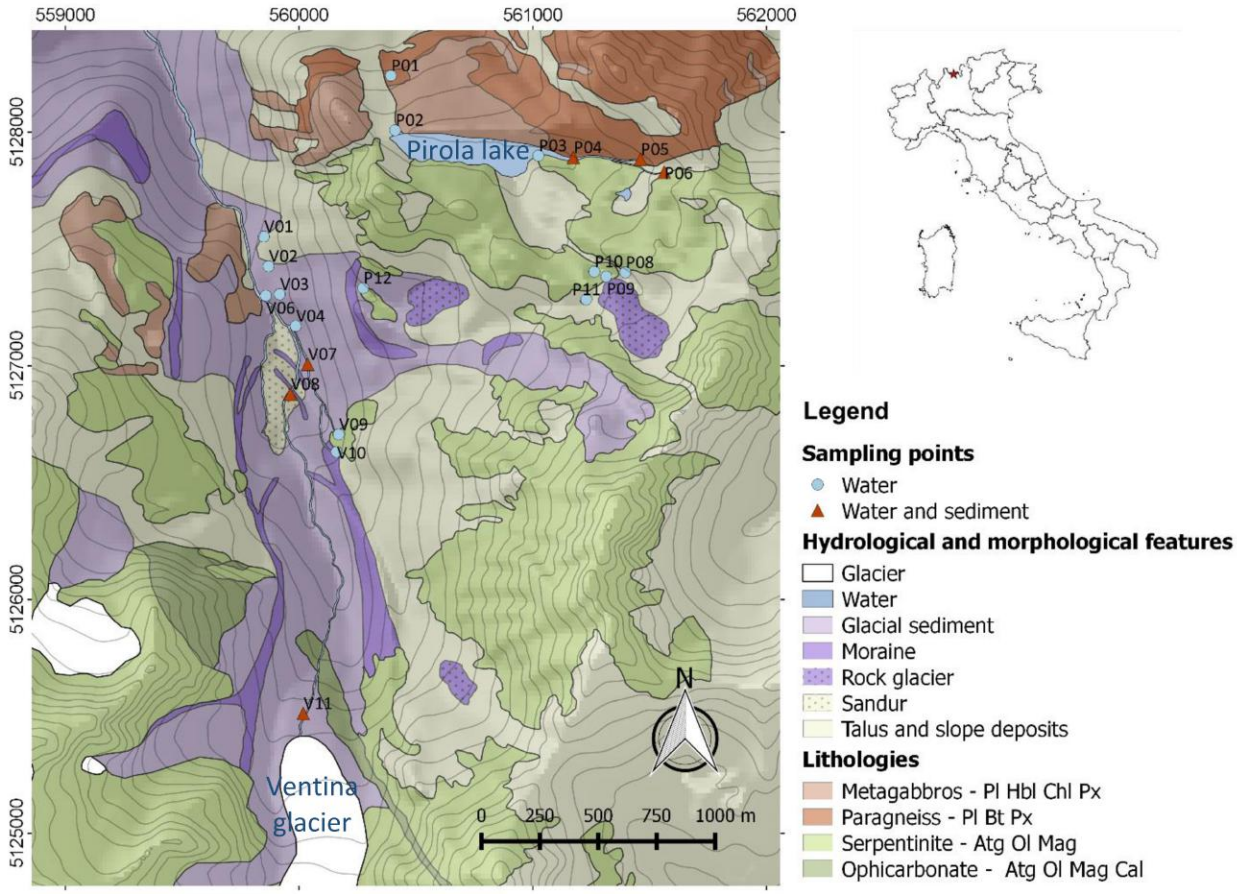

Figure 2.2: study area map (GPS coordinates of sampling points in supplementary material Supplementary_07, chapter 9).

Several water samples were collected at five springs outflowing from fractures in bedrock. Water flow in a fractured aquifer through a low-permeability rock volume, possibly leads to an enrichment in metals, if passing through mineralized bodies and veins (MacQuarrie and Mayer, 2005).

We also collected waters from small lakes and ponds, where the presence of biota is typically scarce and with water bodies sensitive to atmospheric deposition and to temperature changes, usually freezing during winter (Santolaria et al., 2017; Sommaruga-Wögrath et al., 1997).

Two sampling points were obtained at the outlet of an ice glacier (V11) and of a rock glacier (P08). Even if both the waters come from ice thawing, ice glaciers show a faster response in melting during the summer season and are more sensitive to atmospheric deposition than rock glacier sources (Brown, 2002).

Other samples were obtained from stream waters, resulting from a concurrent contribution from the sources described above (Table 2.2).

SAMPLING POINT	SOLID SAMPLE	BEDROCK	TYPE OF WATER SOURCE
P01		Margna nappe	Stream outlet from Pirola lake
P02		Pirola fault zone	Pirola Lake at the outlet
P03			Pirola Lake at the inlet
P04	*		Stream inlet into Pirola lake
P05	*	Margna nappe	Spring from fracture
P06	*		Spring from fracture
P08			Rock glacier melting outflow
P09			Lake
P10			Lake
P11			Lake
P12			Spring from phreatic aquifer into slope deposit close to a moraine ridge
V01		Suretta nappe	Spring from fracture
V02			Spring line from phreatic aquifer in slope deposits
V03			Stream
V04			Spring line from phreatic aquifer in slope deposits
V06			Stream
V07	*		Stream
V08	*		Stream in the *sandur*
V09			Spring from fracture
V10			Spring from fracture
V11			Ventina glacier melting outflow

Table 2.2: typologies of water collected during the sampling campaigns.

Water analyses included:

- Physico-chemical parameters collected on site with probes;
- Major ions: Carbonates (as HCO_3) with colorimetric titrations, and other ions (Cl, NO_3, SO_4, Ca, Mg, Na, NH_4, K) with ionic chromatography;
- Trace elements (Cr, Mn, Fe, Co, Ni, Cu, Zn, Cd, As, Ag and Pb) with ICP-MS.

Specific technical details about sampling and analyses techniques are included in appendix (chapter 7).

2.5.2 solid samples: sampling and analysis

Six outcropping glacial sediments and soils were sampled at the same location of some of the water samples (water and sediment samples collected in the same point have the same name) using plastic bags. Selection of sampling sites was conducted in function to cover the heterogeneities between different bedrock and different morphologies outcropping in the study area. Samples were collected both in the glacier forefield and in the nearby of the glacier front (V11). I also collected sediments in the *sandur* (V08) and from a lateral moraine deposed during the Little Ice Age (V07). Moreover, a sediment sample (P04) was also collected at the contact between the two bedrock terraines (i.e., along the Pirola fault) in order to observe the background values due to the different surrounding lithologies.

Samples were collected in plastic bags, air dried in laboratory and then analyzed through microwave assisted acid digestion (more details about analysis and protocols used are listed in appendix, section 7.5).

Sample	Main lithology	Type of deposit	Grain size distribution
V08	Serpentinite	Sandur	gravelly sand
V11	Serpentinite	Subglacial lodgement till	diamicton (clay/silt and pebbles)
V07	Serpentinite	Little Ice Age morenic ridge	clayey silt
P04	Metagabbros	Poorly developed soil, with sparce vegetation cover	clayey silt
P06	Serpentinite	Poorly developed soil, without vegetation	clayey silt
P05	Metagabbros	Poorly developed soil, with sparce vegetation cover	clayey silt

Table 2.3: classification and bedrock lithology of solid samples

2.5.3 Statistical analysis

After analyses, all the concentration data resulting under the limit of detection (which are called censored data) were substituted with LOD/10 values for both solid and water samples (Alier et al., 2009; Giussani et al., 2016), then a multi-way statistical analysis was performed.

Seasonal variations and trends

Data were firstly divided our dataset in subsets, in function of the sampling period: an early summer dataset (for samplings in June and July, including 74 samples) and a late one (for samplings in September and October, including 76 samples). This arbitrary decision was made to highlight the main temporal trend along the melting season in glacial environment catchments, where elements due to atmospheric deposition concentrate mostly in the first part of summer, with high snow and ice melting, while elements dissolved by water-rock and water-sediment interaction reach their baseline natural concentrations in the late summer (Hindshaw et al., 2011). The snow layer thickness data for long term monitoring in the Alps with similar altitude of the study areas confirm this trend (Marty and Meister, 2012).

In order to investigate if the differences between early and late summer concentrations are statistically significative, a one-way ANOVA test was applied to all the chemical measured variables. This statistical test compares the mean and the variances of two different dataset in function of a categorical variable (in this case the sampling period). The null hypothesis is that these datasets are the same, and the variance among samples is basically the same as the difference between the datasets, and an F value is calculated as the ratio between the variance between the groups and beneath the groups and also a p value is calculated as well (Ross and Willson, 2017). Also, a difference between the means was measured to understand if the trend indicates an increasing or a decreasing in concentration from early to late summer, and then normalized on the total mean as:

$$\frac{\mu_{LS} - \mu_{ES}}{\mu_{TOT}}$$

Where μ_{LS} is the late summer period mean, where μ_{ES} is the early summer period mean, and μ_{TOT} is the total mean of the whole sampling campaigns. This process was applied for all measured chemical variables.

Seasonal clustering

Afterwards, hierarchical cluster analysis was applied to the different datasets for major ions and trace elements variables, using Ward's method (Ward, 1963). This method starts from a singleton (single-point clusters) and aims to create clusters with the lowest possible increment

of sum of squares. We decided to use this method because it creates small clusters. This approach aims to understand which variables present similar features, helping us to understand the possible similar source of metals in the same cluster.

To avoid interferences due to different measure units in the application of cluster analysis, all the measured variables in the data matrix were scaled and centered on mean, using the following equation:

$$x_i' = \frac{x_i - \mu}{s}$$

Where μ is the mean, s is the standard deviation, x_i is the original value and x_i', is the standardize value (Sahariah et al., 2015).

Statistical analysis was performed using the software STATISTICA 8 (StatSoft, Inc., 2007).

Partition between water and sediment

In order to compare water with sediment sample data a partition coefficient between dissolved and liquid phase of metals was calculated through a K_r coefficient (Fdez-Ortiz de Vallejuelo et al., 2014) expressed as:

$$K_r = \frac{C_{metal\ sed}}{C_{metal\ wat}}$$

Were $C_{metal\ sed}$ indicates the total metal concentration in the sediment sample in mg/kg and $C_{metal\ wat}$ indicates the metal concentration in the water in μg/L. The data obtained were expressed after a logarithmic transformation. This approach permits to quantify how likely the concentration of a trace element in water reflects the bedrock concentration.

2.6 Results

2.6.1 Major and trace elements in waters

Waters analyzed in this study, regarding physico-chemical parameters, and all waters present low mineralizations (max EC values is 98 μS/cm), and changes in EC mainly remark seasonal trend increasing in the end of summer. More details about physico-chemical parameters are listed in supplementary material Supplementary_01 (chapter 9). Also, water present principally sourcing from Ca ang Mg, correlated with HCO_3.

Data for trace elements are synthetize in Table 2.3. Observing the threshold limits for drinking water defined by WHO, most of the samples show concentration which are not concerning for

human risk, only the maximum values for Ni slightly goes over, and As show an high maximum value, which is double of the threshold value.

Element	Measure unit	25th percentile	Mean	Median	75th percentile	Maximum	WHO limit
Ag	µg/L	<LOD	0.0526	0.0101	0.0605	0.8382	-
As	µg/L	0.0195	1.2278	0.1074	0.3273	28.5961	10
Cd	µg/L	<LOD	0.0203	0.0032	0.0201	0.1092	3
Co	µg/L	<LOD	0.0561	0.0352	0.0839	0.6696	50
Cr	µg/L	0.4781	1.027	0.9107	1.4003	2.8614	50
Cu	µg/L	0.0001	0.2312	0.1165	0.3136	1.9823	2000
Fe	µg/L	1.6958	8.8737	5.8836	12.1065	41.1742	-
Mn	µg/L	0.0712	0.4812	0.1933	0.4937	6.2423	500
Ni	µg/L	3.8851	6.5436	6.5677	8.4386	20.4384	20
Pb	µg/L	0.0152	0.0907	0.0609	0.1058	1.1055	10
Zn	µg/L	1.4701	6.8391	4.3256	9.4942	39.6039	3000

Table 2.4: descriptive statistics of PTEs concentrations in water samples, and comparison with WHO limits for human consumption of water.

2.6.2 seasonal trends analysis (ANOVA)

Water samples show seasonal differences which can inform about the possible source of potentially toxic elements in the analyzed catchment (Hindshaw et al., 2011; for more details about the single results for every sample, see supplementary material Supplementary_01, chapter 9).

The F value outcoming from ANOVA against the difference between periodical mean normalized is plotted in Figure 2.3 for variables presenting significative difference ($p<0.05$) between early summer and late summer periods. pH, Na, NO_3, K, Pb, Mn, As, Fe were not plotted because these variables show a seasonal difference between early summer and late summer which is not significantly higher than the variance among the different years of sampling.

Elements decreasing from early summer to late summer are: Cu, Zn and Cl; the latter presenting a high F value, as an index of its high significance according to the ANOVA test.

Conversely, variables showing an increment in the late summer are: Ca, Cr, Ni, HCO_3, Mg and SO_4 concentrations.

Electrical conductivity shows a slightly increasing trend from early to late summer, as the elements listed above (but with a higher F value). This effect suggests a similar source for most of the major ions (mainly derived from rock dissolution) and the PTEs which show the same seasonal trend (Ni and Cr).

Also, Ag, Cd, NH_4 and Co show a high increment from early to late summer if normalized to the mean, but for these elements a major warning comes from the fact that several measured concentrations are close to the instrumental LODs, resulting in possible inaccuracies.

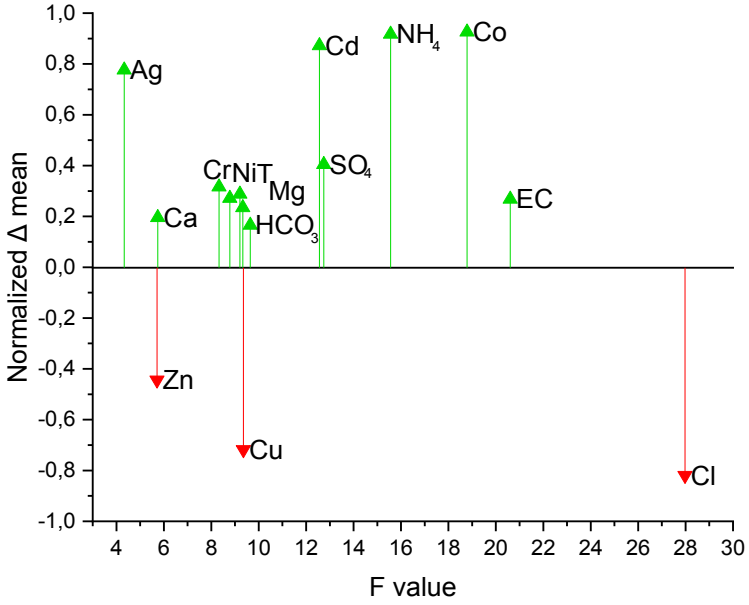

Figure 2.3: plot of F value (x axis) and difference of the early and late summer mean normalized for total mean (y axis) for all variables showing a significant difference (p<0.05).

2.6.3 Seasonal clustering

Figure 2.4 shows the hierarchic clusters for early and late summer including major ions and trace elements. The clustering of elements in the beginning and the end of the melting season can highlight similarity in sources, or same chemical behavior in dissolution from bedrock. In early summer four main clusters are present: one containing nitrogen salts, Cl, As, carbonates, Ni and Cr; one containing Na, K, NH_4 and SO_4; one containing Ag and Cd and one containing the other analyzed trace elements.

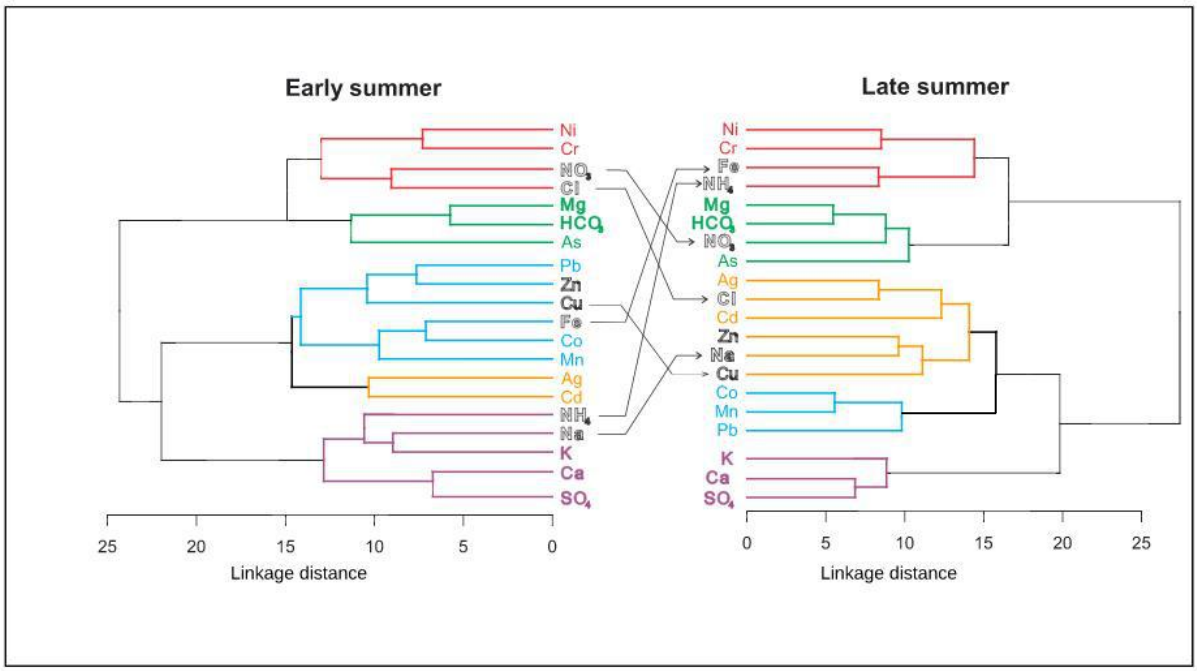

Figure 2.4: cluster diagrams for early and late summer and their clustering changes in the different periods.

Late summer clustering partly remarks the early summer one, but the setting for trace elements changes and highlight the separation in another cluster of Cu, Zn, Ag, Cd, Na and Cl, which plot together in late summer clustering.

2.6.4 Acid digestion of solid samples

Table 2.5 presents acid digestion values for all the analyzed samples. The analyzed samples show a high load of Fe, Cr, Ni and Mn, as typical of ultramafic bedrock lithologies. Also, a clear difference in As concentration from the samples collected in the Ventina valley and in the Pirola basin is observable, with a great increment for the samples close to the Pirola fault. Ag and Cd, instead, results below limit of detections in all sampling points.

Samples	P04	V07	V08	LOD
Measure unit	mg/kg	mg/kg	mg/kg	mg/kg
Co	44.10 ±0.80	75.60±1.80	44.90±2.20	0.3
Cr	454.00±3.00	2160.00±10.30	667.00±1.20	0.22
Cu	40.60±1.60	13.00±0.30	14.10±0.63	0.18
Mn	419.50±3.00	728.00±15.50	389.00±10.00	0.12
Ni	526.00±6.60	1310.00±10.00	941.00±16.70	0.03
Fe	19800.00±15.00	40400.00±25.50	19000.00±24.00	0.08
Zn	43.75±2.00	26.09±1.10	6.47±0.40	0.41
As	154.65±6.70	5.91±0.30	3.68±0.20	0.95
Ag	<LOD	<LOD	<LOD	0.75
Pb	1.02±0.10	0.04±0.01	0.4±0.01	0.03
Cd	<LOD	<LOD	<LOD	0.39
Samples	V11	P05	P06	LOD
Measure unit	mg/kg	mg/kg	mg/kg	mg/kg
Co	52.00±1.60	32.63±1.20	107.95±4.50	0.3
Cr	1080±25.50	345.97±11.00	1119.21±21.00	0.22
Cu	79.20±2.00	120.18±4.30	59.20±2.00	0.18
Mn	494.00±19.00	781.29±23.50	762.09±31.10	0.12
Ni	1090.00±22.20	359.28±12.80	1726.62±11.40	0.03
Fe	27200.00±25.50	48730±21.40	45743.00±34.00	0.08
Zn	11.72±0.40	143.58±4.30	205.14±6.60	0.41
As	10.73±0.50	123.74±2.30	121.40±4.70	0.95
Ag	<LOD	<LOD	<LOD	0.75
Pb	1.19±0.05	24.17±0.90	74.89±1.00	0.03
Cd	<LOD	<LOD	<LOD	0.39

Table 2.5: acid digestion values and standard deviation (based on three replicates of the Ventina solid samples.

In Figure 2.5 acid digestion of the analyzed samples and values from other studies on serpentine derived soils in Greece (Kanellopoulos et al., 2015) and in 2 soil profiles in Poland (Kierczak et al., 2008), are normalized for mean upper crustal values (Wedepohl, 1995), to observe possible geochemical anomalies, assuming the lack of high load of pollutants in sediments due to atmospheric deposition (elements like Cd and Ag are, in fact, lower than the detection limits of acid digestions in all our samples, and they are not in figure).

Fe, Mn, and As data for Poland are not present in graph because they were not analyzed by the authors.

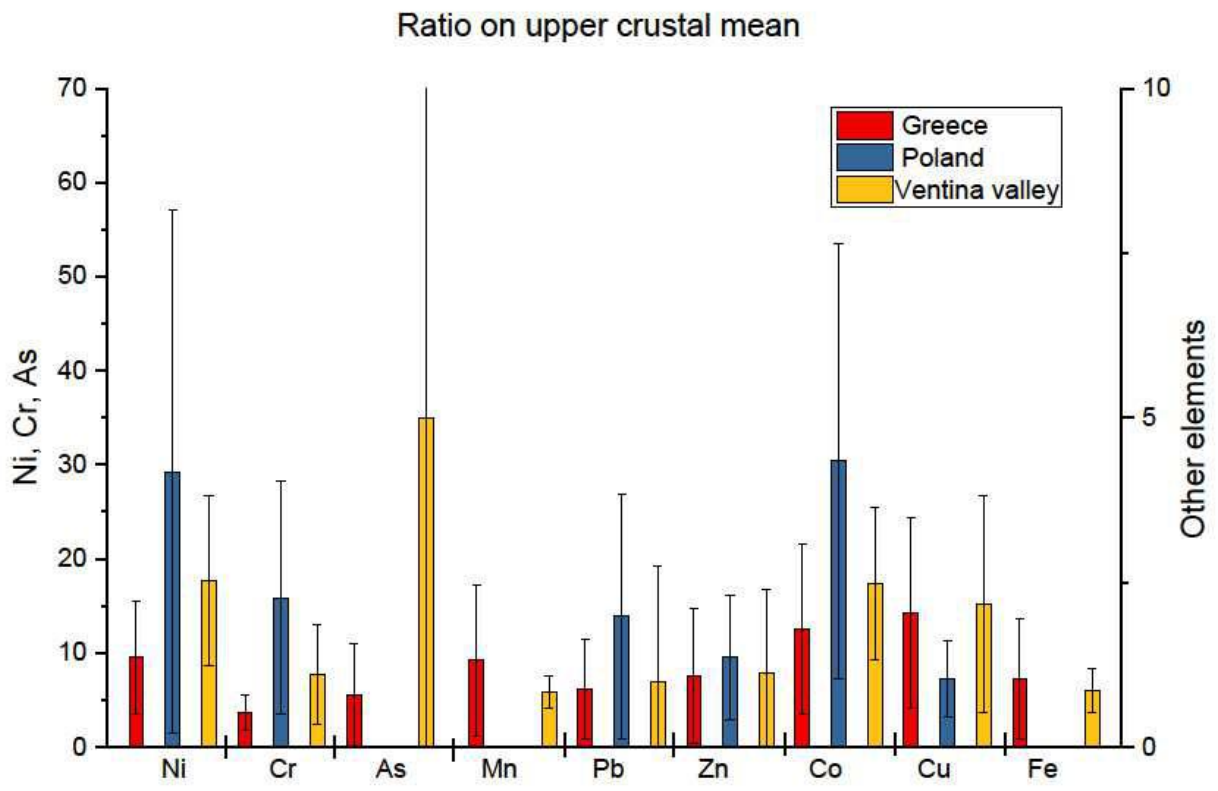

Figure 2.5:Bar graph showing the ratio on the earth crust average abundance (Wedepohl, 1995) of PTEs in Poland (Kierczak et al., 2008) Greece (Kanellopoulos et al., 2015) and this study.

As observable, metals as Co, Ni and Cr already present higher load than the mean crustal one, but this is clearly correlated to the lithology of the site, presenting a high geochemical background (Binda et al., 2018). Thus, sediment samples show mainly a natural load of analyzed metals. The only element showing a higher load compared to other studies is As. This element presents a relatively high concentration in sediment of the study area, especially in the glacial sediment samples collected in the area proximal to the fault, in fact this element also presents a big variance in the different sampling sites (sampling site P06, Table 2.5).

2.6.5 Partition between solid and water compartments

We obtained K_r coefficient of the analyzed metals using the mean concentration in water along the entire time series, and total concentration in solid samples (from pseudo total acid digestion) and is represented in logarithmic scale in Figure 2.6. Lower values of K_r indicate a greater presence in dissolved phase compared to the concentration in the solid phase. It's possible to distinguish 3 main groups of PTEs: a first group (including Fe, Cr, Mn, Co, Cu) with

high values, indicating the typical elements included in serpentinites, which present low dissolution rates, another group indicating Ni, As and Pb, presenting medium values and the third group with values less than 1.5 (including Zn, Cd, and Ag) elements presenting a possible enrichment due to other sources than water/rock interaction, and in this case including the effect of atmospheric deposition.

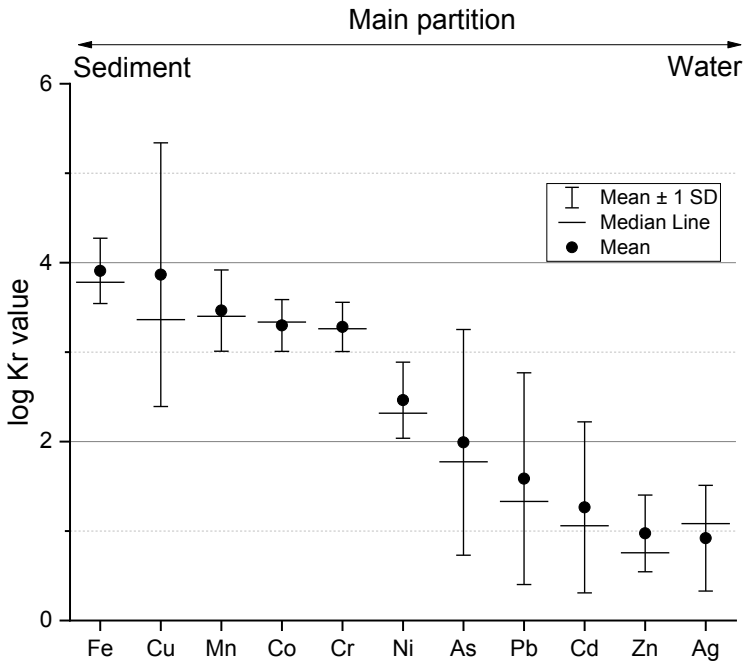

Figure 2.6: Values of Kr index exposed in logarithmic scale for the five water and glacial sediment sampling points, bars indicate the mean values, whiskers indicate the standard deviation.

The water samples analysis reveals a relatively high concentration of Ni respect to other PTEs, and a lower K_r ratio, indicating a major partition in the liquid phase respect to the sediment samples acid digestions, compared to other analyzed elements.

Co and Mn plot together too, but differently from Co, Mn does not show a statistically significant increase during the melting season.

As maintains a clustering with Mg and HCO_3 from early to late summer and does not show a significant seasonal trend.

2.7 Discussion

Results obtained in this study elucidate specific trends during the summer season for trace elements and relevant differences of concentrations between solid and water samples.

Combining the outputs of the proposed integrated approach and analyzing the bedrock main minerals and geochemistry, we can finally infer the sources of elements in the analyzed watershed.

Following the clustering of variables in the different seasons and their trend along the melting season, we recognized groups of PTEs which can possibly have similar sources. Then, analyzing the partition of elements between water and sediment samples, we evaluated if the geochemically available species justify a presence of PTE in water, or whether an enrichment due to atmospheric depositions is present. Table 2.6 summarizes the different approaches and the behavior of different trace elements of water samples, whose results are discussed below. The discussion will firstly focus on the PTEs showing possibly concerning concentrations in water samples, and then will move to other analyzed PTEs.

2.7.1 Source apportionment for concerning PTEs: Ni and As

Among the analyzed elements, the only ones showing possible concerning concentrations are Ni and As. Ni presents a relatively high concentration in waters from all the sampling sites, with higher concentrations close to WHO limits for drinking water, while As presents a lower mean values in the whole study area, but concerning concentrations in the all the sampling campaigns at the same spring.

Ni is an element which could be present in high concentration on mafic and ultramafic terrains and show clustering with other elements defined as natural (i.e., Cr). Also, observing the results in the other approaches this element shows an increase from the melting season through the end of summer (typical of elements outcoming from water-rock interaction), and a partition of solid/water concentration of an intermediate value. Ni shows a relatively high mobility and high concentration in water samples, but this behavior comes from a high dissolution of sulphides in the study area, which was deeply analyzed in another study (Binda et al., 2018).

Moving to As, this PTE does not show a significant seasonal trend, and present a medium-low K_r value, with a high variance in the study area (Figure 2.6), suggesting an anthropic enrichment. Nevertheless, its correlation with Mg and HCO_3, species typically dissolving from rocks, is an indicator for rock dissolution sourcing.

The high As concentration in part of the analyzed sediment samples can support a dissolution from water of this elements (Figure 2.5). The breccias in the fault area present in fact As bearing minerals (Bedogné et al., 1993; Burkhard, 1989) and other authors highlighted the high concentration background of As in freshwaters in other areas of the central Alps (Peña Reyes et al., 2015).

As, also, presents a high concentration along all the sampling sequence in only one spring (P06, with a mean value above WHO limits, supplementary material), while the concentration results lower in all the other springs of the study area. At least for this spring, were high As concentration were observed in sediment sample too, a geochemical anomaly can be the cause of this PTE presence. In fact, as observable in Figure 2.7, the only one spring present values at least closer to P06 is P04, which was collected in the same stream just few meters downvalley and presenting dilution of P06 initial concentration caused by mixing with other waters.

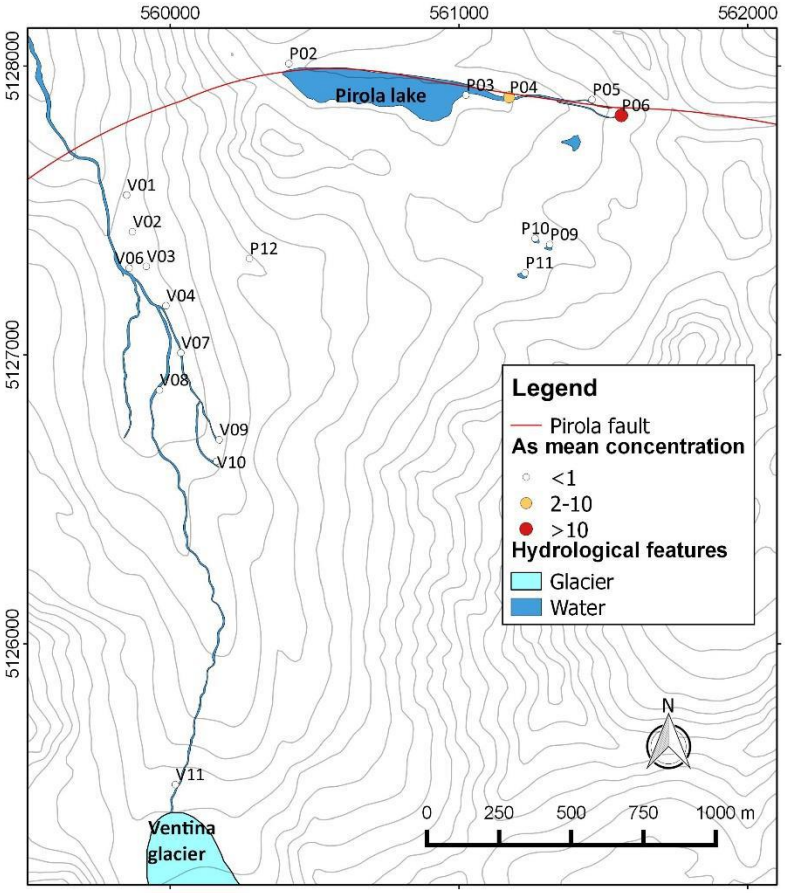

Figure 2.7: distribution map of mean As values in water (in µg/L) for all sampling campaigns.

Consequently, while considering the whole study area As concentrations could be inferred ss coming from a mixed source, surely in the single spring presenting alarming concentrations for human consumption and environmental risk the cause would be a geochemical anomaly.

2.7.2 Source apportionment for other PTEs

Other PTEs from natural sources: Cr, Co and Mn.

Elements such as Ni and Cr maintain a clustering throughout the sampling season and plot together to major ions in the ANOVA test, with a slight increase from early to late summer.
Co and Mn plot together in Figure 2.4, maintaining their clustering, and present similar Kr value. But differently from Co, Mn does not show a statistically significant increase during the melting season.
Mn and Co are elements which can easily dissolve from mafic rocks, and their presence in water can be justified as mainly from water/rock interaction (Kierczak et al., 2016). Also, these elements present quite low concentrations in waters of the study area, especially if compared with solid samples (they present in fact a K_r value which is more than 3, Figure 2.6). Fe does not show a significant change from early summer to late summer (Figure 2.3), and plot with Co and Mn in early summer, and then group with NH_4, Ni and Cr in late summer (Figure 2.4). Also, it presents high K_r value similar to the other elements discussed so far.
These elements show relatively high concentrations in water samples too, consistently with their high concentrations in the bedrock and, in turn, in glacial sediments. Other case studies with serpentinite bedrock reported similar values (Bonifacio et al., 2010; Kierczak et al., 2016; Morrison et al., 2015; Voutsis et al., 2015). Consequently, these PTEs can be considered as sourced by natural water-rock interaction.

PTEs with anthropic enrichment: Ag, Cd, and Zn.

Ag, Cd and Zn present a low value in K_r values and separate from the others PTEs in the late summer cluster plot, as indexes of effects of atmospheric depositions (Figure 2.4). Zn shows a decreasing trend from early to late summer too as an index of higher load at the beginning of summer due to snow and ice melting (Hindshaw et al., 2011).
Differently, the trend of Ag and Cd shows an increment along summer period (Figure 2.3): this effect could be due to the high number of samples which presents values below detection

limits. Ag and Cd, anyway, show too low concentrations in the sediment samples to be considered naturally sourced in the study area.

Cd, Ag, Zn were also reported as anthropic elements in other studies in the Alps (Gabrielli et al., 2008), supporting the possible anthropic enrichment of these elements in our study area too.

Other problematic PTEs: Cu and Pb.

Not all the analyzed elements can be easily attributed to a single source by the approaches applied in this study. Some problems arise, in fact, to interpret result from Cu and Pb.

Pb shows a lower K_r value than metals derived from a natural source (even if this element shows high spatial variability, with large range in the different points values) the difference between early summer and late summer are not statistically significant compared to the inter-annual ones, and the cluster analysis shows that Pb groups with Zn and Cu (considered anthropic) in early summer, but groups with Mn and Co (considered natural) in late summer.

Finally, Cu shows a significant decrease in the mean concentration from the beginning to the end of the melting season (Figure 2.3), as Zn, presents a clustering with other considered anthropically enriched PTEs, and a trend which indicate a lower presence in late summer season. Nonetheless, it shows a high value of K_r ratio which indicates a high availability in sediments for dissolution.

Considering the differences in behavior functionally to the applied approach, these metals can be sourced partly naturally sourced, and then anthropically enriched. Therefore, the application of a single-way approach would probably give misleading source apportionment of these elements, and the different trends observed highlight the need of an integrated approach, with a careful evaluation of statistical outputs.

Element	Presence in minerals of the bedrock	Clustering with (early summer)	Clustering with (late summer)	Trend from early to late summer	Kr	Anthropic influence?
Cr	Minor element in serpentinite rocks	**Ni**, Cl, NO_3	**Ni**, **Fe**, NH_4	increasing	high	no
Mn	Minor element in serpentinite rocks	**Co**, **Fe**	**Co**, **Pb**	not significant	high	no
Co	Minor element in serpentinite rocks	**Mn**, **Fe**	**Mn**, **Pb**	increasing	high	no
Ni	Minor element in serpentinite rocks	**Cr**, Cl, NO_3	**Cr**	increasing	Medium-high	no
Cu	Minor element in serpentinite rocks	**Pb**, **Zn**	**Zn**, Na, **Cd**, Cl, **Ag**	decreasing	Medium-high	partly
Zn	Minor element in metagabbros	**Cu**, **Pb**	**Cu**, Na, Cl, **Ag**, **Cd**	decreasing	low	yes
Cd	Not present	**Ag**	**Ag**, Cl, **Zn**, Na, **Cu**	increasing	low	yes
Pb	Trace element in serpentinites	**Cu**, **Zn**	**Co**, **Mn**	not significant	Medium-low	partly
Fe	Major element in serpentinites and metagabbros	**Co**, **Mn**	NH_4, **Ni**, **Cr**	not significant	high	no
Ag	Not present	**Cd**	**Cd**, Cl, **Zn**, Na^+, **Cu**	increasing	low	yes
As	Trace element in some breccias of the Margna nappe	Mg, HCO_3	Mg, HCO_3, NO_3	not significant	Medium low	partly

Table 2.6: synthesis of approaches outputs and anthropic influence evaluation.

2.8 Geochemical anomalies as source of harmful PTEs concentrations

It is important to highlight, that among all elements analyzed to understand their source in the study area, the ones showing higher and possibly dangerous concentration for human and ecosystem health are characterized as probably from natural source or of a mixed one, and are Ni (with different values close to the WHO limit for concentration in water), and As, which present a concentration higher of WHO limit value in one spring along all the sampling sequence (Table 2.4).

This maximum value outcome from only one spring in the study area (point P06, in every sampling campaign) indicating a geochemical anomaly in the fault zone, possibly related to the presence of veins of As-bearing minerals (e.g., realgar). Similar results are also obtained for solid samples collected in this point, presenting an enrichment in As too (Figure 5 and supplementary table 2). Similar mineral anomalies are observed in a location about 10 km far from the study area (Burkhard, 1989).

2.9 Conclusion and next applications

We propose a method to evaluate the source of natural on anthropic PTEs in freshwaters through the application of a multidisciplinary integrated approach, which include:

- the analyses of waters and sediments functionally to main spatiotemporal trends;
- a multiple statistical treatment of data aiming to understand seasonal clustering of variables, and the partition of elements between solids and waters;
- a combined output evaluation to obtain metals sources in water.

We also applied this approach in to evaluate the sources of 11 PTEs (Cr, Mn, Fe, Co, Ni, Cu, Zn, As, Ag, Cd and Pb) in an alpine catchment in northern Italy.

Mountain aquifers, in fact, are a main source for drinking water (Viviroli et al., 2007), and present sensitive biota in their watersheds (Ilyashuk et al., 2014).

It was observed a high natural background in water for Ni, the natural sources of Fe, Co, Mn, Cr without severe risk for human beings and the biota. Metals observed as coming from anthropic sources are Ag, Cd and Zn. Elements showing controversial trends are instead Cu, As, and Pb, which possibly present a mixed source. Highlighted the presence of a geochemical

anomaly in a spring for As, which show a concentration which is double of the WHO limit for water consuming.

Therefore, also in the single step of the application of the integrated approach part of the elements (i.e., Cu, Ag, Cd) showed controversial trend, which could lead to erroneous source apportionment without considering all the possible influencing factors.

The proposed approach helps to understand trace element sources in waters, especially in areas with a high geochemical load of PTEs where is hard to separate the natural and the anthropic ones. Nonetheless, this approach still requires a big amount of analyses, and a good knowledge of the bedrock geochemistry of the study area to have a clearer idea of the natural background. Also, this kind of approach was applied in a relatively simply structured catchment, but it could be considered as a preliminary application to a following on a regional scale.

This approach could also work better in areas with remote settings, where direct sources of pollution are not immediate to observe.

This approach needs to be validated in other types of study areas, to better observe its applicability.

Through this study, the importance of high mountain catchments monitoring is remarkable: these settings, in fact, need high attention in water quality checks for ecological and human risk assessment, because they present an important water source for human populations (Viviroli et al., 2007), and usually these catchments have ecological communities that are highly sensitive to slightly changes in water chemistry, and potentially toxic elements could increase through the food web (Ilyashuk et al., 2014).

3 Seismically induced geochemical anomalies: the 2016-2017 seismic sequence in Central Italy

In this chapter, geochemical anomalies in karst aquifers which followed the main shock of the 2016 and 2017 seismic sequence in Central Italy will be analyzed. Their analysis will be interpreted to understand the mechanisms inducing hydrogeochemical changes in karst aquifers.

3.1 Hydrogeochemical anomalies caused by earthquakes

Earthquakes are catastrophic events that can dramatically affect groundwater resources, including water quality and flow rates. Observed effects of seismicity on groundwater include transient and non-transient changes in flow rate, flow path, and water chemistry (Doglioni et al., 2014; Montgomery and Manga, 2003; Muir-Wood and King, 1993). These effects do not necessarily occur synchronously and are dependent on crustal response to seismicity, as well as processes both internal and external to the affected aquifer systems. Different parameters can give us information to detect the mechanisms that may cause these responses, including the released seismic energy (function of the magnitude of the earthquake, and therefore of the dimension of faulting and coseismic slip), the distance from the epicenter/hypocenter, the timing (i.e. before/after the earthquake) and the duration of the anomaly, the geochemical variables mainly related to the bedrock of the study area (Geller, 1997; Hammond et al., 1981; Hartmann et al., 2005).

The discipline of earthquake hydrogeology has increased the knowledge about how earthquakes can affect water resources, and numerous examples of shocks altering hydrological flow are known worldwide (Rowland et al., 2008; Wang and Manga, 2015). Less is known about the effect that earthquakes can have on water chemistry. However, our ability to understand the process that control hydrologic and hydrochemical responses has been hindered by a lack of coherent sampling strategy. Normally, these data are collected serendipitously in response to main shocks with scant pre-shock data against which the post-shock response can be evaluated. The first observations of hydrochemical anomalies were conducted in the late 1960's (Ulomov and Mavashev, 1967; Allegri et al., 1983; Scholz, 1977;

Silver and Wakita, 1996; Tsunogai and Wakita, 1995), but the mechanisms driving changes are still not clear and responses vary functionally from local features (i.e., geochemistry or aquifer-flow type).

Groundwater resources are vulnerable to seismic hazards, as supply and water quality can potentially be impacted either by transient or permanent changes to the aquifer. Understanding the mechanism and processes affecting groundwater resources is important in order to manage the response following seismic events, and to assess if possible reliable precursors can be proposed on a regional scale. This can be accomplished by collecting continuous and periodic water quality data and groundwater levels from multiple aquifers near fault zones that can be used in conjunction with available tectonic data to identify specific mechanisms driving transient and non-transient changes observed.

There is robust evidence in the literature that supports groundwater responses to earthquakes worldwide, and these may be grouped into three main categories: 1) changes in water isotopes (oxygen and hydrogen), 2) dissolved gases (as radon, carbon dioxide and methane), and 3) major and trace element concentrations. However, not all parameters are collected at all locations on a consistent basis:

1. Water isotopes: Water isotopes derive their signature at the recharge area and are largely conserved within the aquifer. Studies in Northern America (Rowland et al., 2008; Wang and Manga, 2015), Taiwan (Wang et al., 2005) and India (Reddy et al., 2011) have used changes in water isotopes as a proxy for determining changes in water flow paths caused by seismically induced mixing of aquifers with distinct isotopic signatures. Strontium isotopes derive their ratios from the rocks through which the water flows. The strontium isotopic signature after an earthquake in China (Mw 7.9) changed for a period of 3 years (Jin et al., 2016), indicating different rock sources for the water and relatively long-term transient changes to the aquifer after the earthquake.
2. Dissolved gasses: changes in the concentration of dissolved gasses such as Rn, CH_4 and CO_2 are commonly reported (Allegri et al., 1983; Italiano et al., 2009; Tsunogai and Wakita, 1995). In Japan Rn anomalies were observed prior to the Kobe earthquake in 1995 (Tsunogai and Wakita, 1995), while Rn anomalies aftershocks were observed in

India (Nagabhushanam and Reddy, 2011), California (Hammond et al., 1981) and Italy (Allegri et al., 1983). CO_2 and CH_4 anomalies were observed after strong seismic events in Central Italy (Chiodini et al., 2004; Italiano et al., 2009; Martinelli et al., 2017). These studies show changes in deep seated sources of gasses caused by shaking and fault rupturing in these areas.

3. Anomalies in major and trace elements: one of the first papers that observed earthquake-induced hydrochemical anomalies was published about the 1994 Kobe earthquake where an increase in SO_4 and Cl was observed in an artesian aquifer both before and after the 7.2 Mw earthquake, and was attributed to mixing with deeper water (Tsunogai and Wakita, 1995). A study with the same experimental setting and similar results and interpretations was made in the French Pyrenees: authors found anomalous increase in chloride and lead concentrations, and anomalies in the lead isotopic ratio (Poitrasson et al., 1999). A study in Iceland (Claesson et al., 2004) highlighted continuous changes in different elements, and another study in Iceland showed precursor changes in different chemicals before 2 mainshocks in a long-term monitoring program, with increases in K, Na and changing in water isotopes (Skelton et al., 2014).

The mechanisms proposed to justify hydrological and chemical responses observed in previous studies include two main groups:

- mechanism including the intrusion of water from a different source;
- mechanism internal to the aquifer dynamics, with changes in water-rock interaction.

Mechanisms of the first group include: expulsion of water from compressed aquifers (Doglioni et al., 2014; Muir-Wood and King, 1993), aquifer breaching and fluid mixing (Poitrasson et al., 1999; Reddy et al., 2011; Wang et al., 2005), interactions with deep fluids or gases (Barberio et al., 2017; Ciarletti et al., 2016; Manga and Wang, 2015) consolidation and liquefaction of sediment (Montgomery and Manga, 2003). Mechanisms of the second group are: opening of deep fractures, which can increase chemical release with freshly created rock surface (Skelton et al., 2014) or change groundwater flow and his features, increasing permeability. Even landslides or collapses can influence solute load increasing with the deposition of different fine-grained fresh sediment. In more detail, at shallow depths (centimeters to several meters),

earthquakes trigger extensive co- and post-seismic landslides, which can produce reactive fine-grained sediment (Jin et al., 2016). Table 3.1 synthetize the main mechanism causing changes.

.

Mechanism of water quality changes after earthquake	Flow	Major ions	Trace elements	^{2}H and ^{18}O of water	^{13}C of DIC	References
Strain/rupture of faults	L or T	ND	ND	ND	ND	(Cotecchia et al., 1990)
Near surface dilation and shaking	T	T	T	ND	T	(Charmoille et al., 2005; Pasvanoglu et al., 2004)
dilation and mixing of different aquifers	T	T	T	ND	ND	(Poitrasson et al., 1999)
Release of deep-seated geothermal fluids	L or T	L or T	L or T (Li, B, As)	L or T	L or T	(Barberio et al., 2017)
Release of deep-seated trapped gases	--	T	T (data available only for U)	ND	L or T	(Ciarletti et al., 2016; Favara et al., 2001)

Table 3.1: Major changes expected from different mechanisms of movement after earthquakes in carbonate aquifers. An "L" or "T" marked in the column indicates statistically significant changes in the constituent from pre-earthquake conditions. L = lasting changes.

Transient changes in water chemistry were observed in some instances before earthquakes (Barberio et al., 2017; Ingebritsen and Manga, 2014; Silver and Wakita, 1996; Skelton et al., 2014), and the possibility of earthquake forecasting has been proposed. This area of investigation is problematic because the precursor proxies reported are neither convincing nor consistent, and none of the datasets have a sufficiently long-time series nor sampling frequency to reliably capture a precursor signal, except for one (Skelton et al., 2014). This subject has been explored by multiple directions in previous works, including release of radon, (Silver and Wakita, 1996), chlorides and sulphates (Tsunogai and Wakita, 1995). Despite efforts to locate universal and reliable precursors, these signals are at best inconsistent and unreliable, because they usually indicate other sources of anomalies in concentration (Poitrasson et al., 1999). They do not always occur in the same places preceding major seismic events, nor are there signals that occur consistently within strongly affected areas. Nonetheless, precursor signals are an area that has received lots of interest because of the

strong benefit they could bring in disaster management. Also, skepticism is quite diffused regarding precursors reliability (Geller, 1997).

Understanding the nature of the mechanisms played in the groundwater system would better inform us about whether to expect precursor signals, and under what conditions we might expect them. Also, a long-term monitoring in a high seismic frequency area can be the only way to enforce signals evaluations and understand possible precursory effects (Ingebritsen and Manga, 2014).

3.2 Previously reported changes in Central Italy

There is abundant evidence supporting widespread seismically-induced changes in water table, flowrate, and hydrochemical properties, although responses should be measured consistently, and have been varied in their timing and nature. This is especially the case during sequences with higher magnitude which struck Central Italy in the past 50 years (1980 Irpinia, 1997 Colfiorito, 2009 L'Aquila and 2016-2017 Norcia-Amatrice) and within the historical time-window (1349, 1456 and 1703 seismic sequences).

Observed anomalies include:

- changes in water levels and flow of springs discharge in all the recent seismic sequences (Celico, 1981; Martinelli et al., 2017; Petitta et al., 2018);
- dissolved gases anomalies, in more detail Rn anomalies were observed in springs in Latium (Allegri et al., 1983) and different gases anomalies (He, N_2, CH_4 and CO_2) were observed along the Colfiorito sequence; CO_2 anomalies were reported along the 2012 Po valley sequence too (Martinelli et al., 2017);
- major ions changes were observed after the Irpinia 1980 earthquake (Celico, 1981) and after the 1997 Colfiorito sequence (Italiano et al., 2009); also, in the Modena 2012 sequence anomalous increase in Cl in different deep wells (100-300m) was observed (Martinelli et al., 2017);
- trace elements show changes during 2009 L'Aquila earthquake and during 2016-2017 Norcia - Amatrice sequence; in more detail, an enrichment in U was observed in groundwater in the preparatory phase prior to the mainshock, showing periodical spikes not correlated with seasonal variations (Ciarletti et al., 2016), and along the

2016-2017 sequence different metals show anomalous increases in concentration previously and following (Barberio et al., 2017; Rosen et al., 2018) the mainshocks.

Mechanism proposed to explain these responses mainly include the role of deep fluids changing solubility of elements in water (Barberio et al., 2017; Ciarletti et al., 2016), and changes in permeability due to seismic pressure (Italiano et al., 2009).

3.3 The 2016-2017 Central Italy seismic sequence

The seismic sequence which struck Central Italy in 2016-2017 included a series of moderate to large earthquakes along an Apenninic-trending normal fault system. (Chiaraluce et al., 2017). This sequence included ~26,000 earthquakes, and 16 shocks with Mw >5. The first big shock happened in the night of 24th August 2016 (Mw 6.0) which presented epicenter close to the little town of Amatrice, in the province of Rieti. Then, 2 big shocks followed in a northern area: the largest event of the seismic sequence registered so far (Mw 5.9) on 26th October, and another event (Mw 6.5) few days after, on 30th October. Another big shock (Mw 5.5) happened with epicenter in the southern part on 18th January 2017.

Regrettably, the high vulnerability of the local infrastructure and the shallowness of the largest events (depth around 8 km) resulted in 299 casualties and more than 20,000 homeless, with great difficulties in the disaster management.

This seismic sequence was accompanied by the increased interest in earthquake hydrology, both in documenting the effects and understanding the mechanisms behind them. A study along this sequence (Barberio et al., 2017) infers some trace elements (As, V, Cr, Fe) as possible earthquake precursors, and also reports the increase in water table level in Sulmona (located ca. 90km far from the epicentral area). Flow changes in different aquifers in the epicentral areas and the appearance of a new river in the Norcia plain were also reported (Petitta et al., 2018).

3.4 Aim of the study

This study also took place during this sequence, and shows the groundwater hydrochemical responses from two high flow carbonate springs and one alluvial spring located in the Rieti area (Latium region), within the intermediate field, 30-40 km away from all the epicentral areas, and in 5 carbonate sourced springs in the area within 5 km of the epicentral area (near-

field) for the October shocks, located in Castelsantagelo sul Nera and in Forca di Presta (Marche region). The 3 Rieti basin springs, and one spring in the epicentral area present chemical data even before the first shock of the sequence, giving us a picture of pre-earthquake situation too.

Also, to investigate the role played by minor shocks to changes in water quality, in a seismically quieter period (August 2016-January 2017), a probe was installed in a well located in the epicentral area of October 2016 shocks (about 10 km far from the epicentral area of the October shocks), and continuous interactions of electrical conductivity and water level were monitored.

Main focus of this study involves the comparison of responses in the near and intermediate-field areas, with the goal of better conceptualizing the mechanisms and aiming to understand differences in spatial-temporal differences in responses in carbonate aquifers. The aquifers studied here are subjected to the direct effects of shaking and tectonic displacement of large hydrogeologic structures, causing directly effects on flow and chemical quality of the aquifers.

3.5 Study area

The study took place in 2 main areas struck by the earthquake sequence in Central Italy, including: the Sibillini mountains area, the epicentral area of the October 2016 shocks, and the Rieti plain area, a basin located ca. 40km far west from the epicentral area of the seismic sequence. In more detail, 3 springs were periodically analyzed along the seismic sequence in the Rieti basin, while in the epicentral area a spring was monitored with a high sampling frequency (thanks to a bottling plant managed by Nerea S.p.A), 4 springs were monitored with few sampling campaigns, and a well located about 20 km far from the October shocks epicentral area was continuously monitored for physico-chemical parameters starting from spring 2017 (Figure 3.1).

3.5.1 Tectonic Setting

The Apennines fold-thrust belt is part of the accretionary wedge caused by the roll back of the Adriatic subduction towards the east (Cavinato and Celles, 1999). The Quaternary–Neogene normal faults, formed by the subsequent west-to-east migration of the regional extensional regime, govern the intra-montane basin evolution and its filling through continental clastic deposits and can produce large earthquakes, up to Mw 6-7 (Cowie et al., 2017; Roberts and

Michetti, 2004). These aquifers have demonstrated a hydrochemical response to strong magnitude earthquakes (>Mw 5). Thus, local responses in the area along seismic sequences in the recent years were monitored (Barberio et al., 2017; Ciarletti et al., 2016; Italiano et al., 2009; Martinelli et al., 2017; Petitta et al., 2018).

Central Italy presents an unusually high frequency of shallow earthquakes in a confined geographic area relative to other seismically active parts of the world (Cello et al., 1997; Roberts et al., 2004).

The ruptured faults are located within a relay zone between two major overlapping NNW–SSE trending normal faults in the Central Apennines, with segments are focused on either side of the Olevano–Antrodoco–Sibillini (OAS) thrust system. Surface faulting occurred in between two similar surface rupturing seismic sequences that occurred in the central Apennine in the past 20 years: the 1997 Colfiorito sequence to the north, and the 2009 L'Aquila events to the south (Vittori et al., 2011).

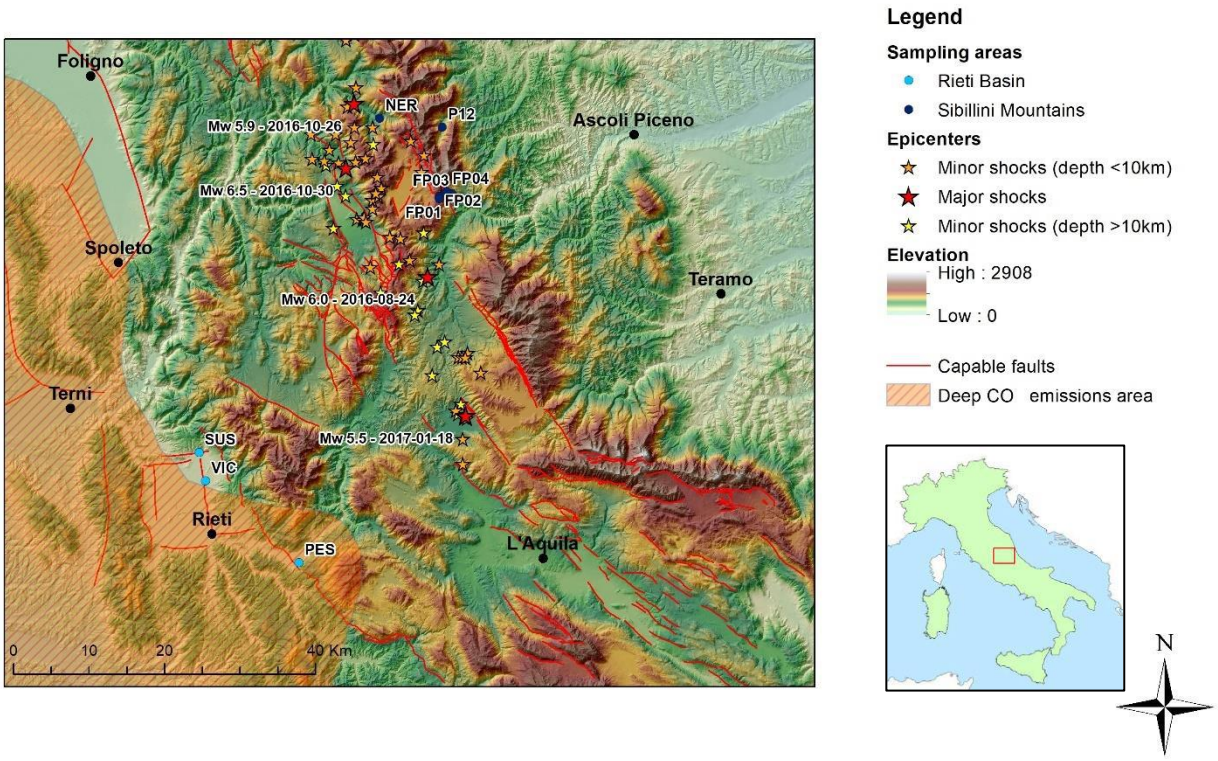

Figure 3.1: study area, including major shocks of the earthquake sequence, and the capable faults (from ITHACA database, http://sgi2.isprambiente.it/ithacaweb/viewer/).GPS coordinates of sampling points in supplementary material Supplementary_07, chapter 9.

3.5.2 Hydrogeological Setting

Sibillini Mountains area

Rocks of the Umbria-Marche succession outcrops in the investigated area. They consist of multiple sedimentary layers from a pelagic environment, which alternate calcareous and calcareous-marly to siliceous lithotypes (Cello et al., 1997). The succession was emplaced over neritic massive limestones, then extensional tectonic movements dismembered them in the middle Lias.

The Nerea spring (NER) recharge area (Figure 3.1) is a major carbonate aquifer within the Umbria-Marche ridge that is characteristic of the central Apennines (Mastrorillo and Petitta, 2014). In these karstic large-area aquifers, faults and fractures within the limestone control flow (Amoruso et al., 2011). The aqueduct flows from the Uccelletto spring, in the Vallinfante springs system, with a discharge measured at 0.57 m^3/s. It is sourced from the Nera-Ussita basal aquifer (Tarragoni, 2006). Pre, co- and post-seismic chemical data was made available from the Uccelleto spring in Castelsantagelo sul Nera through access to the Nerea S.p.A. bottling plant's archived quality control samples.

Other epicentral area springs were analyzed in the Forca di Presta area springs (FP). These springs present fast flow circuits and relatively low flows (around 0.005 m3/s for all the springs) and are located close to the activated fault in the Vettore mountain.

The analyzed well from April 2017 is located in Foce di Montemonaco, an area in the eastern side of the Sibillini mountains. This area is sourced by the eastern Sibillini basal aquifer, which cover about 110km2 of surface (Boni et al., 2010) and is composed by a series of springs outflowing between 830 and 950m a.s.l. with a medium total flow of about 1500 L/s, and part of it (about 530 L/s) are collected with drainage galleries to pipe them in an aqueduct system serving Marche region (Mastrorillo and Petitta, 2010).

Rieti plain Area

The hydrogeological unit (Catena Nuria-Velino-Monte Giano) has an area of about 1200 km^2 and thickness of the carbonate aquifer can reach 3000 – 4000 m (Boni et al., 1986; Celico, 1983; Civita and Fiorucci, 2010). Deep normal faults at the border of the Rieti plain separate the marine Meso-Cenozoic carbonate ridges from Plio-Quaternary continental deposits, as

typical of central Apennine extensional-basins. In this area the regional flow system is hosted by the surrounding carbonate bedrock and springs outflows in contact lower-permeability basin deposits (Martarelli et al., 2008).

Santa Susanna Spring (SUS), supplied by the regional aquifer base-flow, is the spring wtih highest discharge (5.5 m^3/s), and emerges at the intersection of two normal faults at the northeastern edge of the Rieti Plain (Guerrieri et al., 2004). This regional aquifer is hosted in the Terminillo and Reatini mountain carbonates to the east, with infiltration of 545 mm/yr and total recharge area over 300 km2 with main lithology consisting of imbricate thrust carbonates with evaporitic gypsum and anhydrite units in the subsurface (Martarelli et al., 2008; Spadoni et al., 2009). Locally, interbedded Triassic dolomitic limestone outcrops are observed (Martarelli et al., 2008). Water average residence time in the aquifer is about 15-20 years, calculated by aquifer properties values, recharge area extension and Euclidian distance to the spring (Spadoni et al., 2009).

Vicenna Riara Spring (VIC), located inside the Rieti Plain, differently from other analyzed springs, flows mainly from a locally-recharged alluvial aquifer. Water flows to this spring along a buried fault and through preferential flow-paths within the Pleistocene conglomeratic alluvium that lies in the central-eastern part of the plain. This spring has a relatively low discharge (about 0.07 m^3/s), but is the highest discharge alluvially-fed spring in the Rieti Plain (Martarelli et al., 2008).

Peschiera spring (PES) is located about 8 km to the east of the Rieti Plain in the Velino River Valley (Figure 3.1). This spring, with its high flow rate (i.e., 18 m^3/s), represents a major drinking water supply to Rome. The groundwater contribution to the spring is mainly from the aquifer hosted within the uplifted carbonate shelf deposits to the ESE in bedrock consisting of Triassic – Paleocene limestone located in the Giano-Nuria mountains. Two flow paths have been identified to source the spring, with significantly different mean residence times and amounts: 10% of the water has a mean residence time of ~25 – 30 years, and 90% of the water has a mean residence time of thousands of years, both of which contribute to water discharging at the spring (Civita and Fiorucci, 2010).

3.6 Materials and methods

3.6.1 Water analysis and pre-earthquake data collection

Water samples were collected in LPDE bottles and physiochemical parameters (pH, T, EC and alkalinity as HCO_3 by titration) were measured directly on site. Samples were then stabilized and stored refrigerated for laboratory analyses including:

- major ions (Na, Ca, Mg, K, Cl, SO_4) through ionic chromatography;
- trace elements (Al, Cr, Mn, Co, Cu, Ni, Fe, Pb, U, Rb, Sr) were analyzed by Inductively Coupled Plasma -Mass Spectrometry (ICP-MS) to see possible release after the earthquake;
- $\delta^{34}S_{SO4}$ and $\delta^{18}O_{SO4}$ analysis using $BaSO_4$ precipitation;
- $\delta^{13}C_{DIC}$ by precipitation of $SrCO_3$;
- $\delta^{18}O_{H2O}$ using the CO_2 - H_2O equilibration method, and on-line chromium reduction using continuous-flow isotope ratio mass spectrometry for $\delta^{2}H_{H2O}$.

Detailed methods for samples analysis are described in appendix, section 7.

Due to the limited number of samples collected, isotopic analyses were not run on the samples collected in Forca di Presta area, and those include only major ions and trace elements analysis.

For Rieti basin samples, samples were collected starting from 27th August 2016. Pre-earthquake data were collected from a published study and include 4 samples for major ions analysis and a sample for trace element (July 2014, February, May and September 2015; Archer et al., 2016).

Samples from the NER sampling point were collected both directly from the spring and from bottles coming from the bottling plant, to observe possible interferences caused by the bottling process (which mainly consist in a sand filtering). Then, bottles archived in the plant permit us to analyze pre-earthquake values until 2 years before the August shock (Figure 3.2).

3.6.2 Continuous monitoring system data collection and analysis

A Solinst® Levelogger was installed in Foce di Montemonaco locality inside a well on April 2017. This probe registered with a time interval of 20 minutes values for pressure, temperature and Electrical Conducitivity (EC). Also, a Barologger® probe was installed outside of the well to continuously monitor atmospheric pressure, to then used to correct the

measured pressure in the well and calculate water level. Data were downloaded manually, and then hourly and daily means were obtained from the raw data collected (Figure 3.2).

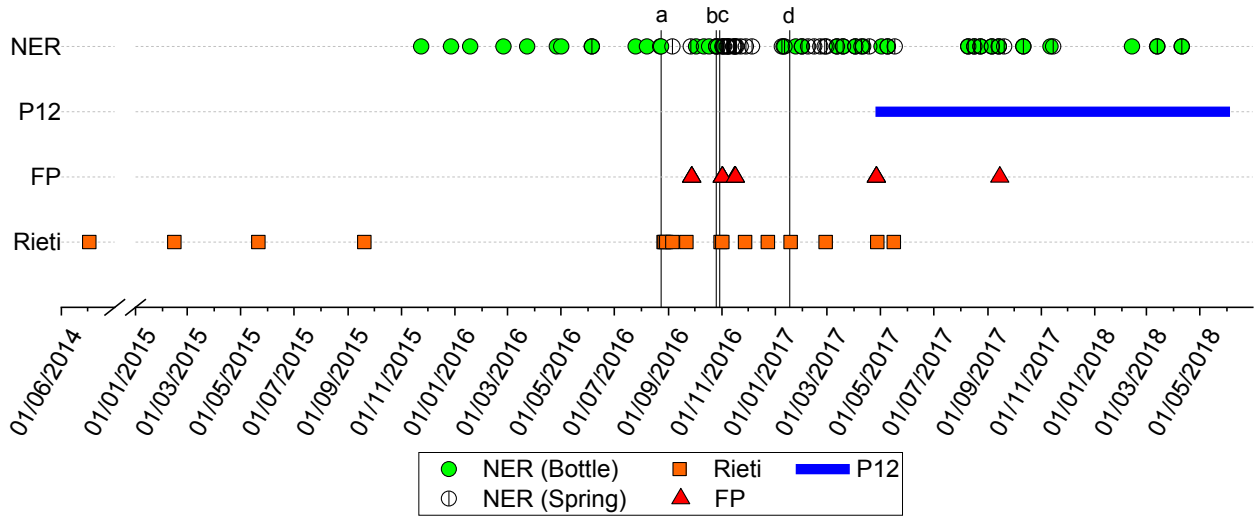

Figure 3.2: Sampling periods (both pre- and post- earthquake) for all analyzed points, vertical lines indicate the major shocks (a: 24th August 2016, b: 26th October 2016, c: 30th October 2016, d: 18th January 2017).

3.6.3 Data analysis

Data analysis was conducted using time series plots to pick up any chemical anomaly that may have occurred during the earthquakes sequence. Afterwards, bivariate correlation matrices and a Principal Component Analysis (PCA) were applied to the dataset to ascertain whether there was a coherent seismic response among the correlated variables. Using correlations between variables it was possible to observed which variables showed same changes possibly related to the mainshocks (Hammond et al., 1981; Hartmann et al., 2005). Chemical data were compared with meteorological (especially rainfalls) and seismic data to check their relevance as drivers of observed chemical variations. Also, to verify the significance of some chemical changes, a binomial test was performed to evaluate if chemical changes did not happen randomly, but where possibly correlated with the mainshocks (Skelton et al., 2014).

Data downloaded from the probe in the P12 well in Foce di Montemonaco were processed to obtain hourly and daily mean of conductivity, temperature and water level. Also, rainfall data were collected from Montemonaco site (7km far from the probe locality) to correlate timing of responses in level. Then, to evaluate possible responses in the Montemonaco probe. We applied a magnitude/distance index to try to weight the possible responses in conductivity or

level recorded by the probe borrowing the following equation from Hammond et al. (1981), used from the authors to normalize Radon anomalies before earthquakes:

$$\frac{M}{D} index = A \frac{\exp(3.4M)}{D^2}$$

where M = magnitude, D = distance between epicenter and sampling point (in km), A = a normalization factor (chosen as 10^{-3} for convenience). We applied a different adjustment factor (10^{-2}), because we did not have as high-magnitude earthquakes as Hammond et al. (1981) during our monitoring time window.

3.7 Results

Results obtained will be organized as follow: firstly, results for Rieti basin and NER spring in the Sibillini mountains will be presented, which present a more complete dataset with an high sampling and consequently high data frequency along the seismic sequence (section 3.7.1), and then main results from the Forca di Presta springs (FP, section 3.7.2) and the monitoring station of Foce di Montemonaco well (P12, 3.7.4) will be presented separately, due to lower sampling frequency and/or different monitoring period from the other monitored springs.

3.7.1 Rieti and Nerea springs

Physico-chemical features

EC values were elevated at SUS, VIC and PES after the 24th August mainshock then decreased over the next two-week period. All four springs were elevated at the onset of sampling after 24th August, into October. After the 30th October mainshock, SUS and PES increase again above the range of pre-earthquake values. NER exhibits an abrupt increase following the near field shocks of 26th October and 30th October and remains elevated until a decrease and return to below reference values by 18th November.

The pH of PES was also within the range of pre-earthquake values for all dates in 2016, but was slightly higher than the pre-seismic range in the February and April 2017 measurements. SUS was slightly elevated after the October event, then decreased and was below the pre-seismic range in February 2017. VIC pH decreases outside of the range of previous values for one sampling, August 30th, then was elevated following the 18th January mainshock. The temperature measured at PES and SUS (detailed data shown in supplementary material Supplementary_02, chapter 9) did not deviate outside the range of previous values during the

post-earthquake time series. The exception was one measurement of PES on 30th August was abnormally high at 15.9°C. The temperature of VIC in all measurements during the post-earthquake time series was 0.4 – 1.0°C higher than the pre-earthquake range.

Major Ions

Most of major ions (i.e. Ca, Mg, NH_4, NO_3, Na, K) show no significant changes throughout the pre-, co- and post-seismic time periods, and both F, PO_4 and NO_2 were below the LOD in most of the samples analyzed (Supporting Information a). Concentrations of SO_4 show no change at VIC, but at PES and SUS there is an abrupt increase after the August earthquake. The alkalinity at SUS and VIC returned to pre-earthquake values by 26th October, becoming elevated again in January 2017. PES values remain elevated until returning to pre-earthquake range by 17th May 2017 (Figure 3.3).

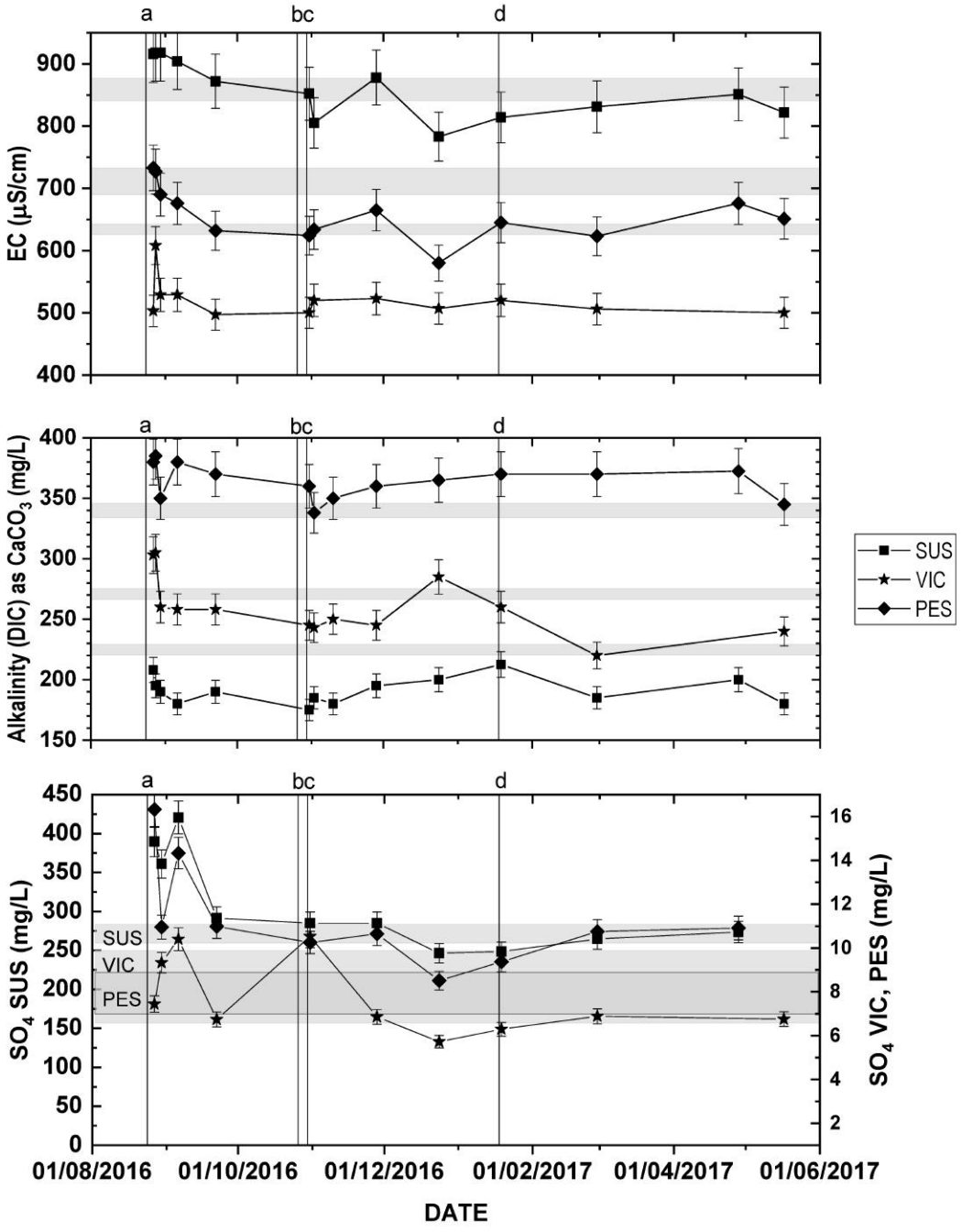

Figure 3.3:EC, alkalinity and SO_4 trend along the seismic sequence for Rieti springs, vertical lines indicate the major shocks (a: 24th August 2016, b: 26th October 2016, c: 30th October 2016, d: 18th January 2017).

NER do not show relevant changes in major ions too, and neither in electrical conductivity, but alkalinity in this spring increased sharply after the near –field shocks of 26th October and 30th October, peaking on 8th November 2016. Both EC and alkalinity show only minor variability after the 18th January 2017 earthquake.

This is followed by a decrease until reaching pre-earthquake concentrations in ca. 3 months, showing a similar trend as trace elements (see below).

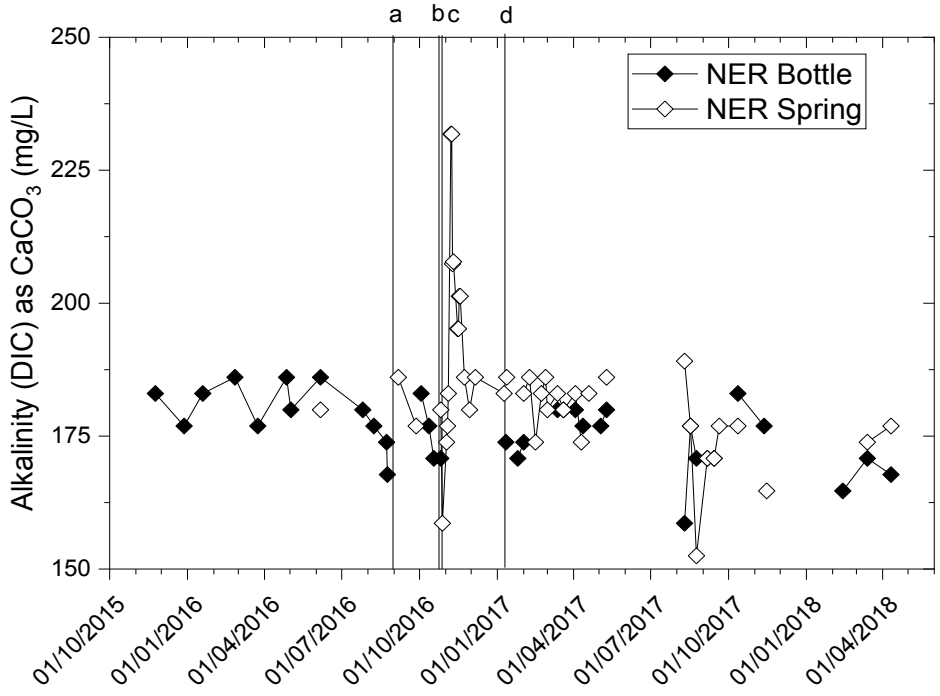

Figure 3.4:alkalinity values for NER samples collected from the bottling plant and directly from the spring, black vertical lines indicate the major mainshocks (a: 24th August 2016, b: 26th October 2016, c: 30th October 2016, d: 18th January 2017).

Trace Elements

Figure 3.6 shows concentrations of representative trace elements (Al, Cu, Pb, Sr, Rb, Mn) in time series for all sampled Rieti springs. Other trace elements (Cr, Co, U, Fe, Ni) not displayed in Figure 3.5 also show similar trends, while elements representing possible interaction with deep fluids (Li, B) did not show significant changes. A significant number of trace elements (Al, Cu, Pb, Sr, Rb, Mn, Cr, Co, U, Fe, Ni) in the three Rieti area springs show elevated concentrations following the 24th August 2016 earthquake, when compared to pre-earthquake values measured from the September 2015 samples (Figure 3.5). For Al, Fe, Ni, Cu, Cr, Mn, Pb, U the null hypothesis of the binomial test could be rejected with p value < 0.001. Two exceptions to this pattern are Rb in SUS and Sr in VIC. The concentrations of Al, Mn, Pb, Co, Fe and Ni in the Rieti springs were strongly correlated, with Pearson correlation coefficients >0.9 (Supplementary material, chapter 9). The trace elements at PES showed two

main peaks in concentration concurrent with the August and October mainshocks, with a smaller peak above pre-earthquake values at the January mainshock. At SUS, the peak concentrations occurred after the 24th August mainshock, then concentrations gradually decreased over the sampling period. Rb and U were highly correlated at all springs and exhibited a slight peak in concentration following the 24th August mainshock (Rieti springs), with a gradual decrease over the rest of the time series. PES values of these elements peaked during the August. sampling then again at the 31st October sampling. Sr concentrations are high after the 24th August event but do not show major change after the 30th October event, then increase again at the end of the sampling (February, April 2017) in PES and SUS. Li and B, instead, did not vary significantly along the sequence. (Figure 3.5).

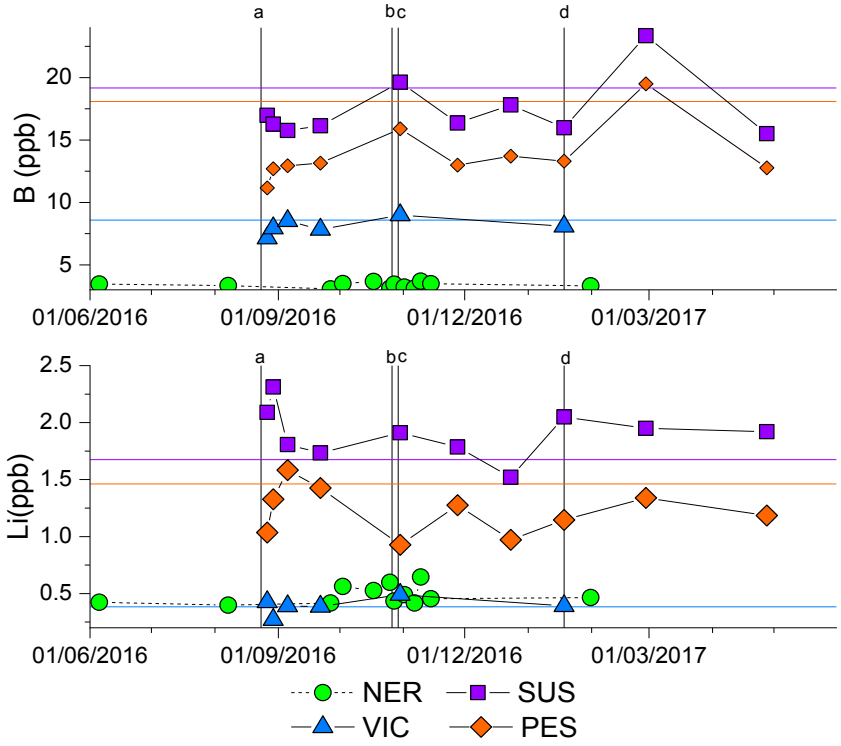

Figure 3.5: Li and B trend along the seismic sequence in Rieti springs and NER. vertical lines indicate the major shocks (a: 24th August 2016, b: 26th October 2016, c: 30th October 2016, d: 18th January 2017), while horizontal colored lines indicate pre-earthquake values for Rieti springs

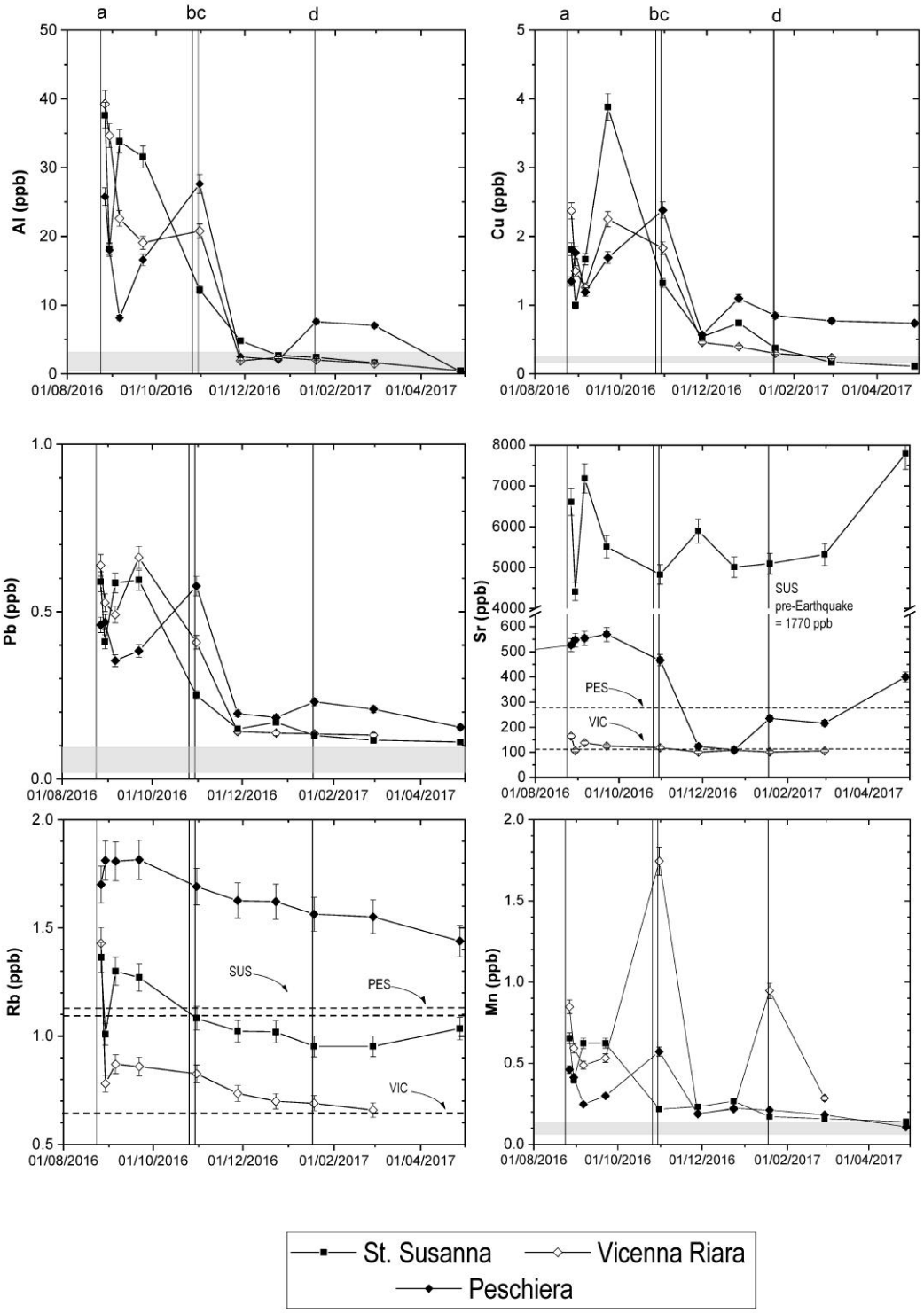

Figure 3.6: temporal trend of some of the analyzed trace elements along the seismic sequence in Rieti springs, vertical black lines indicate the major shocks, and shaded horizontal lines represent pre-earthquake values (a: 24th August 2016, b: 26th October 2016, c: 30th October 2016, d: 18th January 2017).

Similar trend for trace metals was observed in NER, but the main response was observed after the 31st October shock, and the values reach pre-earthquake concentration with a faster rate than in Rieti springs. Al, Cu, Pb and Ni concentrations in NER also exhibited minor peaks during mid-November as well as mid-January, prior to the 18th January mainshock (Figure 3.8), while Sr, Li and B concentration did not show significant variability (Figure 3.5). Al, Fe, Ni, Cu, Cr, Pb the null hypothesis of the binomial test could be rejected with p value 10^{-9}. Also, differences between the archived bottle samples provided from the bottling plant and water collected from the spring are small. This result is significant because the bottled samples were filtered through sand. It appears that the sand filter did not significantly impact the elemental data, so the samples for both NER spring and the bottling plant can be interpreted together. As an example, Figure 3.7 reports linear correlations between samples bottled and collected at the spring concentrations of some elements.

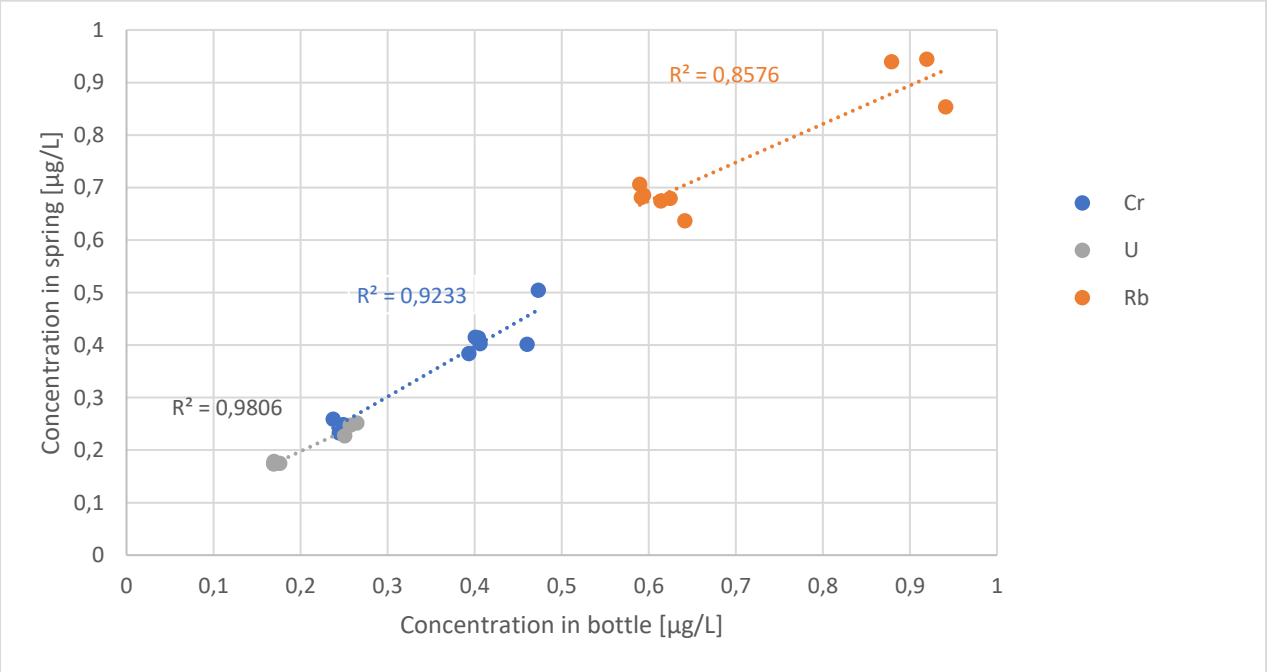

Figure 3.7: correlations between bottled and spring samples concentrations for U (in grey) Cr (in blue) and Rb (in orange) in Nerea.

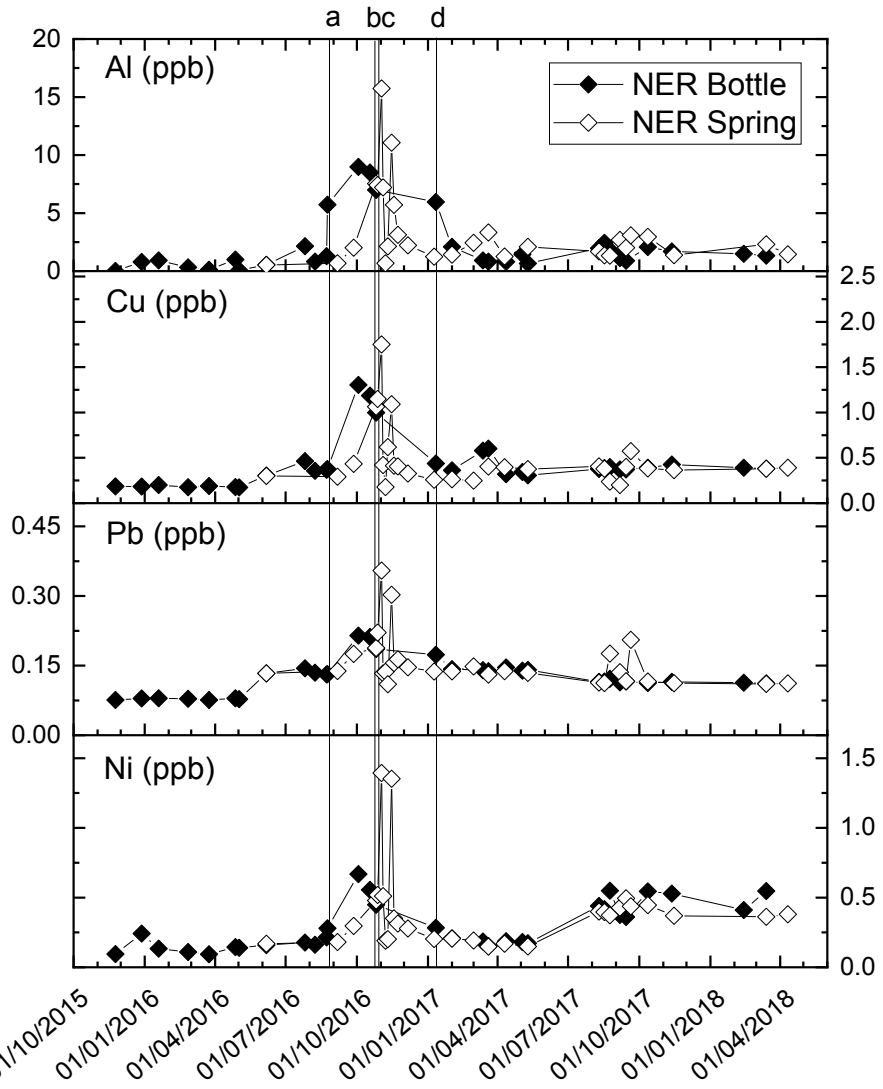

Figure 3.8: Al, Cu, Pb and Ni concentrations for NER samples collected from the bottling plant and directly from the spring, black vertical lines indicate the major mainshocks (a: 24th August 2016, b: 26th October 2016, c: 30th October 2016, d: 18th January 2017).

Stable Isotopes

The $\delta^{13}C_{DIC}$ values (Figure 3.9) of SUS become 1-2‰ enriched above pre-earthquake samples during the August and September samplings. The 31st October and 10th November samples then showed enrichments up to 6‰ greater than before the earthquakes. Values of $\delta^{13}C_{DIC}$ for PES also show enrichment above the range of previous values following the 24th August earthquake, then remain enriched during the post-seismic time series. The most enriched value of $\delta^{13}C_{DIC}$ at PES occurs on 31st October. Values at VIC are slightly heavier than pre-earthquake values and enriched in the November sampling dates following the October

mainshocks. The three pre-earthquake samples at NER are all from 2016, with $\delta^{13}C_{DIC}$ values between -10 and -12‰. The post-earthquake sample values are also within this range except for those within the days following the October mainshocks, where $\delta^{13}C_{DIC}$ values become up to 5‰ more negative. After a t-test evaluation of pre- and post- earthquake data, only PES and SUS data showed a significative statistical difference ($p<0.05$) after the mainshocks.

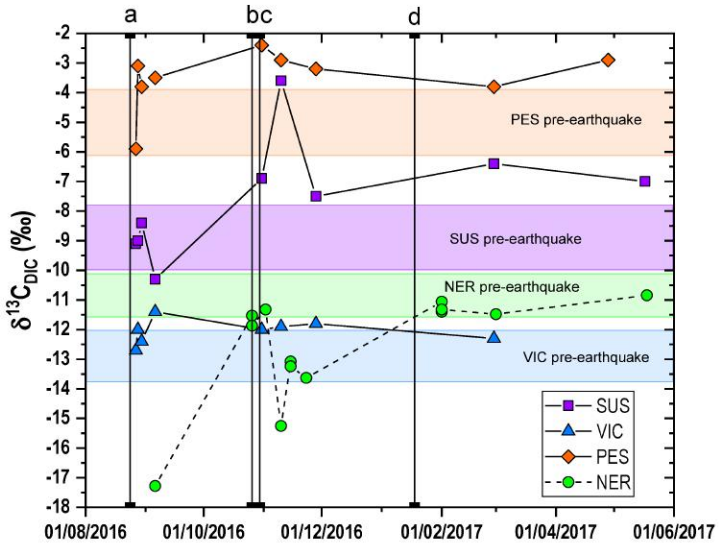

Figure 3.9: carbon 13 isotopic ratio along the seismic sequence for Rieti and NER springs, black vertical lines indicate mainshocks (a: 24th August 2016, b: 26th October 2016,c: 30th October 2016, d: 18th January 2017).

Values of $\delta^{18}O_{H2O}$ and $\delta^{2}H_{H2O}$ are plotted with the global meteoric water line, Mediterranean meteoric water line, and the central Italian meteoric water line in Figure 3.10. The values of VIC, SUS, PES and NER do not change significantly post-earthquake as compared to pre-earthquake value ranges. The pre-earthquake values were collected in all seasons and do not exhibit significant seasonal variability during the years sampled. However, the isotopic values demonstrate that recharge elevations for the springs vary from relatively low elevation at VIC, to recharge elevations >1400 m for NER springs (Figure 3.10, details on isotopic analyses in supplementary material Supplementary_03, chapter 9).

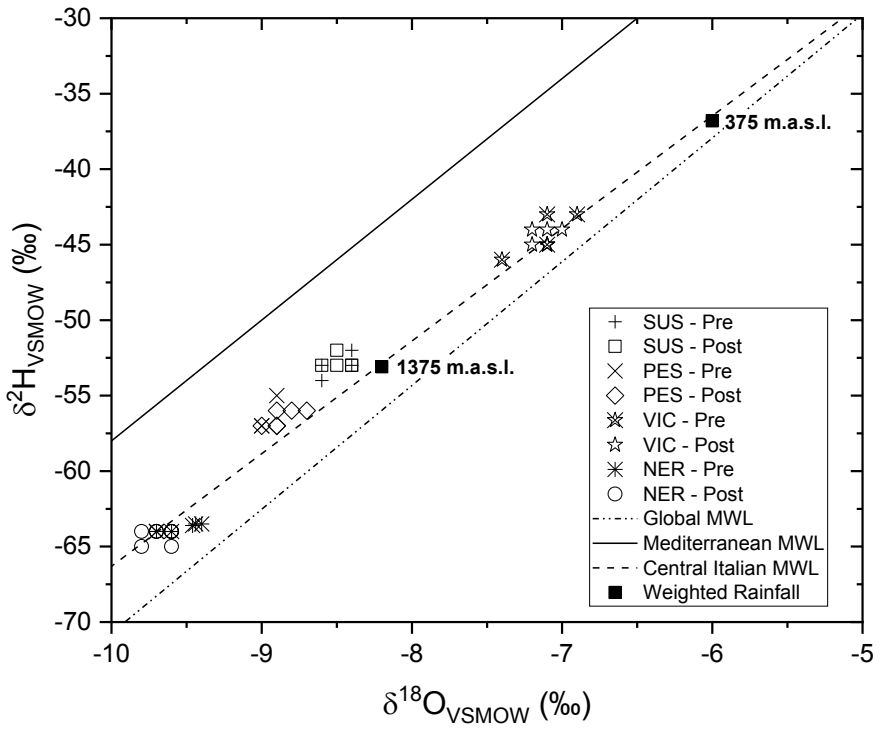

Figure 3.10: Stable isotopes of water from springs pre-earthquake and post-earthquake compared to global, central Italian, and Mediterranean meteoric waterlines: GMWL, cIMWL, and MMWL, respectively. Equations for CIMWL is from Longinelli and Selmo (2003) and rain-gauge measurements at two elevations in the central Apennines (375 and 1,375mabove sea level) is from Spadoni et al. (2009)

3.7.2 Forca di Presta samples

Forca di Presta samples (FP) results will be presented differently from the others, because the low sampling frequency does not permit to treat the data in a statistically significant way through the PCA, and so only peculiar trend of single elements after the main shocks can be discussed.

Only 4 samples from September 2016 until April 2017, but part of the analyzed PTEs show a change possibly ascribable as a seismic response after the October shocks (Figure 3.11).

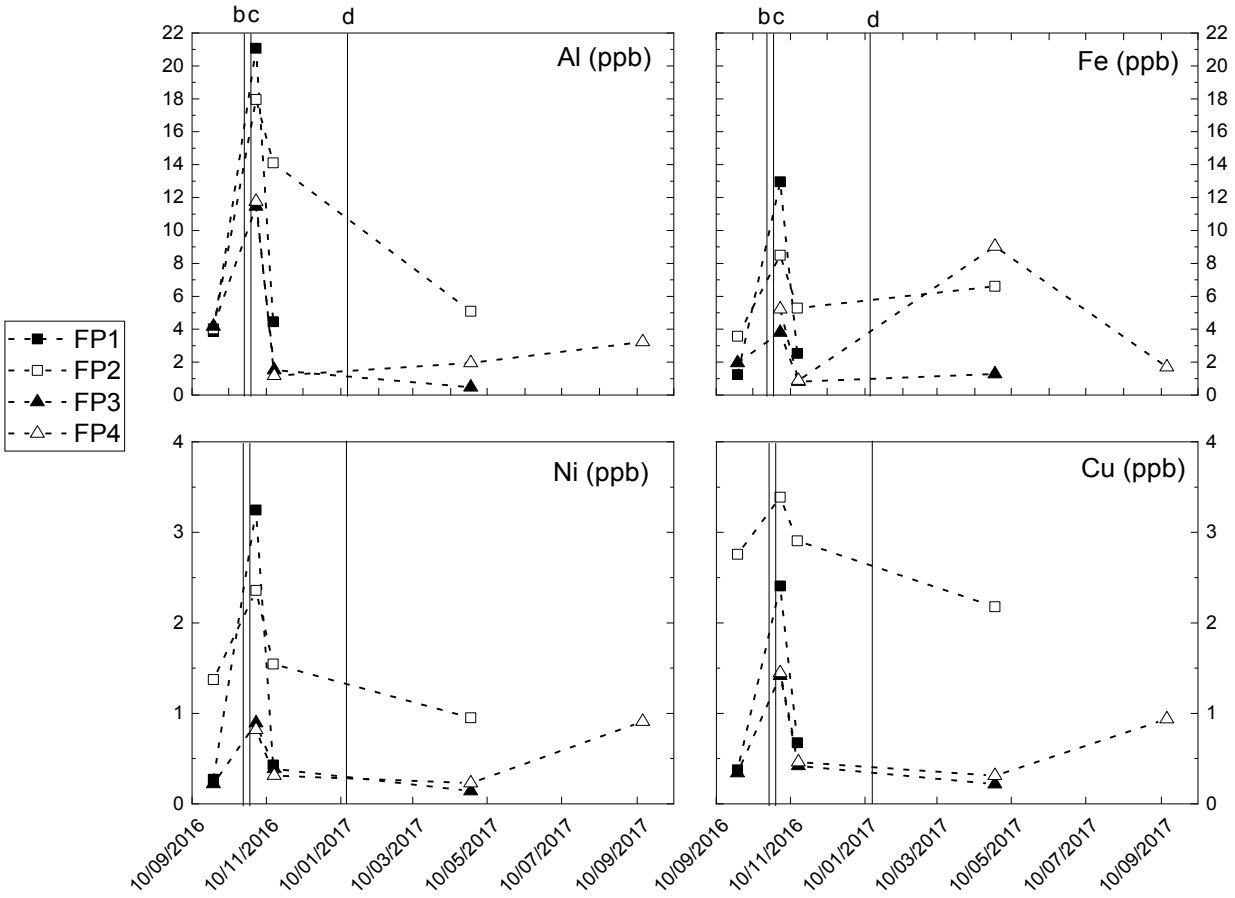

Figure 3.11: Al, Fe, Ni and Cu concentrations (in micrograms per liter) in the Forca di Presta springs along the seismic sequence (mainshocks are indicated on graph with vertical lines, b: 26th October 2016,c: 30th October 2016, d: 18th January 2017).

3.7.3 Multivariate analysis results

Principal Component Analysis (PCA) was performed selecting the springs and period presenting a major number of samples and most variables analyzed, so only Rieti springs and Nerea spring were analyzed with a time span covering the period August 2016-June 2017 for post-earthquake samples, and all pre-earthquake data available for these springs. The trace element and major ion concentration data shows negative loading values for the component 1, which explains ~42% of the total variance. Also, observing component 1 and 2 plot, some trace elements (Ni, Cr, Pb, Al, Cu, Fe) plot separately from the elements typically dissolving from carbonates (Ca, Mg, Pb, Sr, Rb, U; Figure 3.12).

Like the individual time series plots of metals (Figure 3.6), the first component score values plotted in time series, for NER spring and bottle samples (Figure 3.12) show a strong increase in concentration and score values after the 26th October shock then unstable for about 2 months until January 2017, reaching values close to the pre-earthquake ones.

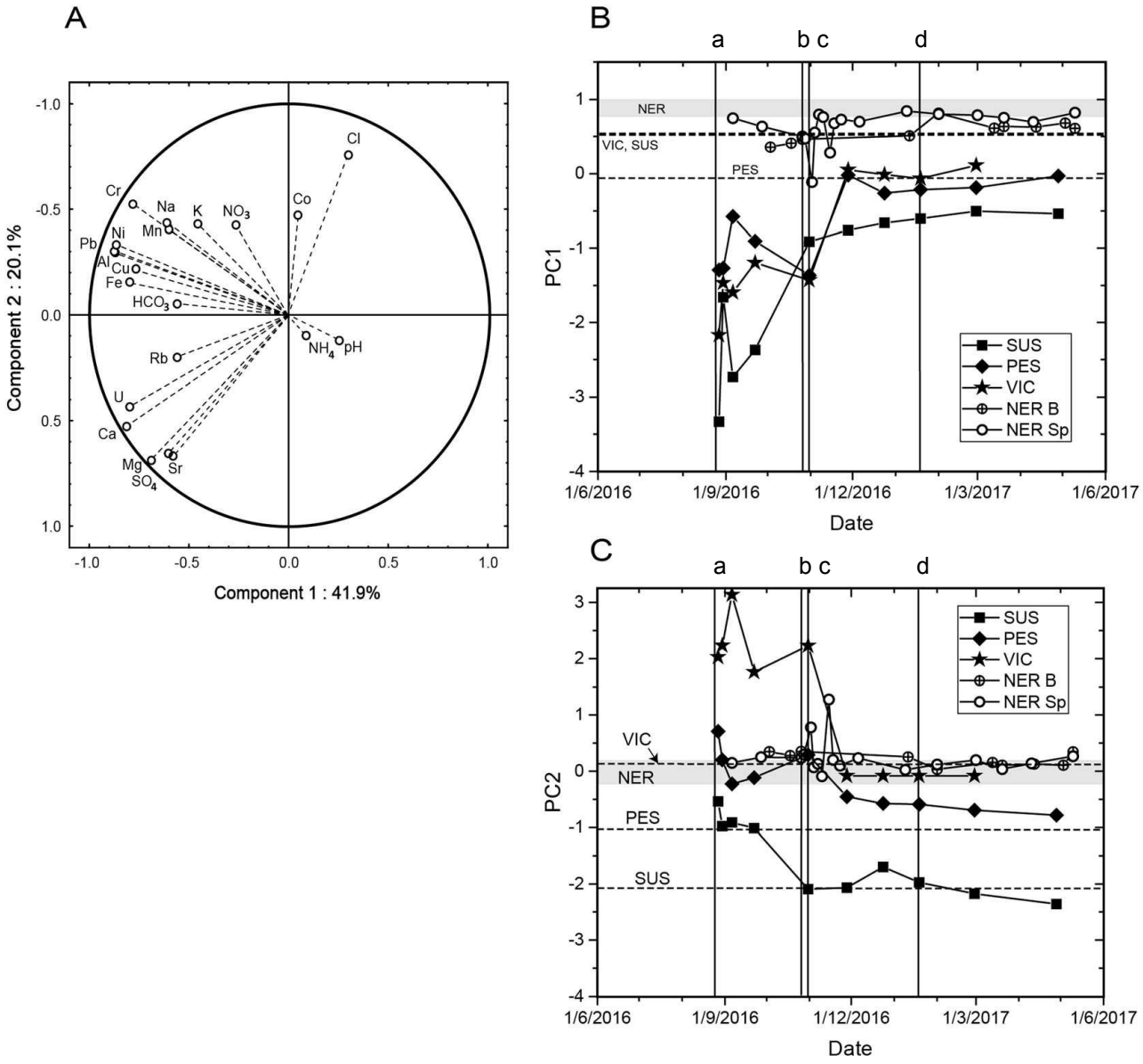

Figure 3.12: (A) PCA loading plot for components 1 and 2 (explaining 62% of the total variance). Metals as Pb, Al, Ni, Cu, Cr, Mn, and Fe are highly correlated in all the springs. (b) Time series of PC1 showing variance over time in relation to the major earthquakes (black vertical lines; a: 24th August 2016, b: 26th October 2016,c: 30th October 2016, d: 18th January 2017) higher numbers show more variance. (c) Time series of PC2 variance in relation to the major earthquakes (black vertical lines). The spring and bottling plant samples are separated here into NER B for bottling plant, and NER Sp for samples from the spring.

A time series plot of component 1 of the Rieti area springs shows that the strong release of metals occurred mainly after the 24th August shock, with some variation in the recovery

between the three springs (Figure 3.12). Similar to the NER samples, the scores return to baseline values that are near those observed prior to the earthquake. Moreover, Rieti springs show scores values larger than NER. This is due to higher constituent concentrations for the metals in Rieti springs, compared to NER.

The PCA also shows that ~20% of the total variance can be explained by Component 2 (Figure 3.12). This variance divides the elements into 2 groups; Sr, SO_4, Mg, Ca, U, Rb with negative loadings, and Fe, Cu, Al, Pb, Na, K, NO_3, Cl, and Co with positive loadings. Alkalinity (HCO_3) has a loading value of the two components which plot this variable between the two groups. Overall, NER samples don't show much variability in component 2 scores, so this response is reflective of the Rieti area springs only. When component 2 is plotted in time series for the Rieti samples (Figure 3.12) there are lower score values following the 24th August event, reflective of increased concentrations of Sr, U, Rb, Ca, Mg, and SO_4.

NH_4 and pH show little variation and do not show any correlation with other major or trace elements (Figure 3.12).

3.7.4 Continuously monitored physico-chemical features

Data downloaded from the probe in Foce di Montemonaco are shown in Figure 3.13.

Electrical conductivity (EC) showed an interesting pattern that may be seismically related in the period April- July 2017. In fact, after the shocks presenting major values of magnitude/distance index, changes in conductivity usually happens few days after, and do not correlate with precipitation data.

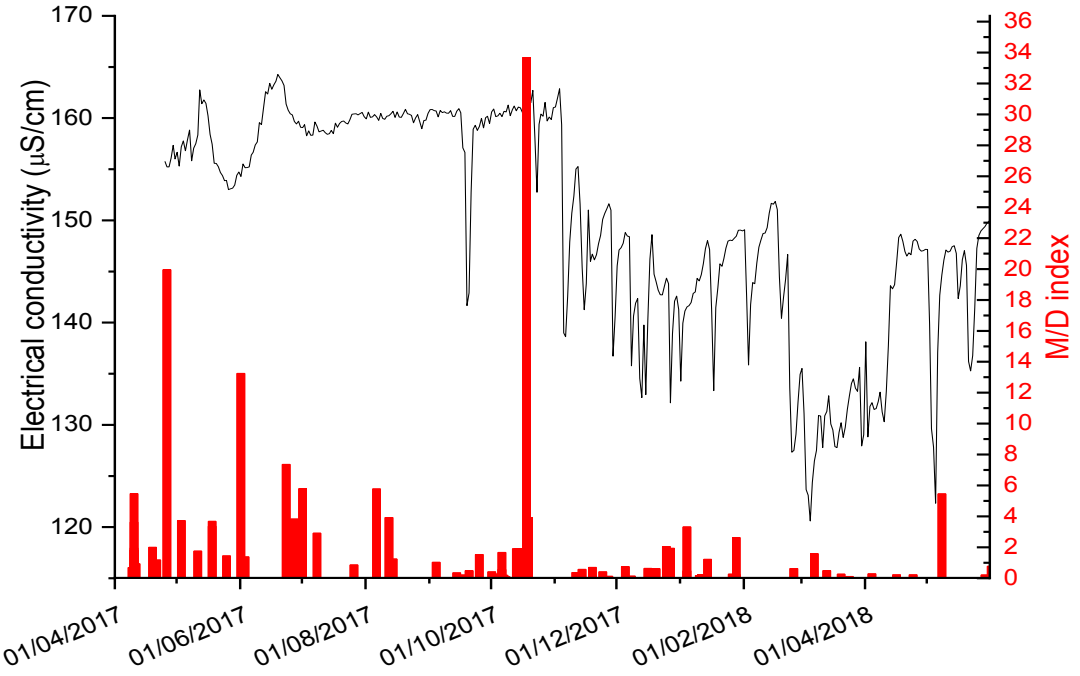

Figure 3.13: electrical conductivity (EC, black line) and magnitude/distance index for all shocks happened (red bars, data on shocks epicenters and magnitude are obtained from ISIDE dataset, http://cnt.rm.ingv.it/iside)

Also, the decrease in level from May 2016 until November 2017 leave us some doubt about a possible response due to a change of flow path after the October shocks. These changes, in fact, did not correlate with changes in EC as happens in the period after November 2017. Also, as observable in Figure 3.14, the level shows a decrease which not correlate with precipitation data collected in Montemonaco (4km far from the probe location), while peaks in level seems to better correlate with rainfall periods after winter 2017-2018. These observations can arise new questions to answer regarding: possible responses to seismicity in EC even after relatively low magnitude events, and possible permanent responses in groundwater level and water flow after the mainshocks, but more data are needed to understand if these changes implicates a definitive change in the level baseline. Daily mean data collected with probe are included in supplementary data Supplementary_05, chapter 9.

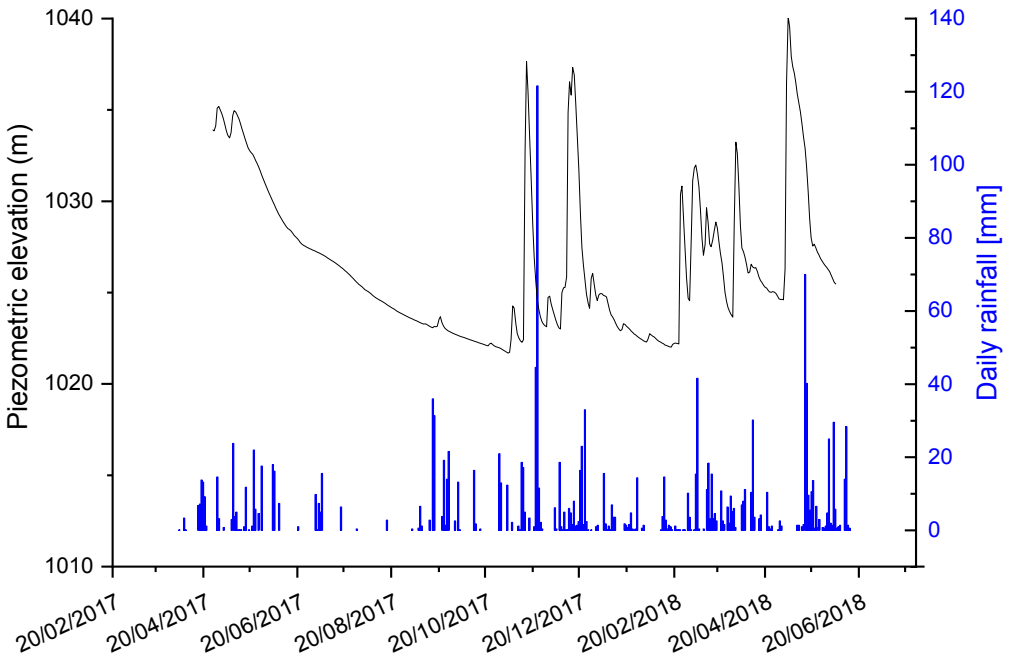

Figure 3.14: piezometric elevation in Foce di Montemonaco (black line)and rainfall data from the Montemonaco station (rainfall data from Marche region monitoring system, http://app.protezionecivile.marche.it/sol/login.php?lang=it)

3.8 Discussion

3.8.1 Natural Variability and background concentrations

To assess whether seismic shaking or changes in pressure, fluid flow, or release of new sources of water to the aquifer caused the changes in groundwater chemistry observed after the earthquake sequence, firstly the natural variation mainly caused by winter precipitation should be evaluate. Previous work on the recharge and discharge processes of SUS and PES springs estimate aquifer mean residence times on the order of 15 – 35 years.

These calculations, however, do not reflect the dual-flow nature of these aquifers, where basal spring discharge contains a mixture of water from the fast (on the order of days), and slow (on the order of years to tens of years) flow paths (Amoruso et al., 2011; Nanni and Rusi, 2003; Petitta et al., 2011). The precipitation patterns characterizing this region predict that the majority of aquifer recharge occurs in the wetter winter months. The Apennine snow pack is between 1 and 3.5 m, on average, and the snow cover usually last less than 100 days, excluding only the highest peaks (Costantini et al., 2013).

To test that the seasonal recharge from snow melt was not influencing the observed hydrochemical trends in these springs, the fastest possible recharge to discharge flow path (i.e. days) was considered in testing for trace element concentration correlation with each other and with precipitation amounts during the month prior to sampling. The amount of precipitation between samplings does not correlate with measured trace element concentrations, indicating that water recharging between an earthquake event and water sampling at the spring did not influence these measurements (correlation tables in supplementary material Supplementary_04, chapter 9). The Fe concentration in PES is negatively correlated with precipitation. This could be caused by a change in redox conditions after oxygenated snow melt, which could make reduced iron to drop out of solution. However, this is the only spring and only element having a correlation with precipitation, and other redox sensitive elements (Mn, Cr, As, Se) do not react the same way.

3.8.2 Response evaluation: changes and timing

Lack of changes of major ions and water isotopes

Generally, significant changes in most of major ions were not detected during the earthquake sequence. Only some constituents (such as Mg, SO_4, and HCO_3) rose in the Rieti area springs, particularly after the 24th August 2016 earthquake (Figure 3.3). The only major component which showed a significant change along the sequence is SO_4 at SUS and PES, its concentration, in fact, almost doubled after the 26th August shock (Figure 3.3), followed by a slighter increase of Ca and Mg. The high concentration of SO_4 could reflect the addition of low flow water having contact with gypsum, which is dominant in the rocks that contribute to these springs. VIC showed few changes too, indicating a possible sourcing from gypsum bearing strata. However, this spring presents pre-earthquake variability close to the post-earthquake response, so may not uniquely be tied to seismicity (Figure 3.3),while NER spring presents low concentrations of SO_4 in the spring and low responses, which reflect the scarce presence of gypsum in the Sibillini area, and geologic cross sections indicate evaporitic beds are only found at considerable depth (Fusari et al., 2017).

Alkalinity also rose slightly after the August earthquake at VIC, and PES and stayed high at PES until sampling stopped. At NER alkalinity rose only after the October earthquakes. The likely reason for the NER response being confined to the October earthquakes is that NER shows a

weak intermediate-field response to the August event, but a strong near-field response to the October events.

The slight change in the major element chemistry indicates possibly a lack of mixing of other water source, and if mixing with water occurred, the new source of water had either a small volume or a similar composition to the aquifer water. Lack of significant changes between the pre- and post-earthquake values of stable isotopes of water for any of the springs (Figure 3.10) are consistent with a lack of mixing, unless the waters mixed shared the same recharge elevation.

The values of $\delta^{18}O_{H2O}$ and $\delta^{2}H_{H2O}$ in Central Apennine groundwater are primarily controlled by recharge elevation (Longinelli and Selmo, 2003; Petitta et al., 2011). Hydrochemical responses have been observed in different settings that include post-seismic changes in $\delta^{18}O_{H2O}$ and $\delta^{2}H_{H2O}$ groundwater values. These changes have been attributed to aquifer breaching causing a change in aquifer structure or mixing of different groundwater components (Barbieri et al., 2005; Claesson et al., 2004; Reddy et al., 2011; Skelton et al., 2014).

The lack of a change in water isotope values of PES, SUS and VIC post-earthquake (Figure 3.10) supports the assumption that increases observed in groundwater chemical constituents are a result of processes occurring within the aquifer instead of addition of water from another aquifer or from a geothermally heated source, which would have a different isotopic composition. The residence time in these aquifers is sufficiently long so that aquifer flow path changes would not be evident in the $\delta^{18}O_{H2O}$ and $\delta^{2}H_{H2O}$ values until several years after the seismic sequence, if at all, especially because both SUS and PES are basal springs and represent an integration of flow within the aquifers (Civita and Fiorucci, 2010; Spadoni et al., 2009). This intra-annual stability is also displayed by the lack of variation in $\delta^{18}O_{H2O}$ and $\delta^{2}H_{H2O}$ during the pre-earthquake sampling period (2014-2015, Figure 3.10).

Trace elements changes

Differently from major ions, trace elements show different changes. This is true especially for all Rieti springs show the greatest change in trace element composition after the 24th August 2016 earthquake and most trace elements remained elevated until after the October 26th and 30th, 2016 earthquakes. Most trace elements returned to background concentrations by the end of November 2016, and were not greatly affected by the 18th January 2017 earthquake,

except Mn concentrations that appear to increase after each earthquake in VIC. Trace element concentrations at NER rise and return to pre-earthquake concentrations by the end of November, similar to Rieti Springs (Figure 3.6). Also, Forca di Presta springs show a slight increase in part of the trace elements showing changes along the seismic sequence, and as NER spring, show a response after the 26th October shock (Figure 3.11).

The concentrations of Rb, Sr, and U do not show the same progressive decrease over the time series as the other elements, but remain elevated above 2015 values for the entire sampling. Rb, Sr and U are likely to substitute for Ca or Mg in the calcite or dolomite crystal lattice and so are likely associated with the carbonate rocks that dominate these aquifers. The other trace elements, in contrast, are more likely associated with clays and organic colloids in the slow-moving fractures and pore spaces. PCA analyses show that Rb, Sr, U, SO_4, Mg and Ca group in same quadrant of the diagram, while all other trace and major elements plot in a different quadrant (Figure 3.12), likely associated with clay minerals.

Conversely, elements as Li and B did not show significant changes along the whole time series (Figure 3.5).

Thus, the temporary increase in trace elements in the aquifer, has implications for providing water to earthquake survivors immediately after earthquakes. Although the trace element concentrations in this study are not above drinking water standards, in places where background concentrations are higher, water supplies could be significantly affected for months after a strong earthquake.

Causes for different responses between the springs

Variability in response among measured trace elements and measured springs could also be due to the properties of the elements such as redox potential or sorption (Drever, 2005) or their abundance in the different aquifers. An example from Al concentration, affected by clays distribution in aquifers (Morgantini et al., 2009), which show high concentrations in VIC, with recharge and discharge occuring in a thick alluvial unit (Martarelli et al., 2008), can be attributed to more available clays within the pore matrix that can be released from co-seismic shaking. Also, Fe and Mn concentrations increasing in VIC may be related to release of more reduced water trapped in isolated pores and fractures.

The difference in response between the NER, the FP and Rieti springs may be related to their location in relation to the major earthquake epicenters (Figure 3.1). As mentioned above, the October earthquakes were centered much closer to NER and FP springs than either the August or January earthquakes and so the response for the August earthquake (which was closer to Rieti springs) may have been delayed at NER. The lack of response to the 18th January 2017 earthquake at all springs sampled, may be because it was the furthest away from all the springs sampled (Figure 3.1), more than 20 km for all sites.

3.8.3 Mechanisms for Transient Increases in Dissolved Ion Concentrations

Various mechanisms have been proposed for transient increases in dissolved ion concentrations after seismic events were partially discussed in section 3.1 and Table 3.1, and are summarized by Ingebritsen and Manga (2014). Fractures clearing and slow-moving water in pore spaces has been invoked in Turkey and Italy after major earthquakes (Galassi et al., 2014; Pasvanoglu et al., 2004). The movement of deep-seated geothermal water has been proposed in Italy (Barberio et al., 2017), and finally dilation of stressed aquifers and mixing with other fluids has been proposed in Iceland (Skelton et al., 2014).

The lack of consistent major element changes and changes in pH, the lack of change in the stable isotopes of water, and the lack of any influx of geothermal indicators (Li, B), as well as the increase immediately after the first mainshocks of the trace element concentrations, indicates that at least in the Rieti and Sibillini Mountains areas, deep-seated geothermal fluids located kilometers below the surface could not be the main drivers of the observed transient changes.

However, the Rieti springs show a component of seismically associated deep-gas release from geothermal or magma sources associated with magma chambers located at depth, as seen in the post-earthquake enrichment of $\delta^{13}C_{DIC}$.

The general stability of the stable isotopes of water and major ions in all springs sampled during the central Italy 2016-17 seismic sequence suggest that possibly the mechanism causing hydrogeochemical responses happened internal to the aquifers, without the effect of deep fluids interactions. Although the change in $\delta^{13}C_{DIC}$ in two of the Rieti springs indicates the possibility of deep gas contributions, fluid flow of deep-seated geothermal fluids to the springs was not observed in the data. The data from the springs sampled indicates that

fracture clearing and shaking of fluids from isolated pores dead-end karstic pore spaces is the likely mechanism for the observed changes (Figure 3.15). This mechanism was also proposed by Pasvanoglu et al (2004) after the Mw 7.4 Marmara earthquake (17th August 1999) in Turkey. They saw minor transient changes in flow, turbidity, and major element composition (trace elements were not analyzed) in karst marble aquifers used for water supply and suggested that shaking and fracture clearing was the reason for these transient changes. These data indicate the importance of local fracture clearing and pore fluid expulsion as the likely mechanism for transient changes in carbonate aquifers after earthquake events, and more collection is needed to confirm the hypothesis. In addition, shaking and fracture clearing results a mechanism to consider even in other rock types affected by earthquakes.

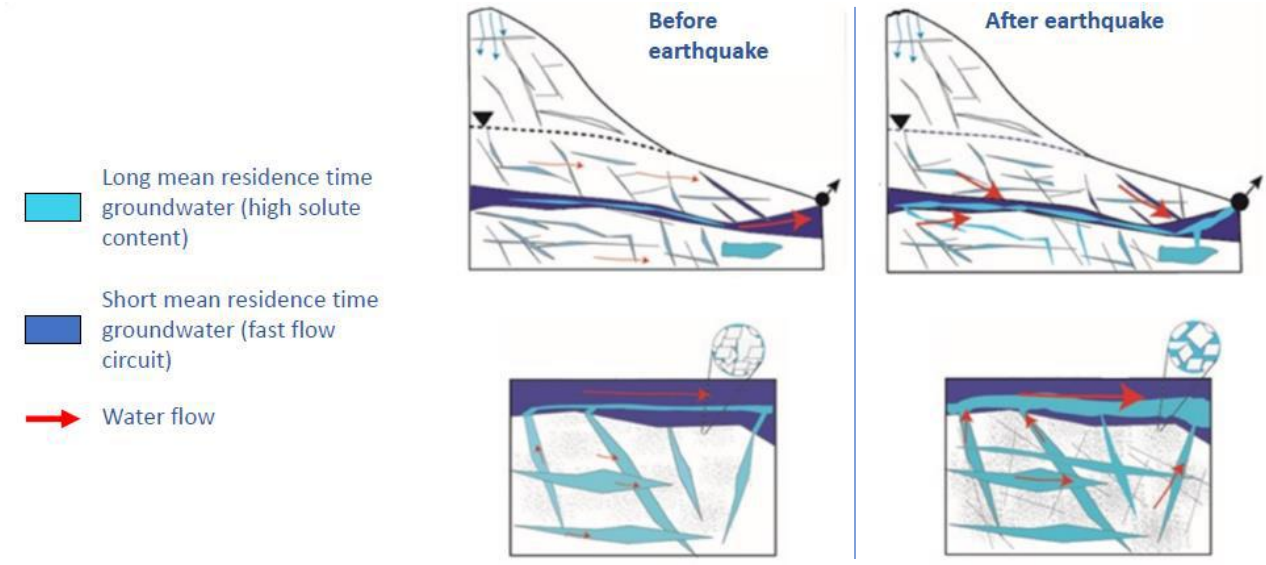

Figure 3.15: conceptual model of the PTEs release after the shock due to shaking, an increase in flow and water conductivity after earthquake increased the dispersion of deep seated high enriched water.

The proposed mechanism for the greatest change in trace element concentration occurring after the first earthquake and diminishing after the October earthquakes, is that the first event effectively cleared, or flushed out, the pore spaces or fractures where longer mean residence time groundwater collected (Pasvanoglu et al., 2004), and none or less longer-residence time water was available for release after following mainshocks (Figure 3.15). Another mechanism which could also be involved include the exposure of fresh rock caused by earthquake pressure and microfracturing, which could enhance water-rock interaction and metals dissolution. PTEs as the one observed with anomalous concentration, in fact, are generally

first elements to be released, because they do not fit well in the mineral lattices of carbonates (Seewald and Seyfried, 1990).

The primary source of dissolved inorganic carbon (DIC) in these aquifers is dissolution of carbonate rock along flow paths, organically-derived soil CO_2 dissolved during infiltration (~-15 – -30‰), and/or CO_2 dissolved in mineralized water with a deep-flow circuit and longer mean residence time (Chiodini et al., 2004, 2000). The $\delta^{13}C$ of the carbonate platform comprising Mt. Terminillo and the Reatini Mountains ranges from ~ +2‰ to +3‰, while in the north, near Nerea, carbonate $\delta^{13}C_{DIC}$ range from ~+2‰ to +3.5‰ (Morettini et al., 2002). The contribution of carbonate dissolution to $\delta^{13}C_{DIC}$ in this region is 2.21‰ ± 0.66‰. The range of $\delta^{13}C_{DIC}$ in central Apennine groundwater containing mantle-derived CO_2 (Figure 3.1), calculated using a carbon mass-balance together with isotopic and hydrogeological data, is -5‰ to -1‰ (Chiodini et al., 2004, 2000). The post-mainshock $\delta^{13}C_{DIC}$ values measured in this study (-5‰ to -3‰, Figure 3.9) fall within this range of previously calculated groundwater with a contribution of mantle-derived CO_2. Also, another explanation includes the contribution of groundwater from longer residence time reservoirs, flow paths, or matrix porosity with a greater degree of water-rock interaction and marine carbonate isotopic signature could have caused this shift to heavier $\delta^{13}C_{DIC}$. The rapid onset of the carbon isotope enrichment suggests multiple drivers of the observed post-seismic $\delta^{13}C_{DIC}$ increase. As suggested by Chiodini et al. (2004), the high pore-pressure from mantle-derived CO_2 gas in these deep reservoirs may have instigated the fault rupture of these earthquakes and released CO_2.

However, at VIC the $\delta^{13}C_{DIC}$ did not change significantly from pre-earthquake values, which is expected at a spring sourcing an aquifer that lacks extensive faulting and connection to a deeper flow circuit.

NER spring present a lighter isotopic DIC after the earthquake, with an opposite effect. The position of this spring in the eastern part of the Apennines, without deep CO_2 source beneath the aquifer can be the cause of this different response (Figure 3.1; Chiodini et al., 2004). The shift to lighter values may be caused by ground shaking and increased flow to NER spring induced more locally derived soil CO_2 to be released into the groundwater.

Assuming the conceptual model as the reason of metals dissolution, possible responses were also observed to lower seismicity in order of magnitude, as happened in P12 well (Figure 3.13).

In fact, a possible slight response was observed in the continuous measurement of EC after earthquake with Mw close to 4, but this possible effect needs to be validated through a more complete seismic monitoring network.

3.8.4 Possible precursory changes

Barberio et al., (2017), after the analysis of 10 springs and wells located in Sulmona (ca. 100 km far from the epicentral area) along the same earthquake sequence of this study, suggested that deep geothermal fluids incursion caused small changes in pH, which elevated Cr, As, and possibly Fe concentrations in springs and a well. They also found that As and Cr concentrations rose 4 months prior to the earthquake sequence, assessing that these elements could be used as precursor indicators of earthquakes. They explained that a slight lowering of the pH of the solution (by 0.4 pH units) could raise the solubility of these elements causing their increase in concentration. Nonetheless, the results of this study, set in nearby localities, along the same earthquake sequence, indicate that As is not a good indicator for earthquake activity as it was not detected either before or after the earthquake sequence in any of spring sampled in our study. Cr and Fe did increase after the earthquakes in all the springs measured in our study, but the pre-earthquake data from NER did not show increases before the 24th August 2016 earthquake. Also, observed pH changes in our study do not correlate with trace element concentrations increasing caused by the earthquakes (Figure 3.12).

Although our data are not sufficient to provide statistical evidence to confirm or deny the ability of trace elements to be used to predict earthquakes in Italy, the data from the Nerea Spring and bottling plant, suggests that at least in this region, few if any of the chemicals measured were elevated before the earthquake mainshock (Figure 3.6).

3.9 Conclusions and future perspectives

Transient changes in the trace element concentrations of springs sampled before and after the central Apennine earthquake sequence from August 2016 to January 2017 show that carbonate aquifers respond more to local shaking that causes fracture and pore fluid clearing than from changes in fluid composition from other sources. This study found that both near-field and intermediate-field springs were affected by fault movement and/or ground shaking that induced aquifer pore pressure change, and that these effects were transient in nature during this earthquake sequence. The three large aquifers sourced by these springs are similar

in hydrogeologic structure but different in proximity to the ruptured faults. The responses, though notable for both near and intermediate field, were different in duration and onset for each of the three carbonate aquifer springs. These complexities indicate a pore pressure response of aquifers to seismic strain and show the probable role of aquifer hydrogeological structure when considering earthquake effects. The enrichment of $\delta^{13}C_{DIC}$ in PES and SUS following the 2016 main shocks was likely influenced by input of deep-sourced CO_2 gas initiated by movement on faults that serve as conduits, in contrast to the mechanism proposed for other chemical enrichments, where solute-rich groundwater trapped in fractures and closed pore pores with more water-rock interaction time is mixed into fast-flowing groundwater and discharged in a post-seismic pulse.

The lack of change in most of the major ions and in $\delta^{18}O_{H2O}$ and $\delta^{2}H_{H2O}$ after the seismic series indicates that the observed hydrochemical dynamics are the result of within-aquifer changes instead of mixing with another aquifer, geothermal fluids, or aquifer breaching.

These local transient changes indicate that carbonate aquifers in general respond more to shaking more than to input from external fluids. This has important implications for supplying water that may have elevated trace element concentrations to earthquake survivors immediately after earthquakes. In addition, the use of trace element concentrations in aquifers as precursors of imminent earthquakes needs considerably more work to ensure that these predictions are accurate.

After the observations made for possible responses in chemistry even after relatively low magnitude earthquakes, the possibility to set-up of a regional monitoring network in Central Italy was considered to observe how water react to this phenomenon in different areas. Also, the increasing of knowledge about how earthquake affect water chemistry could pass through the collection of a bigger data collection, likely from local water managers or EPAs, to create a reliable quantitative model of aquifer seismic responses applying numerical methods. Therefore, the application of Principal Component Analysis, as a preliminary data tool revealed helpful for the interpretation of data, then the application of more complete correlation with earthquake features (i.e., magnitude, fault dynamics) could give us helpful information about a quantitative evaluation of seismic responses from aquifers

4 Secondary projects

The evaluation of geochemical anomalies can be a first step for other applications in water and environmental science. In this chapter, deeper investigations after the geochemical anomalies and human impact evaluation were made in the study area described in chapter 2. The following presented projects include: the anomalous Ni speciation in glacial sediments of Ventina valley (section 4.1) and a fractured aquifer water flow model which was then tested using geochemical markers analyzed from dissolved elements in water (section 4.2).

4.1 Anomalously high concentration of Ni in sediment of Ventina valley as sulphide phase

After the preliminary observation of geochemical background in the Ventina valley, applied to understand the possible exogenous metals present in the watershed (described in chapter 2)part of the glacial sediment samples collected were analyzed to characterize their chemical speciation. This study aims to evaluate the speciation of naturally occurring Ni in serpentinite bedrock glacial sediments. This element, even if coming from a natural source, can be possibly harmful for drinking water quality (Bonifacio et al., 2010; Morrison et al., 2015).

The study then focuses on anomalies in Ni speciation, which showed relatively high dissolution in waters of the study area (chapter 2).

4.1.1 Collection and sequential extractions of sediment samples

3 samples of glacial sediments collected in Ventina valley, in differently developed areas, presenting different morphologies to analyze samples with different deposition and possible difference due to exposure time and grain sizes. A three-step sequential extraction (Pueyo et al., 2008) was performed to analyze the possible dissolution of Ni in water. This procedure includes different leaching solutions to extract metals from the solid sample: each solution contains a series of progressively harsher chemical reagents to dissolve selectively only specific mineral and organic phases of the sample (Filgueiras et al., 2002; Tessier et al., 1979).

The three sequential extraction steps using the following solutions were applied:

• step 1: 4 mL of 0.11M acetic acid. This solution can extract exchangeable metal, and elements bond to labile forms (i.e., carbonates);

• step 2: 4 mL 0.11M hydroxylamine hydrochloride solution, dissolving reducible forms (e.g., Fe and Mn oxides);

• step 3: 1 mL of hydrogen peroxide (33% in weight) and 1M ammonium acetate. This solution can dissolve oxidable species like sulphides and strong organic ligands.

After every separation step, the residual was washed before being extracted with the next solution.

Detailed methods for solid samples analyses will be discussed in section 7.5.

4.1.2 Results of chemical speciation

Ni sequential extractions results highlight a prevailing concentration in the third step (the oxidizing) among the more easily extractable phases. (Figure 4.1). In fact, the extraction on the third step in the 3 samples of the Ventina valley generally presents a major Ni load then the sum of the first 2 steps.

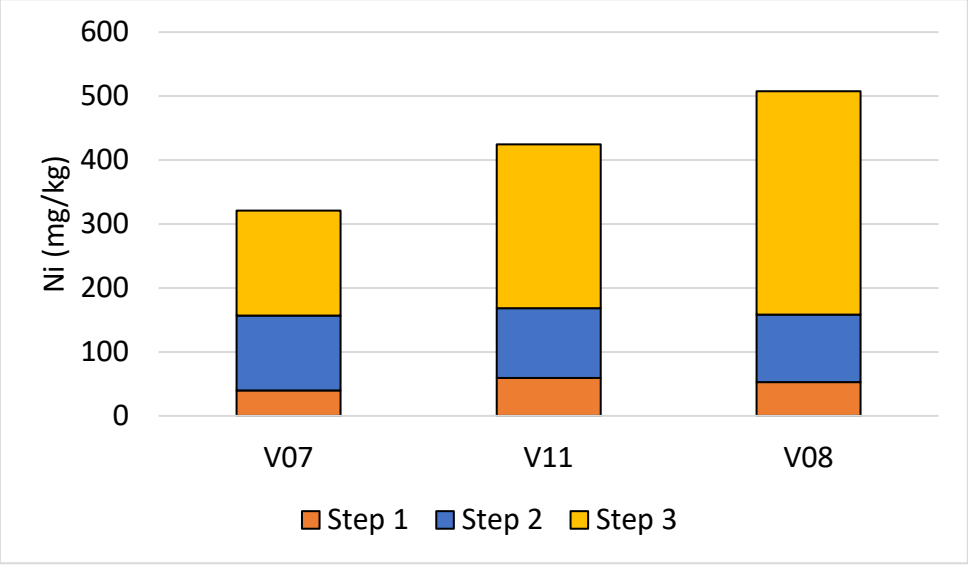

Figure 4.1: Ni chemical speciation in sediment samples.

This partition results different from the typical partition in other studies made on soil developed from serpentine lithologies. In fact, usually Ni substitute to Fe or Mg in serpentine minerals, like olivine, pyroxenes and Fe (hydr)oxides in serpentine soils (Becquer et al., 2005; Morrison et al., 2015), with a main dissolution in the step 2 (Hseu et al., 2017; Kumarathilaka et al., 2016; Rajapaksha et al., 2012), while in this study most of Ni was dissolved in the step 3. So, in Ventina valley, the primary source of labile Ni in the glacial sediment seems to come

from oxidable species, like sulphides, species present in different secondary minerals of the study area.

Thus, comparing the partition of Ni amount in the three extraction steps with other studies results using the same reagents for extractions (Figure 4.2), other studies principally show higher dissolution in the reductive step (step 2), while in the Ventina valley samples Ni present the higher amount in the oxidative step (step 3). Moreover, Ni dissolution in the third step in Ventina valley samples result bigger than in other studies with an overall higher Ni dissolution (Kumarathilaka et al., 2016; Rajapaksha et al., 2012). Only one study shows a comparable trend with a slightly higher dissolution in the third step in part of the samples (Cheng et al., 2011), but the absolute amount of the extracted Ni in mg/kg during the oxidizing extraction results lower. The presence of organic matter, that be dissolved in the step 3 too, can be a confounding factor, but its amount in these sediments result scarce. Moreover, even more developed alpine soils generally present low accumulation of organic matter, because the vegetation cover results scarce and the steep slopes limit pedogenic processes (Bonifacio et al., 2010).

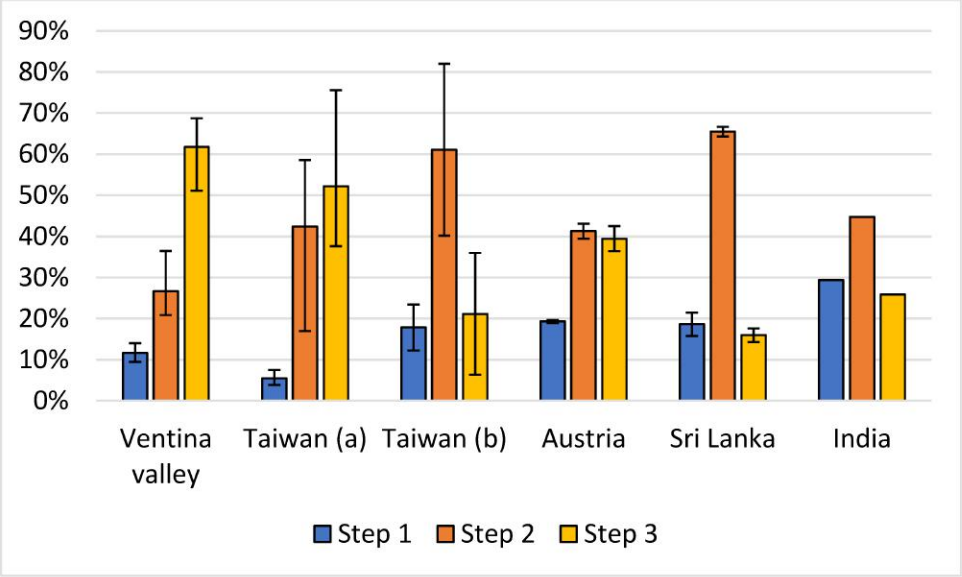

Figure 4.2: Ni percentage partition in different studies (Taiwan (a) data are from Cheng et al., 2011; India data are from Rajapaksha et al., 2012; Taiwan (b) and Austria data are from Hseu et al., 2017; SriLanka data are from Kumarathilaka et al., 2016) and in the Ventina valley. Bars indicate the mean values, while whiskers indicate the maximum and minimum values in the samples analyzed.

4.1.3 Discussion of Ni anomalies

Sulfides in the Ventina glacial sediments, differently from other studies, are primary phases of Ni dissolution. Sulfide minerals (i.e., pentlandite, $(Fe, Ni)_9S_8$, heazlewoodite, Ni_3S_2, and millerite, NiS) are generally observed as small inclusions with alteration rims: serpentine can be Ni enriched after filling the spaces between the residual grains of primary minerals or directly forms the alteration rims (Griffin and Chassé, 2016).

The relatively high dissolution of Ni in the study area, observing the speciation in sediment samples, could be possibly caused by sulfides oxidation: an un-expected result in such a geologic and geomorphologic setting. Glaciated environments, in fact, present principally anoxic condition, especially regarding the solid matrices. Nevertheless, some events can explain a similar event in a high mountain site: oxidation can be promoted by different bacteria who metabolize sulfide oxidation (Fantauzzi et al., 2011; Zhen et al., 2009) and even ferric Fe (Fe^{3+}) can be potentially an oxidant for sulfide minerals in glacial environment (Bottrell and Tranter, 2002). The solubility of metals that can occur as free hydrated cations, such as Ni, generally increases with a decreasing pH since a low acidity in solid–water systems tends to favor the formation of soluble species of many elements. In addition, pH can affect surface charge characteristics and speciation of element ions, thus influencing adsorption–desorption behavior of the involved ions (Miller et al., 2010). We could infer a possible increase of this reaction by an anthropogenic factor (i.e. acid rains, with nitrates) in these sediments.

Another possible reason for a high Ni presence as a sulfide and the relatively high mobility in water is due to the analysis in the primary phases of pedogenetic process in these soils, with very low alteration of the primary bedrock. In fact, other study used to compare our results were applied on more developed pedogenetical phases, while in the Ventina valley samples were at the beginning of pedogenetical process. Only one study (Cheng et al., 2011) analyzed in part of the samples some less developed soils, and the partition of Ni shows more similarities with the Ventina samples than the other ones, suggesting a possible weathering effect for changes in Ni speciation.

4.1.4 Conclusion and next applications of this approach

In summary, this study aims to understand Ni speciation in glacial sediments, after the observation of anomalously high concentration values in water samples, trying to evaluate possible dissolution mechanism. This study reveals a peculiar Ni speciation in the serpentine glacial sediments, differently from the observed partition for serpentine-derived soil samples, indicating a different possible dissolution and leaching mechanism, with consequent different availability pattern for this metal. The relatively high dissolution in waters can be justified by an oxidation of the deposed glacial sediments with glacier regression; this process could be stressed by an anthropogenic factor too (i.e. acid rain). These results leave some open questions regarding the Ni concentration in waters and its possible dissolution. To better understand how Ni could move into the water in the catchment a new approach can include a sequence of extractions with reagent which can better simulate weakly oxidant and organic ligands to simulate bioleaching. Also, the observation of Ni anomalous phase was observed in relatively young glacial deposits: an analysis of samples in more developed stages of the pedological sequence presenting the same bedrock could explain if Ni is present in the earlier stages and then leached or if the anomaly persists.

4.2 Spatial variation of metals as an index for groundwater flow

This chapter will describe the preliminary results of a study set up during my PhD project, where water geochemical features will be used as marker to validate a water flow model applied to the deep fractured aquifer in the study area described in chapter 2, to analyze the possible mixing between the two different basin through the flow in the deep fractured aquifer.

Groundwater flow path modeling is a key tool for hydrological science as well for water supply and management, especially in Alpine areas where, even if water scarcity can be a serious problem due to high seasonality of water availability (Hilberg and Riepler, 2016). Moreover, the accessibility of potentially usable springs in high mountain regions is restricted due to steep slopes and difficult terrain. Thus, although the mountain regions are normally well supplied with precipitation and groundwater recharge (Viviroli et al., 2007) the implementation of sustainable drinking-water supply in mountain settlements represent a particular challenge

Moreover, alpine areas are often hard to reach, and present slope instability which make them less suitable for different operations for groundwater monitoring and management are hard to apply in remote areas (i.e., boreholes drilling). For example, although piezometers can give significant, yet local, insights on the groundwater system (Kosugi et al., 2011), their cost, their short lifespans in unstable areas and their poor representativeness make piezometers not suitable in these areas. Consequently, some classical hydrological techniques (like groundwater head mapping and pumping tests) are not available. Different studies so focus on indirect methods such as hydrochemistry surveys by monitoring springs for natural and artificial tracers, or the analysis through outcrop scale for fractures (Vallet et al., 2015).

The chemical composition of groundwater in glaciated environment is mainly controlled by aquifer lithology and the relative groundwater flow velocity (Brown, 2002; Fortner et al., 2011): hydrochemical *facies* therefore remarks the water enrichment during water-rock interaction, and can work as a marker of groundwater flow.

Rainfall and snowmelt are generally assumed as the main sources of groundwater recharge in high alpine sites, groundwater flow is mainly driven by gravity in these systems. Thus, shallow aquifer flow occurs mainly parallel to the slope, within the weathered or bulked layers in

mountain catchments. Also, shallow aquifer flow in high mountain sites depends on different morphologies typical of this environment, due to high heterogeneity of deposits granulometry (Hilberg and Riepler, 2016). While deeper water circulation is generally present in fractured aquifers. Hard rocks, in fact, provide the second type of groundwater bodies in alpine environments and often occur as fractured aquifers (Hilberg and Riepler, 2016). In fractured rock formations, the rock mass hydraulic behavior is controlled by fractures (also defined joints). In such aquifers, open and well connected fractures constitute high permeability pathways and are orders of magnitude more permeable than the rock matrix (Berkowitz, 2002; Lee et al., 2011; Lei et al., 2017). In this kind of aquifers, Discrete Fracture Network model (DFN) is a widely used technique to model fracture orientations and dimensions, and then permeability and groundwater flow can be modeled, assuming laminar flow inside the fractures and no flow outside from them, with a primary permeability approximated to zero (Lei et al., 2017; Oda, 1985).

To better analyze possible water circulation inside fractured aquifer, an integrated approach is needed. In the following chapter, an hydrochemical evaluation of major ions and a characterization of is used to validate the flow modeling through the application of a DFN after lineaments analysis and outcrops evaluation of joints.

In the following section, groundwater flow will be evaluated in part the study area of chapter 2 through the application of a discrete fracture network, and geochemical markers in water will be used as a validation of modeled flow.

4.2.1 Geological data collection and modeling

Geological data collection and import

22 measurement stations were selected to evaluate fractures orientations and dimensions (Figure 4.3). For outcrop-scale measurements, geological maps were examined prior to fieldwork, in order to find outcrops localized in different bedrocks representing the study area, and to cover different settings compared to the fault, selecting outcrop locations that were representative of lithologically and structurally distinctive rock groups in the study area (Welch and Allen, 2014).

Joints dimensions, frequency and dips were measured on site at an outcrop scale. Dips were obtained through the smartphone app Field MOVE Clino® developed by Midland Valley. This

app works with the tiltmeter and the magnetometer of the mobile phone to measure fracture dips and inclination. Moreover, an analogical compass was used on site to validate data obtained through the mobile app. To evaluate fracture dimensions some references were used on site to measure length and height. Fracture aperture was measured using references too.

Then data were imported on a workstation and analyzed using the software MOVE from Midland valley. Firstly, outliers were removed through observation of data distribution and analyzing the stereoplots. Then, fracture cluster were recognized through the application of a clustering algorithm of orientation values, and agglomeration of cluster was evaluated through Fisher K value (Fisher, 1953). The results obtained from the software were compared with the joint families recognized on site. Data collected on sites and details about recognized cluster of joint through stereoplot analysis are listed in supplementary material Supplementary_06 (chapter 9).

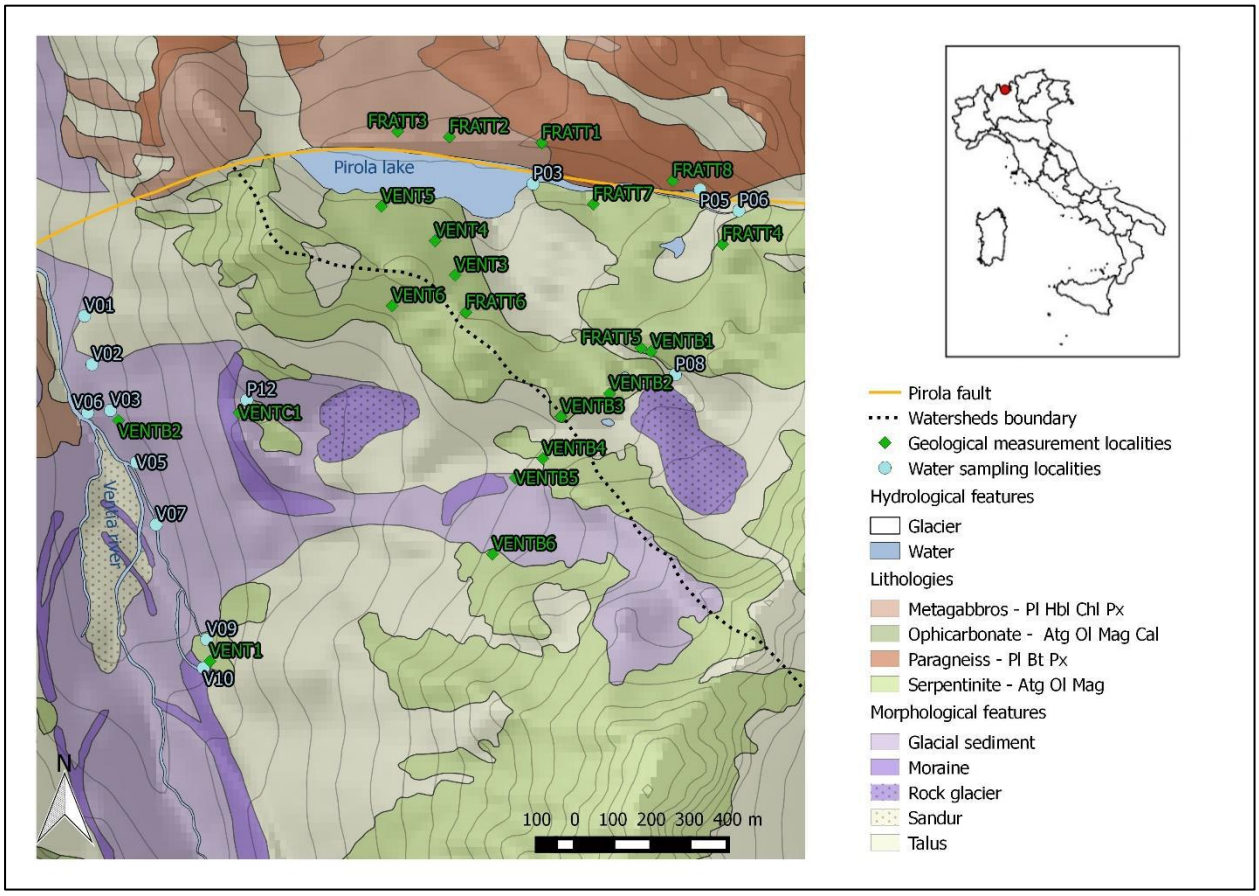

Figure 4.3: map representing the section of the study area of chapter 2 analyzed, the spring considered and the station where fractures were measured (UTM 32N projected coordinates in supplementary file Supplementary_07, chapter 9).

Fracture modelling

To obtain a flow model of the whole study area, the approach used included:

- the subdivision of the study area in sectors functionally to the geological measurement stations creating Voronoi polygons (Berg et al., 2008);
- the creation of different geocellular volumes from grid surfaces, using the digital elevation model of the area as top surface and a flat surface remarking the Ventina valley altitude as a bottom surface;
- the creation of different DFN for every single geocellular volume;
- Permeability and preferential flow modeling after the creation of every DFN (Figure 4.4).

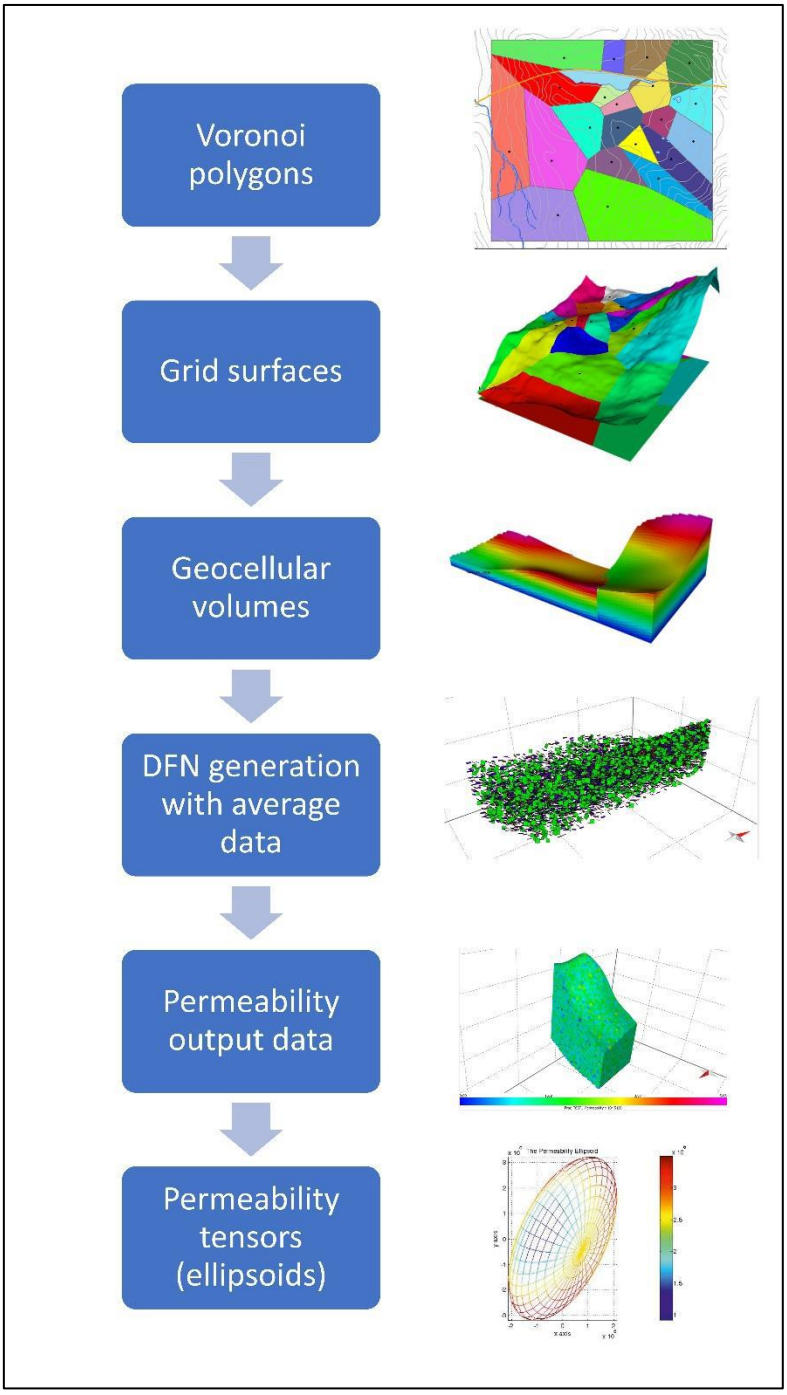

Figure 4.4: workflow of permeability modeling, after data importation.

In more detail, the algorithm to generate DFN is based on a stochastic generation of vectors representing the fractures set observed in field inside a rock volume, basing from the values of orientation, spacing and dimensions and their variance observed in field (Oda, 1985). Permeability and preferential flows direction through the fractured aquifer approximating a laminar flow inside the cracks and approximating the primary permeability of the rock to zero,

which experimentally is evaluated to be considerably low (up to 10^{-24} Darcy, Trimmer et al., 1980)

Once the DFN has been created, the permeability tensor is calculated basing on the geometric methodology of Oda (1985), which is itself based on Darcy's Law and laminar flow between parallel plates. The used equation is:

$$\frac{Q}{A} = \frac{s^3}{12D}\frac{\partial \mathrm{h}}{\partial \mathrm{l}}\frac{\rho g}{\mu}$$

Where:

- Q is the flow rate;
- A is the cross-section area;
- s is the fracture aperture;
- D is fracture spacing;
- $\frac{\partial \mathrm{h}}{\partial \mathrm{l}}$ is the pressure head;
- $\frac{\rho g}{\mu}$ is the fluid density and viscosity.

Permeability tensor is a matrix which indicate heterogenous permeability in space, functionally to the direction. The permeability tensor is a symmetric 3x3 matrix, and hence can be represented by 6 independent numbers: k_{xx}, k_{xy}, k_{xz}, k_{yy}, k_{yz}, k_{zz}. The method of calculating the permeability tensor follows Oda, 1985. This approach essentially derives an equivalent porosity property for each grid cell based on the DFN properties contained in the cell.

4.2.2 Chemical data collection and treatment

In this study the data were collected in part of the sampling points already described in chapters 2.4-2.5, and analyzed variables include the major ions and the trace elements observed as coming from a natural source. Detailed methods for chemical analyses performed are included in section 2.5 and appendix, section 7.

To evaluate variables describing the geochemical trends and anomalies in the study area, collected data where treated through PCA (Kramer, 1998), after normalization and centering on the mean (as in chapter 2.5.3, Sahariah et al., 2015). PCA was performed using all sampling

periods and points to evaluate spatial and temporal variations, and F NO_3 NH_4 were removed from analyzed list because these variables present low variance.

Then, mean values of principal component scores of every sampling point among the different sampling periods were obtained to not lose the temporal variability, and highlight spatial variations.

Finally, inverse distant weighting (IDW) algorithm was used (Sarma, 2010) to generate a interpolation surface of score value, to discriminate geochemical differences and similarities among the analyzed springs.

4.2.3 Results and discussion

Geological model results

After the geological modeling for every area separated through Voronoi polygons described in section 4.2.1, mapping the difference in permeability and preferential flow (Figure 4.5), is observable that generally permeability increases in the SW part of the study area, with a general direction of referential flow with a direction NW-SE. Also, the area crossed by the fault show a general lower permeability, as an index of the effect caused by the fault. Detailed data collected in site are listed in supplementary material Supplementary_06 (chapter 9).

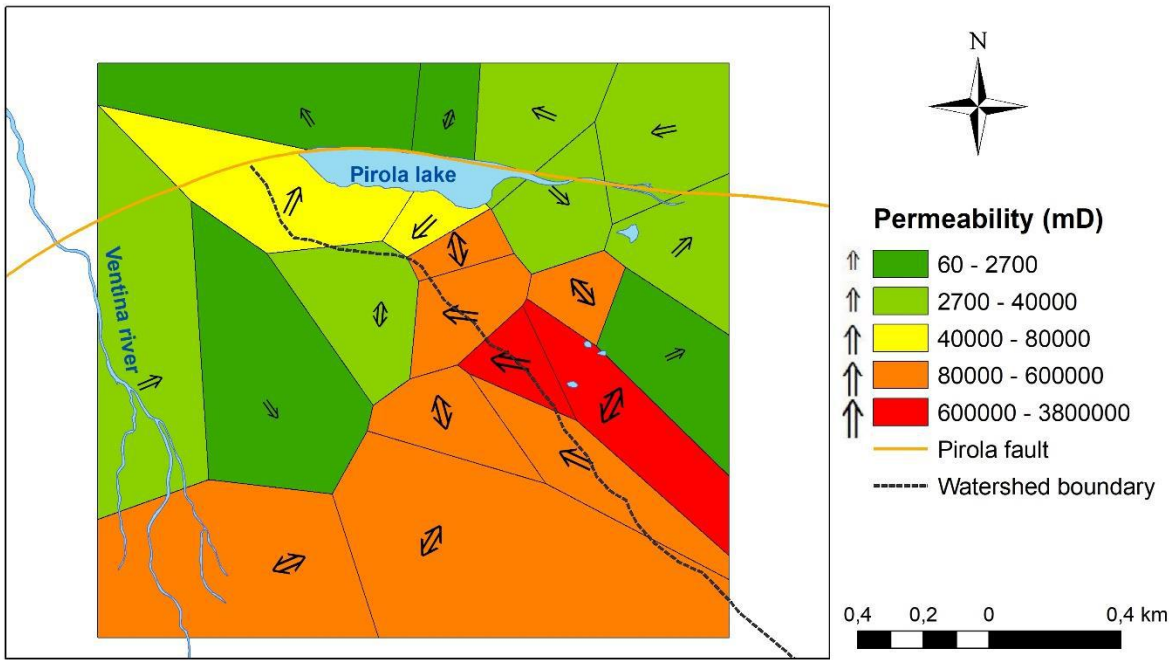

Figure 4.5: map of the study area after the flow modeling of every subdivision of the study area, color scale indicate the permeability grade (in millidarcy), and arrows indicate preferential 2D flow after the computation of permeability tensor ellipsoids.

Geological model validation through geochemical markers

PCA loading plot on all the data from the analyzed springs in Figure 4.6 shows mainly two clusters of variables, which mainly separates on component 1 (explaining 30% of the total variance of the system). This component separates ions mainly dissolving from serpentinite minerals (Ni, Cr, Fe, Mg) and ions mainly dissolving from gabbros rocks and minerals.

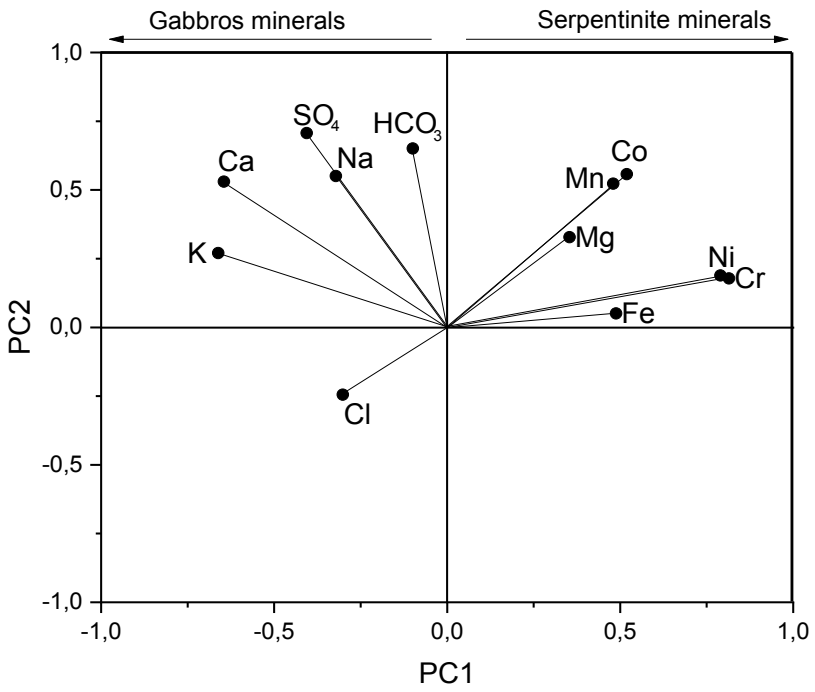

Figure 4.6: loading plot for the analyzed chemical variables in all the considered springs of this stud. First component partly remarks the differences in geochemistry of the site.

Observing the interpolation surface of score values in the sampled springs, it is clear that generally the different basin remarks differences in water chemistry, with the Pirola lake influenced more by gabbros type waters (Figure 4.7). Nonetheless, a spring in the Ventina basins show a clear similarity with the Pirola basin spring, and spring P08 show a chemical fingerprint typical of serpentinites. Therefore, observing the model output, the similarities between spring P08 and the spring in the Ventina valley suggest that a communication between the basins is possible due to the high permeability observed in the SW part of the area. The difference between V05 and the other Ventina valley spring is instead surprising, and can be justified with a mixing of shallow surface aquifer and the deep aquifer due to the very low permeability in the central part of the analyzed area, as observable in Figure 4.5.

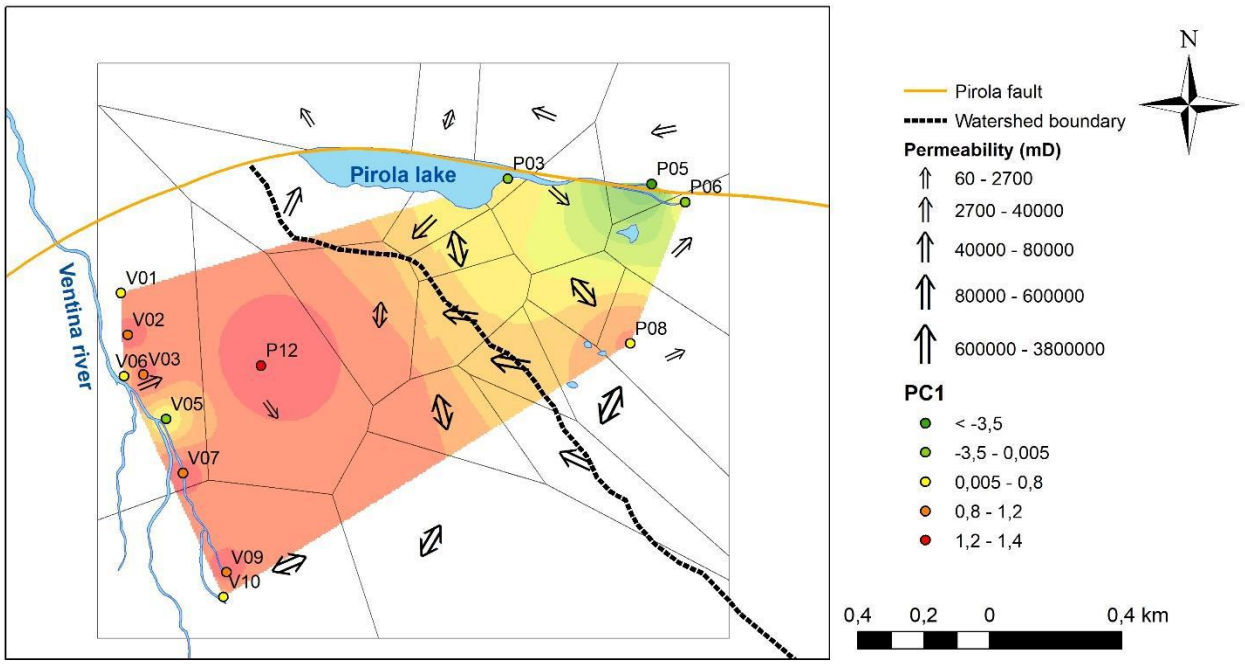

Figure 4.7: map showing the 2D projection of the permeability tensors and the color map of PCA scores values in all the sampled springs.

4.2.4 Conclusion and next application

After the geological data collection and modeling, a possible communication between the two aquifer is observable in the SW part, and the chemical data confirm similarities between the springs in that part.

The central part of the area shows low permeability and a mixing of shallow and deeper aquifer

After these observations, I conclude that the application of an integrated approach can be an helpful tool to validate the groundwater flow geological modeling through geochemical markers.

This preliminary study requires anyway more analyses to have a deeper understanding of water flow and a more complete modeling approach. Further improvements include:

- 3D modeling using permeability decrement with depth (Jiang et al., 2010), and a 3D evaluation of permeability tensors;
- Integration of weather data and flow measurements in the shallow and deep aquifer, to quantify water recharge and possible evapotranspiration and runoff;

- Analysis of lineaments observation through aerial photographs or Unmanned Aerial Vehicle (UAV) flights to compare field scale and regional scale measurements

5 General remarks and conclusions

After the presentation of different case studies where geochemical anomalies were observed and human impact in a remote setting was assessed, general observation can be made regarding the techniques used to obtain the presented results.

The observations of chapter 2.3 highlight the need to applicate of an integrated approach to understand PTEs sources in the analyzed water catchment: the application of only one of the methods along the approach, in fact, for some elements represented confounding results (i.e., seasonal trends and clustering of Cd and Ag).

Also, the presented case studies highlight the importance of an adequate long time span to observe the temporal variation of background values and sampling frequency in water monitoring. In fact, this environmental compartment requires a sharp observation of temporal trends to understand the natural variability, due to the high dynamicity of this compartment, differently from soils and sediments, which clearly complicates the modeling of geochemical anomalies and background values for water compared with other more stable compartments (Galuszka, 2007).

Surely multivariate statistics, as in other applications in environmental geochemistry, showed its value to understand natural phenomena (as in chapter 2 with cluster analysis and in chapter 3 and 4.2 with PCA). In this dissertation, in fact, multivariate statistic was used with different application and gave useful information regarding earthquake response evaluation, to evaluate the geochemical markers in different springs, and to classify differences in clustering of variables following seasonal trends.

As a negative aspect, a big number of samples and data analyses is still needed, especially in water samples, to assess the background value concentration. While preliminary modeling techniques are used in geochemical background evaluation from remote sensing collected data, modeling techniques are still limited for geochemical water sciences, but these techniques, after good data management and validation, could become the next approaches to this environmental issue (Kirkwood et al., 2016).

Therefore, while different data analysis tools are useful to understand PTEs sources in water, modeling techniques still results limited in the understanding of PTEs dissolution, weathering

and possible anthropic enrichment, due to high spatial and temporal heterogeneity, and a high number of factors which can change dissolution patterns (i.e., anthropic stress, biota interaction; Gaillardet et al., 2003; Galuszka, 2007; Zhen et al., 2009).

Then, once their mechanism and causes are known, geochemical anomalies can work as a marker and can become helpful tools in field geochemical applications. In fact, as observed in chapter 4.2, the natural anomalies of metals concentration explained water similarities between springs, and therefore a possible communication. Also, as observed in chapter 3 and references therein, geochemical anomalies work as a marker of seismic activity, and even if still quite debated and not completely reliable yet, geochemical anomalies can work as precursors of seismic activity too.

Concluding, the multidisciplinary approaches are winning strategies for the evaluation of geochemical anomalies in water, and as presented through my dissertation, mechanism causing anomalies can be explained and understood with careful evaluation of chemical and hydrogeological data.

6 References

Albanese, S., De Vivo, B., Lima, A., Cicchella, D., 2007. Geochemical background and baseline values of toxic elements in stream sediments of Campania region (Italy). Journal of Geochemical Exploration 93, 21–34. https://doi.org/10.1016/j.gexplo.2006.07.006

Alier, M., Felipe-Sotelo, M., Hernàndez, I., Tauler, R., 2009. Variation patterns of nitric oxide in Catalonia during the period from 2001 to 2006 using multivariate data analysis methods. Analytica chimica acta 642, 77–88.

Allegri, L., Bella, F., Della Monica, G., Ermini, A., Improta, S., Sgrigna, V., Biagi, P.F., 1983. Radon and tilt anomalies detected before the Irpinia (south Italy) earthquake of November 23, 1980 at great distances from the epicenter. Geophysical Research Letters 10, 269–272. https://doi.org/10.1029/GL010i004p00269

Ambrosetti, P., Anfossi, D., Cieslik, S., Graziani, G., Lamprecht, R., Marzorati, A., Nodop, K., Sandroni, S., Stingele, A., Zimmermann, H., 1998. Mesoscale transport of atmospheric trace constituents across the central Alps: Transalp tracer experiments. Atmospheric Environment 32, 1257–1272. https://doi.org/10.1016/S1352-2310(97)00185-4

Amoruso, A., Crescentini, L., Petitta, M., Rusi, S., Tallini, M., 2011. Impact of the 6 April 2009 L'Aquila earthquake on groundwater flow in the Gran Sasso carbonate aquifer, Central Italy. Hydrological Processes 25, 1754–1764. https://doi.org/10.1002/hyp.7933

Ander, E.L., Johnson, C.C., Cave, M.R., Palumbo-Roe, B., Nathanail, C.P., Lark, R.M., 2013. Methodology for the determination of normal background concentrations of contaminants in English soil. Science of The Total Environment 454–455, 604–618. https://doi.org/10.1016/j.scitotenv.2013.03.005

Archer, C., Noble, P., Kreamer, D., Piscopo, V., Petitta, M., Rosen, M.R., Poulson, S.R., Piovesan, G., Mensing, S., 2016. Hydrochemical determination of source water contributions to Lake Lungo and Lake Ripasottile (central Italy). Journal of Limnology. 10.4081/jlimnol.2016.1576

Arpine, H., Gayane, S., 2016. Determination of background concentrations of hydrochemical parameters and water quality assessment in the Akhuryan River Basin (Armenia). Physics and Chemistry of the Earth, Parts A/B/C, 3rd International Conference on Ecohydrology, Soil and Climate Change, EcoHCC'14 94, 2–9. https://doi.org/10.1016/j.pce.2016.03.011

Barberio, M.D., Barbieri, M., Billi, A., Doglioni, C., Petitta, M., 2017. Hydrogeochemical changes before and during the 2016 Amatrice-Norcia seismic sequence (central Italy). Scientific Reports 7. https://doi.org/10.1038/s41598-017-11990-8

Barbieri, M., Boschetti, T., Petitta, M., Tallini, M., 2005. Stable isotope (2H, 18O and 87Sr/86Sr) and hydrochemistry monitoring for groundwater hydrodynamics analysis in a karst aquifer (Gran Sasso, Central Italy). Applied Geochemistry, vol. 20, issue 11, pp. 2063-2081 20, 2063–2081. https://doi.org/10.1016/j.apgeochem.2005.07.008

Becquer, T., C. Quantin, S. Rotte-Capet, J. Ghanbaja, C. Mustin, A. J. Herbillon, 2005. Sources of trace metals in Ferralsols in New Caledonia. European Journal of Soil Science 57, 200–213. https://doi.org/10.1111/j.1365-2389.2005.00730.x

Bedogné, F., Montrasio, A., Sciesa, E., 1993. I minerali della provincia di Sondrio, Valmalenco.

Bella, F., Biagi, P.F., Caputo, M., Cozzi, E., Monica, G.D., Ermini, A., Gordeez, E.I., Khatkevich, Y.M., Martinelli, G., Plastino, W., Scandone, R., Sgrigna, V., Zilpimiani, D., 1998. Hydrogeochemical anomalies in Kamchatka (Russia). Physics and Chemistry of the Earth 23, 921–925. https://doi.org/10.1016/S0079-1946(98)00120-7

Berg, M. de, Cheong, O., Kreveld, M. van, Overmars, M., 2008. Computational geometry: algorithms and applications. Springer-Verlag TELOS.

Berkowitz, B., 2002. Characterizing flow and transport in fractured geological media: A review. Advances in Water Resources 25, 861–884. https://doi.org/10.1016/S0309-1708(02)00042-8

Binda, G., Pozzi, A., Livio, F., Piasini, P., Zhang, C., 2018. Anomalously high concentration of Ni as sulphide phase in sediment and in water of a mountain catchment with serpentinite bedrock. Journal of Geochemical Exploration 190, 58–68. https://doi.org/10.1016/j.gexplo.2018.02.014

Bloise, A., Barca, D., Gualtieri, A.F., Pollastri, S., Belluso, E., 2016. Trace elements in hazardous mineral fibres. Environ. Pollut. 216, 314–323. https://doi.org/10.1016/j.envpol.2016.06.007

Boni, C., Baldoni, T., Banzato, F., Cascone, D., Petitta, M., 2010. Hydrogeological Study for Identification, Characterisation and Management of Groundwater Resources in the Sibillini Mountains National Park (central Italy). Italian Journal of Engineering Geology and Environment 21–39. https://doi.org/10.4408/IJEGE.2010-02.O-02

Boni, C., Bono, P., Capelli, G., 1986. Schema idrogeologico dell'Italia centrale. Mem. Soc. Geol. It. 35, 991 – 1012.

Bonifacio, E., Falsone, G., Piazza, S., 2010. Linking Ni and Cr concentrations to soil mineralogy: does it help to assess metal contamination when the natural background is high? Journal of Soils and Sediments 10, 1475–1486.

Bonsignore, G., Casati, P., Crespi, R., Fagnani, G., Liborio, G., Montrasio, A., Mottana, A., Ragni, U., Schiavinato, G., Venzo, S., 1971. Note Illustrative della Carta Geologica d'Italia alla scala 1: 100.000, Fogli 7 e 18: Pizzo Bernina e Sondrio. Nuova Tecnica Grafica, Serv Geol It, Roma 1–130.

Bottrell, S.H., Tranter, M., 2002. Sulphide oxidation under partially anoxic conditions at the bed of the Haut Glacier d'Arolla, Switzerland. Hydrological Processes 16, 2363–2368.

Brown, A.L., Martin, J.B., Screaton, E.J., Ezell, J.E., Spellman, P., Gulley, J., 2014. Bank storage in karst aquifers: The impact of temporary intrusion of river water on carbonate dissolution and trace metal mobility. Chemical Geology 385, 56–69. https://doi.org/10.1016/j.chemgeo.2014.06.015

Brown, G.H., 2002. Glacier meltwater hydrochemistry. Applied Geochemistry 17, 855–883.

Burkhard, D.J., 1989. Co-Ni-As sulphides in serpentinites of different metamorphic grade in the eastern Central Alps (Switzerland and Italy). Mineralogy and Petrology 41, 65–71.

Busico, G., Cuoco, E., Kazakis, N., Colombani, N., Mastrocicco, M., Tedesco, D., Voudouris, K., 2018. Multivariate statistical analysis to characterize/discriminate between anthropogenic and geogenic trace elements occurrence in the Campania Plain, Southern Italy. Environmental Pollution 234, 260–269. https://doi.org/10.1016/j.envpol.2017.11.053

Cameron, E.M., Leybourne, M.I., Kelley, D.L., 2002. Exploring for deeply covered mineral deposits: Formation of geochemical anomalies in northern Chile by earthquake-induced surface flooding of mineralized groundwaters. Geology 30, 1007–1010. https://doi.org/10.1130/0091-7613(2002)030<1007:EFDCMD>2.0.CO;2

Carrivick, J.L., Russell, A.J., 2007. GLACIAL LANDFORMS, SEDIMENTS | Glacifluvial Landforms of Deposition, in: Elias, S.A. (Ed.), Encyclopedia of Quaternary Science. Elsevier, Oxford, pp. 909–920. https://doi.org/10.1016/B0-44-452747-8/00087-9

Castorina, F., Petrini, R., Galic, A., Slejko, F.F., Aviani, U., Pezzetta, E., Cavazzini, G., 2013. The fate of iron in waters from a coastal environment impacted by metallurgical industry in Northern Italy: hydrochemistry and Fe-isotopes. Applied Geochemistry, Special issue dedicated to Giovanni Maria (Gian Maria) Zuppi (1947-2011) 34, 222–230. https://doi.org/10.1016/j.apgeochem.2013.04.003

Cavallo, A., 2018. Serpentinitic waste materials from the dimension stone industry: Characterization, possible reuses and critical issues. Resour. Policy 59, 17–23. https://doi.org/10.1016/j.resourpol.2018.08.003

Cavinato, G.P., Celles, P.D., 1999. Extensional basins in the tectonically bimodal central Apennines fold-thrust belt, Italy: response to corner flow above a subducting slab in retrograde motion. Geology 27, 955–958.

Celico, P., 1981. Relazioni tra idrodinamica sotterranea e terremoti in Irpinia (Campania). Rend. Soc. Geol. It 4, 103–108.

Celico, P.B., 1983. Idrogeologia dei massicci carbonatici, delle piane quaternarie e delle aree vulcaniche dell'Italia centro-meridionale: Marche e Lazio meridionali, Abruzzo, Molise e Campania. Cassa per il Mezzogiorno.

Cello, G., Mazzoli, S., Tondi, E., Turco, E., 1997. Active tectonics in the central Apennines and possible implications for seismic hazard analysis in peninsular Italy. Tectonophysics 272, 43–68. https://doi.org/10.1016/S0040-1951(96)00275-2

Charmoille, A., Fabbri, O., Mudry, J., Guglielmi, Y., Bertrand, C., 2005. Post-seismic permeability change in a shallow fractured aquifer following a ML 5.1 earthquake (Fourbanne karst aquifer, Jura outermost thrust unit, eastern France). Geophysical Research Letters 32, n/a-n/a. https://doi.org/10.1029/2005GL023859

Cheng, C.-H., Jien, S.-H., Iizuka, Y., Tsai, H., Chang, Y.-H., Hseu, Z.-Y., 2011. Pedogenic Chromium and Nickel Partitioning in Serpentine Soils along a Toposequence. Soil Science Society of America journal.

Chiaraluce, L., Stefano, R.D., Tinti, E., Scognamiglio, L., Michele, M., Casarotti, E., Cattaneo, M., Gori, P.D., Chiarabba, C., Monachesi, G., Lombardi, A., Valoroso, L., Latorre, D., Marzorati, S., 2017. The 2016 Central Italy Seismic Sequence: A First Look at the Mainshocks, Aftershocks,

and Source Models. Seismological Research Letters 88, 757–771. https://doi.org/10.1785/0220160221

Chiodini, G., Cardellini, C., Amato, A., Boschi, E., Caliro, S., Frondini, F., Ventura, G., 2004. Carbon dioxide Earth degassing and seismogenesis in central and southern Italy. Geophysical Research Letters 31, n/a-n/a. https://doi.org/10.1029/2004GL019480

Chiodini, G., Frondini, F., Cardellini, C., Parello, F., Peruzzi, L., 2000. Rate of diffuse carbon dioxide Earth degassing estimated from carbon balance of regional aquifers: The case of central Apennine, Italy. J. Geophys. Res. 105, 8423–8434. https://doi.org/10.1029/1999JB900355

Ciarletti, M., Plastino, W., Peresan, A., Nisi, S., Copia, L., Panza, G.F., Povinec, P.P., 2016. Uranium Groundwater Monitoring and Seismic Analysis: A Case Study of the Gran Sasso Hydrogeological Basin, Italy. Pure and Applied Geophysics 173, 1079–1095. https://doi.org/10.1007/s00024-015-1152-4

Civita, M.V., Fiorucci, A., 2010. The recharge - discharge process of the Peschiera spring system (central Italy). AQUAmundi - Journal of water sciences 161–178. https://doi.org/10.4409/Am-014-10-0019

Claesson, L., Skelton, A., Graham, C., Dietl, C., Mörth, M., Torssander, P., Kockum, I., 2004. Hydrogeochemical changes before and after a major earthquake. Geology 32, 641–644.

Clark, P.U., Dyke, A.S., Shakun, J.D., Carlson, A.E., Clark, J., Wohlfarth, B., Mitrovica, J.X., Hostetler, S.W., McCabe, A.M., 2009. The Last Glacial Maximum. Science 325, 710–714. https://doi.org/10.1126/science.1172873

Costantini, E.A., Fantappié, M., L'Abate, G., 2013. Climate and pedoclimate of Italy, in: The Soils of Italy. Springer, pp. 19–37.

Cotecchia, V., Salvemini, A., Ventrella, N.A., 1990. Interpretazione degli abbassamenti territoriali indotti dal terremoto del 23 Novembre 1980 e correlazioni con i danni osservati su talune strutture ingegneristiche dell'area epicentrale irpina. Rivista italiana di geotecnica 24, 4.

Coward, M., Dietrich, D., 1989. Alpine tectonics—an overview. Geological Society, London, Special Publications 45, 1–29.

Cowie, P.A., Phillips, R.J., Roberts, G.P., McCaffrey, K., Zijerveld, L.J.J., Gregory, L.C., Faure Walker, J., Wedmore, L.N.J., Dunai, T.J., Binnie, S.A., Freeman, S.P.H.T., Wilcken, K., Shanks, R.P., Huismans, R.S., Papanikolaou, I., Michetti, A.M., Wilkinson, M., 2017. Orogen-scale uplift in the central Italian Apennines drives episodic behaviour of earthquake faults. Scientific Reports 7, 44858. https://doi.org/10.1038/srep44858

Dalla Libera, N., Fabbri, P., Mason, L., Piccinini, L., Pola, M., 2017. Geostatistics as a tool to improve the natural background level definition: An application in groundwater. Science of The Total Environment 598, 330–340. https://doi.org/10.1016/j.scitotenv.2017.04.018

de Vallejuelo, S.F.-O., Gredilla, A., de Diego, A., Arana, G., Madariaga, J.M., 2014. Methodology to assess the mobility of trace elements between water and contaminated estuarine sediments as a function of the site physico-chemical characteristics. Science of the Total Environment 473, 359–371.

Devic, G., Djordjevic, D., Sakan, S., 2014. Natural and anthropogenic factors affecting the groundwater quality in Serbia. Science of The Total Environment 468–469, 933–942. https://doi.org/10.1016/j.scitotenv.2013.09.011

Doglioni, C., Barba, S., Carminati, E., Riguzzi, F., 2014. Fault on–off versus coseismic fluids reaction. Geoscience Frontiers 5, 767–780. https://doi.org/10.1016/j.gsf.2013.08.004

Dossi, C., Ciceri, E., Giussani, B., Pozzi, A., Galgaro, A., Viero, A., Viganò, A., 2007. Water and snow chemistry of main ions and trace elements in the karst system of Monte Pelmo massif (Dolomites, Eastern Alps, Italy). Mar. Freshwater Res. 58, 649–656. https://doi.org/10.1071/MF06170

Drever, J.I., 2005. Surface and Ground Water, Weathering, and Soils: Treatise on Geochemistry. Elsevier.

Dung, T.T.T., Cappuyns, V., Swennen, R., Phung, N.K., 2013. From geochemical background determination to pollution assessment of heavy metals in sediments and soils. Reviews in Environmental Science and Bio/Technology 12, 335–353.

Evans, D.J.A., 2013. Glaial landforms, sediments | Tills, in: Elias, S.A., Mock, C.J. (Eds.), Encyclopedia of Quaternary Science (Second Edition). Elsevier, Amsterdam, pp. 62–75. https://doi.org/10.1016/B978-0-444-53643-3.00088-1

Fantauzzi, M., Licheri, C., Atzei, D., Loi, G., Elsener, B., Rossi, G., Rossi, A., 2011. Arsenopyrite and pyrite bioleaching: evidence from XPS, XRD and ICP techniques. Anal Bioanal Chem 401, 2237–2248. https://doi.org/10.1007/s00216-011-5300-0

Favara, R., Italiano, F., Martinelli, G., 2001. Earthquake-induced chemical changes in the thermal waters of the Umbria region during the 1997–1998 seismic swarm. Terra Nova 13, 227–233. https://doi.org/10.1046/j.1365-3121.2001.00347.x

Filgueiras, A.V., Lavilla, I., Bendicho, C., 2002. Chemical sequential extraction for metal partitioning in environmental solid samples. Journal of Environmental Monitoring 4, 823–857. https://doi.org/10.1039/B207574C

Finardi, S., Silibello, C., D'Allura, A., Radice, P., 2014. Analysis of pollutants exchange between the Po Valley and the surrounding European region. Urban Climate 10, 682–702. https://doi.org/10.1016/j.uclim.2014.02.002

Fisher, R.A., 1953. Dispersion on a sphere. Proc. R. Soc. Lond. A 217, 295–305. https://doi.org/10.1098/rspa.1953.0064

Flem, B., Reimann, C., Fabian, K., Birke, M., Filzmoser, P., Banks, D., 2018. Graphical statistics to explore the natural and anthropogenic processes influencing the inorganic quality of drinking water, ground water and surface water. Applied Geochemistry, SI: ISEG 2016 88, 133–148. https://doi.org/10.1016/j.apgeochem.2017.09.006

Förstner, U., Wittmann, G.T., 1979. Metal pollution in the aquatic environment. Springer Science & Business Media.

Fortner, S.K., Mark, B.G., McKenzie, J.M., Bury, J., Trierweiler, A., Baraer, M., Burns, P.J., Munk, L., 2011. Elevated stream trace and minor element concentrations in the foreland of receding tropical glaciers. Applied Geochemistry 26, 1792–1801.

Fusari, A., Carroll, M.R., Ferraro, S., Giovannetti, R., Giudetti, G., Invernizzi, C., Mussi, M., Pennisi, M., 2017. Circulation path of thermal waters within the Laga foredeep basin inferred from chemical and isotopic (δ18O, δD, 3H, 87Sr/86Sr) data. Applied Geochemistry 78, 23–34. https://doi.org/10.1016/j.apgeochem.2016.11.021

Gabrielli, P., Cozzi, G., Torcini, S., Cescon, P., Barbante, C., 2008. Trace elements in winter snow of the Dolomites (Italy): A statistical study of natural and anthropogenic contributions. Chemosphere 72, 1504–1509. https://doi.org/10.1016/j.chemosphere.2008.04.076

Gaillardet, J., Viers, J., Dupré, B., 2003. Trace elements in river waters. Treatise on geochemistry 5, 605.

Galassi, D.M., Lombardo, P., Fiasca, B., Di Cioccio, A., Di Lorenzo, T., Petitta, M., Di Carlo, P., 2014. Earthquakes trigger the loss of groundwater biodiversity. Scientific reports 4, 6273.

Galuszka, A., 2007. A review of geochemical background concepts and an example using data from Poland. Environ Geol 52, 861–870. https://doi.org/10.1007/s00254-006-0528-2

Gaus, I., Kinniburgh, D.G., Talbot, J.C., Webster, R., 2003. Geostatistical analysis of arsenic concentration in groundwater in Bangladesh using disjunctive kriging. Environmental geology 44, 939–948.

Geller, R.J., 1997. Earthquake prediction: a critical review. Geophys J Int 131, 425–450. https://doi.org/10.1111/j.1365-246X.1997.tb06588.x

Giussani, B., Roncoroni, S., Recchia, S., Pozzi, A., 2016. Bidimensional and Multidimensional Principal Component Analysis in Long Term Atmospheric Monitoring. Atmosphere 7, 155.

Gong, M., Wu, L., Bi, X., Ren, L., Wang, L., Ma, Z., Bao, Z., Li, Z., 2010. Assessing heavy-metal contamination and sources by GIS-based approach and multivariate analysis of urban–rural topsoils in Wuhan, central China. Environmental Geochemistry and Health 32, 59–72. https://doi.org/10.1007/s10653-009-9265-2

Griffin, W.L., Chassé, M., 2016. Nickel, in: White, W.M. (Ed.), Encyclopedia of Geochemistry. Springer International Publishing Switzerland, pp. 1–4. https://doi.org/10.1007/978-3-319-39193-9_243-1

Guerrieri, L., Brunamonte, F., Comerci, V., Ferreli, L., Michetti, A.M., Pompili, R., Serva, L., 2004. Geological evolution of the intermountain Rieti basin (Central Apennines). Mapping Geology in Italy. SELCA, Firenze.

Hammond, D.E., Teng, T.L., Miller, L., Haraguchi, G., 1981. A search for Co-variance among seismicity, groundwater chemistry, and groundwater radon in southern California. Geophys. Res. Lett. 8, 445–448. https://doi.org/10.1029/GL008i005p00445

Hartmann, J., Berner, Z., Stüben, D., Henze, N., 2005. A statistical procedure for the analysis of seismotectonically induced hydrochemical signals: A case study from the Eastern Carpathians, Romania. Tectonophysics 405, 77–98. https://doi.org/10.1016/j.tecto.2005.05.014

Hartmann, J., Levy, J.K., 2005. Hydrogeological and gasgeochemical earthquake precursors–A review for application. Natural Hazards 34, 279–304.

Hilberg, S., Riepler, F., 2016. Interaction of various flow systems in small alpine catchments: conceptual model of the upper Gurk Valley aquifer, Carinthia, Austria. Hydrogeol J 1–14. https://doi.org/10.1007/s10040-016-1396-9

Hindshaw, R.S., Tipper, E.T., Reynolds, B.C., Lemarchand, E., Wiederhold, J.G., Magnusson, J., Bernasconi, S.M., Kretzschmar, R., Bourdon, B., 2011. Hydrological control of stream water chemistry in a glacial catchment (Damma Glacier, Switzerland). Chemical Geology 285, 215–230.

Hinsby, K., Condesso de Melo, M.T., Dahl, M., 2008. European case studies supporting the derivation of natural background levels and groundwater threshold values for the protection of dependent ecosystems and human health. Science of The Total Environment 401, 1–20. https://doi.org/10.1016/j.scitotenv.2008.03.018

Hseu, Z.-Y., Su, Y.-C., Zehetner, F., Hsi, H.-C., 2017. Leaching potential of geogenic nickel in serpentine soils from Taiwan and Austria. Journal of Environmental Management, Biogeochemistry of trace elements in the environment 186, 151–157. https://doi.org/10.1016/j.jenvman.2016.02.034

Ilyashuk, B.P., Ilyashuk, E.A., Psenner, R., Tessadri, R., Koinig, K.A., 2014. Rock Glacier Outflows May Adversely Affect Lakes: Lessons from the Past and Present of Two Neighboring Water Bodies in a Crystalline-Rock Watershed. Environmental Science & Technology 48, 6192–6200. https://doi.org/10.1021/es500180c

Ingebritsen, S.E., Manga, M., 2014. Earthquakes: Hydrogeochemical precursors. Nature Geoscience 7, 697. https://doi.org/10.1038/ngeo2261

Italiano, F., Martinelli, G., Bonfanti, P., Caracausi, A., 2009. Long-term (1997-2007) geochemical monitoring of gases from the Umbria-Marche region. Tectonophysics, Ten years after the Umbria-Marche earthquake, Central Italy 476, 282–296. https://doi.org/10.1016/j.tecto.2009.02.040

Jiang, X.-W., Wang, X.-S., Wan, L., 2010. Semi-empirical equations for the systematic decrease in permeability with depth in porous and fractured media. Hydrogeology Journal 18, 839–850.

Jiang, Y., Chao, S., Liu, J., Yang, Y., Chen, Y., Zhang, A., Cao, H., 2017. Source apportionment and health risk assessment of heavy metals in soil for a township in Jiangsu Province, China. Chemosphere 168, 1658–1668. https://doi.org/10.1016/j.chemosphere.2016.11.088

Jin, Z., West, A.J., Zhang, F., An, Z., Hilton, R.G., Yu, J., Wang, J., Li, G., Deng, L., Wang, X., 2016. Seismically enhanced solute fluxes in the Yangtze River headwaters following the AD 2008 Wenchuan earthquake. Geology 44, 47–50.

Kanellopoulos, C., Argyraki, A., Mitropoulos, P., 2015. Geochemistry of serpentine agricultural soil and associated groundwater chemistry and vegetation in the area of Atalanti, Greece. Journal of Geochemical Exploration 158, 22–33. https://doi.org/10.1016/j.gexplo.2015.06.013

Kara, G.T., Kara, M., Bayram, A., Gündüz, O., 2017. Assessment of seasonal and spatial variations of physicochemical parameters and trace elements along a heavily polluted effluent-dominated stream. Environ Monit Assess 189, 585. https://doi.org/10.1007/s10661-017-6309-4

Kierczak, J., Neel, C., Aleksander-Kwaterczak, U., Helios-Rybicka, E., Bril, H., Puziewicz, J., 2008. Solid speciation and mobility of potentially toxic elements from natural and contaminated soils: a combined approach. Chemosphere 73, 776–784.

Kierczak, J., Neel, C., Bril, H., Puziewicz, J., 2007. Effect of mineralogy and pedoclimatic variations on Ni and Cr distribution in serpentine soils under temperate climate. Geoderma 142, 165–177.

Kierczak, J., Pędziwiatr, A., Waroszewski, J., Modelska, M., 2016. Mobility of Ni, Cr and Co in serpentine soils derived on various ultrabasic bedrocks under temperate climate. Geoderma 268, 78–91.

Kirkwood, C., Cave, M., Beamish, D., Grebby, S., Ferreira, A., 2016. A machine learning approach to geochemical mapping. Journal of Geochemical Exploration 167, 49–61. https://doi.org/10.1016/j.gexplo.2016.05.003

Kosugi, K., Fujimoto, M., Katsura, S., Kato, H., Sando, Y., Mizuyama, T., 2011. Localized bedrock aquifer distribution explains discharge from a headwater catchment. Water Resources Research 47. https://doi.org/10.1029/2010WR009884

Kramer, R., 1998. Chemometric techniques for quantitative analysis. Marcel Dekker New York.

Kumarathilaka, P., Oze, C., Vithanage, M., 2016. Perchlorate mobilization of metals in serpentine soils. Applied Geochemistry 74, 203–209. https://doi.org/10.1016/j.apgeochem.2016.10.009

Lecomte, K.L., Milana, J.P., Formica, S.M., Depetris, P.J., 2008. Hydrochemical appraisal of ice- and rock-glacier meltwater in the hyperarid Agua Negra drainage basin, Andes of Argentina. Hydrological processes 22, 2180–2195.

Ledin, A., Pettersson, C., Allard, B., Aastrup, M., 1989. Background concentration ranges of heavy metals in Swedish groundwaters from crystalline rocks: A review. Water Air Soil Pollut 47, 419–426. https://doi.org/10.1007/BF00279333

Lee, C.-C., Lee, C.-H., Yeh, H.-F., Lin, H.-I., 2011. Modeling spatial fracture intensity as a control on flow in fractured rock. Environmental Earth Sciences 63, 1199–1211. https://doi.org/10.1007/s12665-010-0794-x

Lei, Q., Latham, J.-P., Tsang, C.-F., 2017. The use of discrete fracture networks for modelling coupled geomechanical and hydrological behaviour of fractured rocks. Computers and Geotechnics 85, 151–176. https://doi.org/10.1016/j.compgeo.2016.12.024

Liang, J., Feng, C., Zeng, G., Gao, X., Zhong, M., Li, Xiaodong, Li, Xin, He, X., Fang, Y., 2017. Spatial distribution and source identification of heavy metals in surface soils in a typical coal mine city, Lianyuan, China. Environmental Pollution 225, 681–690. https://doi.org/10.1016/j.envpol.2017.03.057

Ling, K.-Y., Zhu, X.-Q., Tang, H.-S., Du, S.-J., Gu, J., 2018. Geology and geochemistry of the Xiaoshanba bauxite deposit, Central Guizhou Province, SW China: Implications for the behavior of trace and rare earth elements. Journal of Geochemical Exploration 190, 170–186. https://doi.org/10.1016/j.gexplo.2018.03.007

Longinelli, A., Selmo, E., 2003. Isotopic composition of precipitation in Italy: a first overall map. Journal of Hydrology 270, 75–88. https://doi.org/10.1016/S0022-1694(02)00281-0

Loska, K., Wiechuła, D., 2003. Application of principal component analysis for the estimation of source of heavy metal contamination in surface sediments from the Rybnik Reservoir. Chemosphere 51, 723–733.

MacQuarrie, K.T., Mayer, K.U., 2005. Reactive transport modeling in fractured rock: A state-of-the-science review. Earth-Science Reviews 72, 189–227.

Manga, M., Wang, C.-Y., 2015. 4.12 - Earthquake Hydrology, in: Schubert, G. (Ed.), Treatise on Geophysics (Second Edition). Elsevier, Oxford, pp. 305–328. https://doi.org/10.1016/B978-0-444-53802-4.00082-8

Martarelli, L., Petitta, M., Scalise, A.R., Silvi, A., 2008. Cartografia idrogeologica sperimentale della Piana Reatina (Lazio). Mem. Descr. Carta Geol. d'It 81, 137–156.

Martinelli, G., Dadomo, A., Italiano, F., Petrini, R., Slejko, F.F., 2017. Geochemical monitoring of the 2012 Po Valley seismic sequence: A review and update. Chemical Geology 469, 147–162. https://doi.org/10.1016/j.chemgeo.2016.12.013

Martins, V.T. de S., Pino, D.S., Bertolo, R., Hirata, R., Babinski, M., Pacheco, D.F., Rios, A.P., 2018. Who to blame for groundwater fluoride anomaly in São Paulo, Brazil? Hydrogeochemistry and isotopic evidence. Applied Geochemistry 90, 25–38. https://doi.org/10.1016/j.apgeochem.2017.12.020

Marty, C., Meister, R., 2012. Long-term snow and weather observations at Weissfluhjoch and its relation to other high-altitude observatories in the Alps. Theor Appl Climatol 110, 573–583. https://doi.org/10.1007/s00704-012-0584-3

Mastrorillo, L., Petitta, M., 2014. Hydrogeological conceptual model of the upper Chienti River Basin aquifers (Umbria-Marche Apennines). Italian Journal of Geosciences 133, 396–408.

Mastrorillo, L., Petitta, M., 2010. Effective infiltration variability in the Umbria-Marche carbonate aquifers of central Italy. Journal of Mediterranean Earth Sciences 2.

Matschullat, J., Ottenstein, R., Reimann, C., 2000. Geochemical background – can we calculate it? Environmental Geology 39, 990–1000. https://doi.org/10.1007/s002549900084

Matthews, J.A., Briffa, K.R., 2005. The 'little ice age': re-evaluation of an evolving concept. Geografiska Annaler: Series A, Physical Geography 87, 17–36. https://doi.org/10.1111/j.0435-3676.2005.00242.x

Miller, F.S., Kilminster, K.L., Degens, B., Firns, G.W., 2010. Relationship between Metals Leached and Soil Type from Potential Acid Sulphate Soils under Acidic and Neutral Conditions in Western Australia. Water Air Soil Pollut 205, 133. https://doi.org/10.1007/s11270-009-0061-5

Montgomery, D.R., Manga, M., 2003. Streamflow and Water Well Responses to Earthquakes. Science 300, 2047–2049. https://doi.org/10.1126/science.1082980

Morelli, G., Rimondi, V., Benvenuti, M., Medas, D., Costagliola, P., Gasparon, M., 2017. Experimental simulation of arsenic desorption from Quaternary aquifer sediments following sea water intrusion. Applied Geochemistry 87, 176–187. https://doi.org/10.1016/j.apgeochem.2017.10.024

Morettini, E., Santantonio, M., Bartolini, A., Cecca, F., Baumgartner, P.., Hunziker, J.., 2002. Carbon isotope stratigraphy and carbonate production during the Early–Middle Jurassic: examples from the Umbria–Marche–Sabina Apennines (central Italy). Palaeogeography, Palaeoclimatology, Palaeoecology 184, 251–273. https://doi.org/10.1016/S0031-0182(02)00258-4

Morgantini, N., Frondini, F., Cardellini, C., 2009. Natural trace elements baselines and dissolved loads in groundwater from carbonate aquifers of central Italy. Physics and Chemistry of the Earth, Parts A/B/C, Advances in Sustainable Management of Water Quality on Catchment Scale 34, 520–529. https://doi.org/10.1016/j.pce.2008.05.004

Morrison, J.M., Goldhaber, M.B., Mills, C.T., Breit, G.N., Hooper, R.L., Holloway, J.M., Diehl, S.F., Ranville, J.F., 2015. Weathering and transport of chromium and nickel from serpentinite in the Coast Range ophiolite to the Sacramento Valley, California, USA. Applied Geochemistry 61, 72–86.

Muhammad, S., Shah, M.T., Khan, S., 2011. Health risk assessment of heavy metals and their source apportionment in drinking water of Kohistan region, northern Pakistan. Microchemical Journal 98, 334–343. https://doi.org/10.1016/j.microc.2011.03.003

Muir-Wood, R., King, G.C.P., 1993. Hydrological signatures of earthquake strain. J. Geophys. Res. 98, 22035–22068. https://doi.org/10.1029/93JB02219

Muntener, O., Hermann, J., Trommsdorff, V., 2000. Cooling History and Exhumation of Lower-Crustal Granulite and Upper Mantle (Malenco, Eastern Central Alps). J. Petrol. 41, 175–200. https://doi.org/10.1093/petrology/41.2.175

Nagabhushanam, P., Reddy, D.V., 2011. Groundwater electrical conductivity and soil radon gas monitoring for earthquake precursory studies in Koyna, India. Applied Geochemistry 26, 731–737. https://doi.org/10.1016/j.apgeochem.2011.01.031

Nanni, T., Rusi, S., 2003. Idrogeologia del massiccio carbonatico della montagna della Majella (Appennino centrale). Bollettino della Società geologica italiana 122, 173–202.

Nriagu, J.O., 1989. A global assessment of natural sources of atmospheric trace metals. Nature 338, 47–49.

Oda, M., 1985. Permeability tensor for discontinuous rock masses. Géotechnique 35, 483–495. https://doi.org/10.1680/geot.1985.35.4.483

Ou, C., St-Hilaire, A., Ouarda, T.B.M.J., Conly, F.M., Armstrong, N., Khalil, B., Proulx-McInnis, S., 2012. Coupling geostatistical approaches with PCA and fuzzy optimal model (FOM) for the integrated assessment of sampling locations of water quality monitoring networks (WQMNs). Journal of Environmental Monitoring 14, 3118. https://doi.org/10.1039/c2em30372h

Pasvanoglu, S., Canik, B., Rosen, M.R., 2004. Hydrogeology and Possible Effects of the Mw 7.4 Marmara Earthquake (17 August 1999) on the Spring Waters in the Orhangazi-Bursa Area, Hirkey. Geological Society of India 63, 313–322.

Pelica, J., Barbosa, S., Reboredo, F., Lidon, F., Pessoa, F., Calvão, T., 2018. The paradigm of high concentration of metals of natural or anthropogenic origin in soils – The case of Neves-Corvo mine area (Southern Portugal). Journal of Geochemical Exploration 186, 12–23. https://doi.org/10.1016/j.gexplo.2017.11.021

Peña Reyes, F.A., Crosta, G.B., Frattini, P., Basiricò, S., Della Pergola, R., 2015. Hydrogeochemical overview and natural arsenic occurrence in groundwater from alpine springs (upper Valtellina, Northern Italy). Journal of Hydrology 529, 1530–1549. https://doi.org/10.1016/j.jhydrol.2015.08.029

Petitta, M., Mastrorillo, L., Preziosi, E., Banzato, F., Barberio, M.D., Billi, A., Cambi, C., De Luca, G., Di Carlo, G., Di Curzio, D., Di Salvo, C., Nanni, T., Palpacelli, S., Rusi, S., Saroli, M., Tallini, M., Tazioli, A., Valigi, D., Vivalda, P., Doglioni, C., 2018. Water-table and discharge changes associated with the 2016–2017 seismic sequence in central Italy: hydrogeological data and a conceptual model for fractured carbonate aquifers. Hydrogeology Journal. https://doi.org/10.1007/s10040-017-1717-7

Petitta, M., Primavera, P., Tuccimei, P., Aravena, R., 2011. Interaction between deep and shallow groundwater systems in areas affected by Quaternary tectonics (Central Italy): a geochemical and isotope approach. Environmental Earth Sciences 63, 11–30. https://doi.org/10.1007/s12665-010-0663-7

Poitrasson, F., Dundas, S.H., Toutain, J.-P., Munoz, M., Rigo, A., 1999. Earthquake-related elemental and isotopic lead anomaly in a springwater. Earth and Planetary Science Letters 169, 269–276. https://doi.org/10.1016/S0012-821X(99)00085-0

Pozzorini, D., FruhGreen, G.L., 1996. Stable isotope systematics of the Ventina ophicarbonate zone, Bergell contact aureole. Schweizerische Mineralogische und Petrographische Mitteilungen 76, 549–564.

Pueyo, M., Mateu, J., Rigol, A., Vidal, M., López-Sánchez, J.F., Rauret, G., 2008. Use of the modified BCR three-step sequential extraction procedure for the study of trace element dynamics in contaminated soils. Environmental pollution 152, 330–341.

Rajapaksha, A.U., Vithanage, M., Oze, C., Bandara, W.M.A.T., Weerasooriya, R., 2012. Nickel and manganese release in serpentine soil from the Ussangoda Ultramafic Complex, Sri Lanka. Geoderma 189–190, 1–9. https://doi.org/10.1016/j.geoderma.2012.04.019

Reddy, D.V., Nagabhushanam, P., Sukhija, B.S., 2011. Earthquake (M 5.1) induced hydrogeochemical and δ18O changes: validation of aquifer breaching—mixing model in Koyna, India. Geophysical Journal International 184, 359–370. https://doi.org/10.1111/j.1365-246X.2010.04838.x

Reimann, C., Fabian, K., Birke, M., Filzmoser, P., Demetriades, A., Négrel, P., Oorts, K., Matschullat, J., de Caritat, P., 2018. GEMAS: Establishing geochemical background and threshold for 53 chemical elements in European agricultural soil. Applied Geochemistry, SI: ISEG 2016 88, 302–318. https://doi.org/10.1016/j.apgeochem.2017.01.021

Reimann, C., Filzmoser, P., Garrett, R.G., 2005. Background and threshold: critical comparison of methods of determination. Science of The Total Environment 346, 1–16. https://doi.org/10.1016/j.scitotenv.2004.11.023

Reimann, C., Garrett, R.G., 2005. Geochemical background—concept and reality. Science of The Total Environment 350, 12–27. https://doi.org/10.1016/j.scitotenv.2005.01.047

Renberg, I., Brännvall, M.-L., Bindler, R., Emteryd, O., 2002. Stable lead isotopes and lake sediments—a useful combination for the study of atmospheric lead pollution history. Science of The Total Environment, Peat Bog Archives of Atmospheric Metal Deposition 292, 45–54. https://doi.org/10.1016/S0048-9697(02)00032-3

Roberts, G.P., Cowie, P., Papanikolaou, I., Michetti, A.M., 2004. Fault scaling relationships, deformation rates and seismic hazards: an example from the Lazio–Abruzzo Apennines, central Italy. Journal of Structural Geology 26, 377–398. https://doi.org/10.1016/S0191-8141(03)00104-4

Roberts, G.P., Michetti, A.M., 2004. Spatial and temporal variations in growth rates along active normal fault systems: an example from The Lazio–Abruzzo Apennines, central Italy. Journal of Structural Geology 26, 339–376. https://doi.org/10.1016/S0191-8141(03)00103-2

Rose, A.W., Hawkes, H.E., Webb, J.S., 1979. Geochemistry in mineral exploration. Academic press London.

Rosen, M.R., Binda, G., Archer, C., Pozzi, A., Michetti, A.M., Noble, P.J., 2018. Mechanisms of earthquake induced chemical and fluid transport to carbonate groundwater springs after earthquakes. Water Resources Research. https://doi.org/10.1029/2017WR022097

Ross, A., Willson, V.L., 2017. One-Way Anova, in: Basic and Advanced Statistical Tests. Sense Publishers, Rotterdam, pp. 21–24. https://doi.org/10.1007/978-94-6351-086-8_5

Rowland, J.C., Manga, M., Rose, T.P., 2008. The influence of poorly interconnected fault zone flow paths on spring geochemistry. Geofluids 8, 93–101. https://doi.org/10.1111/j.1468-8123.2008.00208.x

Runnells, D.D., Shepherd, T.A., Angino, E.E., 1992. Metals in water. Determining natural background concentrations in mineralized areas. Environ. Sci. Technol. 26, 2316–2323. https://doi.org/10.1021/es00036a001

Sahariah, B., Goswami, L., Farooqui, I.U., Raul, P., Bhattacharyya, P., Bhattacharya, S., 2015. Solubility, hydrogeochemical impact, and health assessment of toxic metals in municipal wastes of two differently populated cities. Journal of Geochemical Exploration 157, 100–109.

Santolaria, Z., Arruebo, T., Pardo, A., Rodríguez-Casals, C., Matesanz, J.M., Lanaja, F.J., Urieta, J.S., 2017. Natural and anthropic effects on hydrochemistry and major and trace elements in the water mass of a Spanish Pyrenean glacial lake set. Environmental Monitoring and Assessment 189. https://doi.org/10.1007/s10661-017-6023-2

Sarma, D.D., 2010. Geostatistics with applications in earth sciences. Springer Science & Business Media.

Schmid, S.M., Fügenschuh, B., Kissling, E., Schuster, R., 2004. Tectonic map and overall architecture of the Alpine orogen. Eclogae Geologicae Helvetiae 97, 93–117.

Schneider, P., Nilius, U., Gottschalk, N., Süß, A., Schaffrath, M., Löser, R., Lange, T., 2017. Determination of the Geogenic Metal Background in Surface Water: Benchmarking Methodology for the Rivers of Saxony-Anhalt, Germany. Water 9, 75. https://doi.org/10.3390/w9020075

Scholz, C.H., 1977. A physical interpretation of the Haicheng earthquake prediction. Nature 267, 121. https://doi.org/10.1038/267121a0

Seewald, J.S., Seyfried, W.E., 1990. The effect of temperature on metal mobility in subseafloor hydrothermal systems: Constraints from basalt alteration experiments: Earth and Planetary Science Letters, 101, 388 403.

Shah, M.H., Iqbal, J., Shaheen, N., Khan, N., Choudhary, M.A., Akhter, G., 2012. Assessment of background levels of trace metals in water and soil from a remote region of Himalaya. Environmental Monitoring and Assessment 184, 1243–1252. https://doi.org/10.1007/s10661-011-2036-4

Silver, P.G., Wakita, H., 1996. A search for earthquake precursors. Science; Washington 273, 77.

Skelton, A., Andrén, M., Kristmannsdóttir, H., Stockmann, G., Mörth, C.-M., Sveinbjörnsdóttir, Á., Jónsson, S., Sturkell, E., Guðrúnardóttir, H.R., Hjartarson, H., Siegmund, H., Kockum, I., 2014. Changes in groundwater chemistry before two consecutive earthquakes in Iceland. Nature Geoscience 7, 752. https://doi.org/10.1038/ngeo2250

Sollitto, D., Romic, M., Castrignanò, A., Romic, D., Bakic, H., 2010. Assessing heavy metal contamination in soils of the Zagreb region (Northwest Croatia) using multivariate geostatistics. Catena 80, 182–194.

Sommaruga-Wögrath, S., Koinig, K.A., Schmidt, R., Sommaruga, R., Tessadri, R., Psenner, R., 1997. Temperature effects on the acidity of remote alpine lakes. Nature 387, 64–67.

Spadoni, M., Brilli, M., Giustini, F., Petitta, M., 2009. Using GIS for modelling the impact of current climate trend on the recharge area of the S. Susanna spring (central Apennines, Italy). Hydrological Processes 24, 50–64. https://doi.org/10.1002/hyp.7452

StatSoft, Inc., 2007. STATISTICA (data analysis software system), version 8.0. www.statsoft.com.

Su, S., Li, D., Zhang, Q., Xiao, R., Huang, F., Wu, J., 2011. Temporal trend and source apportionment of water pollution in different functional zones of Qiantang River, China. Water Research 45, 1781–1795. https://doi.org/10.1016/j.watres.2010.11.030

Tarragoni, C., 2006. Determinazione della "quota isotopica" del bacino di alimentazione delle principali sorgenti dell'alta Valnerina. Geologica Romana 8.

Tassi, E., Grifoni, M., Bardelli, F., Aquilanti, G., La Felice, S., Iadecola, A., Lattanzi, P., Petruzzelli, G., 2018. Evidence for the natural origins of anomalously high chromium levels in soils of the Cecina Valley (Italy). Environmental Science: Processes & Impacts. https://doi.org/10.1039/C8EM00063H

Tessier, A., Campbell, P.G., Bisson, M., 1979. Sequential extraction procedure for the speciation of particulate trace metals. Analytical chemistry 51, 844–851.

Tranter, M., 2003. Geochemical weathering in glacial and proglacial environments. Treatise on geochemistry 5, 605.

Trimmer, D., Bonner, B., Heard, H.C., Duba, A., 1980. Effect of pressure and stress on water transport in intact and fractured gabbro and granite. Journal of Geophysical Research: Solid Earth 85, 7059–7071.

Trommsdorff, V., Evans, B.W., 1977. Antigorite-ophicarbonates: contact metamorphism in Valmalenco, Italy. Contributions to Mineralogy and Petrology 62, 301–312.

Trommsdorff, V., Montrasio, A., Hermann, J., Muntener, O., Spillmann, P., Giere, R., 2007. The geological map of Valmalenco.

Tsunogai, U., Wakita, H., 1995. Precursory chemical changes in ground water: Kobe earthquake, Japan. Science 61–61.

Ulomov, V. I., Mavashev, B. Z., 1967. On Forerunner of a Strong Tectonic Earthquake, Doklady Akademii nauk SSSR, 176, 319-322

Vallet, A., Bertrand, C., Mudry, J., Bogaard, T., Fabbri, O., Baudement, C., Régent, B., 2015. Contribution of time-related environmental tracing combined with tracer tests for characterization of a groundwater conceptual model: a case study at the Séchilienne landslide,

western Alps (France). Hydrogeology Journal 23, 1761–1779. https://doi.org/10.1007/s10040-015-1298-2

Vaselli, O., Buccianti, A., De Siena, C., Bini, C., Coradossi, N., Angelone, M., 1997. Geochemical characterization of ophiolitic soils in a temperate climate: a multivariate statistical approach. Geoderma 75, 117–133.

Vittori, E., Di Manna, P., Blumetti, A.M., Comerci, V., Guerrieri, L., Esposito, E., Michetti, A.M., Porfido, S., Piccardi, L., Roberts, G.P., 2011. Surface faulting of the 6 April 2009 M w 6.3 L'Aquila earthquake in Central Italy. Bulletin of the Seismological Society of America 101, 1507–1530.

Viviroli, D., Dürr, H.H., Messerli, B., Meybeck, M., Weingartner, R., 2007. Mountains of the world, water towers for humanity: Typology, mapping, and global significance. Water Resources Research 43. https://doi.org/10.1029/2006WR005653

von Gunten, H.R., Sturm, M., Moser, R.N., 1997. 200-Year Record of Metals in Lake Sediments and Natural Background Concentrations. Environ. Sci. Technol. 31, 2193–2197. https://doi.org/10.1021/es960616h

Voutsis, N., Kelepertzis, E., Tziritis, E., Kelepertsis, A., 2015. Assessing the hydrogeochemistry of groundwaters in ophiolite areas of Euboea Island, Greece, using multivariate statistical methods. Journal of Geochemical Exploration 159, 79–92.

Wang, C.-H., Wang, C.-Y., Kuo, C.-H., Chen, W.-F., 2005. Some isotopic and hydrological changes associated with the 1999 Chi-Chi earthquake, Taiwan. Island Arc 14, 37–54.

Wang, C.-Y., Manga, M., 2015. New streams and springs after the 2014 Mw6.0 South Napa earthquake. Nature Communications 6, 7597. https://doi.org/10.1038/ncomms8597

Ward, J.H., 1963. Hierarchical Grouping to Optimize an Objective Function. Journal of the American Statistical Association 58, 236–244. https://doi.org/10.1080/01621459.1963.10500845

Wedepohl, K.H., 1995. The composition of the continental crust. Geochimica et Cosmochimica Acta 59, 1217–1232. https://doi.org/10.1016/0016-7037(95)00038-2

Welch, L.A., Allen, D.M., 2014. Hydraulic conductivity characteristics in mountains and implications for conceptualizing bedrock groundwater flow. Hydrogeol J 22, 1003–1026. https://doi.org/10.1007/s10040-014-1121-5

Woith, H., Wang, R., Maiwald, U., Pekdeger, A., Zschau, J., 2013. On the origin of geochemical anomalies in groundwaters induced by the Adana 1998 earthquake. Chemical Geology 339, 177–186. https://doi.org/10.1016/j.chemgeo.2012.10.012

Yuan, Y., Cave, M., Zhang, C., 2018. Using Local Moran's I to identify contamination hotspots of rare earth elements in urban soils of London. Applied Geochemistry, SI: ISEG 2016 88, 167–178. https://doi.org/10.1016/j.apgeochem.2017.07.011

Zhang, C., Luo, L., Xu, W., Ledwith, V., 2008. Use of local Moran's I and GIS to identify pollution hotspots of Pb in urban soils of Galway, Ireland. Science of The Total Environment 398, 212–221. https://doi.org/10.1016/j.scitotenv.2008.03.011

Zhen, S., Yan, Z., Zhang, Y., Wang, J., Campbell, M., Qin, W., 2009. Column bioleaching of a low grade nickel-bearing sulfide ore containing high magnesium as olivine, chlorite and antigorite. Hydrometallurgy 96, 337–341. https://doi.org/10.1016/j.hydromet.2008.11.007

Zhou, J., Ma, D., Pan, J., Nie, W., Wu, K., 2008. Application of multivariate statistical approach to identify heavy metal sources in sediment and waters: a case study in Yangzhong, China. Environmental Geology 54, 373–380.

7 Appendix 1: Detailed methods for samples chemical analyses and QA/QC protocols

The methods applied in all the provided case studies follow techniques usually applied for water quality analyses.

These methods can be firstly classified in on-site analysis, directly made in the spring, and off-site analyses, including the collection of samples in bottles, to process them after in laboratory for analyses. The off-site analyses include, moreover, a pretreatment of the glassware due to type of analyses.

On site analyses include the measurement of physio-chemical parameters, and the analyses of alkalinity and hardness through MERCK titration kit.

Data reliability was obtained through the application of Quality Assurance/Quality control protocols: for examples, laboratory, environmental and instrumental blank were analyzed, instrumental and sampling precision were analyzed through analysis of replicates and using internal and external standards.

Most of the analysis applied during my PhD dissertation were performed in the Università degli Studi dell'Insubria, Dipartimento di Scienza e Alta Tecnologia, Como, Italy laboratories, only isotopic analyses were performed at the stable isotopes laboratory in University of Nevada, Reno, USA.

If not different specified along the other chapters of the dissertation, the methods used are listed in the following sections.

7.1 Reagents and solutions

All the solutions used in Università dell'Insubria laboratories in Como (Italy) for the study presented in this dissertation were made using ultrapure water from a Millipore (USA) MilliQ system (18.8MΩcm resistivity). Nitric and hydrochloric acid solutions were obtained from a Carlo Erba® (Italy) reagents 65% volume solution; ultrapure nitric acid for trace element analysis was obtained by subboiling distillation of 65% acid using Milestone (USA) duoPUR. Washing solution for all laboratory and sampling glassware was obtained from dilution of NALGENE® (USA) L900 in ultrapure water. Standard solutions for ionic chromatography were obtained from single analyte standard solutions from MERCK (Germany), and standard

solutions for trace-element analysis were obtained from dilution of certiPUR® ICP multi-elemental standard MERCK (Germany). All reagents used in extraction solutions (acetic acid, hydroxylamine hydrochloride, hydrogen peroxide and ammonium acetate) were diluted from Carlo Erba® pure reagent grade (Italy).

7.2 Glassware preparation and washing

All laboratory and field operation were made using nitrile gloves to avoid any kind of samples contamination.

All LPDE bottles used were pre-washed using a NALGENE L900 (USA) soap solution with ultrapure water. Then bottles and vials were differently washed functionally to the analysis to perform:

- Glassware for major anions analysis was just rinsed with ultrapure water and then air dried;
- Glassware for major cations was washed with a solution of 2% HNO3 after the first washing, and then rinsed and air dried;
- Glassware for trace metals analysis

7.3 Water On-site analyses and samples collection

The physio-chemical parameters of pH, temperature and electrical conductivity (EC) were evaluated on site using specific field probes: a HANNA Instruments (USA) HI 9025 pH-meter equipped with sensors for pH and temperature and a HANNA Instruments HI 9033 conductivity probe for electrical conductivity. Hardness and alkalinity were directly evaluated on site using MERCK (Germany) titration kits. All field sampling and analysis procedures were made wearing nitrile gloves to avoid samples contaminations.

Samples for laboratory analysis were filtered on site with a 0.45 micrometer sterile Millex-GS millipore MCE membrane and transferred to LPDE bottles (washed as described in section 7.2). sample bottles were rinsed three times with the water to be collected before being filled.

7.4 Waters off-site analyses

7.4.1 Alkalinity colorimetric titration

Carbonates as HCO_3 were estimated by colorimetric titration using 0,01 M HCl and Bromocresol Green as indicator.

7.4.2 Ionic chromatography

Chromatography is a separation technique used for the analysis of complex environmental matrices, to separate different analytes in function of their retention times and quantify them through an external calibration with standards. For this technique are fundamental a regular flow, because the analytes are recognized for time, and the right choice for column (stationary phase) and carrier (mobile phase).

The basic scheme of a liquid chromatographer includes a pump to keep a regular flow in the system, a samples injector, a column to separate of the different analytes and a detector to observe signal intensities in function of the concentration. In more detail, ionic chromatography permits the separation of major anions and cations in water samples using low salinity solutes as mobile phase, a ionic change resin-filled column as stationary phase,

Major anions (F, Cl, NO_2, NO_3, SO_4, PO_4) and cations (Ca, Mg, Na, NH_4, K) were estimated using an ionic chromatography Metrohm Eco IC equipped with an 883 Compact Autosampler, with different settings for the analysis of anions and cations. More specifically for anion test samples were filtered through 0,45 µm polypropylene filters and analyzed using a Metrohm Metrosep A Supp 5 column and a 3,2 mmol/l Sodium carbonate and 1 mmol/l sodium bicarbonate solution as eluent; while cation samples after filtration were acidified with 1M nitric acid to obtain a pH 2 solution, and then analyzed using a Metrohm Metrosep C4- 150 column and a 5mmol/l phosphoric acid solution as eluent.

The limit of detection (LOD) of the technique was calculated as 0.05 ppm. Ionic balances were calculated to assess data reliability following the equation:

$$\frac{\sum anions - \sum cations}{\sum anions + \sum cations}$$

Where cations and anions concentrations are expressed as milliequivalent per liter (Chapra, 2008).

7.4.3 Inductively Coupled Plasma – Mass Spectrometry (ICP-MS)

Trace elements were analyzed in Insubria University laboratory using a ICP-MS Icap-Q Thermo Scientific (USA). This instrument includes a plasma source with quartz torch and plastic nebulizer with a platinum injector and it is equipped with a collision chamber to avoid different interferences due to polyatomic species usually formed in the plasma (i.e., ArCl with the same mass of As, or ArO with the same mass of Fe; Fishman and Friedman, 1989). The instrument is also equipped with a Cetac ASX 260 autosampler.

Samples for trace element analysis were acidified with 2% ultrapure HNO_3. LODs were calculates as three times the standard deviations of blank samples and the values for all trace metals analyzed in this dissertation are included in Table 7.1

Element	LOD (µg/L)
Li	0.08300
B	0.02568
Al	0.05350
V	0.00070
Cr	0.00310
Mn	0.00216
Fe	0.01888
Co	0.00024
Ni	0.00475
Cu	0.00105
As	0.00181
Rb	0.00151
Sr	0.00115
Cd	0.00042
Pb	0.00021
U	0.00002

Table 7.1: limit of detections of trace elements analyzed through ICP-MS.

7.4.4 Isotopes

Water, sulfate and dissolved inorganic carbon isotopes were analyzed along the 2016-2017 seismic sequence in Central Italy (chapter 3). Waters were prepared for isotopic analysis by precipitation of dissolved sulfate as $BaSO_4$. $BaSO_4$ precipitates were analyzed for $\delta^{34}S_{SO4}$ using V_2O_5 as a combustion aid and followed the methods of Giesemann et al. (1994). $BaSO_4$ precipitates were analyzed for $\delta^{18}O_{SO4}$ following the method of Kornexl et al. (1999). The analytical error (one sigma), estimated by replicate analysis, was ±0.2‰ and ± 0.4 ‰ for $\delta^{34}S_{SO4}$ and $\delta^{18}O_{SO4}$, respectively.

Water samples were prepared for isotopic analysis of dissolved inorganic carbon by precipitation as $SrCO_3$ after the method of Usdowski et al. (1979), and then analyzed using the method of Harris et al. (1997), with analytical error within ±0.2‰. Waters were analyzed for $\delta^{18}O_{H2O}$ using the CO_2 - H_2O equilibration method of Epstein and Mayeda (1953), and for $\delta^{2}H_{H2O}$ using the method of Morrison et al. (2001). The analytical error of these measurements was ±0.1‰ and ±1.0 ‰ for $\delta^{18}O_{H2O}$ and $\delta^{2}H_{H2O}$, respectively. All stable isotope analyses were carried out at the University of Nevada, Reno Stable Isotope lab. All values are reported using delta notation (δ‰), and the standards used were V-SMOW for oxygen and hydrogen, V-PDB for carbon and V-CDT for sulfur. Between 5 and 10% of all analyses were run as replicates to determine reproducibility of the results. All replicates were within 10% of the original value.

7.4.5 QA/QC protocols for water analysis

Precision for the different techniques for water analysis was obtained through analysis of replicates.

Solutions for major ions and trace elements analysis were spiked with internal standards to control and correct instrument drifts through the samples analyses. To certify the quality of analysis and observe possible instrumental bias, an internal standard with 10 ppb of indium (In) was spiked in all the samples. The recovery of In spikes were all within 10% of the value of the spiked added.

Sampling and analysis errors were evaluated through the analysis of blank samples.

7.5 Solid samples chemical analyses

The analysis of the geochemical background in the study area (chapter 2) requested the solid samples analyses for total load of metal in solid phase, and also speciation understanding through sequential extractions in part of the samples was performed to observe Ni anomalies (chapter 4.1).

Sequential extractions we applied using a protocol modified from the European standardized extraction

7.5.1 Samples collection and pre-treatment

Once in laboratory, samples were air-dried in oven at 105 °C for 3 h (Quevauviller, 1998), coarser grains were removed and the finer fraction (< 2 mm) was homogenized and pulverized to<0.075mm in an agate mill (Chabukdhara and Nema, 2012).

7.5.2 Samples sequential extractions

A three-step sequential extraction (Pueyo et al., 2008) was performed to analyze the possible dissolution of different metals species in water. This procedure includes different leaching solutions to extract metals from the soil sample: each solution contains a series of progressively harsher chemical reagents to dissolve selectively only specific mineral and organic phases of the sample (Filgueiras et al., 2002; Tessier et al., 1979).

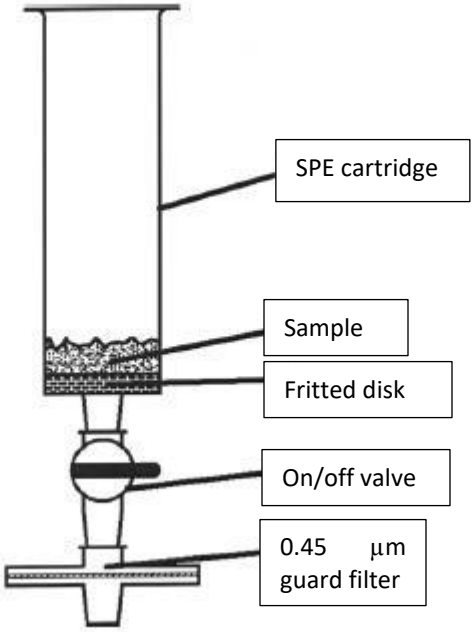

Figure 7.1: representation of the system used for the sequential extractions in our laboratory (modified from Ciceri et al., 2008)

Speciation analysis was performed using a methodology implemented in our laboratory using the BCR-701 as reference material (Ciceri et al., 2008). 100 mg of dry solid sample are weighted and collected in polypropylene special Solid Phase Extraction (SPE) empty column with a valve put at the end. The three sequential extraction steps make use of the following solutions:

• step 1: 4 mL of 0.11M acetic acid. This solution can extract exchangeable metal, and elements bond to labile forms (i.e., carbonates);

• step 2: 4 mL 0.11M hydroxylamine hydrochloride solution, dissolving reducible forms (e.g., Fe and Mn oxides);

• step 3: 1 mL of hydrogen peroxide (33% in weight), then left in digestion 1 h at 85 ± 2 °C in a water bath. Another 1 mL aliquot and another digestion a room temperature. Then 5 mL of 1M ammonium acetate was added to the residue. This solution can dissolve oxidable species like sulphides and strong organic ligands.

For every step, the solution was added in the SPE column and then shaken overnight, the solution was separated from the solid using a filtration system and not by centrifugation, as in the standard protocol of sequential extractions (Pueyo et al., 2008); this approach was

applied because filtering avoids any loss of sample for the following extraction step, especially with fine grained ones.

After every separation step, the residual was washed before being extracted with the next solution: firstly, it was rinsed with a 2 mL aliquot of the same step extracting solution, then washed two times with ultrapure water and sonicated for 20 min. All the separations of solid and liquid phase during the wash were done filtering as done in the extractions. Finally, the solid residual was air-dried before the application of the following step. All the solutions were then analyzed with ICP-MS instrumentation for metals concentrations (section 7.4.3 for more details).

7.5.3 Acid micro wave assisted digestion

All sediment samples were digested using a pure hydrochloric and nitric acid solution in proportion 1:3 (aqua regia). 500 mg of sample were inserted in Teflon vessels, and 3 mL of solution were added. The digestion was made in a MLS-1200 Mega, Milestone (USA) microwave. After cooling, the solution was diluted with ultrapure water. Differently from other digestion with different acids which can dissolve even most resistant silicates phases (i.e., hydrofluoric acid), this digestion (also called pseudo-total digestion) could underestimate the overall load of metals, but different studies and procedures applied it to understand the ratio between the exchangeable phase and the total (Kanellopoulos et al., 2015).

The solutions extracted from sequential extractions and from acid digestions were analyzed using a Thermo-scientific (USA) Icap Q ICP-MS instrument, as the water samples.

7.5.4 QA/QC protocols for solid samples analyses

The digestion was applied to bulk solid samples and from the residual of the 3 extraction steps to calculate the extraction recoveries as in the equation:

$$recovery = \frac{s1 + s2 + s3 + ad_r}{ad_b}$$

where s1, s2 and s3 are the extraction steps, ad_r is the acid digestion of the residual and ad_b is the acid digestion value from the bulk sample (Cheng et al., 2011; Rajapaksha et al., 2012).

Samples were run in triplicate and present less than 5% of relative standard deviation. LODs were calculated as three times the standard deviation of blank samples and are listed in Table 7.2. Blanks were made analyzing only the extracting solution for every single step.

Acid digestion and sequential extraction methods were standardized in our laboratory using BCR-701 reference material (Ciceri et al., 2008).

Technique	acid digestion	Step 1	Step 2	Step 3
Measure unit	**mg/kg**	**mg/kg**	**mg/kg**	**mg/kg**
Co	0.3	0.41	0.11	0.5
Cr	0.22	0.07	0.12	0.44
Cu	0.18	0.03	0.02	0.11
Mn	0.12	0.2	0.33	0.05
Ni	0.03	0.22	0.19	0.11
Fe	0.08	0.1	0.14	0.12
Zn	0.41	-	-	-
As	0.95	-	-	-
Ag	0.75	-	-	-
Pb	0.03	-	-	-
Cd	0.39	-	-	-

Table 7.2: LODs for the different extraction techniques.

8 Appendix 2: published papers through the PhD project

Along my PhD project, papers regarding geochemical anomalies were submitted and published, and also 2 papers regarding geological data collected along the 2016-2017 sequence were published (which are not discussed in my dissertation). I suggest consulting the papers for major details. Published papers include:

- Rosen, M.R., Binda, G., Archer, C., Pozzi, A., Michetti, A.M., Noble, P.J., 2018. Mechanisms of earthquake induced chemical and fluid transport to carbonate groundwater springs after earthquakes. Water Resources Research. https://doi.org/10.1029/2017WR022097 (discussed in chapter 3)
- Binda, G., Pozzi, A., Livio, F., Piasini, P., Zhang, C., 2018. Anomalously high concentration of Ni as sulphide phase in sediment and in water of a mountain catchment with serpentinite bedrock. Journal of Geochemical Exploration 190, 58–68. https://doi.org/10.1016/j.gexplo.2018.02.014 (discussed in chapter 4.1)
- Villani, F., Civico, R., Pucci, S., Pizzimenti, L., Nappi, R., De Martini, P. M., et al., 2018. A database of the coseismic effects following the 30 October 2016 Norcia earthquake in Central Italy. Scientific data, 5, 180049. https://doi.org/10.1038/sdata.2018.49
- Civico, R., Pucci, S., Villani, F., Pizzimenti, L., De Martini, P. M., Nappi, R. et al., 2018. Surface ruptures following the 30 October 2016 M_w 6.5 Norcia earthquake, central Italy. Journal of Maps, 14:2, 151-160. https://doi.org/10.1080/17445647.2018.1441756

9 Appendix 3: Supplementary material

Supplementary material is included in .zip format.

This material includes 7 files, indexes as follow:

- Supplementary_01: all chemical measured variables of water samples in the Ventina valley (chapter 2 and 4.2);
- Supplementary_02: all measured variables and sites for physico-chemical parameters, major ions and trace elements in Central Italy (chapter 3);
- Supplementary_03: table for isotopic data for water samples in Central Italy;
- Supplementary_04: rainfall data and correlation matrices with trace elements for Central Italy;
- Supplementary_05: probe data and collected rainfall data for Central Italy;
- Supplementary_06: Detailed fracture data collected on site and stereoplots;
- Supplementary_07: gps projected coordinates (in UTM32N format) of all sampling sites.

10 Appendix references

Chabukdhara, M., Nema, A.K., 2012. Assessment of heavy metal contamination in Hindon River sediments: a chemometric and geochemical approach. Chemosphere 87, 945–953.

Chapra, S.C., 2008. Surface water-quality modeling. Waveland press.

Cheng, C.-H., Jien, S.-H., Iizuka, Y., Tsai, H., Chang, Y.-H., Hseu, Z.-Y., 2011. Pedogenic Chromium and Nickel Partitioning in Serpentine Soils along a Toposequence. Soil Science Society of America journal.

Ciceri, E., Giussani, B., Pozzi, A., Dossi, C., Recchia, S., 2008. Problems in the application of the three-step BCR sequential extraction to low amounts of sediments: an alternative validated route. Talanta 76, 621–626.

Epstein, S., Mayeda, T., 1953. Variation of O18 content of waters from natural sources. Geochimica et Cosmochimica Acta 4, 213–224. https://doi.org/10.1016/0016-7037(53)90051-9

Filgueiras, A.V., Lavilla, I., Bendicho, C., 2002. Chemical sequential extraction for metal partitioning in environmental solid samples. Journal of Environmental Monitoring 4, 823–857. https://doi.org/10.1039/B207574C

Fishman, M.J., Friedman, L.C., 1989. Methods for determination of inorganic substances in water and fluvial sediments. Geological Survey (US).

Giesemann, A., Jaeger, H.-J., Norman, A.L., Krouse, H.R., Brand, W.A., 1994. Online Sulfur-Isotope Determination Using an Elemental Analyzer Coupled to a Mass Spectrometer. Analytical Chemistry 66, 2816–2819. https://doi.org/10.1021/ac00090a005

Harris, D., Porter, L.K., Paul, E.A., 1997. Continuous flow isotope ratio mass spectrometry of carbon dioxide trapped as strontium carbonate. Communications in Soil Science and Plant Analysis 28, 747–757. https://doi.org/10.1080/00103629709369827

Kanellopoulos, C., Argyraki, A., Mitropoulos, P., 2015. Geochemistry of serpentine agricultural soil and associated groundwater chemistry and vegetation in the area of Atalanti, Greece. Journal of Geochemical Exploration 158, 22–33. https://doi.org/10.1016/j.gexplo.2015.06.013

Kornexl, B.E., Gehre, M., Höfling, R., Werner, R.A., 1999. On-line δ18O measurement of organic and inorganic substances. Rapid Communications in Mass Spectrometry 13, 1685–

1693. https://doi.org/10.1002/(SICI)1097-0231(19990830)13:16<1685::AID-RCM699>3.0.CO;2-9

Morrison, J., Brockwell, T., Merren, T., Fourel, F., Phillips, A.M., 2001. On-Line High-Precision Stable Hydrogen Isotopic Analyses on Nanoliter Water Samples. Analytical Chemistry 73, 3570–3575. https://doi.org/10.1021/ac001447t

Pueyo, M., Mateu, J., Rigol, A., Vidal, M., López-Sánchez, J.F., Rauret, G., 2008. Use of the modified BCR three-step sequential extraction procedure for the study of trace element dynamics in contaminated soils. Environmental pollution 152, 330–341.

Quevauviller, P., 1998. Operationally defined extraction procedures for soil and sediment analysis I. Standardization. TrAC Trends in Analytical Chemistry 17, 289–298.

Rajapaksha, A.U., Vithanage, M., Oze, C., Bandara, W.M.A.T., Weerasooriya, R., 2012. Nickel and manganese release in serpentine soil from the Ussangoda Ultramafic Complex, Sri Lanka. Geoderma 189–190, 1–9. https://doi.org/10.1016/j.geoderma.2012.04.019

Tessier, A., Campbell, P.G., Bisson, M., 1979. Sequential extraction procedure for the speciation of particulate trace metals. Analytical chemistry 51, 844–851.

Usdowski, E., Hoefs, J., Menschel, G., 1979. Relationship between13C and18O fractionation and changes in major element composition in a recent calcite-depositing spring — A model of chemical variations with inorganic CaCO3 precipitation. Earth and Planetary Science Letters 42, 267–276. https://doi.org/10.1016/0012-821X(79)90034-7

Acknoledgments

During the period of my PhD project I had the opportunity to enrich my culture over than my academic skills, and this is also due to the people which I met along my path.

Firstly, I would thank my supervisor Prof. Andrea Pozzi for giving me this great opportunity, and geology colleagues Prof. Franz Livio and Prof. Alessandro Michetti, who shared their knowledge with me to help me in improving my skills.

I would also thank the reviewer of this dissertation, Prof. Alasdair Skelton from University of Stockholm and Prof. Francesca Castorina from the “La Sapienza” University in Rome, for their helpful comments which improve the quality of the whole text.

I would thank all the professors and staff of the analytical chemistry lab for the technical and personal support with my works and the analytical instruments (special thanks to Prof. Damiano Monticelli and Lele for their help with the instruments, and to Ross for the fundamental material and reagents supply). A special thank also goes to my neighbour colleagues Spanu and Moscheni which shared with me happy and sad moments about all the work made throughout the PhD course.

I would thank the people who helped me sampling in the campaigns in Central Italy and in the Ventina valley, and also who gave me logistical support on field: Christian, Paolino, Lorenzo, all the staff of the “Gerli Porro” hut, Pierluigi Mariani from the Nerea s.p.a., and Paolo Bellezza from the “Riserva di lago Lungo e Ripasottile”.

I would also thank Dr. Chaosheng Zhang from University of Ireland, in Galway to host me a couple of months in a beautiful place as Ireland and share his great knowledge with me, and the people of the geography and chemistry departments for the funny moments spent together.

Also, many thanks to Dr. Paula Noble and Dr. Michael Rosen who gave me the possibility to live an amazing experience, over than a greatly productive working period in Nevada, I had the time of my life there.

Last, but surely not least, I would thank my family for their continuous support, and my girlfriend Federica who still bear with me, and became by now part of my family too.

Supplementary_01: All water samples values and limits of detection for physicochemical parameters, major ions and trace elements in Ventina valley

		Physico-chemical parameters			Major ions (milligrams per liter)									
	Measure unit	°C	-	µS/cm	mg/L	mg/L	mg/L	mg/L	mg/L	mg/L	mg/L	mg/L	mg/L	
Sample	Date	Temperature	pH	Electrical conductivity	HCO_3	Cl	NO_3	SO_4	NH_4	Ca	Mg	Na	K	Ionic Balance
P01	30/07/2014	6.6	7.1	26	18.04	0.27	1.13	3.36	0.11	3.1463348	1.7121991	0.69	0.13	-7.42%
P02	30/07/2014	12.5	7.35	27	17.31	0.29	1.07	2.76	0.12	2.4986855	2.1007887	0.66	0.05	-4.60%
V10	30/07/2014	3.1	7.68	45.3	28.04	0.05	1.18	5.74	0.12	3.6614467	3.803132	0.12	<LOD	-8.32%
V09	30/07/2014	3.1	7.64	46.5	31.52	0.06	1.21	5.94	<LOD	4.1886633	4.686802	0.10	<LOD	-4.92%
V08	30/07/2014	5.5	7.31	21.4	11.08	0.24	0.97	4.44	<LOD	4.0196601	0.588204	0.05	<LOD	-8.19%
V06	30/07/2014	6.1	7.33	31.6	14.79	0.04	0.89	3.92	0.28	2.4469619	2.1318229	0.04	<LOD	-3.74%
P09	30/07/2014	6.3	7.5	30	25.27	0.57	1.08	1.71	0.01	3.4636184	4.721829	0.28	<LOD	8.61%
P10	30/07/2014	10.5	7.55	26	18.17	0.28	0.85	1.45	0.12	2.0072145	3.5956713	0.03	<LOD	7.24%
P03	30/07/2014	14.9	7.35	28	17.12	0.30	0.90	2.79	0.09	2.3144525	1.8033285	0.66	0.06	-9.39%
P12	31/07/2014	6.5	8.8	39	24.19	0.47	0.73	1.88	<LOD	2.6873623	3.1875826	0.04	<LOD	-7.26%
P08	31/07/2014	0.7	7.1	29	22.12	0.24	1.08	3.08	0.06	2.5804358	3.2517385	0.14	<LOD	-5.28%
V11	31/07/2014	1.8	7.38	14.7	9.88	0.23	0.89	2.38	0.04	2.2524885	1.0485069	<LOD	<LOD	-7.19%
P04	31/07/2014	0.8	7.23	40	28.68	0.20	0.38	6.95	1.11	8.2917156	1.6249706	0.72	0.23	1.59%
P05	31/07/2014	5.6	7.53	52	25.07	0.24	0.52	10.44	<LOD	8.4876764	0.9073942	0.78	0.55	-8.10%
P06	31/07/2014	2.3	8.1	49	26.03	0.28	1.06	4.63	<LOD	2.2618153	4.6429108	0.07	<LOD	-4.82%
V01	31/07/2014	4.3	7.4	43.7	30.84	0.01	1.40	3.19	0.02	3.3296399	4.0022161	0.10	<LOD	-8.52%
V02	31/07/2014	5.6	7.62	34.5	22.72	0.05	0.75	1.76	0.04	2.021438	2.9871372	0.12	<LOD	-8.80%
V03	31/07/2014	6.4	7.32	34	23.86	0.03	0.84	1.23	0.46	2.024	2.921	0.09	<LOD	-7.46%
V04	31/07/2014	3.3	7.36	39.5	31.71	0.01	1.13	3.13	0.06	3.5528478	4.4682913	0.17	0.01	-4.09%
V07	25/06/2014	3.66	7.73	48.3	24.77	0.25	1.21	5.66	0.04	3.2937895	4.0237263	0.12	0.01	-4.49%
V08	25/06/2014	4.31	8.01	30.9	14.60	0.26	1.47	5.25	0.02	4.0481969	1.7710818	0.03	<LOD	-3.99%
V06	25/06/2014	3.66	7.73	42.5	21.67	0.22	1.38	4.83	0.16	3.1400207	2.9159876	0.09	0.11	-8.03%
P09	25/06/2014	1	8.25	17.1	16.91	0.86	0.89	1.42	0.24	2.0078996	2.7952602	0.55	0.13	3.52%
P10	25/06/2014	4.45	7.79	5.2	3.14	0.25	0.46	0.73	0.04	0.6276197	0.5	0.03	<LOD	-3.14%
P03	25/06/2014	4.36	7.97	26.9	19.13	0.43	1.30	3.06	0.26	2.5707009	2.0575794	0.71	0.13	-8.49%
P08	25/06/2014	0.12	8.44	27.7	16.35	0.30	1.27	2.88	0.06	1.9417932	2.4349241	0.18	<LOD	-7.30%
V11	26/06/2014	0.76	8.27	20.8	12.69	0.34	1.61	5.05	0.01	3.1864544	1.6881273	0.02	<LOD	-7.65%
P04	26/06/2014	0.8	8.01	35.8	20.84	0.27	0.70	5.31	0.21	7.5301868	1.4818879	0.73	0.21	7.48%
V01	26/06/2014	3.28	7.61	41	24.28	0.14	1.41	3.15	0.12	2.6904955	3.1857027	0.20	<LOD	-8.73%
V02	26/06/2014	4.73	7.54	32.4	20.40	0.11	0.86	1.86	0.03	1.928008	2.6831952	0.15	0.03	-8.95%
V03	26/06/2014	4.59	7.91	30.7	21.03	0.13	0.97	1.62	0.24	1.822	2.65	0.21	<LOD	-9.03%
V04	26/06/2014	2.29	7.61	41.8	31.72	0.18	1.39	2.15	0.50	3.3026488	3.7784107	0.40	0.10	-6.17%
P01	01/10/2014	9.1	7.37	27.6	17.08	0.32	0.92	3.34	0.12	3.2928368	1.6242979	0.75	0.18	-4.37%
P02	01/10/2014	11.7	7.79	27.3	17.73	0.27	0.80	2.82	0.11	2.5466978	2.0719813	0.66	0.06	-5.13%
P03	01/10/2014	12	7.75	26.8	16.75	0.28	0.79	2.90	0.10	2.5678094	2.0593144	0.69	0.08	-2.98%
P04	01/10/2014	8.3	7.23	54.4	29.93	0.16	0.40	9.96	0.11	9.7975021	1.9214988	0.80	0.32	-0.85%
P05	01/10/2014	5.2	7.8	57.2	25.07	0.25	0.63	13.74	0.10	9.6174177	0.8295494	0.85	0.64	-8.04%
P06	01/10/2014	9.8	7.99	85	52.05	0.04	1.64	10.18	0.03	4.0675528	8.3594683	0.17	<LOD	-9.64%
P08	01/10/2014	2.3	7.6	41.4	27.32	0.28	1.95	6.90	<LOD	3.1577579	4.1053453	0.55	<LOD	-9.68%
P09	01/10/2014	7.8	7.94	39.2	25.21	0.59	1.18	3.23	<LOD	2.6071253	4.4357248	0.11	<LOD	-1.58%
P10	01/10/2014	11.4	8.42	37.9	21.21	0.26	1.06	2.88	<LOD	2.0809074	3.5514556	0.06	<LOD	-3.99%
P12	01/10/2014	8.4	7.73	40	25.37	1.29	1.02	2.48	0.01	2.6230415	3.2261751	0.59	0.54	-8.77%
V01	02/10/2014	4.9	7.43	49.1	32.12	0.07	1.64	3.70	<LOD	4.1836543	4.6898074	0.16	<LOD	-2.42%
V02	02/10/2014	7	7.42	41.9	24.02	0.04	1.22	2.94	<LOD	2.4278941	3.3432635	0.19	<LOD	-8.08%
V03	02/10/2014	6.7	6.58	35	27.16	0.02	1.13	3.03	0.06	2.686	3.702	0.18	0.03	-7.85%
V04	02/10/2014	3.4	6.6	53.9	35.54	0.01	1.67	5.22	0.00	4.3416138	4.5950317	0.43	0.12	-7.58%

		Physico-chemical parameters			Major ions (milligrams per liter)									
	Measure unit	°C	-	µS/cm	mg/L	mg/L	mg/L	mg/L	mg/L	mg/L	mg/L	mg/L	mg/L	
Sample	Date	Temperature	pH	Electrical conductivity	HCO_3	Cl	NO_3	SO_4	NH_4	Ca	Mg	Na	K	Ionic Balance
V06	02/10/2014	5	6.62	43.3	25.21	0.06	1.01	5.99	<LOD	4.580888	3.8514672	0.05	<LOD	-0.71%
V07	02/10/2014	4.1	7.48	38.4	20.45	0.25	1.11	6.52	<LOD	3.9582349	2.8616251	0.07	<LOD	-6.39%
V08	02/10/2014	8.3	7.36	26.1	14.48	0.23	0.87	4.44	0.03	3.1710412	1.6973753	0.03	<LOD	-7.58%
V10	02/10/2014	4	6.95	38.1	22.26	0.06	1.08	5.74	0.01	3.3029473	3.1823165	0.09	0.00	-7.68%
V11	02/10/2014	2	6.6	19.3	12.04	0.25	1.04	4.19	<LOD	3.3957808	1.5625315	0.05	<LOD	-1.29%
P01	02/09/2014	9.5	7.74	26.6	15.26	0.27	0.83	3.23	<LOD	3.2581049	1.6451371	0.69	0.17	-0.84%
P02	02/09/2014	11.6	7.61	26.1	14.30	0.26	0.82	2.80	<LOD	2.5214565	2.0871261	0.66	0.04	2.23%
P03	02/09/2014	12.1	7.13	47.3	14.66	0.25	0.84	2.75	0.10	2.4811231	1.9753261	0.67	0.09	0.80%
P04	02/09/2014	8.1	7.05	45.6	27.07	<LOD	0.20	8.09	<LOD	8.1643732	1.7013761	0.74	0.28	-2.32%
P05	02/09/2014	5.9	7.24	49.1	24.14	0.24	0.41	12.12	<LOD	8.603278	0.8380332	0.82	0.55	-9.30%
P06	02/09/2014	5	8.25	76.6	36.85	0.02	1.41	8.72	<LOD	3.1222535	6.5266479	0.12	<LOD	-7.32%
P08	02/09/2014	1.9	7.79	39.2	25.87	0.25	1.50	5.22	<LOD	3.2339507	4.0596296	0.35	<LOD	-4.92%
P09	02/09/2014	9.3	8.39	30.5	26.94	0.23	0.73	1.91	<LOD	3.5245162	4.6852903	0.11	<LOD	6.29%
P10	02/09/2014	10.6	8.41	28.4	16.95	0.21	0.47	1.65	<LOD	1.4320599	3.2607641	0.06	<LOD	2.51%
P12	02/09/2014	7.1	7.4	39.7	24.20	0.26	1.06	2.26	0.02	2.5932841	3.2440295	0.17	<LOD	-7.22%
V01	03/09/2014	5.1	7.54	44.6	28.49	0.04	1.44	3.11	<LOD	3.4808239	3.9115057	0.14	<LOD	-5.14%
V02	03/09/2014	7.5	7.66	38.5	22.30	0.02	0.76	1.66	<LOD	2.1242276	3.0454634	0.16	0.11	-5.95%
V03	03/09/2014	7.4	7.8	36.6	21.10	0.01	1.02	2.34	<LOD	2.477	3.345	0.17	0.08	-0.35%
V04	03/09/2014	3.8	7.63	50	30.00	0.04	1.40	4.50	<LOD	3.3730803	3.9761518	0.31	0.07	-8.76%
V06	03/09/2014	6.4	7.54	37.9	18.75	0.06	0.99	4.07	<LOD	2.6866841	2.5879896	0.01	0.07	-7.89%
V07	03/09/2014	4	6.82	37.2	22.17	0.28	1.40	6.33	1.77	4.2910759	3.4253545	0.10	<LOD	6.51%
V08	03/09/2014	6.7	6.85	27.8	15.36	0.23	1.04	4.95	0.05	4.7503821	1.2149771	0.05	<LOD	-5.00%
V09	03/09/2014	3.7	7.9	38.5	20.36	0.06	1.07	5.73	<LOD	3.2524358	2.8485385	0.08	0.01	-8.17%
V10	03/09/2014	5.2	7.2	39.8	22.06	0.08	1.12	5.47	0.04	3.5928669	3.1242798	0.17	0.01	-5.20%
V11	03/09/2014	2.4	7.72	18.8	10.85	0.23	0.91	3.63	<LOD	2.797654	1.3214076	<LOD	<LOD	-4.99%
P01	23/06/2015	4.87	7.6	27	16.47	0.35	1.80	1.88	<LOD	3	1.426	0.30	0.40	-9.00%
P02	23/06/2015	6.72	7.95	30	15.86	0.39	1.32	1.39	0.53	2.547	2.055	0.17	0.22	2.71%
P03	23/06/2015	8.41	8.6	29	16.35	0.34	1.33	1.38	0.54	2.593	2.059	0.16	0.23	2.12%
P04	23/06/2015	6.93	7.56	41	23.18	0.33	0.51	2.53	0.42	4.97	1.837	0.29	0.46	-0.32%
P05	23/06/2015	3.8	7.76	40	25.01	0.32	0.72	4.18	0.48	8.722	0.793	0.46	0.82	4.69%
P06	23/06/2015	0.59	9.11	31	20.01	0.33	1.10	1.19	0.66	1.705	3.41	0.42	<LOD	5.10%
P08	23/06/2015	0.35	8.41	19	12.20	0.33	0.95	0.70	0.31	1.298	1.684	<LOD	<LOD	-4.02%
P09	23/06/2015	9.52	8.02	23	12.20	0.36	0.83	0.60	0.37	1.099	1.997	<LOD	<LOD	0.74%
P10	23/06/2015	11.51	8.02	17	4.25	0.35	0.80	0.53	0.30	0.342	0.661	<LOD	<LOD	-8.09%
P11	23/06/2015	6.94	8.16	44	26.11	0.40	1.57	2.08	0.47	3.305	3.873	0.23	<LOD	1.16%
P12	23/06/2015	6.26	7.96	33	20.01	0.32	1.12	0.80	0.28	2.346	2.896	<LOD	<LOD	-0.12%
V01	24/06/2015	3.38	7.95	42.5	26.84	0.38	1.39	1.35	0.37	3.317	3.998	0.12	0.19	2.36%
V02	24/06/2015	5.55	7.86	34.1	22.20	0.39	1.08	0.91	0.51	2.229	3.266	0.17	<LOD	0.57%
V03	24/06/2015	4.51	8.32	33.1	20.74	0.36	1.07	0.88	0.35	2.19	3.095	0.11	<LOD	0.35%
V04	24/06/2015	2.49	8.07	45.9	29.28	0.37	1.42	1.64	0.61	3.959	4.091	0.25	0.25	3.36%
V06	24/06/2015	5.71	8.23	39.7	21.96	0.35	1.44	2.17	0.80	3.413	2.996	<LOD	<LOD	2.59%
V07	24/06/2015	2.5	8.08	47.1	26.27	0.37	1.41	2.52	0.35	3.88	4.033	0.15	<LOD	3.32%
V08	24/06/2015	4.18	8.39	32	16.59	0.36	1.86	1.95	0.14	3.139	1.905	<LOD	<LOD	-4.68%
V09	24/06/2015	2.09	8.17	46.2	28.30	0.35	1.70	2.54	0.33	3.911	4.116	0.14	<LOD	0.40%
V10	24/06/2015	2.12	7.95	47.5	27.98	0.36	2.02	2.39	0.64	3.719	4.589	0.15	0.26	5.26%
V11	24/06/2015	0.75	7.8	25	11.96	0.39	1.63	1.66	0.28	2.44	1.348	<LOD	<LOD	-3.73%
P05	12/10/2015	6.7	8.12	63.5	32.04	<LOD	0.59	4.76	3.96	8.61	0.866	0.39	0.70	8.83%
P06	12/10/2015	3.4	8.67	84.3	42.70	<LOD	2.30	3.83	1.95	3.776	7.393	0.00	0.03	5.19%
P08	12/10/2015	2.7	8.1	98	42.78	<LOD	2.69	9.93	1.62	5.422	6.766	1.89	0.11	2.61%

		Physico-chemical parameters			Major ions (milligrams per liter)									
	Measure unit	°C	-	µS/cm	mg/L	mg/L	mg/L	mg/L	mg/L	mg/L	mg/L	mg/L	mg/L	
Sample	Date	Temperature	pH	Electrical conductivity	HCO_3	Cl	NO_3	SO_4	NH_4	Ca	Mg	Na	K	Ionic Balance
P09	12/10/2015	4.6	8.22	63	35.48	<LOD	1.69	2.17	3.64	3.063	5.173	0.12	<LOD	9.19%
P11	12/10/2015	2.6	8.2	75.1	35.99	<LOD	1.95	4.84	2.07	5.121	5.332	0.18	0.09	6.34%
V01	13/10/2015	5.1	7.38	46.9	28.30	<LOD	1.63	0.91	2.06	3.397	3.872	0.05	<LOD	8.61%
V02	13/10/2015	6.2	7.71	35.7	23.98	<LOD	0.79	0.43	2.62	2.154	3.025	0.03	<LOD	9.63%
V03	13/10/2015	7.64	5.9	35.4	22.29	<LOD	0.93	0.37	1.71	2.137	3.128	0.00	<LOD	8.40%
V04	13/10/2015	3.5	7.53	54.2	34.65	<LOD	1.69	1.72	1.94	3.97	4.438	0.23	0.11	4.02%
V07	13/10/2015	4	7.87	55.7	32.05	<LOD	1.44	3.64	2.91	4.965	3.948	0.06	<LOD	8.28%
V11	13/10/2015	2.5	7.29	35.3	18.71	<LOD	1.97	3.08	1.91	3.896	2.031	<LOD	<LOD	7.50%
P03	28/09/2015	10.7	8.37	33.7	21.32	<LOD	1.35	1.16	2.35	2.458	2.1	0.13	0.05	4.55%
P05	28/09/2015	5.3	7.98	60	30.26	<LOD	0.56	4.63	1.87	9.52	0.879	0.40	0.71	6.72%
P06	28/09/2015	2.1	8.51	75.1	43.43	<LOD	2.00	3.97	1.64	3.736	7.421	<LOD	0.03	3.63%
P08	28/09/2015	1.6	7.7	83.8	42.70	<LOD	2.24	7.68	2.59	5.299	6.625	1.55	0.08	6.62%
P09	28/09/2015	5	8.34	56.8	33.72	<LOD	1.70	2.29	3.10	3.043	4.929	0.40	0.21	9.06%
P10	28/09/2015	6.2	8.64	40.1	28.23	<LOD	1.28	1.65	2.37	2.551	4.084	0.09	0.01	7.31%
P11	28/09/2015	5.4	8.21	66.5	39.65	<LOD	1.88	3.81	4.30	4.663	5.241	0.18	0.10	9.22%
P12	28/09/2015	6.1	6.78	28.5	26.30	<LOD	1.09	0.78	2.52	2.449	3.166	0.41	0.23	8.07%
V01	29/09/2015	6.6	6.7	60.4	29.70	<LOD	2.00	0.80	2.99	3.277	3.82	0.05	<LOD	9.35%
V02	29/09/2015	7.6	6.75	40.1	22.31	<LOD	1.34	0.27	1.77	2.14	3.112	0.02	<LOD	8.08%
V03	29/09/2015	7.6	6.72	40.1	22.50	<LOD	1.37	0.15	1.80	2.128	3.079	0.05	<LOD	7.93%
V04	29/09/2015	3.6	7.54	43.1	31.07	<LOD	1.93	1.56	1.33	3.808	4.334	0.22	0.08	4.95%
V06	29/09/2015	5.4	7.67	59.7	32.47	<LOD	2.12	2.44	3.52	4.279	4.039	0.13	0.06	9.64%
V07	29/09/2015	3.3	8.04	60	29.03	<LOD	1.61	3.04	2.63	4.571	3.734	0.06	0.01	9.55%
V08	29/09/2015	7.2	7.9	58.8	28.47	<LOD	1.69	2.69	2.42	4.973	2.564	0.34	<LOD	5.06%
V10	29/09/2015	3.1	7.74	58	28.95	<LOD	1.53	3.00	2.56	4.416	3.537	0.04	<LOD	7.73%
V11	29/09/2015	1.6	7.2	37.3	18.43	<LOD	2.18	2.28	2.52	3.429	1.79	<LOD	<LOD	8.80%
P05	25/07/2016	5	6.95	57.9	27.15	0.64	0.87	4.13	0.83	7.76	0.879	0.70	0.87	-0.40%
P06	25/07/2016	3.4	7	79.3	45.14	0.68	2.40	2.77	0.72	3.311	6.38	<LOD	0.31	-7.36%
P08	25/07/2016	1.3	6.93	52.9	26.54	0.68	2.24	2.80	0.32	2.9	3.479	0.85	<LOD	-6.05%
P11	25/07/2016	1.6	7.09	61.1	30.81	0.87	2.13	2.75	0.29	3.633	4.098	0.50	0.32	-4.78%
P12	25/07/2016	7.9	7.14	39.5	24.71	0.64	1.24	1.20	0.28	2.397	2.95	0.46	0.32	-7.07%
V01	26/07/2016	4.8	6.76	49.7	27.76	0.66	1.84	1.55	0.30	3.078	3.473	<LOD	0.25	-7.30%
V02	26/07/2016	5.81	5.81	36.9	22.88	0.74	1.59	1.19	0.98	2.074	2.954	<LOD	<LOD	-5.33%
V03	26/07/2016	6.5	6.71	34.1	22.88	0.66	1.23	1.14	0.66	2.059	2.863	<LOD	0.32	-6.60%
V04	26/07/2016	4	6.85	52.5	28.37	0.65	1.55	2.33	0.89	3.448	3.438	<LOD	0.30	-4.16%
V07	26/07/2016	3.2	6.4	46.6	24.40	0.65	1.92	2.53	0.65	3.496	3.047	<LOD	0.31	-3.37%
V10	26/07/2016	3.1	6.4	45.5	23.49	0.73	1.56	2.56	0.28	4.293	3.907	<LOD	<LOD	6.49%
V11	26/07/2016	1.8	6.15	15	9.15	0.65	1.83	1.27	0.79	1.606	0.922	<LOD	<LOD	-5.69%
P05	23/06/2016	4.3	5.93	49.2	28.49	0.01	0.57	0.73	0.26	5.079	2.155	<LOD	<LOD	-4.87%
P06	23/06/2016	0.8	6.07	27	17.17	<LOD	1.11	4.41	0.64	6.713	0.531	0.66	0.91	8.83%
P08	23/06/2016	0.6	6.28	25.6	16.17	<LOD	1.60	1.45	0.52	1.326	1.878	0.54	<LOD	-8.02%
P11	23/06/2016	1.1	6.1	38.5	23.49	<LOD	0.89	1.66	0.71	2.318	3.004	0.45	0.56	0.27%
P12	23/06/2016	5.7	7.12	31.1	20.96	<LOD	0.29	0.57	0.42	1.624	2.218	0.47	<LOD	-7.91%
V07	24/06/2016	3.11	7.1	48.7	29.59	<LOD	1.07	2.46	0.78	3.138	3.801	0.48	0.52	-0.59%
V09	24/06/2016	2.8	6.73	51.9	29.59	<LOD	1.15	2.55	0.67	2.973	3.693	0.44	<LOD	-4.48%
V10	24/06/2016	2.9	6.47	48.4	28.37	<LOD	1.91	2.70	0.78	3.05	3.744	0.49	0.52	-1.24%
V11	24/06/2016	0.75	7.8	22	10.98	<LOD	1.08	1.32	0.71	1.731	0.879	0.44	<LOD	-1.73%
P03	10/10/2016	2.6	8.28	37	10.60	0.44	1.66	2.27	<LOD	2.492	2.119	<LOD	<LOD	6.90%
P08	10/10/2016	2.6	8.28	95.2	31.65	0.24	2.40	6.17	<LOD	5.645	6.373	0.47	<LOD	8.84%
P11	10/10/2016	1.6	8.9	87	26.57	0.19	2.33	5.41	<LOD	5.089	5.622	<LOD	<LOD	9.61%

		Physico-chemical parameters			Major ions (milligrams per liter)									
	Measure unit	°C	-	µS/cm	mg/L	mg/L	mg/L	mg/L	mg/L	mg/L	mg/L	mg/L	mg/L	
Sample	Date	Temperature	pH	Electrical conductivity	HCO_3	Cl	NO_3	SO_4	NH_4	Ca	Mg	Na	K	Ionic Balance
V01	11/10/2016	3.7	6.89	57.8	20.47	0.43	1.56	1.89	<LOD	3.194	3.706	<LOD	0.12	6.30%
V02	11/10/2016	4.1	6.09	46.2	20.40	0.18	1.76	1.45	<LOD	2.101	3.423	<LOD	<LOD	-1.46%
V03	11/10/2016	5.3	6.19	48.2	20.42	0.26	1.60	1.65	<LOD	1.676	3.048	<LOD	<LOD	-9.20%
V04	11/10/2016	3.6	5.23	57.3	30.50	0.32	1.53	4.06	<LOD	6.323	4.321	<LOD	<LOD	4.14%
V07	11/10/2016	3.5	5.98	57.1	24.52	0.16	1.55	4.36	<LOD	4.791	3.094	<LOD	<LOD	-2.77%
V11	11/10/2016	1.5	6.55	36.1	8.50	0.16	1.58	3.31	<LOD	3.65	0.789	<LOD	<LOD	1.89%
LOD	-	-	-	-	0.05	0.05	0.05	0.05	0.05	0.05	0.05	0.05	0.05	-

		Trace elements (micrograms per liter)										
	Measure unit	µg/L	µg/L	µg/L	µg/L	µg/L	µg/L	µg/L	µg/L	µg/L	µg/L	µg/L
Sample	Date	Cr	Mn	Co	Ni	Cu	Zn	Cd	Pb	Fe	Ag	As
P01	30/07/2014	0.1927	0.0394	0.0254	2.2680	<LOD	1.3378	0.0121	0.0669	<LOD	0.0131	0.2248
P02	30/07/2014	0.2164	0.2121	0.0228	3.0105	<LOD	0.8367	0.0120	0.0694	<LOD	0.0058	0.2859
V10	30/07/2014	0.7044	0.0214	<LOD	2.1898	0.0177	1.2938	<LOD	0.0507	2.0844	<LOD	0.2866
V09	30/07/2014	0.7396	0.0367	<LOD	1.4181	0.0165	<LOD	<LOD	0.0512	2.4061	<LOD	0.2705
V08	30/07/2014	0.1700	1.8925	<LOD	1.1041	0.0270	1.6388	<LOD	0.0528	1.6976	<LOD	0.0580
V06	30/07/2014	0.4683	0.1758	0.0383	4.5947	<LOD	6.7501	0.0117	0.0769	3.0206	0.0100	0.1522
P09	30/07/2014	0.6229	0.3163	0.0541	3.8381	0.1990	3.7127	0.0121	0.0943	24.2178	0.0354	0.0201
P10	30/07/2014	0.4830	0.4235	0.0479	3.3732	0.1375	5.8318	0.0133	0.0883	21.1254	0.0139	0.0248
P03	30/07/2014	0.1966	0.2401	0.0185	2.7984	<LOD	0.4201	0.0122	0.0674	<LOD	0.0040	0.2713
P12	31/07/2014	0.9180	0.0467	0.0300	7.0068	<LOD	0.6500	0.0117	0.0685	0.0479	0.0042	0.0459
P08	31/07/2014	0.1653	0.0829	0.0266	3.1029	<LOD	0.1499	0.0117	0.0693	2.3733	0.0022	0.0276
V11	31/07/2014	0.1865	0.2598	0.0412	4.3880	<LOD	0.5657	0.0114	0.0696	<LOD	0.0024	0.0421
P04	31/07/2014	0.1337	0.0271	0.0198	1.1773	<LOD	1.2934	0.0121	0.0679	<LOD	0.0089	1.2219
P05	31/07/2014	0.0126	0.0353	0.0224	0.1199	<LOD	1.2178	0.0115	0.0668	<LOD	0.0049	0.0105
P06	31/07/2014	0.5105	0.1512	0.1196	2.1160	<LOD	3.6820	0.1028	0.1520	7.0157	0.1125	10.2861
V01	31/07/2014	1.2277	0.0547	0.0281	4.3019	<LOD	<LOD	0.0115	0.0677	1.8097	0.0028	0.1175
V02	31/07/2014	0.9329	0.0456	0.0293	5.1985	0.0419	2.7324	0.0118	0.0703	1.6958	0.0034	0.0464
V03	31/07/2014	0.9800	0.0712	0.0334	5.7628	0.0735	1.4026	0.0116	0.0730	4.6946	0.0083	0.0485
V04	31/07/2014	0.8639	0.0639	0.0262	2.8241	0.0064	1.7149	0.0113	0.0683	4.2935	0.0060	0.1958
V07	25/06/2014	1.1154	2.1885	0.0308	3.0479	0.2934	7.5424	<LOD	0.1057	8.7146	0.0116	0.2414
V08	25/06/2014	0.6610	0.6436	0.0843	5.4859	0.1642	10.1346	<LOD	0.0821	15.9300	0.0067	0.1201
V06	25/06/2014	0.8009	0.2741	0.0351	4.3580	0.5281	10.4480	<LOD	0.1926	7.9297	0.0685	0.2086
P09	25/06/2014	0.4882	0.6090	0.0434	3.3535	0.2869	3.2210	<LOD	0.1178	19.3810	0.0195	0.0165
P10	25/06/2014	0.3538	0.5407	0.0113	2.2769	0.6417	8.1410	<LOD	0.1904	8.9193	0.0125	0.0156
P03	25/06/2014	0.3021	0.2716	0.0072	3.4377	0.1773	12.7743	<LOD	0.1120	8.5983	0.1026	0.3152
P08	25/06/2014	0.2257	0.2029	0.0114	3.3709	0.1927	4.4305	<LOD	0.0934	7.4787	0.0078	0.0366
V11	26/06/2014	0.9519	1.4917	0.2638	8.4669	0.4738	9.0653	<LOD	0.1771	41.1742	0.0042	0.1447
P04	26/06/2014	0.6563	0.1583	<LOD	2.4295	1.8462	10.3203	<LOD	0.2115	3.4899	0.0031	1.6117
V01	26/06/2014	1.2156	1.0596	<LOD	3.8851	0.7163	8.8587	<LOD	0.1203	3.7692	0.0103	0.1059
V02	26/06/2014	1.1338	0.1845	0.0054	4.8327	0.4766	4.3933	<LOD	0.1049	9.8186	<LOD	0.0520
V03	26/06/2014	0.8863	0.1809	0.0351	5.2195	0.2261	37.1396	0.0122	1.1055	4.1940	0.0375	0.0483
V04	26/06/2014	0.7708	1.2469	<LOD	2.3484	0.1408	5.5545	<LOD	0.1043	9.1478	<LOD	0.1700
P01	01/10/2014	0.8243	0.2413	0.1137	6.8778	0.4826	39.6039	0.0536	0.1461	<LOD	0.0413	0.3981
P02	01/10/2014	0.6841	0.5441	0.0837	8.5818	<LOD	7.4811	0.0512	0.0435	2.1769	0.0390	0.5393
P03	01/10/2014	0.6476	0.7597	0.0828	7.5663	0.0040	2.1734	0.0512	0.0477	<LOD	0.0234	0.5117
P04	01/10/2014	0.3898	0.2526	0.0870	3.1117	<LOD	5.1087	0.0510	0.0442	<LOD	0.0429	2.0388

		Trace elements (micrograms per liter)										
	Measure unit	µg/L	µg/L	µg/L	µg/L	µg/L	µg/L	µg/L	µg/L	µg/L	µg/L	µg/L
Sample	**Date**	**Cr**	**Mn**	**Co**	**Ni**	**Cu**	**Zn**	**Cd**	**Pb**	**Fe**	**Ag**	**As**
P05	01/10/2014	0.0652	0.0943	0.0774	0.0643	0.1319	12.0513	0.0509	0.0358	8.6292	0.0285	0.0126
P06	01/10/2014	1.2876	0.1727	0.0871	6.6036	<LOD	23.0707	0.0508	0.0587	<LOD	0.0932	22.4182
P08	01/10/2014	2.4646	6.2423	0.6696	15.8359	0.7753	37.2064	<LOD	0.6447	5.5976	0.0604	0.0304
P09	01/10/2014	1.3603	0.6354	0.1602	9.2838	0.1652	0.2474	0.0502	0.0796	<LOD	0.0385	0.0585
P10	01/10/2014	1.3029	0.6713	0.1323	7.0584	0.1614	<LOD	0.0525	0.0513	<LOD	0.0266	0.0562
P12	01/10/2014	2.8614	1.5685	0.2118	20.4384	0.1015	23.3075	0.0506	0.1107	<LOD	2.7856	0.0945
V01	02/10/2014	2.8234	0.0533	0.0440	7.6585	<LOD	1.1671	0.0178	0.0027	19.8175	<LOD	0.1758
V02	02/10/2014	2.5145	0.1693	0.0622	10.8107	<LOD	5.6289	0.0182	0.0249	<LOD	<LOD	0.0475
V03	02/10/2014	2.2344	0.3737	0.0685	13.8737	0.1210	1.6062	0.0196	0.0563	<LOD	<LOD	0.0356
V04	02/10/2014	2.4145	2.0007	0.2467	7.6412	0.1501	<LOD	0.0184	0.0360	<LOD	<LOD	0.3458
V06	02/10/2014	1.1860	0.1205	0.0645	8.4346	<LOD	<LOD	0.0180	0.0035	8.4155	<LOD	0.3939
V07	02/10/2014	0.9718	0.0929	0.0528	6.4391	<LOD	4.8809	0.0182	0.0095	28.5621	0.0056	0.7303
V08	02/10/2014	0.5100	0.2313	0.0974	11.6599	<LOD	<LOD	0.0186	0.0248	<LOD	<LOD	0.0709
V10	02/10/2014	1.1343	0.1087	0.0548	4.8931	<LOD	5.3339	0.0184	0.0150	12.4403	<LOD	0.3817
V11	02/10/2014	0.4274	0.1524	0.0595	7.1968	<LOD	<LOD	0.0180	0.0035	13.3203	<LOD	0.1212
P01	02/09/2014	0.3922	0.1531	0.1259	3.1153	1.1471	14.5109	0.1045	0.1995	<LOD	0.1179	0.2408
P02	02/09/2014	0.3970	0.4093	0.1259	3.6751	0.0738	9.5794	0.1041	0.1621	1.9990	0.1143	0.2911
P03	02/09/2014	0.5876	0.5847	0.0490	6.7323	0.0284	9.9141	0.0226	0.0260	<LOD	2.2391	0.4260
P04	02/09/2014	0.5866	0.0758	0.0383	3.5296	<LOD	12.7703	0.0214	0.0192	25.5338	0.0019	2.5201
P05	02/09/2014	0.1696	0.1028	0.0368	0.3267	<LOD	19.2157	0.0196	0.0634	<LOD	0.0951	<LOD
P06	02/09/2014	1.2371	0.1892	0.0604	5.0973	<LOD	12.8428	0.0195	0.0613	<LOD	0.5990	21.5234
P08	02/09/2014	0.7810	0.2487	0.0687	7.5384	0.1097	10.1829	0.0195	0.0510	<LOD	0.2839	0.0041
P09	02/09/2014	0.9404	0.7247	0.1801	4.4348	0.2220	2.3892	0.1038	0.1761	29.3556	0.1757	0.0347
P10	02/09/2014	1.2359	1.2364	0.1010	7.2831	0.2843	11.6822	0.0226	0.0510	<LOD	0.1048	<LOD
P12	02/09/2014	2.1841	0.1072	0.0522	16.1672	0.2680	20.1891	0.0193	0.0386	<LOD	0.0814	0.0231
V01	03/09/2014	1.4407	0.1462	0.1215	4.5515	<LOD	1.8618	0.1030	0.1519	0.1667	0.1000	0.1441
V02	03/09/2014	1.2547	0.1706	0.1288	6.0824	0.1196	1.2612	0.1040	0.1690	7.1718	0.1437	0.0617
V03	03/09/2014	1.2365	0.2162	0.1318	7.2012	0.0971	1.9407	0.1038	0.1584	9.5569	0.1172	0.0541
V04	03/09/2014	1.0586	0.1557	0.1204	2.4389	<LOD	<LOD	0.1028	0.1454	1.7698	0.2569	0.2617
V06	03/09/2014	0.6732	0.2193	0.1362	5.1766	<LOD	2.3403	0.1031	0.1492	5.6035	0.0915	0.1956
V07	03/09/2014	0.7603	0.4396	0.1622	3.6611	<LOD	3.6324	0.1035	0.1576	14.4641	0.0947	0.3402
V08	03/09/2014	0.3903	3.9531	0.1370	5.5708	<LOD	0.2243	0.1092	0.1466	1.2519	0.0988	0.0451
V09	03/09/2014	0.7987	0.3059	0.1452	2.8384	<LOD	1.8018	0.1046	0.1518	9.7726	0.1033	0.2454
V10	03/09/2014	0.7596	0.1915	0.1278	2.7732	<LOD	2.5844	0.1039	0.1553	2.0935	0.1560	0.2278
V11	03/09/2014	0.3474	0.3811	0.1492	5.9951	<LOD	0.3683	0.1032	0.1599	2.9774	0.0973	0.0575
P01	23/06/2015	0.3187	0.1886	0.0173	4.7373	0.9112	14.6293	<LOD	0.2330	4.2323	<LOD	0.5117
P02	23/06/2015	0.9190	0.8222	0.1395	7.8706	0.5446	19.8755	0.0330	0.0998	34.8329	0.0528	0.7745
P03	23/06/2015	0.8599	0.6183	0.0717	8.4507	1.0151	15.3242	<LOD	0.0833	34.8827	<LOD	0.7157
P04	23/06/2015	0.3757	0.1733	<LOD	2.1275	0.5184	26.8058	<LOD	0.1370	3.9600	0.0069	2.4722
P05	23/06/2015	0.1520	0.0613	<LOD	0.2542	0.3982	15.1542	<LOD	0.0394	2.1842	<LOD	<LOD
P06	23/06/2015	0.4869	0.1285	0.0038	3.9539	0.1562	8.2499	<LOD	0.0418	8.4524	<LOD	11.2179
P08	23/06/2015	0.3603	0.4145	0.0345	5.9874	0.3401	11.5610	<LOD	0.0266	11.0895	<LOD	<LOD
P09	23/06/2015	0.8354	1.4009	0.0974	7.2028	1.9823	13.6632	<LOD	0.1799	34.6013	<LOD	<LOD
P10	23/06/2015	0.9251	1.2282	0.0821	6.6186	1.4345	31.4627	<LOD	0.3450	29.3738	<LOD	0.0021
P11	23/06/2015	1.2830	2.1854	0.2002	6.8896	0.8273	22.6271	<LOD	0.0980	33.8500	0.7623	0.2146
P12	23/06/2015	1.8013	0.3899	0.0636	13.9366	0.8478	32.8039	0.0354	0.3077	12.2741	0.0442	0.1052
V01	24/06/2015	1.8992	0.0554	<LOD	6.7597	0.0603	11.1537	<LOD	0.0011	5.2086	<LOD	0.1306
V02	24/06/2015	1.7410	0.1016	0.0013	9.0707	0.3194	17.5410	<LOD	0.1041	7.5661	<LOD	0.0369
V03	24/06/2015	1.6272	0.3218	0.0092	9.6094	0.2913	8.4541	<LOD	0.0411	13.9030	<LOD	0.0313
V04	24/06/2015	1.3665	0.1199	<LOD	4.2355	0.0983	8.1149	<LOD	<LOD	6.5564	<LOD	0.3230

		Trace elements (micrograms per liter)										
	Measure unit	µg/L	µg/L	µg/L	µg/L	µg/L	µg/L	µg/L	µg/L	µg/L	µg/L	µg/L
Sample	Date	Cr	Mn	Co	Ni	Cu	Zn	Cd	Pb	Fe	Ag	As
V06	24/06/2015	0.7819	0.2057	0.0182	6.9426	0.0268	9.7612	<LOD	0.0962	5.7262	<LOD	0.2039
V07	24/06/2015	1.3010	0.3047	0.0359	6.5719	0.1045	9.4658	<LOD	<LOD	9.6491	<LOD	0.4196
V08	24/06/2015	0.5684	0.3050	0.0353	8.2240	0.0404	7.9515	<LOD	0.0005	5.6195	<LOD	0.0997
V09	24/06/2015	1.3873	0.4212	0.0673	6.8884	0.0607	5.5008	<LOD	<LOD	11.9873	<LOD	0.3003
V10	24/06/2015	1.5005	0.1283	0.0073	4.5953	0.0869	10.1622	<LOD	0.0036	6.4715	0.0609	0.4199
V11	24/06/2015	0.6597	1.5684	0.2064	9.5064	0.1605	25.6465	<LOD	0.0848	22.6217	<LOD	0.1001
P05	12/10/2015	0.0131	<LOD	<LOD	0.7814	0.0337	2.4666	<LOD	<LOD	0.9642	0.0521	<LOD
P06	12/10/2015	1.2642	0.0981	<LOD	5.2142	<LOD	4.8950	<LOD	0.0362	7.2303	0.0183	28.5961
P08	12/10/2015	0.9034	0.3828	0.0101	10.6127	0.2055	8.8092	<LOD	0.0208	7.7266	0.0240	0.0208
P09	12/10/2015	1.3201	1.8061	0.0789	9.7118	0.3706	3.8666	<LOD	<LOD	32.8388	<LOD	<LOD
P11	12/10/2015	1.9787	1.1630	0.0956	9.9013	0.3415	2.5941	<LOD	0.2339	20.6075	0.0458	0.2339
V01	13/10/2015	2.5717	0.0035	<LOD	8.3660	0.0587	0.8612	<LOD	0.1677	4.0400	<LOD	0.1677
V02	13/10/2015	2.2128	0.2437	0.0072	10.6791	0.4019	2.2447	<LOD	0.0186	13.0002	0.0183	0.0186
V03	13/10/2015	2.2784	0.0804	<LOD	11.3713	0.2129	1.4701	<LOD	0.0198	9.6604	<LOD	0.0198
V04	13/10/2015	2.1867	0.0780	<LOD	4.9331	0.0604	1.2141	<LOD	0.5908	5.1881	0.0209	0.5908
V07	13/10/2015	1.8909	1.2196	0.2116	12.6913	0.1935	3.2475	<LOD	0.8441	21.6360	<LOD	0.8441
V11	13/10/2015	0.8370	0.2315	0.0098	6.5635	0.0124	1.7758	<LOD	0.3813	4.3799	0.0295	0.3813
P03	28/09/2015	0.9198	0.4780	0.0641	6.9876	0.3374	3.1971	0.0046	0.0584	22.1001	0.0220	0.5631
P05	28/09/2015	0.0475	0.0227	0.0206	0.1137	0.0892	0.9755	0.0068	0.0163	3.2806	0.1894	0.0152
P06	28/09/2015	0.9443	0.1952	0.0417	4.2995	0.1172	2.1097	0.0059	0.0362	7.8156	0.0149	20.9975
P08	28/09/2015	0.7018	0.2837	0.0451	8.1305	0.1688	0.9188	0.0065	0.0205	9.6210	0.5179	0.0763
P09	28/09/2015	1.3114	1.3551	0.1151	8.8060	0.6838	4.8253	0.0083	0.0688	31.9581	0.0236	0.0423
P10	28/09/2015	1.2159	2.1919	0.1077	7.4735	0.4014	4.9527	0.0093	0.0604	29.5194	0.0127	0.0451
P11	28/09/2015	2.4315	0.9168	0.1300	5.9161	0.3570	4.0716	0.0055	0.0551	28.8869	0.0350	0.2572
P12	28/09/2015	1.9473	0.1565	0.0395	12.7868	0.2358	5.7730	0.0065	0.1053	7.0419	0.0090	0.1545
V01	29/09/2015	2.3566	0.1375	0.0410	6.6472	0.1581	1.1013	0.0022	0.0152	7.3954	0.0102	0.2160
V02	29/09/2015	1.9107	0.3180	0.0426	9.1055	0.2582	0.8797	0.0024	0.0148	15.2622	0.8382	0.0840
V03	29/09/2015	1.9940	0.2365	0.0397	9.7084	0.2941	11.9288	0.0038	0.0339	12.6040	0.0347	0.0856
V04	29/09/2015	1.7526	0.0970	0.0201	3.5602	0.1116	0.5576	0.0022	0.0103	7.5755	0.0147	0.4602
V06	29/09/2015	1.4576	0.4237	0.0750	8.4542	0.1244	1.1810	0.0026	0.0203	14.1798	0.0174	0.5115
V07	29/09/2015	1.5636	0.4069	0.1101	6.8331	0.1159	0.6216	0.0024	0.0264	17.5790	0.0143	0.6624
V08	29/09/2015	0.8625	0.1375	0.0503	12.6804	0.0681	2.1875	0.0025	0.0125	4.5031	0.0038	0.1588
V10	29/09/2015	1.8372	0.7823	0.1611	7.3906	0.2012	3.3742	0.0026	0.0375	30.7425	0.0511	0.4437
V11	29/09/2015	0.5437	0.3587	0.0387	6.8564	0.0505	0.8616	0.0026	0.0222	5.9659	0.0176	0.2394
P05	25/07/2016	0.8708	0.4158	<LOD	6.9837	1.3976	6.7914	<LOD	<LOD	5.8444	<LOD	0.1706
P06	25/07/2016	1.2395	<LOD	<LOD	9.3492	<LOD	3.6884	<LOD	<LOD	10.9767	<LOD	28.2497
P08	25/07/2016	0.4781	<LOD	<LOD	10.0636	<LOD	4.9548	<LOD	<LOD	19.7701	<LOD	<LOD
P11	25/07/2016	1.3811	<LOD	<LOD	5.2231	0.4311	4.2578	<LOD	<LOD	11.6616	<LOD	<LOD
P12	25/07/2016	2.1286	5.7420	<LOD	16.6693	0.3592	13.1957	<LOD	<LOD	32.8403	<LOD	<LOD
V01	26/07/2016	2.2017	<LOD	<LOD	8.7168	<LOD	3.3448	<LOD	<LOD	5.0186	<LOD	0.0195
V02	26/07/2016	1.4391	<LOD	<LOD	8.4163	0.6808	2.6200	<LOD	<LOD	4.5514	<LOD	<LOD
V03	26/07/2016	2.1520	<LOD	<LOD	14.1992	0.7092	5.7241	<LOD	<LOD	7.7993	<LOD	<LOD
V04	26/07/2016	1.2724	<LOD	<LOD	8.9297	<LOD	5.0603	<LOD	<LOD	6.2071	<LOD	0.1597
V07	26/07/2016	<LOD	<LOD	<LOD	0.0280	<LOD	6.9079	<LOD	<LOD	4.8823	<LOD	<LOD
V10	26/07/2016	0.6551	<LOD	<LOD	4.4764	<LOD	5.4233	<LOD	<LOD	4.0051	<LOD	<LOD
V11	26/07/2016	<LOD	1.0643	<LOD	10.8461	<LOD	4.5394	<LOD	<LOD	3.9131	<LOD	<LOD
P05	23/06/2016	<LOD	<LOD	<LOD	0.0733	0.1891	6.6373	0.0536	0.0671	0.4893	0.0886	<LOD
P06	23/06/2016	0.1113	<LOD	<LOD	4.9346	0.1659	2.8510	0.0522	0.0922	3.0191	0.0969	8.5224
P08	23/06/2016	0.2173	0.9080	<LOD	7.9790	0.3402	5.8740	0.0522	0.0877	20.1192	0.1085	<LOD
P11	23/06/2016	0.9320	0.0876	<LOD	4.9804	0.4079	5.2438	0.0534	0.0970	11.5722	0.0918	<LOD

		Trace elements (micrograms per liter)										
	Measure unit	µg/L	µg/L	µg/L	µg/L	µg/L	µg/L	µg/L	µg/L	µg/L	µg/L	µg/L
Sample	**Date**	**Cr**	**Mn**	**Co**	**Ni**	**Cu**	**Zn**	**Cd**	**Pb**	**Fe**	**Ag**	**As**
P12	23/06/2016	2.0503	<LOD	<LOD	13.0241	0.3117	7.0406	0.0519	0.0636	6.3211	0.0950	<LOD
V07	24/06/2016	1.8132	<LOD	<LOD	8.2155	0.2691	16.9710	0.0516	0.0794	9.4472	0.0862	0.3913
V09	24/06/2016	2.0956	0.1341	<LOD	6.3207	0.4067	4.9496	0.0518	0.1061	13.8999	0.1148	0.6811
V10	24/06/2016	2.0527	0.5666	<LOD	6.9724	0.3026	8.1028	0.0516	0.0891	12.0506	0.0895	0.1088
V11	24/06/2016	0.2952	0.5617	<LOD	7.7324	0.4559	2.6209	0.0555	0.1297	5.9228	0.1314	<LOD
P03	10/10/2016	<LOD	<LOD	<LOD	5.4226	<LOD	1.1578	<LOD	<LOD	0.1371	<LOD	<LOD
P08	10/10/2016	0.1818	<LOD	<LOD	5.3343	<LOD	2.7949	<LOD	<LOD	<LOD	<LOD	<LOD
P11	10/10/2016	0.4237	<LOD	<LOD	16.4020	1.0034	2.0326	<LOD	<LOD	0.1210	<LOD	<LOD
V01	11/10/2016	1.7462	<LOD	<LOD	5.6864	0.2350	1.6870	<LOD	<LOD	0.3408	<LOD	<LOD
V02	11/10/2016	1.1148	<LOD	<LOD	7.9568	<LOD	1.4302	<LOD	<LOD	0.1975	<LOD	<LOD
V03	11/10/2016	1.1929	<LOD	<LOD	15.8066	<LOD	2.5720	<LOD	<LOD	4.6111	<LOD	<LOD
V04	11/10/2016	0.5398	<LOD	<LOD	8.3775	<LOD	1.6220	<LOD	<LOD	1.1918	<LOD	0.0149
V07	11/10/2016	0.3945	<LOD	<LOD	8.7079	<LOD	0.8864	<LOD	<LOD	<LOD	<LOD	<LOD
V11	11/10/2016	0.0490	<LOD	<LOD	5.3870	<LOD	0.5952	<LOD	<LOD	0.0399	<LOD	<LOD
LOD	-	0.0031	0.002	0.0002	0.0047	0.001	0.0096	0.0004	0.0002	0.0188	0.0003	0.0018

Supplementary_02: Major ions and trace elements analyzed in all the springs along the 2016-2017 Seismic sequence

SAMPLE	DATE	T	pH	Electrical conductivity	HCO_3	F	Cl	NO_2	NO_3	PO_4	SO_4	NH_4	Ca	Mg	Na	K	Ionic balance
	Measure unit	°C	-	µS/cm	mg/L	mg/L	mg/L	mg/L	mg/L	mg/L	mg/L	mg/L	mg/L	mg/L	mg/L	mg/L	-
NER (Bottle)	24/11/2015	-	7.98	292	183.00	0.05	6.27	<LOD	1.81	<LOD	1.62	1.00	69.40	1.14	2.34	1.43	7.36%
NER (Bottle)	28/12/2015	-	7.95	290	176.90	0.04	5.89	<LOD	1.63	<LOD	1.67	1.02	66.91	1.03	2.31	1.28	7.27%
NER (Bottle)	19/01/2016	-	7.95	286	183.00	0.02	6.26	<LOD	1.84	<LOD	1.72	<LOD	60.91	0.93	2.36	1.59	0.35%
NER (Bottle)	26/02/2016	-	8.03	296	186.05	0.05	6.48	<LOD	1.56	<LOD	1.74	<LOD	69.44	1.08	2.38	1.91	5.94%
NER (Bottle)	24/03/2016	-	8.14	306	176.90	0.05	6.72	<LOD	1.48	<LOD	1.84	<LOD	61.41	0.96	2.44	1.19	2.05%
NER (Bottle)	27/04/2016	-	8.06	297	186.05	<LOD	7.29	<LOD	1.61	<LOD	1.76	0.91	62.39	0.98	2.60	2.34	1.56%
NER (Bottle)	02/05/2016	-	8.15	299	179.95	0.02	7.41	<LOD	1.71	<LOD	1.76	1.05	68.43	1.06	2.49	1.64	7.10%
NER (Bottle)	06/06/2016	-	7.85	289	186.05	0.04	6.63	<LOD	1.51	<LOD	1.79	2.37	60.93	1.14	2.52	1.81	1.88%
NER (Bottle)	26/07/2016	-	7.94	292	179.95	0.04	6.48	<LOD	1.58	<LOD	1.72	2.70	54.80	1.01	2.37	1.64	-1.24%
NER (Bottle)	08/08/2016	-	7.88	301	176.90	0.05	6.50	<LOD	1.79	<LOD	1.73	2.26	62.10	1.04	2.56	1.72	4.85%
NER (Bottle)	23/08/2016	-	8.09	288	173.85	<LOD	5.11	<LOD	1.02	<LOD	1.43	<LOD	54.99	1.98	2.17	1.05	-0.11%
NER (Bottle)	24/08/2016	-	8.12	271	167.75	<LOD	5.08	<LOD	0.99	<LOD	1.42	<LOD	57.46	1.99	2.19	1.04	3.61%
NER (Bottle)	03/10/2016	-	7.42	312	183.00	0.05	5.90	<LOD	0.87	<LOD	1.47	2.72	52.63	1.38	3.13	1.86	-2.13%
NER (Bottle)	12/10/2016	-	7.57	268	176.90	-	-	-	-	-	-	-	-	-	-	-	-
NER (Bottle)	18/10/2016	-	7.68	267	170.80	0.05	5.50	<LOD	0.81	<LOD	1.40	2.63	54.05	1.35	2.82	2.07	2.21%
NER (Bottle)	26/10/2016	-	6.66	272	170.80	0.04	6.03	<LOD	1.76	<LOD	1.69	<LOD	61.53	1.02	2.79	2.12	4.71%
NER (Bottle)	11/01/2017	-	7.46	230	173.85	0.04	5.25	<LOD	0.69	<LOD	1.38	2.64	54.11	1.68	3.58	2.31	2.64%
NER (Bottle)	25/01/2017	-	7.64	247	170.80	-	-	-	-	-	-	-	-	-	-	-	-
NER (Bottle)	01/02/2017	-	7.95	232	173.85	0.05	5.71	<LOD	1.38	<LOD	1.75	1.99	53.45	1.07	2.35	1.69	-0.92%
NER (Bottle)	13/03/2017	-	7.66	294	179.95	0.04	5.44	<LOD	0.66	<LOD	1.51	2.72	57.81	1.39	2.95	2.52	3.10%
NER (Bottle)	20/03/2017	-	7.72	281	179.95	0.04	5.45	<LOD	0.67	<LOD	1.54	2.55	57.11	1.58	3.41	2.28	2.84%
NER (Bottle)	03/04/2017	-	8	279	179.95	0.04	6.14	<LOD	1.35	<LOD	1.77	2.08	58.59	1.19	2.58	1.83	1.81%
NER (Bottle)	12/04/2017	-	7.71	276	176.90	0.06	5.64	<LOD	0.64	<LOD	1.52	2.61	57.06	1.31	3.08	1.85	2.85%
NER (Bottle)	03/05/2017	-	7.68	288	176.90	0.04	5.98	<LOD	0.62	<LOD	1.59	2.67	56.14	1.39	2.77	2.10	2.05%
NER (Bottle)	10/05/2017	-	7.78	281	179.95	0.02	6.53	<LOD	1.45	<LOD	1.80	3.09	58.89	1.21	2.84	2.37	3.09%
NER (Bottle)	10/08/2017	-	7.9	301	158.60	<LOD	4.21	<LOD	0.86	<LOD	1.60	1.66	58.00	1.95	1.27	1.07	7.82%
NER (Bottle)	17/08/2017	-	8.02	245	176.90	<LOD	4.16	<LOD	0.87	<LOD	1.60	<LOD	55.95	2.02	2.15	1.04	0.30%
NER (Bottle)	24/08/2017	-	8.02	275	170.80	<LOD	4.06	<LOD	0.84	<LOD	1.61	<LOD	54.25	2.00	2.09	1.02	0.54%
NER (Bottle)	06/09/2017	-	8.2	254	170.80	<LOD	3.95	<LOD	0.84	<LOD	1.58	<LOD	55.25	2.01	2.09	1.06	1.46%
NER (Bottle)	14/09/2017	-	8.7	290	170.80	<LOD	3.95	<LOD	0.82	<LOD	1.61	<LOD	53.84	1.98	2.00	1.03	0.17%
NER (Bottle)	12/10/2017	-	7.17	291	183.00	<LOD	3.93	<LOD	0.86	<LOD	1.62	<LOD	54.89	2.01	2.16	1.07	-2.06%
NER (Bottle)	12/11/2017	-	8.06	236	176.90	<LOD	3.80	<LOD	0.93	<LOD	1.65	<LOD	53.63	2.02	2.07	1.04	-1.53%
NER (Bottle)	13/02/2018	-	8.05	248	164.70	<LOD	5.54	<LOD	0.80	<LOD	1.61	<LOD	61.30	2.05	2.22	1.09	7.28%
NER (Bottle)	14/03/2018	-	8.16	239	170.80	<LOD	5.81	<LOD	0.75	<LOD	1.67	<LOD	67.30	2.01	2.19	1.10	9.66%
NER (Bottle)	11/04/2018	-	8.09	305	167.75	<LOD	6.27	<LOD	0.73	<LOD	1.67	<LOD	62.84	2.00	2.22	1.04	7.13%
NER (Spring)	06/06/2016	-	6.81	296	179.95	0.04	6.84	<LOD	1.73	<LOD	1.71	2.67	62.61	1.06	2.65	1.67	4.68%
NER (Spring)	06/09/2016	-	7.91	288	186.05	0.04	6.74	<LOD	1.82	<LOD	1.64	3.03	59.14	1.30	2.50	2.15	1.34%
NER (Spring)	27/09/2016	9.5	7.52	314	176.90	0.02	5.94	<LOD	0.83	<LOD	1.33	3.84	48.81	0.93	3.19	2.16	-3.07%
NER (Spring)	26/10/2016	-	6.62	278	179.95	0.02	5.92	<LOD	0.74	<LOD	1.79	5.33	50.73	1.15	2.83	2.05	-1.03%
NER (Spring)	28/10/2016	-	6.63	271	158.60	0.04	5.75	<LOD	0.76	<LOD	1.34	4.63	42.57	1.18	3.02	1.99	-2.54%
NER (Spring)	02/11/2016	-	6.72	288	173.85	0.05	6.36	0.03	1.92	<LOD	1.67	2.47	61.41	1.29	2.69	2.10	5.85%
NER (Spring)	03/11/2016	9.6	7.63	312	176.90	-	-	-	-	-	-	-	-	-	-	-	-
NER (Spring)	04/11/2016	-	7.04	290	183.00	0.04	5.70	<LOD	0.90	<LOD	1.34	2.95	61.94	1.21	2.75	1.64	4.71%
NER (Spring)	07/11/2016	-	7.72	286	231.80	0.04	6.30	<LOD	1.72	<LOD	1.64	2.17	60.33	1.08	2.73	2.08	-8.66%
NER (Spring)	08/11/2016	-	6.89	285	231.80	-	-	-	-	-	-	-	-	-	-	-	-

SAMPLE	DATE	T	pH	Electrical conductivity	HCO_3	F	Cl	NO_2	NO_3	PO_4	SO_4	NH_4	Ca	Mg	Na	K	Ionic balance
	Measure unit	°C	-	µS/cm	mg/L	mg/L	mg/L	mg/L	mg/L	mg/L	mg/L	mg/L	mg/L	mg/L	mg/L	mg/L	-
NER (Spring)	09/11/2016	-	6.82	287	207.40	-	-	-	-	-	-	-	-	-	-	-	-
NER (Spring)	10/11/2016	-	7.02	285	219.60	0.04	5.73	<LOD	0.91	<LOD	1.38	2.59	59.59	1.20	2.32	1.95	-6.04%
NER (Spring)	10/11/2016	-	7.05	288	195.20	-	-	-	-	-	-	-	-	-	-	-	-
NER (Spring)	15/11/2016	-	6.94	287	195.20	0.05	6.27	<LOD	1.80	<LOD	1.62	2.50	59.22	1.01	2.51	1.80	-1.53%
NER (Spring)	16/11/2016	-	7.71	287	195.20	-	-	-	-	-	-	-	-	-	-	-	-
NER (Spring)	17/11/2016	-	7.72	286	201.30	-	-	-	-	-	-	-	-	-	-	-	-
NER (Spring)	18/11/2016	8.7	8.44	253.5	201.30	0.04	6.23	<LOD	1.65	<LOD	1.63	1.97	55.22	1.02	2.57	1.80	-6.42%
NER (Spring)	23/11/2016	-	7.67	247	186.05	0.04	5.75	<LOD	0.91	<LOD	1.35	4.65	46.05	1.14	2.76	1.77	-7.20%
NER (Spring)	29/11/2016	-	7.32	250	179.95	-	-	-	-	-	-	-	-	-	-	-	-
NER (Spring)	06/12/2016	-	7.55	248	186.05	0.04	6.28	<LOD	1.82	<LOD	1.61	<LOD	61.21	1.14	2.81	1.96	0.51%
NER (Spring)	09/01/2017	-	7.4	243	183.00	0.04	5.72	<LOD	0.89	<LOD	1.35	3.44	47.47	0.98	2.76	1.77	-6.59%
NER (Spring)	12/01/2017	-	7.43	247	186.05	-	-	-	-	-	-	-	-	-	-	-	-
NER (Spring)	01/02/2017	-	7.63	256	183.00	0.04	6.38	<LOD	1.76	<LOD	1.62	1.91	59.18	1.05	2.58	1.71	0.96%
NER (Spring)	08/02/2017	-	7.62	260	186.05	-	-	-	-	-	-	-	-	-	-	-	-
NER (Spring)	15/02/2017	-	7.2	239	173.85	-	-	-	-	-	-	-	-	-	-	-	-
NER (Spring)	22/02/2017	-	7.51	242	183.00	-	-	-	-	-	-	-	-	-	-	-	-
NER (Spring)	27/02/2017	-	7.79	243	186.05	-	-	-	-	-	-	-	-	-	-	-	-
NER (Spring)	01/03/2017	-	7.49	248	179.95	0.04	6.52	<LOD	1.70	<LOD	1.70	2.35	53.41	1.04	2.38	1.98	-2.53%
NER (Spring)	13/03/2017	-	7.75	300	183.00	-	-	-	-	-	-	-	-	-	-	-	-
NER (Spring)	20/03/2017	-	7.667	292	179.95	0.04	5.99	<LOD	0.83	<LOD	1.51	2.86	53.86	1.27	2.79	1.78	-0.68%
NER (Spring)	03/04/2017	-	7.7	303	183.00	0.05	6.61	<LOD	1.57	<LOD	1.77	1.86	60.44	1.17	2.63	1.94	2.03%
NER (Spring)	10/04/2017	-	7.803	283	173.85	0.04	6.18	<LOD	0.81	<LOD	1.69	2.72	57.61	1.01	2.69	2.36	3.41%
NER (Spring)	19/04/2017	-	7.71	311	183.00	-	-	-	-	-	-	-	-	-	-	-	-
NER (Spring)	10/05/2017	-	7.71	304	186.05	0.04	7.60	<LOD	1.61	<LOD	1.82	2.35	56.29	0.97	2.49	1.84	-2.31%
NER (Spring)	18/05/2017	14.5	8.45	305	-	-	-	-	-	-	-	-	-	-	-	-	-
NER (Spring)	10/08/2017	-	7.86	286	189.10	<LOD	6.13	<LOD	1.00	<LOD	1.51	<LOD	55.22	1.97	2.14	1.06	-4.35%
NER (Spring)	17/08/2017	-	7.27	242	176.90	<LOD	6.03	<LOD	0.99	<LOD	1.48	<LOD	55.31	2.00	2.17	1.05	-1.07%
NER (Spring)	24/08/2017	-	7.95	310	152.50	<LOD	6.01	<LOD	1.00	<LOD	1.47	<LOD	56.86	1.98	2.19	1.04	7.03%
NER (Spring)	06/09/2017	-	7.94	282	170.80	<LOD	6.11	<LOD	1.01	<LOD	1.58	<LOD	56.17	1.99	2.16	1.01	1.15%
NER (Spring)	14/09/2017	-	7.83	270	170.80	<LOD	6.17	<LOD	1.01	<LOD	1.50	<LOD	56.18	1.98	2.17	1.07	1.18%
NER (Spring)	20/09/2017	-	7.9	240	176.90	<LOD	6.17	<LOD	1.01	<LOD	1.48	<LOD	56.21	1.97	2.09	1.03	-0.51%
NER (Spring)	12/10/2017	-	7.91	342	176.90	<LOD	6.13	<LOD	1.01	<LOD	1.46	<LOD	63.48	1.96	2.13	1.06	5.10%
NER (Spring)	15/11/2017	-	6.99	258	164.70	<LOD	6.53	<LOD	1.07	<LOD	1.52	<LOD	50.90	1.52	2.20	0.99	-2.48%
NER (Spring)	14/03/2018	-	6.96	301	173.85	<LOD	7.15	<LOD	0.78	<LOD	1.94	<LOD	56.54	2.02	2.25	1.03	0.20%
NER (Spring)	11/04/2018	-	7.68	302	176.90	<LOD	6.95	<LOD	0.77	<LOD	1.95	<LOD	59.04	2.05	2.29	1.06	1.54%
VIC	03/07/2014	13	7.3	534	292.00	<LOD	5.50	<LOD	<LOD	<LOD	6.30	<LOD	96.00	2.00	4.20	1.20	1.02%
VIC	15/02/2015	13	7.4	527	357.00	<LOD	4.80	<LOD	<LOD	<LOD	10.00	<LOD	100.00	2.10	3.00	0.78	-7.58%
VIC	22/05/2015	13.2	7	506	299.00	<LOD	6.60	<LOD	<LOD	<LOD	6.80	<LOD	94.00	2.10	5.20	1.70	-0.84%
VIC	20/09/2015	12.2	7.4	520	304.00	<LOD	6.70	<LOD	<LOD	<LOD	7.00	<LOD	95.00	2.00	5.30	1.20	-1.36%
VIC	27/08/2016	-	7.06	503	366.00	0.08	6.00	<LOD	<LOD	0.12	7.44	<LOD	101.81	3.02	5.85	2.50	-5.63%
VIC	28/08/2016	-	7.11	608	-	-	-	-	-	-	-	-	-	-	-	-	-
VIC	30/08/2016	14.2	6.37	529	353.80	0.09	7.99	1.08	<LOD	<LOD	9.33	<LOD	97.03	2.60	6.06	2.94	-7.24%
VIC	06/09/2016	13.8	7.42	529	341.60	0.07	10.25	1.69	21.03	<LOD	10.40	<LOD	107.90	2.49	7.45	3.15	-3.85%
VIC	22/09/2016	-	8.13	497	314.15	0.07	6.13	<LOD	14.15	0.05	6.74	<LOD	100.54	2.56	5.29	2.43	-1.49%
VIC	31/10/2016	-	8.1	500	298.90	0.08	5.71	<LOD	9.04	0.09	10.53	3.23	84.96	2.68	5.78	3.86	-4.17%
VIC	02/11/2016	-	7.78	520	295.85	-	-	-	-	-	-	-	-	-	-	-	-
VIC	28/11/2016	-	7.53	516	329.40	0.06	6.44	<LOD	14.84	<LOD	6.86	2.13	106.50	2.33	5.21	2.57	-0.33%

SAMPLE	DATE	T	pH	Electrical conductivity	HCO_3	F	Cl	NO_2	NO_3	PO_4	SO_4	NH_4	Ca	Mg	Na	K	Ionic balance
	Measure unit	°C	-	µS/cm	mg/L	mg/L	mg/L	mg/L	mg/L	mg/L	mg/L	mg/L	mg/L	mg/L	mg/L	mg/L	-
VIC	24/12/2016	-	7.8	507	347.70	0.07	5.50	<LOD	9.90	0.09	5.72	3.51	88.51	3.19	6.24	2.53	-8.11%
VIC	19/01/2017	-	7.66	520	317.20	0.06	5.67	<LOD	9.25	0.08	6.29	3.43	86.27	2.89	6.28	2.57	-5.27%
VIC	28/02/2017	-	7.67	506	268.40	0.06	6.25	<LOD	14.44	0.05	6.89	3.01	103.62	2.42	5.60	2.46	8.29%
VIC	17/05/2017	13.5	7.34	500	292.80	0.06	6.35	<LOD	14.49	0.05	6.76	2.70	105.09	2.40	5.60	2.40	4.87%
SUS	03/07/2014	10.9	7.4	835	266.00	<LOD	3.70	<LOD	<LOD	<LOD	270.00	<LOD	110.00	27.00	2.00	<LOD	-12.74%
SUS	15/02/2015	10.7	7.6	851	296.00	<LOD	3.70	<LOD	<LOD	<LOD	280.00	<LOD	120.00	30.00	2.60	0.56	-11.32%
SUS	22/05/2015	10.4	7.1	798	235.00	<LOD	3.00	<LOD	<LOD	<LOD	260.00	<LOD	130.00	29.00	2.80	0.68	-1.78%
SUS	20/09/2015	10.3	7.3	855	275.00	<LOD	3.60	<LOD	<LOD	<LOD	270.00	<LOD	140.00	30.00	2.90	0.55	-3.15%
SUS	27/08/2016	-	7.35	916	227.23	0.76	5.00	<LOD	3.74	<LOD	389.69	1.88	161.79	38.67	3.73	2.48	-2.04%
SUS	28/08/2016	-	7.22	918	-	-	-	-	-	-	-	-	-	-	-	-	-
SUS	30/08/2016	10.3	7.14	918	256.20	0.65	4.80	<LOD	3.44	<LOD	360.93	2.08	138.33	33.50	3.16	2.49	-8.91%
SUS	06/09/2016	10.3	7.05	904	244.00	0.88	5.48	<LOD	<LOD	<LOD	420.52	2.00	161.32	39.48	3.98	2.43	-5.28%
SUS	22/09/2016	-	8.12	872	231.80	0.53	3.73	<LOD	2.76	<LOD	291.40	2.75	148.52	35.41	3.44	2.30	3.15%
SUS	31/10/2016	-	8.13	852	213.50	0.63	3.42	<LOD	1.13	<LOD	284.93	3.54	115.24	35.93	4.05	<LOD	-2.63%
SUS	02/11/2016	-	7.85	805	225.70	-	-	-	-	-	-	-	-	-	-	-	-
SUS	28/11/2016	-	7.87	873	253.15	0.52	3.77	<LOD	2.63	<LOD	285.08	3.26	144.00	36.24	3.40	2.27	1.46%
SUS	24/12/2016	-	7.43	783	244.00	0.50	3.30	<LOD	1.49	<LOD	246.39	2.05	106.59	33.63	3.82	2.88	-4.66%
SUS	19/01/2017	-	7.63	814	259.25	0.49	3.29	<LOD	3.75	<LOD	248.44	1.95	129.50	41.22	3.72	2.54	3.02%
SUS	28/02/2017	-	6.68	831	225.70	0.55	3.50	<LOD	2.60	<LOD	264.67	2.43	140.30	34.03	3.32	1.93	3.90%
SUS	28/04/2017	10.8	7.7	851	244.00	0.51	3.72	<LOD	3.07	<LOD	273.63	2.07	140.46	33.68	3.21	1.98	1.09%
SUS	17/05/2017	10.4	7.44	822	219.60	1.06	3.18	<LOD	2.59	<LOD	276.11	<LOD	148.66	30.27	3.78	0.98	2.88%
PES	03/07/2014	12.8	7.2	617	404.00	<LOD	4.10	<LOD	<LOD	<LOD	8.40	<LOD	94.00	19.00	2.60	<LOD	-4.04%
PES	15/02/2015	10	7	653	540.00	<LOD	7.00	<LOD	<LOD	<LOD	6.80	<LOD	100.00	20.00	4.90	<LOD	-14.53%
PES	22/05/2015	11.4	7	594.8	409.00	<LOD	3.40	<LOD	<LOD	<LOD	8.90	<LOD	100.00	19.00	3.10	<LOD	-2.10%
PES	20/09/2015	12.4	7.2	597	411.00	<LOD	4.00	<LOD	<LOD	<LOD	6.80	<LOD	100.00	18.00	4.40	<LOD	-2.34%
PES	27/08/2016	-	7.1	733	439.20	0.12	6.70	2.03	3.90	<LOD	16.32	1.97	102.84	23.86	4.07	2.69	-2.50%
PES	28/08/2016	-	7.11	727	469.70	-	-	-	-	-	-	-	-	-	-	-	-
PES	30/08/2016	15.9	7.33	690	488.00	0.11	4.71	<LOD	<LOD	0.06	10.95	2.09	90.22	27.81	4.11	2.65	-7.77%
PES	06/09/2016	12.9	7.4	676	506.30	0.09	5.90	1.00	<LOD	<LOD	14.33	2.22	92.98	28.56	4.08	2.69	-8.80%
PES	22/09/2016	-	7.85	632	451.40	0.09	4.39	0.20	2.76	<LOD	10.98	1.97	94.63	22.49	4.04	2.32	-5.97%
PES	31/10/2016	-	7.67	624	439.20	0.06	4.10	<LOD	1.47	<LOD	10.25	3.10	96.52	20.64	4.16	2.27	-4.28%
PES	02/11/2016	-	7.64	634	411.75	-	-	-	-	-	-	-	-	-	-	-	-
PES	28/11/2016	-	7.56	484	305.00	0.10	4.52	<LOD	2.94	0.03	10.65	0.76	87.37	14.96	4.05	2.12	4.16%
PES	24/12/2016	-	7.17	580	445.30	0.09	3.93	<LOD	1.51	0.07	8.51	3.07	91.70	21.50	3.75	2.55	-6.03%
PES	19/01/2017	-	7.71	645	451.40	0.13	3.91	0.06	1.48	<LOD	9.37	2.92	93.18	22.83	3.97	2.57	-5.45%
PES	28/02/2017	-	7.38	623	451.40	0.09	4.34	<LOD	2.60	<LOD	10.75	2.44	116.83	22.27	3.88	2.11	1.51%
PES	28/04/2017	12.2	7.42	676	454.45	0.09	4.36	<LOD	2.71	0.03	10.91	<LOD	120.60	23.01	3.94	2.04	1.86%
PES	17/05/2017	15	6.95	651	420.90	0.83	4.57	<LOD	2.97	<LOD	9.39	<LOD	94.82	22.98	2.93	0.77	-3.81%
FP01	28/09/2016	11.9	7.27	233	134.20	0.81	2.32	<LOD	2.11	<LOD	8.65	<LOD	38.86	5.08	0.88	0.25	-2.36%
FP01	02/11/2016	9.3	7.63	222	128.10	0.84	2.42	<LOD	2.18	1.56	7.96	<LOD	39.22	4.73	1.08	0.25	-1.22%
FP01	16/11/2016	4.2	7.9	222.2	140.30	0.81	2.39	<LOD	2.13	<LOD	9.20	<LOD	38.69	5.30	1.02	0.24	-4.25%
FP02	28/09/2016	9.7	6.89	586	256.20	0.81	22.17	<LOD	28.87	<LOD	5.03	<LOD	104.52	1.48	8.87	1.29	2.93%
FP02	02/11/2016	8.3	7.22	592	271.45	0.79	19.97	0.79	28.33	<LOD	4.87	<LOD	108.23	1.47	8.35	1.24	2.57%
FP02	16/11/2016	6.7	7.56	579	266.88	0.80	16.88	<LOD	26.25	<LOD	4.59	<LOD	99.46	1.40	7.51	1.08	0.28%
FP02	27/04/2017	7.3	6.87	597	298.90	0.80	20.01	<LOD	27.95	<LOD	5.34	<LOD	118.48	1.73	8.61	1.59	3.29%
FP03	28/09/2016	11.4	7.22	505	323.30	0.79	3.95	<LOD	1.63	<LOD	2.68	<LOD	52.37	18.91	2.70	0.14	-12.62%
FP03	02/11/2016	10.8	7.58	546	320.25	0.77	3.92	0.90	1.65	1.48	2.71	<LOD	72.17	19.37	2.84	0.19	-2.02%

SAMPLE	DATE	T	pH	Electrical conductivity	HCO_3	F	Cl	NO_2	NO_3	PO_4	SO_4	NH_4	Ca	Mg	Na	K	Ionic balance
	Measure unit	°C	-	µS/cm	mg/L	mg/L	mg/L	mg/L	mg/L	mg/L	mg/L	mg/L	mg/L	mg/L	mg/L	mg/L	-
FP03	17/11/2016	8.6	7.95	504	311.10	0.79	3.99	<LOD	1.73	<LOD	2.74	<LOD	77.21	20.23	2.75	0.23	2.84%
FP03	27/04/2017	9.5	6.94	485	347.70	0.79	3.90	<LOD	1.61	<LOD	2.73	<LOD	77.69	17.24	2.43	0.39	-4.54%
FP04	02/11/2016	10.4	7.3	556	312.63	0.79	5.51	0.89	1.99	1.49	11.85	<LOD	74.21	23.42	6.25	0.82	2.28%
FP04	17/11/2016	9.2	7.85	574	329.40	0.79	5.48	<LOD	1.91	<LOD	12.32	<LOD	72.95	22.77	6.02	0.79	-0.68%
FP04	27/04/2017	-	7.76	567	283.65	0.79	5.73	<LOD	1.73	<LOD	16.85	<LOD	65.28	16.78	5.07	0.52	-3.50%
FP04	15/09/2017	-	7.26	560	274.50	0.80	6.87	<LOD	2.17	<LOD	21.31	0.13	78.99	20.17	7.23	0.77	6.59%

SAMPLE	DATE	Li	B	Al	Cr	Mn	Fe	Co	Ni	Cu	Rb	Sr	Pb	U
	Measure unit	µg/L	µg/L	µg/L	µg/L	µg/L	µg/L	µg/L	µg/L	µg/L	µg/L	µg/L	µg/L	µg/L
NER (Bottle)	24/11/2015	-	-	0.0193	0.2262	0.0803	<LOD	0.0866	0.0945	0.1848	0.7976	72.2382	0.0761	0.2201
NER (Bottle)	28/12/2015	-	-	0.7912	0.2779	0.1364	1.0966	0.0900	0.2414	0.1823	0.7180	65.7642	0.0793	0.2103
NER (Bottle)	19/01/2016	-	-	0.9136	0.2130	0.0900	0.0576	0.0865	0.1337	0.1997	0.7037	64.4979	0.0795	0.2049
NER (Bottle)	26/02/2016	-	-	0.3280	0.2119	0.0792	<LOD	0.0855	0.1095	0.1761	0.7456	68.8134	0.0784	0.2141
NER (Bottle)	24/03/2016	-	-	0.1098	0.2031	0.0725	<LOD	0.0851	0.0940	0.1883	0.7683	74.7810	0.0759	0.2197
NER (Bottle)	27/04/2016	-	-	0.9881	0.1988	0.0985	0.0804	0.0953	0.1448	0.1780	0.7286	67.0645	0.0796	0.2089
NER (Bottle)	02/05/2016	-	-	0.0672	0.2104	0.0884	<LOD	0.0969	0.1392	0.1740	0.7015	66.5900	0.0779	0.2090
NER (Bottle)	06/06/2016	0.4240	3.4570	0.5432	0.2443	0.1363	0.4167	0.1304	0.1595	0.3042	0.9412	84.4620	0.1333	0.2506
NER (Bottle)	26/07/2016	-	-	2.1493	0.2499	0.1571	1.5986	0.1313	0.1772	0.4631	0.9961	87.2803	0.1443	0.2550
NER (Bottle)	08/08/2016	0.3980	3.3360	0.8160	0.2508	0.1448	0.3174	0.1532	0.1619	0.3566	1.0038	89.0507	0.1346	0.2582
NER (Bottle)	23/08/2016	0.3340	3.4930	1.2851	0.2002	0.1345	0.8228	0.1320	0.1366	0.3679	0.6331	-	0.1166	0.2701
NER (Bottle)	24/08/2016	0.3804	3.5120	5.7233	0.2653	0.1357	1.6399	0.1352	0.1479	0.3763	0.6250	-	0.1349	0.2744
NER (Bottle)	03/10/2016	-	-	8.9830	0.4641	0.2164	2.8884	0.1369	0.6680	1.3051	0.9776	71.2059	0.2147	0.2395
NER (Bottle)	12/10/2016	-	-	-	-	-	-	-	-	-	-	-	-	-
NER (Bottle)	18/10/2016	0.5285	3.6990	8.4929	0.4316	0.2086	2.5666	0.1351	0.5551	1.1856	0.8681	69.2057	0.2116	0.2314
NER (Bottle)	26/10/2016	-	-	7.0000	0.4107	0.1874	1.7661	0.1343	0.4480	0.9979	0.8688	69.2630	0.1858	0.2314
NER (Bottle)	11/01/2017	-	-	5.9526	0.2958	0.2374	5.3633	0.1333	0.2827	0.4379	0.8060	68.4945	0.1732	0.1683
NER (Bottle)	25/01/2017	-	-	-	-	-	-	-	-	-	-	-	-	-
NER (Bottle)	01/02/2017	0.5090	3.1330	2.0893	0.2991	0.1748	1.5033	0.1314	0.2075	0.3627	0.7234	63.4491	0.1422	0.2110
NER (Bottle)	13/03/2017	-	-	0.9211	0.2316	0.3263	0.6893	0.1309	0.1845	0.5800	0.8486	85.6616	0.1401	0.2527
NER (Bottle)	20/03/2017	-	-	0.8200	0.2374	0.2402	0.3174	0.1299	0.1516	0.6019	0.8790	88.0210	0.1378	0.2570
NER (Bottle)	03/04/2017	-	-	-	-	-	-	-	-	-	-	-	-	-
NER (Bottle)	12/04/2017	-	-	0.8014	0.2547	0.4940	1.0594	0.1313	0.1869	0.3197	0.9299	91.3352	0.1461	0.2676
NER (Bottle)	03/05/2017	-	-	1.4427	0.2473	0.3033	1.0832	0.1306	0.1805	0.3432	0.9675	96.1248	0.1390	0.2689
NER (Bottle)	10/05/2017	-	-	0.6617	0.2492	0.4933	1.8789	0.1303	0.1730	0.3058	0.9194	93.6049	0.1409	0.2645
NER (Bottle)	10/08/2017	0.4128	-	1.9644	0.4730	0.3564	1.9257	0.1337	0.4404	0.3768	0.6138	-	0.1151	0.1707
NER (Bottle)	17/08/2017	0.4081	-	2.4395	0.4061	0.3459	1.1991	0.1328	0.4169	0.3870	0.5915	-	0.1157	0.1692
NER (Bottle)	24/08/2017	0.4025	-	1.8199	0.4603	0.3676	1.8656	0.1342	0.5488	0.3977	0.6244	-	0.1214	0.1706
NER (Bottle)	06/09/2017	0.4109	-	1.1207	0.4042	0.3322	0.7472	0.1308	0.3753	0.3715	0.5939	-	0.1139	0.1693
NER (Bottle)	14/09/2017	0.3999	-	0.8948	0.4005	0.3311	0.7293	0.1310	0.3611	0.3711	0.5897	-	0.1156	0.1691
NER (Bottle)	12/10/2017	0.4022	-	2.0658	0.5122	0.4027	3.1776	0.1349	0.5446	0.3915	0.7156	-	0.1125	0.1775
NER (Bottle)	12/11/2017	0.3763	-	1.6987	0.4262	0.3690	1.5271	0.1342	0.5291	0.4253	0.5929	-	0.1149	0.1669
NER (Bottle)	13/02/2018	0.4344	-	1.4844	0.4028	0.3439	1.6360	0.1331	0.4107	0.3910	0.6413	-	0.1133	0.1748

SAMPLE	DATE	Li	B	Al	Cr	Mn	Fe	Co	Ni	Cu	Rb	Sr	Pb	U
	Measure unit	µg/L	µg/L	µg/L	µg/L	µg/L	µg/L	µg/L	µg/L	µg/L	µg/L	µg/L	µg/L	µg/L
NER (Bottle)	14/03/2018	0.4150	-	1.3233	0.3934	0.3929	0.9281	0.1363	0.5473	0.3821	0.6415	-	0.1116	0.1760
NER (Bottle)	11/04/2018	-	-	-	-	-	-	-	-	-	-	-	-	-
NER (Spring)	06/06/2016	-	-	0.5193	0.2327	0.1456	0.3552	0.1302	0.1688	0.3003	0.8534	66.0871	0.1331	0.2272
NER (Spring)	06/09/2016	-	-	0.6657	0.2508	0.1689	0.4339	0.1315	0.1811	0.2921	1.0596	86.0341	0.1384	0.2592
NER (Spring)	27/09/2016	0.4170	3.0690	2.0168	0.3282	0.2977	1.1496	0.1367	0.2959	0.4339	0.9310	72.3627	0.1750	0.2364
NER (Spring)	26/10/2016	0.5990	3.1220	7.5327	0.4337	0.1888	1.9165	0.1353	0.4785	1.0640	0.9615	70.1495	0.1879	0.2317
NER (Spring)	28/10/2016	0.4350	3.4530	7.4144	0.4201	0.1990	2.1762	0.1353	0.5195	1.1486	0.9445	67.9247	0.2212	0.2303
NER (Spring)	02/11/2016	0.4900	3.2230	15.7299	0.6426	0.3885	7.1851	0.1420	1.3935	1.7503	1.0379	71.8298	0.3548	0.2378
NER (Spring)	03/11/2016	-	-	-	-	-	-	-	-	-	-	-	-	-
NER (Spring)	04/11/2016	-	-	7.2171	0.5475	0.2256	5.9853	0.1019	0.5102	0.4208	0.8159	62.0918	0.1333	0.1991
NER (Spring)	07/11/2016	0.4170	3.1390	0.6723	0.2421	0.1721	0.2920	0.1301	0.1906	0.1767	0.8306	65.0097	0.1364	0.2279
NER (Spring)	08/11/2016	-	-	-	-	-	-	-	-	-	-	-	-	-
NER (Spring)	09/11/2016	-	-	-	-	-	-	-	-	-	-	-	-	-
NER (Spring)	10/11/2016	0.6450	3.6950	2.1376	0.2705	0.1221	1.8035	0.0986	0.2017	0.6183	0.8253	64.8185	0.1099	0.2042
NER (Spring)	10/11/2016	-	-	-	-	-	-	-	-	-	-	-	-	-
NER (Spring)	15/11/2016	0.4580	3.4915	11.0652	0.3330	0.2781	4.0328	0.4498	1.3532	1.0917	0.9509	67.8928	0.3026	0.2456
NER (Spring)	16/11/2016	-	-	-	-	-	-	-	-	-	-	-	-	-
NER (Spring)	17/11/2016	-	-	-	-	-	-	-	-	-	-	-	-	-
NER (Spring)	18/11/2016	-	-	5.7089	0.2891	0.2194	2.0697	0.1332	0.3511	0.4135	0.8530	66.5913	0.1557	0.2325
NER (Spring)	23/11/2016	-	-	3.1260	0.3149	0.2165	2.5613	0.1359	0.3140	0.4058	0.8513	60.1163	0.1635	0.2204
NER (Spring)	29/11/2016	-	-	-	-	-	-	-	-	-	-	-	-	-
NER (Spring)	06/12/2016	-	-	2.2192	0.3041	0.1799	1.9160	0.1352	0.2780	0.3272	0.8194	58.9669	0.1464	0.2163
NER (Spring)	09/01/2017	-	-	1.2385	0.2866	0.1710	0.5731	0.1316	0.2029	0.2580	0.8071	57.5206	0.1371	0.2146
NER (Spring)	12/01/2017	-	-	-	-	-	-	-	-	-	-	-	-	-
NER (Spring)	01/02/2017	0.4650	3.3120	1.4109	0.3022	0.1726	1.3685	0.1319	0.2050	0.2627	0.8144	59.0888	0.1377	0.2165
NER (Spring)	08/02/2017	-	-	-	-	-	-	-	-	-	-	-	-	-
NER (Spring)	15/02/2017	-	-	-	-	-	-	-	-	-	-	-	-	-
NER (Spring)	22/02/2017	-	-	-	-	-	-	-	-	-	-	-	-	-
NER (Spring)	27/02/2017	-	-	-	-	-	-	-	-	-	-	-	-	-
NER (Spring)	01/03/2017	-	-	2.4392	0.2971	0.1754	1.7740	0.1324	0.1924	0.2492	0.8329	60.4489	0.1480	0.2209
NER (Spring)	13/03/2017	-	-	-	-	-	-	-	-	-	-	-	-	-
NER (Spring)	20/03/2017	-	-	3.3349	0.2588	0.1788	0.5726	0.1309	0.1485	0.4043	0.9391	75.0576	0.1306	0.2471
NER (Spring)	03/04/2017	-	-	-	-	-	-	-	-	-	-	-	-	-
NER (Spring)	10/04/2017	-	-	1.2604	0.2733	0.1631	1.6814	0.1311	0.1694	0.3955	0.9605	79.3543	0.1378	0.2544
NER (Spring)	19/04/2017	-	-	-	-	-	-	-	-	-	-	-	-	-
NER (Spring)	10/05/2017	-	-	2.0868	0.2485	0.1489	0.5111	0.1309	0.1498	0.3753	0.9442	78.0286	0.1344	0.2517
NER (Spring)	18/05/2017	-	-	-	-	-	-	-	-	-	-	-	-	-
NER (Spring)	10/08/2017	0.3846	-	1.7003	0.5045	0.3424	1.4344	0.1318	0.4001	0.4049	0.6743	-	0.1135	0.1754
NER (Spring)	17/08/2017	0.3895	-	1.3549	0.4026	0.3410	1.3720	0.1325	0.3964	0.3793	0.6812	-	0.1124	0.1749
NER (Spring)	24/08/2017	0.3940	-	1.3216	0.4011	0.3305	0.8430	0.1319	0.3736	0.2372	0.6791	-	0.1760	0.1755
NER (Spring)	06/09/2017	0.4040	-	2.6803	0.4134	0.3473	6.3337	0.1337	0.4272	0.2000	0.6855	-	0.1359	0.1782
NER (Spring)	14/09/2017	0.3615	-	2.0076	0.4145	0.3712	1.5108	0.1336	0.4943	0.3995	0.7058	-	0.1164	0.1735
NER (Spring)	20/09/2017	0.8073	-	3.0839	0.4172	0.3605	2.3644	0.1330	0.4378	0.5735	0.6569	-	0.2056	0.1841
NER (Spring)	12/10/2017	0.3833	-	2.9477	0.4174	0.3596	1.1125	0.1337	0.4455	0.3838	0.5915	-	0.1157	0.1680
NER (Spring)	15/11/2017	0.3920	-	1.3698	0.3999	0.3345	0.8049	0.1318	0.3689	0.3636	0.6660	-	0.1119	0.1732
NER (Spring)	14/03/2018	0.3572	-	2.3049	0.3834	0.3335	0.5820	0.1324	0.3616	0.3796	0.6363	-	0.1108	0.1745
NER (Spring)	11/04/2018	0.3923	-	1.4512	0.3899	0.3342	0.8384	0.1327	0.3801	0.3908	0.6940	-	0.1118	0.1770
VIC	03/07/2014	-	-	-	-	-	-	-	-	-	-	-	-	-

SAMPLE	DATE	Li	B	Al	Cr	Mn	Fe	Co	Ni	Cu	Rb	Sr	Pb	U
	Measure unit	µg/L	µg/L	µg/L	µg/L	µg/L	µg/L	µg/L	µg/L	µg/L	µg/L	µg/L	µg/L	µg/L
VIC	15/02/2015	-	-	-	-	-	-	-	-	-	-	-	-	-
VIC	22/05/2015	-	-	-	-	-	-	-	-	-	-	-	-	-
VIC	20/09/2015	0.3840	8.5850	1.8400	0.9605	0.1426	<LOD	0.0935	0.1172	0.1793	0.6461	113.3348	0.1045	0.3131
VIC	27/08/2016	0.4260	7.1360	39.2592	2.5683	0.8471	20.0874	0.1725	4.9866	2.3705	1.4288	164.5908	0.6384	0.6768
VIC	28/08/2016	-	-	-	-	-	-	-	-	-	-	-	-	-
VIC	30/08/2016	0.2710	7.9350	34.6647	2.7120	0.5924	14.2267	0.1540	3.9135	1.4960	0.7813	106.7138	0.5269	0.4542
VIC	06/09/2016	0.3900	8.5260	22.6007	3.0751	0.4884	12.1754	0.1550	4.1922	1.2572	0.8700	138.2297	0.4914	0.5621
VIC	22/09/2016	0.3835	7.8400	19.0669	1.8217	0.5318	7.5437	0.1461	2.0010	2.2510	0.8602	125.0932	0.6620	0.5321
VIC	31/10/2016	0.4900	8.9880	20.7716	1.7130	1.7449	9.1439	0.1513	2.1182	1.8275	0.8265	118.5304	0.4085	0.5389
VIC	02/11/2016	-	-	-	-	-	-	-	-	-	-	-	-	-
VIC	28/11/2016	-	-	1.9136	1.0262	0.1897	3.5217	0.1354	0.3470	0.4568	0.7355	100.9961	0.1420	0.4620
VIC	24/12/2016	-	-	2.3496	1.1422	0.2180	7.9305	0.1344	0.2811	0.3934	0.6993	108.2338	0.1375	0.4899
VIC	19/01/2017	0.3960	8.0935	2.0438	0.9780	0.9463	1.1149	0.1383	0.2471	0.2970	0.6903	101.7461	0.1350	0.4830
VIC	28/02/2017	-	-	1.4738	1.0110	0.2846	1.7445	0.1336	0.2424	0.2376	0.6586	105.7201	0.1311	0.4869
VIC	17/05/2017	-	-	-	-	-	-	-	-	-	-	-	-	-
SUS	03/07/2014	-	-	-	-	-	-	-	-	-	-	-	-	-
SUS	15/02/2015	-	-	-	-	-	-	-	-	-	-	-	-	-
SUS	22/05/2015	-	-	-	-	-	-	-	-	-	-	-	-	-
SUS	20/09/2015	1.6750	19.1750	3.2668	0.2204	0.1313	<LOD	0.0940	0.1881	0.2749	1.0971	1770.2146	0.1046	0.8235
SUS	27/08/2016	2.1010	16.8765	37.6126	2.0520	0.6541	45.1859	0.1163	4.6531	1.8136	1.3640	6607.3405	0.5892	1.5605
SUS	28/08/2016	-	-	-	-	-	-	-	-	-	-	-	-	-
SUS	30/08/2016	2.3120	16.2780	18.1832	1.4535	0.3968	10.0898	0.1035	3.2847	0.9981	1.0085	4411.6220	0.4102	1.2291
SUS	06/09/2016	1.8070	15.7570	33.8270	1.8761	0.6227	17.5514	0.1172	4.1402	1.6670	1.2996	7186.6700	0.5856	1.4607
SUS	22/09/2016	1.7340	16.1350	31.5638	0.7630	0.6233	10.1000	0.1040	2.3475	3.8812	1.2710	5511.2055	0.5941	1.4413
SUS	31/10/2016	1.8965	19.6790	12.2111	0.6304	0.2177	4.4585	0.0946	1.6314	1.3206	1.0828	4831.1488	0.2507	1.3673
SUS	02/11/2016	-	-	-	-	-	-	-	-	-	-	-	-	-
SUS	28/11/2016	1.7860	16.3550	4.8096	0.2098	0.2317	3.4188	0.1014	0.7221	0.5378	1.0227	5898.0712	0.1499	1.2223
SUS	24/12/2016	1.5265	17.8535	2.6797	0.2736	0.2676	3.8405	0.0907	0.4460	0.7399	1.0195	5012.9942	0.1694	1.1490
SUS	19/01/2017	2.0500	15.9880	2.4028	0.2687	0.1709	2.1248	0.0904	0.3833	0.3747	0.9525	5095.7306	0.1301	1.1171
SUS	28/02/2017	1.9500	23.3610	1.6172	0.2649	0.1587	3.5824	0.0884	0.3680	0.1676	0.9527	5322.3451	0.1163	1.1923
SUS	28/04/2017	1.9200	15.5120	0.4566	0.2572	0.1390	1.2394	0.0911	0.3847	0.1120	1.0352	7794.8854	0.1112	1.1487
SUS	17/05/2017	2.3533	-	0.8748	0.6303	0.3512	1.0355	0.1328	0.6693	0.3695	2.1072	<LOD	0.3130	1.2066
PES	03/07/2014	-	-	-	-	-	-	-	-	-	-	-	-	-
PES	15/02/2015	-	-	-	-	-	-	-	-	-	-	-	-	-
PES	22/05/2015	-	-	-	-	-	-	-	-	-	-	-	-	-
PES	20/09/2015	1.4620	18.0910	0.9078	0.2756	0.1014	0.2727	0.0876	0.0961	0.2379	1.1254	293.1330	0.1017	0.2134
PES	27/08/2016	1.0360	11.1680	25.7753	1.6026	0.4606	8.6403	0.1043	3.0991	1.3453	1.7003	527.3513	0.4604	0.6992
PES	28/08/2016	-	-	-	-	-	-	-	-	-	-	-	-	-
PES	30/08/2016	1.3310	12.7065	18.0001	1.5525	0.4124	8.4853	0.1028	2.9540	1.7616	1.8111	547.3522	0.4685	0.7185
PES	06/09/2016	1.5830	12.9410	8.1494	0.7759	0.2472	3.3278	0.0945	1.0317	1.1898	1.8074	554.0308	0.3536	0.7285
PES	22/09/2016	1.4300	13.0930	16.5904	0.9573	0.2990	6.3029	0.0968	1.8156	1.6907	1.8146	569.4720	0.3831	0.7106
PES	31/10/2016	0.9315	15.8900	27.6199	0.9623	0.5712	10.8741	0.1023	2.1648	2.3816	1.6908	466.8747	0.5764	0.6270
PES	02/11/2016	-	-	-	-	-	-	-	-	-	-	-	-	-
PES	28/11/2016	1.2760	12.9860	2.4870	0.4457	0.1874	1.7531	0.0930	0.5213	0.5681	1.6262	123.6484	0.1959	0.6298
PES	24/12/2016	0.9710	13.7040	2.0437	0.4519	0.2230	9.4014	0.0914	0.4426	1.0984	1.6210	109.3463	0.1834	0.6261
PES	19/01/2017	1.1460	13.3000	7.5932	0.4727	0.2110	1.3337	0.0900	0.4119	0.8464	1.5629	234.8874	0.2308	0.6308
PES	28/02/2017	1.3390	19.4940	7.0198	0.4591	0.1828	1.2497	0.0889	0.3317	0.7722	1.5513	216.0093	0.2088	0.6327
PES	28/04/2017	1.1850	12.7670	0.3005	0.4198	0.1079	0.3916	0.0908	0.2811	0.7357	1.4391	400.2776	0.1548	0.5948

SAMPLE	DATE	Li	B	Al	Cr	Mn	Fe	Co	Ni	Cu	Rb	Sr	Pb	U
	Measure unit	µg/L	µg/L	µg/L	µg/L	µg/L	µg/L	µg/L	µg/L	µg/L	µg/L	µg/L	µg/L	µg/L
PES	17/05/2017	0.8362	-	1.1788	0.5512	0.3343	0.7927	0.1276	0.3958	0.3885	1.2168	-	0.3137	0.6354
FP01	28/09/2016	-	-	3.8513	0.0986	2.7351	1.2389	<LOD	0.2719	0.3754	0.3013	206.2559	0.0074	<LOD
FP01	02/11/2016	-	-	21.0689	0.5072	0.3934	12.9524	<LOD	3.2468	2.4070	0.4054	152.5290	0.8148	<LOD
FP01	16/11/2016	-	-	4.4529	0.0554	0.1019	2.5293	<LOD	0.4300	0.6741	0.3410	171.5209	0.0733	<LOD
FP02	28/09/2016	-	-	4.0201	0.2789	0.1024	3.5738	0.0972	1.3722	2.7562	1.2152	290.0807	0.0306	0.1023
FP02	02/11/2016	-	-	17.9593	0.4817	0.3011	8.4883	0.0950	2.3574	3.3882	0.9131	204.5233	0.1603	0.0548
FP02	16/11/2016	-	-	14.1035	0.3803	0.1353	5.2809	0.1258	1.5437	2.9055	1.2120	315.0094	0.0928	0.1190
FP02	27/04/2017	-	-	5.0942	0.1320	0.0674	6.6125	0.0664	0.9506	2.1779	0.9939	239.6750	<LOD	0.0541
FP03	28/09/2016	-	-	4.1643	0.2171	0.1764	1.9500	<LOD	0.2196	0.3416	0.0943	93.4984	<LOD	<LOD
FP03	02/11/2016	-	-	11.4685	0.3670	0.3647	3.7998	<LOD	0.8937	1.4165	0.1388	110.3734	0.0568	0.0390
FP03	17/11/2016	-	-	1.5212	0.0849	2.1719	0.8132	<LOD	0.3874	0.4199	0.0904	79.5211	<LOD	<LOD
FP03	27/04/2017	-	-	0.4736	0.1481	0.2244	1.2788	<LOD	0.1405	0.2170	0.1147	112.3144	<LOD	0.0218
FP04	02/11/2016	-	-	11.7631	0.6708	0.5225	5.2224	<LOD	0.8184	1.4480	0.3322	208.2504	0.0725	0.2322
FP04	17/11/2016	-	-	1.1704	0.4573	0.5087	0.8797	<LOD	0.3124	0.4616	0.3253	213.3281	<LOD	0.2263
FP04	27/04/2017	-	-	1.9529	0.4229	0.0807	9.0283	<LOD	0.2305	0.3118	0.2225	149.0388	<LOD	0.1487
FP04	15/09/2017	-	-	3.2301	1.0702	0.6710	1.7022	0.6725	0.9096	0.9360	0.9683	-	0.6300	0.9609

Supplementary_03: Isotopes ratios of analyzed samples in Rieti and Sibillini mountains springs

Sample	Date	Area	Replicates	$\delta^{18}O_{H2O}$ ‰	$\delta^{2}H_{H2O}$ ‰	$\delta^{18}O_{SO4}$ ‰	$\delta34S_{SO4}$ ‰	$\delta^{13}C_{DIC}$ ‰
NER (Bottle)	06/06/2016	Nerea		-9.60	-64.00	-	-	-12.04
NER (Bottle)	07/26/2016	Nerea		-9.70	-64.00	-	-	-
NER (Bottle)	08/08/2016	Nerea		-9.70	-64.00	-	-	-
NER (Bottle)	10/26/2016	Nerea		-9.70	-64.00	-	-	-11.53
NER (Bottle)	10/26/2016	Nerea		-9.80	-64.00	-	-	-11.87
NER (Bottle)	02/01/2017	Nerea		-9.80	-65.00	-	-	-11.06
NER (Spring)	06/06/2016	Nerea		-9.70	-64.00	-	-	-11.55
NER (Spring)	09/06/2016	Nerea		-9.60	-64.00	-	-	-17.28
NER (Spring)	11/02/2016	Nerea		-9.70	-64.00	-	-	-11.32
NER (Spring)	11/10/2016	Nerea		-9.60	-64.00	-	-	-15.25
NER (Spring)	11/15/2016	Nerea	Replicate1	-9.70	-64.00	-	-	-13.08
NER (Spring)	11/15/2016	Nerea	Replicate2	-	-	-	-	-13.24
NER (Spring)	11/23/2016	Nerea		-9.60	-64.00	-	-	-13.63
NER (Spring)	02/01/2017	Nerea	Replicate1	-9.60	-64.00	-	-	-11.40
NER (Spring)	02/01/2017	Nerea	Replicate2	-	-	-	-	-11.32
NER (Spring)	03/01/2017	Nerea		-9.70	-64.00	-	-	-11.48
NER (Spring)	05/10/2017	Nerea	Replicate1	-9.60	-65.00	-	-	-10.84
NER (Spring)	05/10/2017	Nerea	Replicate2	-9.60	-64.00	-	-	-
PES	07/03/2014	Rieti		-9.00	-57.00	8.00	10.20	-6.10
PES	02/15/2015	Rieti		-8.90	-55.00	9.00	12.20	-3.90
PES	05/22/2015	Rieti		9.00	-57.00	8.30	12.10	-4.20
PES	09/20/2015	Rieti		-9.00	-57.00	9.00	12.10	-4.80
PES	08/27/2016	Rieti		-8.90	-57.00	16.00	11.50	-5.90
PES	08/28/2016	Rieti		-8.90	-57.00	11.75	12.00	-3.10
PES	08/30/2016	Rieti		-9.00	-57.00	9.90	12.00	-3.80
PES	09/06/2016	Rieti		-9.00	-57.00	9.60	12.20	-3.50
PES	09/22/2016	Rieti		-	-	-	-	-
PES	10/31/2016	Rieti		-8.70	-56.00	8.80	11.90	-2.40
PES	10/31/2016	Rieti		-8.70	-56.00	-	-	-
PES	11/02/2016	Rieti		-	-	9.00	-	-
PES	11/10/2016	Rieti		-8.90	-57.00	8.30	11.10	-2.90
PES	11/28/2016	Rieti		-8.90	-57.00	8.90	11.50	-3.20
PES	02/28/2017	Rieti	Replicate1	-8.90	-57.00	-	-	-
PES	02/28/2017	Rieti	Replicate2	-8.80	-56.00	-	-	-3.80
PES	04/28/2017	Rieti		-8.90	-56.00	-	-	-2.90
SUS	07/03/2014	Rieti		-8.60	-53.00	10.70	15.30	-10.00
SUS	02/15/2015	Rieti		-8.40	-52.00	9.30	15.40	-9.00
SUS	05/22/2015	Rieti		-8.60	-54.00	10.00	14.90	-8.90
SUS	09/15/2015	Rieti		-8.40	-53.00	9.60	15.50	-8.80
SUS	08/27/2016	Rieti		-8.60	-53.00	10.10	15.20	-9.10
SUS	08/28/2016	Rieti		-8.60	-53.00	10.30	15.00	-9.00
SUS	08/30/2016	Rieti		-8.60	-53.00	9.30	15.20	-8.40
SUS	09/06/2016	Rieti		-8.60	-53.00	10.30	14.90	-10.30
SUS	09/22/2016	Rieti		-	-	-	-	-
SUS	10/31/2016	Rieti		-8.40	-53.00	10.60	15.30	-6.90
SUS	11/02/2016	Rieti		-	-	10.50	-	-
SUS	11/10/2016	Rieti		-8.50	-53.00	10.30	15.20	-3.60
SUS	11/28/2016	Rieti		-8.40	-53.00	10.10	14.20	-7.50
SUS	02/28/2017	Rieti		-8.40	-53.00	-	-	-6.40
SUS	04/28/2017	Rieti		-8.50	-52.00	-	-	-7.00
VIC	07/03/2014	Rieti		-6.90	-43.00	-0.70	-9.90	-13.80
VIC	02/15/2015	Rieti		-7.10	-43.00	5.20	8.80	-13.50
VIC	05/22/2015	Rieti		-7.40	-46.00	4.20	8.60	-12.00
VIC	09/15/2015	Rieti		-7.10	-45.00	6.00	15.20	-13.50
VIC	08/27/2016	Rieti		-7.10	-45.00	6.40	7.40	-12.70
VIC	08/28/2016	Rieti		-7.10	-45.00	7.90	7.50	-12.00
VIC	08/30/2016	Rieti		-7.20	-45.00	6.20	8.10	-12.40
VIC	09/06/2016	Rieti		-7.20	-45.00	5.70	8.40	-11.40
VIC	09/22/2016	Rieti		-7.20	-45.00	-	-	-
VIC	10/31/2016	Rieti	Replicate1	-7.00	-44.00	-	-	-
VIC	10/31/2016	Rieti	Replicate2	-7.00	-44.00	5.40	9.00	-12.00
VIC	11/10/2016	Rieti		-7.10	-45.00	5.60	-	-
VIC	11/10/2016	Rieti		-7.10	-45.00	-	8.20	-11.90
VIC	11/28/2016	Rieti		-7.10	-45.00	-	-	-11.80
VIC	02/28/2017	Rieti		-7.10	-44.00	-	-	-12.30
VIC	02/28/2017	Rieti		-7.10	-44.00	-	-	-
VIC	05/17/2017	Rieti		-7.20	-44.00	-	-	-

Supplementary_04: Precipitation data and correlation matrices for Rieti and Nerea springs

Precipitation data retrieved from http://www.idrografico.roma.it/annali/

LEONESSA (used for NER)

	January mm	February mm	March mm	April mm	May mm	June mm	July mm	August mm	September mm	October mm	November mm	December mm	*average* mm
2012	23.6	35.8	5.8	175.4	125	25.8	27.6	24.2	134.2	242.6	291.2	129.2	103.3667
2013	140.4	163.8	268.6	99.8	188.2	104	105.8	69.8	134	105.8	279.2	57.3	143.0583
2014	224.3	173.6	89.4	187	96	110.5	131.5	13.1	86.5	25.2	206.4	71.4	117.9083
2015	110.5	78	129.2	55.1	42.2	39.2	41	70.3	92.9	265.6	80.8	0.2	83.75
2016	203.5	279.5	99.1	142.5	159.6	85.5	67.5	55.9	77.4	166	134.7	3	122.85
average	140.46	146.14	118.42	131.96	122.2	73	74.68	46.66	105	161.04	198.46	52.22	114.1867

PESCHIERA (used for PES, VIC and SUS)

	January mm	February mm	March mm	April mm	May mm	June mm	July mm	August mm	September mm	October mm	November mm	December mm	*average* mm
2012	32.4	26.6	23.4	108.6	177.6	27.2	12.4	29	186.2	190.6	163.4	149.6	93.91667
2013	154	131	233.2	79.4	136.4	73	23.2	45.6	66.6	107.8	270	56	114.6833
2014	193.6	143	80.4	154.2	95.6	142.4	103.6	25.6	113.2	30.2	180.6	81.4	111.9833
2015	115	85.6	111.6	59	46.6	55.4	45.4	49.2	93.4	253.8	54.2	4.4	81.13333
2016	173.4	183.6	84.2	105.8	174.6	139.6	93	22	93.2	100.8	110.6	3.2	107
average	133.68	113.96	106.56	101.4	126.16	87.52	55.52	34.28	110.52	136.64	155.76	58.92	101.7433

Correlation matrices

Pearson's correlations

values >0.5 potentially correlated, highlighted in bold

values >0.9 strongly correlated, hilighted in bold and red

VIC correlation matrix

	Precip.	Al	Co	Cr	Cu	Fe	Mn	Ni	Pb	Rb	Sr	U
Precip.	**1**	-0.123	-0.09	-0.097	0.09	-0.301	0.258	-0.105	0.007	-0.136	-0.109	-0.085
Al	-0.123	**1**	**0.946**	**0.882**	**0.859**	**0.926**	0.361	**0.958**	**0.895**	**0.754**	**0.724**	**0.619**
Co	-0.09	**0.946**	**1**	**0.836**	**0.83**	**0.921**	0.422	**0.95**	**0.833**	**0.89**	**0.872**	**0.812**
Cr	-0.097	**0.882**	**0.836**	**1**	**0.677**	**0.846**	0.15	**0.962**	**0.813**	**0.572**	**0.681**	**0.518**
Cu	0.09	**0.859**	**0.83**	**0.677**	**1**	**0.757**	0.46	**0.774**	**0.955**	**0.739**	**0.742**	**0.685**
Fe	-0.301	**0.926**	**0.921**	**0.846**	**0.757**	**1**	0.207	**0.925**	**0.781**	**0.82**	**0.8**	**0.703**
Mn	0.258	0.361	0.422	0.15	0.46	0.207	**1**	0.252	0.287	0.25	0.219	0.328
Ni	-0.105	**0.958**	**0.95**	**0.962**	**0.774**	**0.925**	0.252	**1**	**0.855**	**0.757**	**0.797**	**0.672**
Pb	0.007	**0.895**	**0.833**	**0.813**	**0.955**	**0.781**	0.287	**0.855**	**1**	**0.686**	**0.734**	**0.621**
Rb	-0.136	**0.754**	**0.89**	**0.572**	**0.739**	**0.82**	0.25	**0.757**	**0.686**	**1**	**0.93**	**0.926**
Sr	-0.109	**0.724**	**0.872**	**0.681**	**0.742**	**0.8**	0.219	**0.797**	**0.734**	**0.93**	**1**	**0.972**
U	-0.085	**0.619**	**0.812**	**0.518**	**0.685**	**0.703**	0.328	**0.672**	**0.621**	**0.926**	**0.972**	**1**

SUS correlation matrix

	Precip.	Al	Co	Cr	Cu	Fe	Mn	Ni	Pb	Rb	Sr	U
Precip.	**1**	0.031	0.106	-0.142	0.131	-0.208	-0.081	-0.054	-0.021	0.054	0.086	0.221
Al	0.031	**1**	**0.915**	**0.886**	**0.792**	**0.8**	**0.975**	**0.937**	**0.989**	**0.935**	**0.224**	**0.936**
Co	0.106	**0.915**	**1**	**0.904**	**0.56**	**0.797**	**0.901**	**0.933**	**0.887**	**0.864**	**0.363**	**0.845**
Cr	-0.142	**0.886**	**0.904**	**1**	**0.443**	**0.844**	**0.841**	**0.987**	**0.865**	**0.774**	**0.235**	**0.79**
Cu	0.131	**0.792**	**0.56**	**0.443**	**1**	**0.406**	**0.806**	**0.562**	**0.826**	**0.756**	**-0.025**	**0.747**
Fe	-0.208	**0.8**	**0.797**	**0.844**	**0.406**	**1**	**0.771**	**0.837**	**0.735**	**0.803**	**0.301**	**0.801**
Mn	-0.081	**0.975**	**0.901**	**0.841**	**0.806**	**0.771**	**1**	**0.892**	**0.982**	**0.92**	0.221	**0.871**
Ni	-0.054	**0.937**	**0.933**	**0.987**	**0.562**	**0.837**	**0.892**	**1**	**0.92**	**0.824**	**0.201**	**0.852**
Pb	-0.021	**0.989**	**0.887**	**0.865**	**0.826**	**0.735**	**0.982**	**0.92**	**1**	**0.902**	**0.173**	**0.888**
Rb	0.054	**0.935**	**0.864**	**0.774**	**0.756**	**0.803**	**0.92**	**0.824**	**0.902**	**1**	**0.457**	**0.945**
Sr	0.086	**0.224**	**0.363**	**0.235**	**-0.025**	**0.301**	0.221	**0.201**	**0.173**	**0.457**	**1**	**0.267**
U	0.221	**0.936**	**0.845**	**0.79**	**0.747**	**0.801**	**0.871**	**0.852**	**0.888**	**0.945**	**0.267**	**1**

PES correlation matrix

	Precip.	U	Sr	Rb	Fe	Cu	Al	Mn	Cr	Pb	Co	Ni
Precip.	1	-0.434	-0.199	-0.488	-0.775	-0.369	-0.324	-0.451	-0.612	-0.361	-0.58	-0.587
U	-0.434	1	**0.721**	**0.903**	**0.324**	**0.398**	0.463	**0.386**	**0.715**	**0.561**	**0.558**	**0.653**
Sr	-0.199	**0.721**	1	**0.642**	**0.344**	**0.647**	**0.663**	**0.551**	**0.74**	**0.742**	**0.696**	**0.734**
Rb	-0.488	**0.903**	**0.642**	1	**0.557**	**0.635**	**0.567**	**0.572**	**0.674**	**0.703**	**0.649**	**0.683**
Fe	-0.775	**0.324**	**0.344**	**0.557**	1	**0.82**	**0.713**	**0.833**	**0.646**	**0.734**	**0.764**	**0.722**
Cu	-0.369	**0.398**	**0.647**	**0.635**	**0.82**	1	**0.844**	**0.889**	**0.645**	**0.914**	**0.783**	**0.747**
Al	-0.324	0.463	**0.663**	**0.567**	**0.713**	**0.844**	1	**0.955**	**0.824**	**0.953**	**0.896**	**0.893**
Mn	-0.451	**0.386**	**0.551**	**0.572**	**0.833**	**0.889**	**0.955**	1	**0.783**	**0.957**	**0.913**	**0.867**
Cr	-0.612	**0.715**	**0.74**	**0.674**	**0.646**	**0.645**	**0.824**	**0.783**	1	**0.822**	**0.932**	**0.983**
Pb	-0.361	**0.561**	**0.742**	**0.703**	**0.734**	**0.914**	**0.953**	**0.957**	**0.822**	1	**0.916**	**0.891**
Co	-0.58	**0.558**	**0.696**	**0.649**	**0.764**	**0.783**	**0.896**	**0.913**	**0.932**	**0.916**	1	**0.974**
Ni	-0.587	**0.653**	**0.734**	**0.683**	**0.722**	**0.747**	**0.893**	**0.867**	**0.983**	**0.891**	**0.974**	1

NER correlation matrix

	Precip.	Al	Co	Cr	Cu	Fe	Mn	Ni	Pb	Rb	Sr	U
Precip.	1	0.5	0.036	0.437	**0.567**	0.172	-0.018	0.3	0.348	0.356	0.413	0.186
Al	0.5	1	**0.341**	**0.834**	**0.941**	**0.785**	**0.613**	**0.908**	**0.938**	**0.725**	**0.694**	0.243
Co	0.036	**0.341**	1	**-0.136**	**0.175**	**0.216**	0.299	**0.614**	**0.52**	**0.342**	**0.09**	**0.408**
Cr	0.437	**0.834**	**-0.136**	1	**0.911**	**0.579**	**0.544**	**0.676**	**0.735**	**0.696**	**0.661**	0.307
Cu	**0.567**	**0.941**	**0.175**	**0.911**	1	**0.576**	0.491	**0.811**	**0.85**	**0.777**	**0.739**	**0.392**
Fe	0.172	**0.785**	**0.216**	**0.579**	**0.576**	1	**0.706**	**0.695**	**0.749**	**0.397**	**0.481**	**-0.25**
Mn	-0.018	**0.613**	0.299	**0.544**	0.491	**0.706**	1	**0.705**	**0.766**	**0.667**	**0.62**	0.202
Ni	0.3	**0.908**	**0.614**	**0.676**	**0.811**	**0.695**	**0.705**	1	**0.983**	**0.752**	**0.536**	**0.436**
Pb	0.348	**0.938**	**0.52**	**0.735**	**0.85**	**0.749**	**0.766**	**0.983**	1	**0.776**	**0.633**	0.379
Rb	0.356	**0.725**	**0.342**	**0.696**	**0.777**	**0.397**	**0.667**	**0.752**	**0.776**	1	**0.751**	**0.649**
Sr	0.413	**0.694**	**0.09**	**0.661**	**0.739**	**0.481**	**0.62**	**0.536**	**0.633**	**0.751**	1	**0.219**
U	0.186	0.243	**0.408**	0.307	**0.392**	**-0.25**	0.202	**0.436**	0.379	**0.649**	**0.219**	1

Supplementary_05: Daily means of P12 probe recorded variables and precipitation data from Montemonaco

Date	Piezometric elevation (m)	Temperature (°C)	Electrical conductivity (µS/cm)	Rainfall (mm)
26/04/2017	1033.92	7.06	155.78	0
27/04/2017	1033.85	6.96	155.22	14.6
28/04/2017	1034.13	6.97	155.23	3.2
29/04/2017	1035.1	6.98	156.1	0
30/04/2017	1035.19	7.04	157.34	0
01/05/2017	1034.99	6.96	156	0.8
02/05/2017	1034.78	6.97	156.67	0
03/05/2017	1034.51	6.95	155.32	0
04/05/2017	1034.16	7.04	157.18	0
05/05/2017	1033.82	7.08	157.77	0
06/05/2017	1033.6	7.08	156.8	3
07/05/2017	1033.46	7.08	157.89	23.8
08/05/2017	1033.75	7.07	158.83	3.8
09/05/2017	1034.68	6.99	155.83	5
10/05/2017	1034.95	7.02	157.06	0.2
11/05/2017	1034.88	7.01	157.5	0.2
12/05/2017	1034.71	7.03	158.35	0.2
13/05/2017	1034.52	7.05	162.75	0
14/05/2017	1034.27	7.06	161.4	1
15/05/2017	1033.99	7.06	161.78	11.8
16/05/2017	1033.71	7.06	161.44	0
17/05/2017	1033.45	7.06	160.23	0.2
18/05/2017	1033.18	7.06	158.42	0
19/05/2017	1032.94	7.04	157.44	1.2
20/05/2017	1032.77	6.93	155.59	22
21/05/2017	1032.67	6.93	155.56	5.8
22/05/2017	1032.57	6.89	155.25	0
23/05/2017	1032.42	6.84	154.69	4.6
24/05/2017	1032.23	6.8	154.38	0
25/05/2017	1032.06	6.77	153.87	17.6
26/05/2017	1031.87	6.75	153.92	0
27/05/2017	1031.64	6.74	153	0
28/05/2017	1031.41	6.73	153.09	0
29/05/2017	1031.19	6.73	153.15	0
30/05/2017	1030.99	6.74	153.46	0
31/05/2017	1030.78	6.75	154.4	0
01/06/2017	1030.57	6.76	154.73	18
02/06/2017	1030.39	6.76	154.3	16.2
03/06/2017	1030.2	6.77	155.52	0
04/06/2017	1030.02	6.79	155.15	0
05/06/2017	1029.83	6.82	155.16	7.4
06/06/2017	1029.64	6.85	155.22	0
07/06/2017	1029.45	6.88	156.39	0
08/06/2017	1029.28	6.91	156.66	0

Date	Piezometric elevation (m)	Temperature (°C)	Electrical conductivity (µS/cm)	Rainfall (mm)
09/06/2017	1029.13	6.93	157.37	0
10/06/2017	1028.99	6.92	157.68	0
11/06/2017	1028.86	6.91	159.55	0
12/06/2017	1028.72	6.92	159.37	0
13/06/2017	1028.6	6.96	160.99	0
14/06/2017	1028.49	6.99	162.58	0
15/06/2017	1028.45	7.02	162.36	0
16/06/2017	1028.37	7.03	163.41	0
17/06/2017	1028.26	7.04	162.83	1
18/06/2017	1028.13	7.04	163.25	0
19/06/2017	1028.05	7.04	163.61	0
20/06/2017	1027.96	7.04	164.28	0
21/06/2017	1027.86	7.03	163.95	0
22/06/2017	1027.74	7.01	163.65	0
23/06/2017	1027.65	6.95	163.19	0
24/06/2017	1027.59	6.91	161.37	0
25/06/2017	1027.54	6.91	160.78	0
26/06/2017	1027.49	6.92	160.43	0
27/06/2017	1027.45	6.92	160.32	0
28/06/2017	1027.41	6.92	159.67	9.8
29/06/2017	1027.37	6.92	159.43	0.2
30/06/2017	1027.33	6.92	159.7	7.4
01/07/2017	1027.3	6.92	159.1	5
02/07/2017	1027.26	6.93	159.07	15.6
03/07/2017	1027.21	6.92	159.37	0
04/07/2017	1027.18	6.92	158.27	0
05/07/2017	1027.14	6.92	158.76	0
06/07/2017	1027.09	6.92	158.31	0
07/07/2017	1027.05	6.92	158.34	0
08/07/2017	1027	6.92	159.63	0
09/07/2017	1026.94	6.92	159.22	0
10/07/2017	1026.88	6.92	158.66	0
11/07/2017	1026.83	6.92	158.74	0
12/07/2017	1026.77	6.92	158.82	0
13/07/2017	1026.72	6.92	158.57	0
14/07/2017	1026.67	6.92	158.42	6.4
15/07/2017	1026.61	6.92	158.47	0
16/07/2017	1026.54	6.92	158.79	0
17/07/2017	1026.48	6.91	158.47	0
18/07/2017	1026.42	6.91	159.51	0
19/07/2017	1026.35	6.91	159.1	0
20/07/2017	1026.28	6.91	159.47	0
21/07/2017	1026.21	6.91	159.67	0
22/07/2017	1026.13	6.92	159.72	0
23/07/2017	1026.05	6.92	159.53	0
24/07/2017	1025.97	6.92	159.43	0.4
25/07/2017	1025.89	6.92	159.85	0

Date	Piezometric elevation (m)	Temperature (°C)	Electrical conductivity (µS/cm)	Rainfall (mm)
26/07/2017	1025.8	6.92	160.38	0
27/07/2017	1025.71	6.92	160.42	0
28/07/2017	1025.62	6.92	160.43	0
29/07/2017	1025.54	6.92	160.31	0
30/07/2017	1025.46	6.92	160.44	0
31/07/2017	1025.38	6.92	160.56	0
01/08/2017	1025.33	6.92	160.14	0
02/08/2017	1025.24	6.92	159.93	0
03/08/2017	1025.16	6.92	160.58	0
04/08/2017	1025.1	6.92	160.07	0
05/08/2017	1025.06	6.92	160.12	0
06/08/2017	1025	6.92	160.35	0
07/08/2017	1024.93	6.92	160.12	0
08/08/2017	1024.85	6.92	159.78	0
09/08/2017	1024.78	6.92	160.46	0
10/08/2017	1024.72	6.92	159.98	0
11/08/2017	1024.67	6.92	159.88	0
12/08/2017	1024.61	6.91	160.18	2.8
13/08/2017	1024.57	6.91	160.23	0
14/08/2017	1024.52	6.91	160.43	0
15/08/2017	1024.47	6.91	160.67	0
16/08/2017	1024.42	6.91	160.07	0
17/08/2017	1024.36	6.91	160.6	0
18/08/2017	1024.3	6.91	160.1	0
19/08/2017	1024.25	6.91	160.08	0
20/08/2017	1024.2	6.91	160.44	0
21/08/2017	1024.14	6.91	160.87	0
22/08/2017	1024.09	6.91	160.42	0
23/08/2017	1024.04	6.9	160.38	0
24/08/2017	1023.97	6.9	160.27	0
25/08/2017	1023.93	6.9	159.53	0
26/08/2017	1023.88	6.9	160.03	0
27/08/2017	1023.84	6.9	160.35	0
28/08/2017	1023.79	6.9	159.65	0.4
29/08/2017	1023.75	6.9	158.96	0
30/08/2017	1023.71	6.9	159.77	0
31/08/2017	1023.66	6.9	159.79	0
01/09/2017	1023.63	6.9	160.46	0.6
02/09/2017	1023.59	6.9	160.83	6.6
03/09/2017	1023.55	6.9	160.85	1.2
04/09/2017	1023.51	6.9	160.74	0
05/09/2017	1023.47	6.9	160.7	0
06/09/2017	1023.43	6.89	160.12	0
07/09/2017	1023.39	6.89	160.75	0
08/09/2017	1023.35	6.89	160.54	2.8
09/09/2017	1023.31	6.89	160.62	0
10/09/2017	1023.28	6.89	160.5	36

Date	Piezometric elevation (m)	Temperature (°C)	Electrical conductivity (µS/cm)	Rainfall (mm)
11/09/2017	1023.29	6.89	160.48	31.4
12/09/2017	1023.27	6.89	160.73	0
13/09/2017	1023.21	6.88	160.17	0
14/09/2017	1023.15	6.88	160.17	0
15/09/2017	1023.11	6.89	160.69	0
16/09/2017	1023.08	6.88	160.93	3.8
17/09/2017	1023.15	6.88	160.53	19.2
18/09/2017	1023.13	6.88	157.1	1.4
19/09/2017	1023.16	6.87	156.65	14
20/09/2017	1023.51	6.79	141.66	21.6
21/09/2017	1023.69	6.81	142.9	0
22/09/2017	1023.38	6.87	152.76	0
23/09/2017	1023.17	6.88	158.92	0
24/09/2017	1023.05	6.88	159.3	2.6
25/09/2017	1022.97	6.88	158.8	0
26/09/2017	1022.91	6.88	159.19	13.2
27/09/2017	1022.86	6.88	159.98	0.2
28/09/2017	1022.82	6.88	159.05	0
29/09/2017	1022.78	6.88	160.04	0
30/09/2017	1022.75	6.88	160.19	0
01/10/2017	1022.71	6.88	159.47	0
02/10/2017	1022.67	6.88	160.61	0
03/10/2017	1022.64	6.88	160.9	0
04/10/2017	1022.61	6.88	160.15	0
05/10/2017	1022.58	6.88	160.22	0
06/10/2017	1022.55	6.87	160.47	16.4
07/10/2017	1022.52	6.87	160.15	1.8
08/10/2017	1022.49	6.87	160.66	0
09/10/2017	1022.46	6.87	160.61	0
10/10/2017	1022.43	6.87	161.28	0.4
11/10/2017	1022.4	6.87	160.24	0
12/10/2017	1022.37	6.87	160.81	0
13/10/2017	1022.34	6.87	161.18	0
14/10/2017	1022.31	6.87	160.72	0
15/10/2017	1022.28	6.87	161.08	0
16/10/2017	1022.25	6.87	161	0
17/10/2017	1022.23	6.87	160.53	0
18/10/2017	1022.2	6.87	160.95	0
19/10/2017	1022.17	6.87	160.84	0
20/10/2017	1022.14	6.87	161.89	0
21/10/2017	1022.11	6.87	161.5	0
22/10/2017	1022.08	6.87	162.71	21
23/10/2017	1022.19	6.86	158.03	13
24/10/2017	1022.23	6.85	152.75	0
25/10/2017	1022.15	6.86	159.4	0
26/10/2017	1022.09	6.87	160.39	0
27/10/2017	1022.04	6.87	160.18	12.4

Date	Piezometric elevation (m)	Temperature (°C)	Electrical conductivity (µS/cm)	Rainfall (mm)
28/10/2017	1022.01	6.87	161.53	0
29/10/2017	1021.99	6.87	159.73	0
30/10/2017	1021.95	6.87	160.1	2.2
31/10/2017	1021.9	6.87	159.87	0
01/11/2017	1021.85	6.87	161.03	0
02/11/2017	1021.79	6.87	161.08	0
03/11/2017	1021.74	6.87	161.95	1.2
04/11/2017	1021.69	6.87	162.87	0.2
05/11/2017	1021.73	6.86	159.35	18.6
06/11/2017	1022.43	6.8	139	17.2
07/11/2017	1024.27	6.79	138.63	5
08/11/2017	1024.15	6.83	142.56	0
09/11/2017	1023.33	6.86	147.89	0
10/11/2017	1022.75	6.87	150.71	3.4
11/11/2017	1022.51	6.87	152.38	0
12/11/2017	1022.36	6.87	155.02	0
13/11/2017	1022.28	6.87	155.26	1
14/11/2017	1022.42	6.85	151.59	44.6
15/11/2017	1032.74	6.88	145.39	121.6
16/11/2017	1037.65	6.68	141.27	11.6
17/11/2017	1035.99	6.71	143.82	2.2
18/11/2017	1033.52	6.83	151.01	0.4
19/11/2017	1031.33	6.79	145.99	0
20/11/2017	1028.74	6.82	146.7	0
21/11/2017	1026.92	6.85	146.14	0
22/11/2017	1025.58	6.87	146.63	0
23/11/2017	1024.62	6.87	147.72	0
24/11/2017	1024.04	6.87	148.53	0
25/11/2017	1023.68	6.87	150.1	0
26/11/2017	1023.42	6.87	150.68	6.2
27/11/2017	1023.27	6.87	151.13	0.4
28/11/2017	1023.19	6.87	151.62	0
29/11/2017	1023.13	6.87	151	18.6
30/11/2017	1024.73	6.81	136.72	1
01/12/2017	1024.81	6.82	140.55	0.2
02/12/2017	1024.39	6.85	145.53	5
03/12/2017	1024.06	6.86	147.11	0.2
04/12/2017	1023.79	6.87	147.32	0.2
05/12/2017	1023.52	6.87	147.76	6
06/12/2017	1023.25	6.87	148.81	4.8
07/12/2017	1023.07	6.87	148.47	1.6
08/12/2017	1023.01	6.87	148.4	8
09/12/2017	1024.99	6.83	135.78	1.2
10/12/2017	1025.26	6.83	140.66	1.4
11/12/2017	1025.28	6.84	141.91	2.4
12/12/2017	1025.85	6.85	142.36	16.4
13/12/2017	1034.86	6.93	134.54	23

Date	Piezometric elevation (m)	Temperature (°C)	Electrical conductivity (µS/cm)	Rainfall (mm)
14/12/2017	1036.54	6.86	132.67	1.6
15/12/2017	1035.81	6.9	139.77	33
16/12/2017	1037.33	6.84	132.96	2.4
17/12/2017	1036.92	6.86	140.28	0.2
18/12/2017	1035.36	6.88	146.2	0
19/12/2017	1033.46	6.89	148.6	0.2
20/12/2017	1031.75	6.85	144.74	0
21/12/2017	1029.26	6.85	143.99	0
22/12/2017	1027.45	6.88	143.18	1
23/12/2017	1026.52	6.88	142.73	1.4
24/12/2017	1025.67	6.89	142.72	0
25/12/2017	1024.9	6.9	143.57	0
26/12/2017	1024.43	6.9	144.35	0
27/12/2017	1024.14	6.9	143.8	15.6
28/12/2017	1025.79	6.87	132.16	1.8
29/12/2017	1026.05	6.87	138.95	0.2
30/12/2017	1025.41	6.89	142.1	1.2
31/12/2017	1024.87	6.9	142.59	0.2
01/01/2018	1024.56	6.89	141.28	7
02/01/2018	1024.88	6.87	134.28	3.6
03/01/2018	1024.95	6.88	139.94	3.6
04/01/2018	1024.94	6.89	141.14	0
05/01/2018	1024.85	6.89	141.53	0
06/01/2018	1024.81	6.9	141.66	0
07/01/2018	1024.76	6.9	141.96	0
08/01/2018	1024.38	6.9	142.85	0
09/01/2018	1024.03	6.9	143	1.8
10/01/2018	1023.79	6.9	144.33	1.4
11/01/2018	1023.66	6.9	144.08	0.8
12/01/2018	1023.51	6.9	144.69	1.6
13/01/2018	1023.3	6.9	145.77	4.8
14/01/2018	1023.14	6.89	147.23	0.4
15/01/2018	1023	6.89	148.03	0.2
16/01/2018	1022.91	6.89	147.14	0.4
17/01/2018	1022.98	6.89	141.19	14.4
18/01/2018	1023.3	6.89	133.34	0
19/01/2018	1023.26	6.89	141.47	0
20/01/2018	1023.16	6.89	143.39	0.6
21/01/2018	1023.09	6.89	145.75	1.4
22/01/2018	1023	6.89	145.51	0
23/01/2018	1022.9	6.89	146.26	0
24/01/2018	1022.81	6.89	147.29	0
25/01/2018	1022.74	6.89	147.98	0
26/01/2018	1022.67	6.89	148.07	0
27/01/2018	1022.6	6.89	148.01	0
28/01/2018	1022.53	6.89	148.24	0
29/01/2018	1022.48	6.89	148.45	0

Date	Piezometric elevation (m)	Temperature (°C)	Electrical conductivity (µS/cm)	Rainfall (mm)
30/01/2018	1022.43	6.89	149.03	0
31/01/2018	1022.37	6.89	149.04	0
01/02/2018	1022.32	6.89	148.97	0.2
02/02/2018	1022.3	6.89	149.08	3.8
03/02/2018	1022.46	6.89	142.46	14.6
04/02/2018	1022.75	6.9	135.86	2.8
05/02/2018	1022.68	6.89	141.77	0.4
06/02/2018	1022.61	6.89	143.92	1.4
07/02/2018	1022.56	6.89	143.8	1
08/02/2018	1022.49	6.89	145.83	0.2
09/02/2018	1022.4	6.89	147.38	0
10/02/2018	1022.34	6.89	148.08	1.2
11/02/2018	1022.3	6.89	148.7	0.2
12/02/2018	1022.25	6.89	148.75	0.2
13/02/2018	1022.2	6.89	149.29	0.2
14/02/2018	1022.13	6.89	150.71	0
15/02/2018	1022.1	6.89	151.67	0.2
16/02/2018	1022.07	6.89	151.57	0.2
17/02/2018	1022.03	6.89	151.84	0
18/02/2018	1022.01	6.89	151.05	10.2
19/02/2018	1022.16	6.89	144.47	3.6
20/02/2018	1022.23	6.89	140.42	0.2
21/02/2018	1022.24	6.89	142.48	0
22/02/2018	1022.22	6.89	144.26	0.2
23/02/2018	1022.19	6.89	146.68	15.4
24/02/2018	1030.39	7.04	133.63	41.6
25/02/2018	1030.83	7.05	127.33	0.4
26/02/2018	1029.19	7.18	127.5	0
27/02/2018	1027.39	7.11	129.08	0
28/02/2018	1025.83	7.04	132.25	0.4
01/03/2018	1024.69	6.99	134.93	0
02/03/2018	1024.55	7.02	135.51	11.2
03/03/2018	1027.9	7.14	131.09	18.4
04/03/2018	1031.13	7	123.68	3.2
05/03/2018	1031.83	7.04	123.11	15.4
06/03/2018	1031.98	7.06	120.61	3.2
07/03/2018	1031.53	7.15	124.36	4.6
08/03/2018	1030.82	7.24	126.48	2.6
09/03/2018	1029.62	7.35	127.5	0
10/03/2018	1027.99	7.23	130.91	0
11/03/2018	1027.05	7.18	130.86	10.8
12/03/2018	1027.62	7.15	127.77	2.6
13/03/2018	1029.64	7.12	130.88	1.6
14/03/2018	1028.8	7.12	131.32	0
15/03/2018	1027.66	7.11	132.84	6.4
16/03/2018	1027.51	7.12	130.1	2
17/03/2018	1027.88	7.12	129.49	9.4

Date	Piezometric elevation (m)	Temperature (°C)	Electrical conductivity (µS/cm)	Rainfall (mm)
18/03/2018	1028.37	7.12	127.88	5.2
19/03/2018	1028.86	7.12	127.78	6
20/03/2018	1028.55	7.15	129.27	0.8
21/03/2018	1027.78	7.13	130.21	0
22/03/2018	1027.16	7.15	128.77	0
23/03/2018	1026.62	7.08	129.77	0
24/03/2018	1025.87	7.05	131.51	7
25/03/2018	1025.03	7.04	132.84	8
26/03/2018	1024.5	7.03	134.05	11.2
27/03/2018	1024.18	7.03	134.5	0
28/03/2018	1023.95	7.04	133.59	0
29/03/2018	1023.8	7.04	133.28	0
30/03/2018	1023.66	7.02	135.63	10.4
31/03/2018	1028.79	7.04	127.94	30.2
01/04/2018	1033.24	6.95	129.03	3.6
02/04/2018	1032.61	7.02	138.12	0
03/04/2018	1030.92	7.11	128.82	0
04/04/2018	1028.64	7.14	131.8	3.2
05/04/2018	1027.44	7.14	132.17	4.2
06/04/2018	1027.23	7.16	131.51	0
07/04/2018	1026.94	7.15	131.59	0
08/04/2018	1026.52	7.1	132.27	0
09/04/2018	1026.07	7.08	133.2	10.4
10/04/2018	1026.12	7.09	131.27	1
11/04/2018	1026.55	7.1	130.3	0.4
12/04/2018	1026.4	7.08	133.27	1.2
13/04/2018	1026.34	7.07	137.73	0
14/04/2018	1026.37	7.07	143.6	0
15/04/2018	1026.16	7.07	143.3	0
16/04/2018	1025.88	7.07	143.7	0.2
17/04/2018	1025.66	7.07	145.9	2.6
18/04/2018	1025.56	7.07	148.32	1.2
19/04/2018	1025.4	7.07	148.65	0
20/04/2018	1025.3	7.07	147.93	0
21/04/2018	1025.24	7.07	146.96	0
22/04/2018	1025.12	7.08	146.5	0
23/04/2018	1025.03	7.08	146.82	0
24/04/2018	1025.02	7.08	146.64	0
25/04/2018	1025.05	7.08	147.97	0
26/04/2018	1025.03	7.08	148.15	0
27/04/2018	1024.97	7.08	147.94	0
28/04/2018	1024.82	7.08	147.19	1.4
29/04/2018	1024.67	7.08	146.99	1.4
30/04/2018	1024.62	7.08	147.04	0
01/05/2018	1024.64	7.08	147.16	1
02/05/2018	1024.6	7.08	147.15	1.6
03/05/2018	1026.28	7.05	139.88	70

Date	Piezometric elevation (m)	Temperature (°C)	Electrical conductivity (µS/cm)	Rainfall (mm)
04/05/2018	1036.46	6.53	129.63	40.2
05/05/2018	1040.11	6.57	127.82	9.6
06/05/2018	1039.54	6.53	122.33	5.6
07/05/2018	1037.93	6.78	137.1	10.6
08/05/2018	1037.38	6.87	142.67	13.6
09/05/2018	1037.01	6.92	144.64	0.6
10/05/2018	1036.48	6.92	146.12	6.6
11/05/2018	1035.87	6.94	147.1	0.8
12/05/2018	1035.37	6.96	146.89	3
13/05/2018	1034.91	6.97	146.98	0
14/05/2018	1034.22	6.95	147.43	0.8
15/05/2018	1033.54	6.96	147.52	0.6
16/05/2018	1032.89	6.97	146.77	1.2
17/05/2018	1031.91	6.99	142.35	4.8
18/05/2018	1030.51	6.97	143.6	25
19/05/2018	1029.03	7	146.15	2
20/05/2018	1027.99	7.01	147.03	1.4
21/05/2018	1027.54	7	145.6	29.6
22/05/2018	1027.65	7	136.21	5.8
23/05/2018	1027.45	7.02	135.28	0.6
24/05/2018	1027.23	7.03	136.77	1
25/05/2018	1027.07	7.02	141.44	1.4
26/05/2018	1026.88	7.03	147.26	0
27/05/2018	1026.73	7.03	148.53	0
28/05/2018	1026.61	7.03	148.97	14
29/05/2018	1026.5	7.03	149.2	28.4
30/05/2018	1026.39	7.04	149.39	1.4
31/05/2018	1026.27	7.04	149.73	0.6

Supplementary_06: Ventina fracture dimensions and orientation

In the following supplementary material, tables of data collected station for fracture dimension and orientation, and the stereoplots of the observed clusters selected for DFN generation will be listed for measurement localities.

Tables include 7 columns for every measurement station, which contains:

- Cluster: number of joint cluster observed in field and then verified on MOVE software;
- Spacing: distance (in centimeters) between fractures observed on field, as an index of fracture intensity;
- Length: fracture length in meters
- Opening: fracture void opening in centimeters
- Fisher K: the K value calculated on software to observe homogeneity in fractures orientations;
- Mean dip angle: mean dip angle calculated for the cluster
- Mean dip azimuth: mean dip azimuth calculated for the cluster.

FRATT1

Cluster	Spacing (cm)	Length (m)	Opening (mm)	Fisher K	Mean dip angle (°)	Mean dip azimuth (°)
0	40	100	5	50.6	30.68	54.9
3	15	30	10	86.11	77.58	198
2	100	20	7	55.52	72.32	285.68
1	200	14	2.5	48.09	65.36	83.3

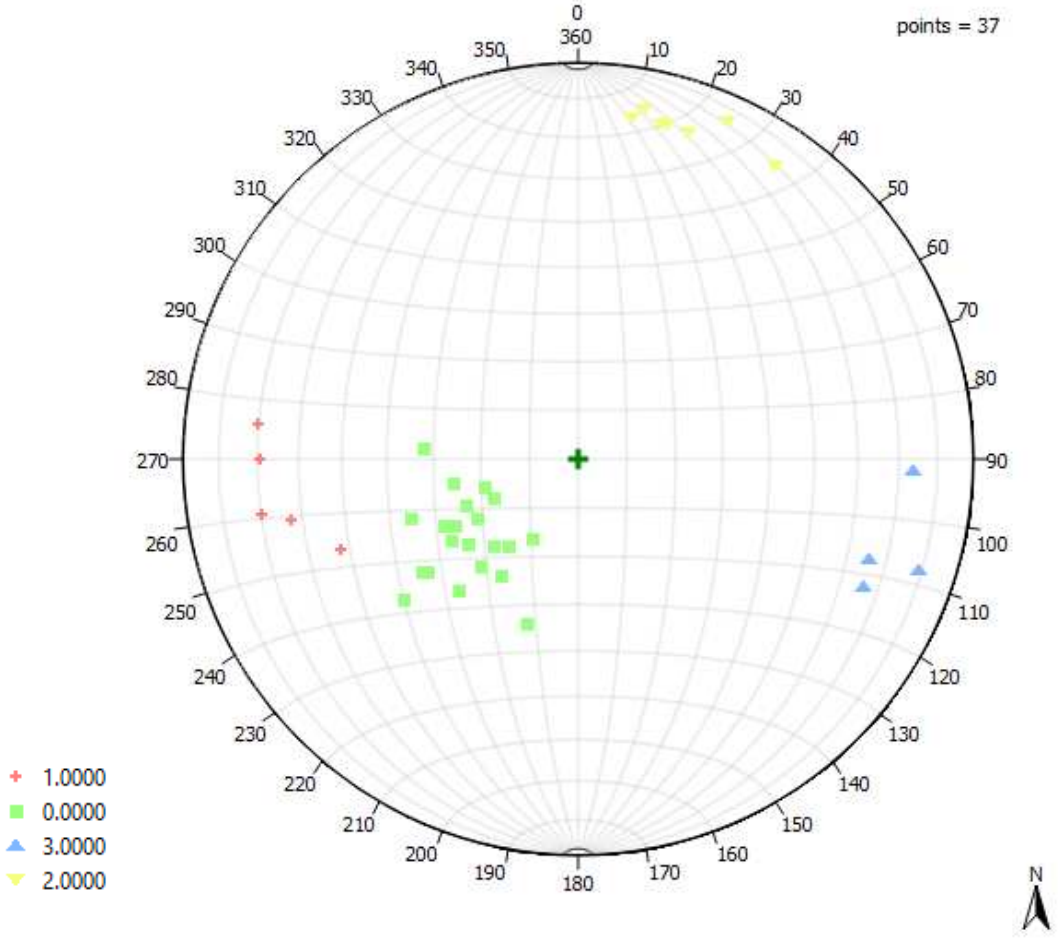

FRATT2

Cluster	Spacing (cm)	Length (m)	Opening (mm)	Fisher K	Mean dip angle (°)	Mean dip azimuth (°)
0	40	20	5	46.7	78.35	83.9
1	40	60	5	115.9	18.85	342.21
2	10	120	10	81.7	66.11	170.38
3	50	10	2.5	31.8	55.67	302.56

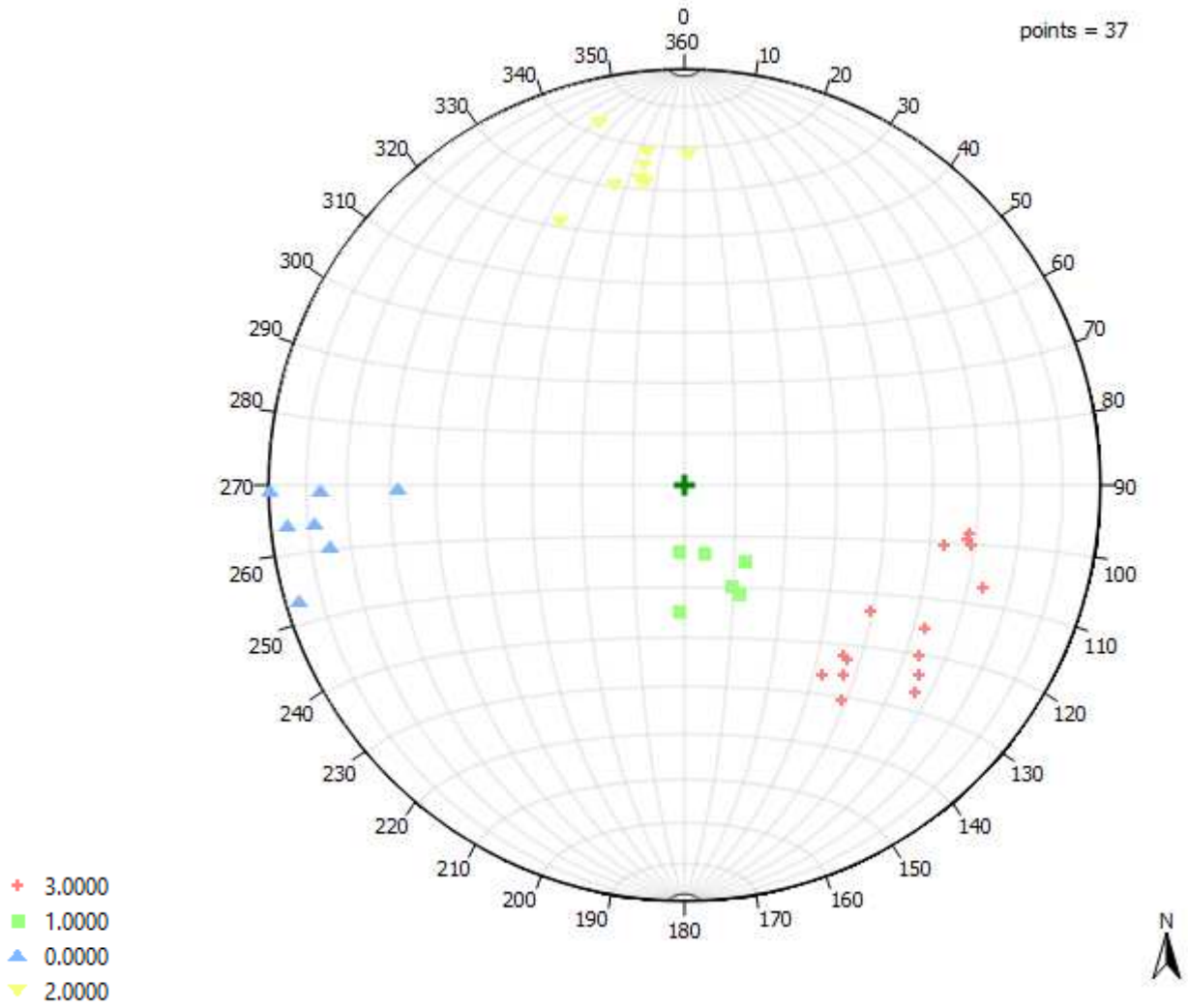

FRATT3

Cluster	Spacing (cm)	Length (m)	Opening (mm)	Fisher K	Mean dip angle (°)	Mean dip azimuth (°)
0	50	14	10	54.7	45.91	339.89
1	30	40	5	41.1	74.07	229.12
2	50	50	5	41.5	28.42	22.18
3	100	8	5	63.4	66.79	87.04

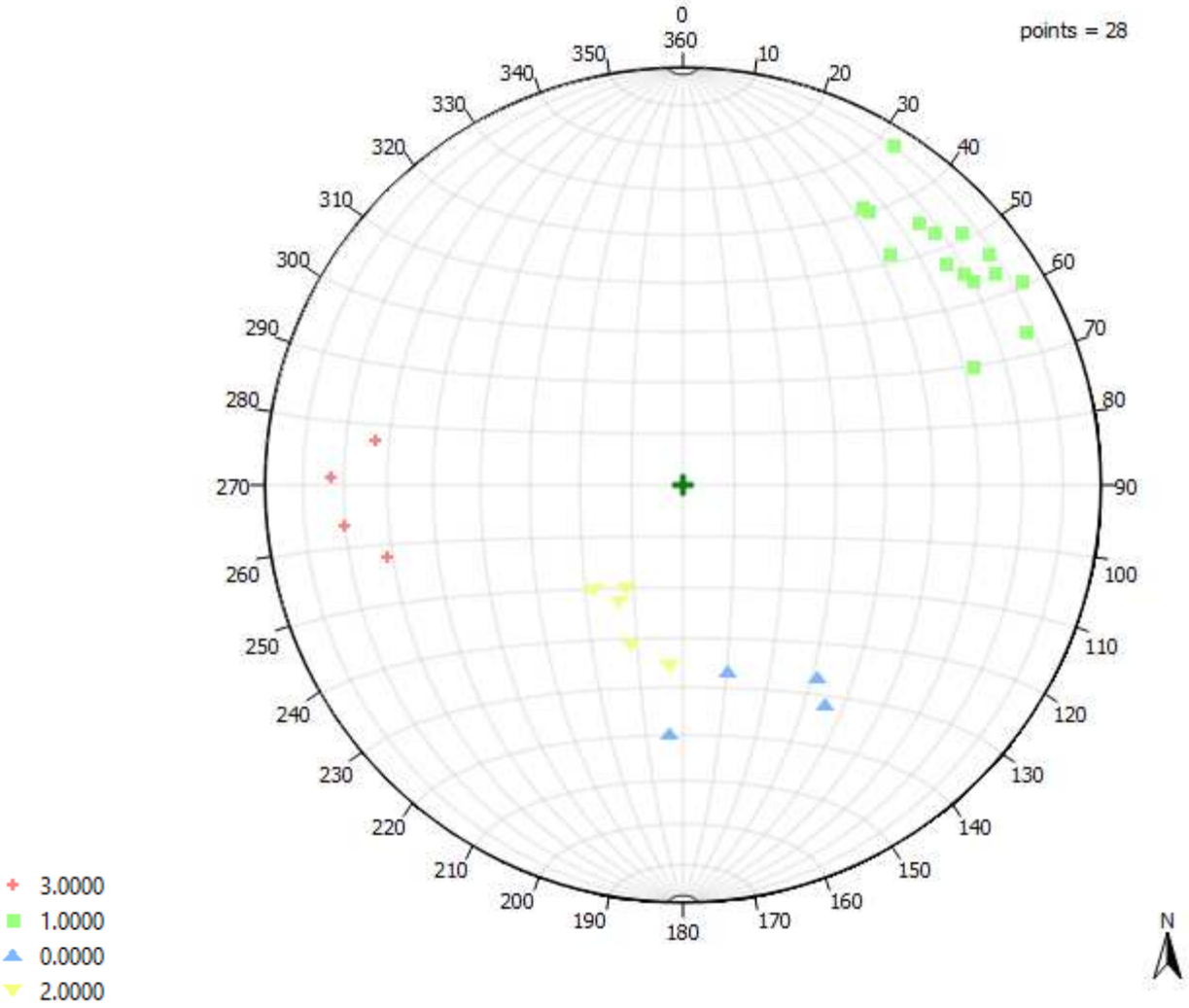

FRATT4

Cluster	Spacing (cm)	Length (m)	Opening (mm)	Fisher K	Mean dip angle (°)	Mean dip azimuth (°)
4	100	40	5	59.45	74.9	286.14
3	100	60	10	35.8	79.35	313.27
0	100	20	7	-	37	350
1	50	60	7	58.52	20.08	4
2	20	80	5	90.55	75.04	191.94

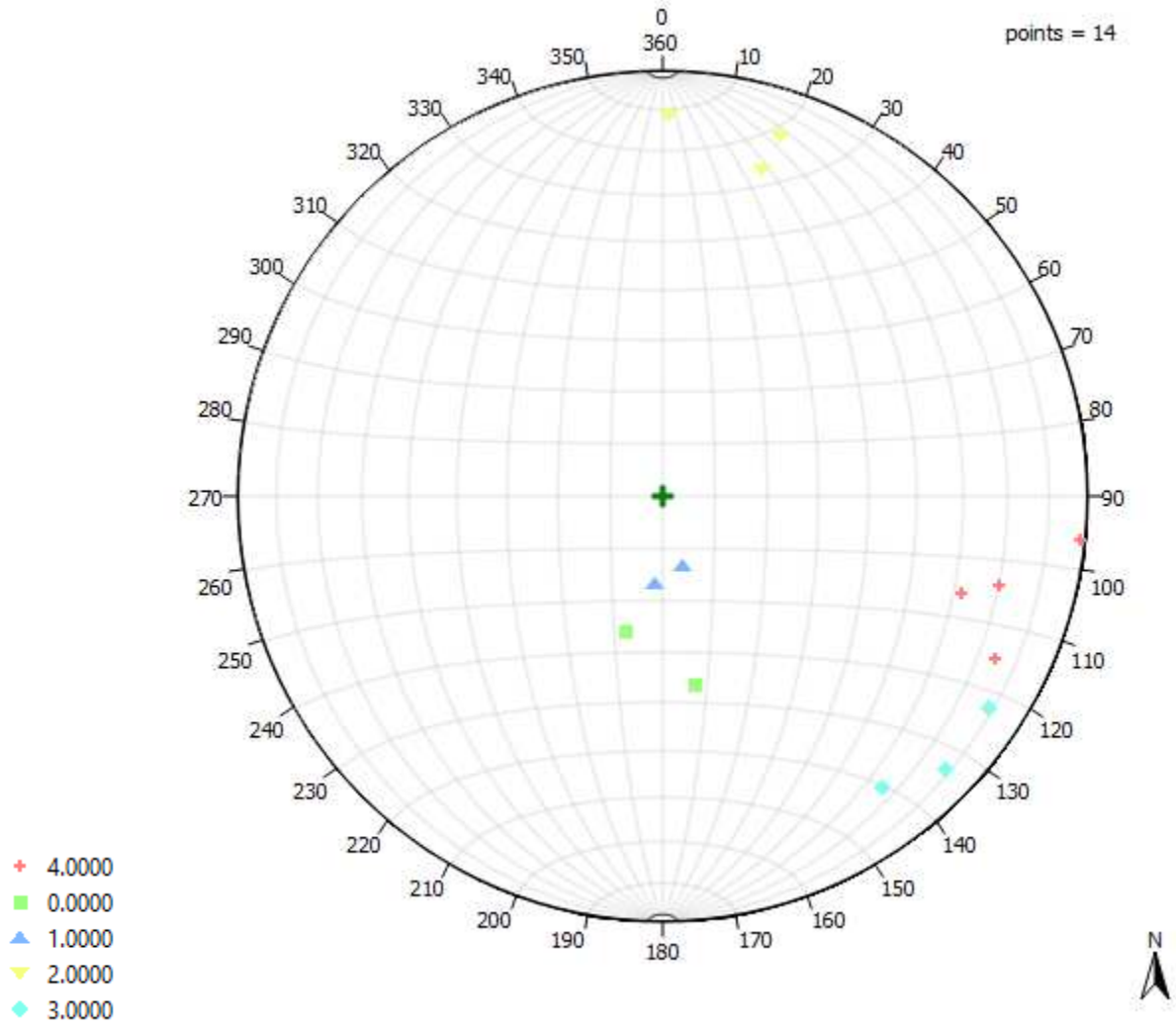

FRATT5

Cluster	Spacing (cm)	Length (m)	Opening (mm)	Fisher K	Mean dip angle (°)	Mean dip azimuth (°)
3	350	40	2	7.37	68.68	117.02
1	100	50	7	30.78	82.01	307.07
0	50	60	5	19.57	21.38	56.58
2	10	40	20	8.3	53.66	229.47

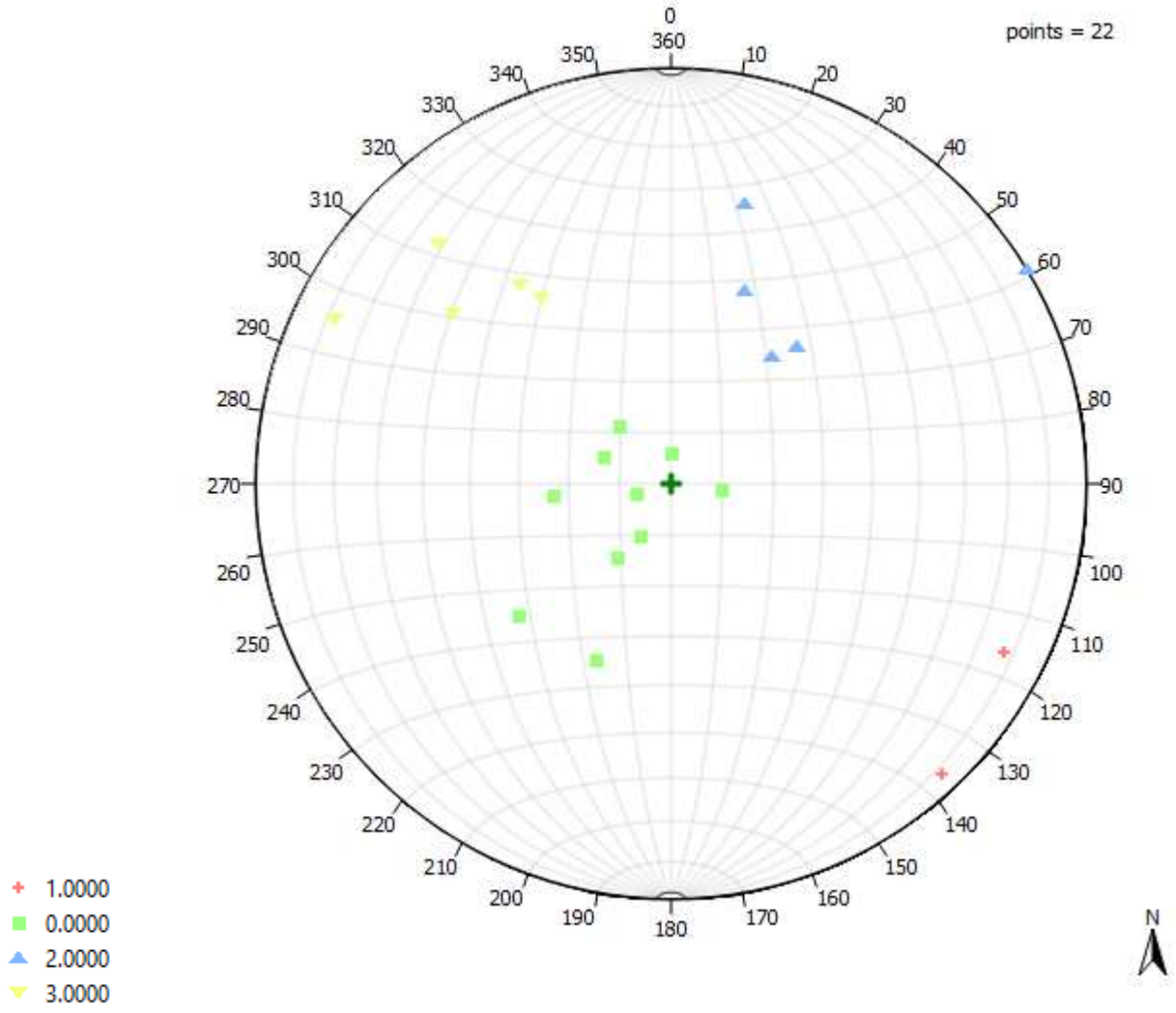

FRATT6

Cluster	Spacing (cm)	Length (m)	Opening (mm)	Fisher K	Mean dip angle (°)	Mean dip azimuth (°)
2	30	40	5	58	57.2	306.97
1	70	50	25	-	67.07	184.33
0	30	8	3	24.3	74.24	239.9
3	50	30	5	30	31.79	314.96
4	35	40	20	-	28.74	197.43

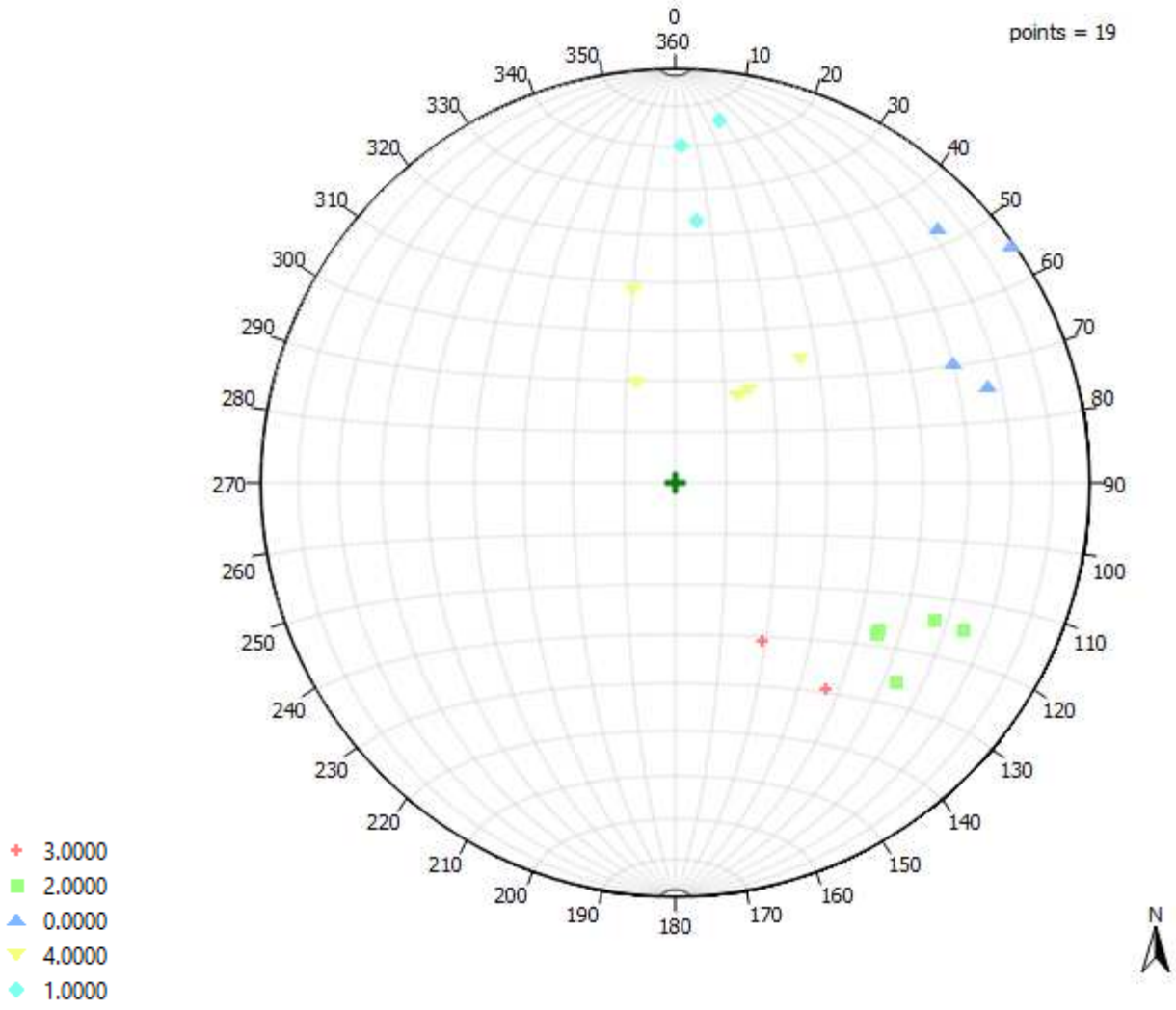

FRATT7

Cluster	Spacing (cm)	Length (m)	Opening (mm)	Fisher K	Mean dip angle (°)	Mean dip azimuth (°)
4	100	40	3	38.25	40.84	343.12
1	150	20	3	179	49.12	0.88
0	80	120	5	206.9	12.56	47.55
3	100	40	10	364.8	63.04	41
2	50	30	5	730	32	110

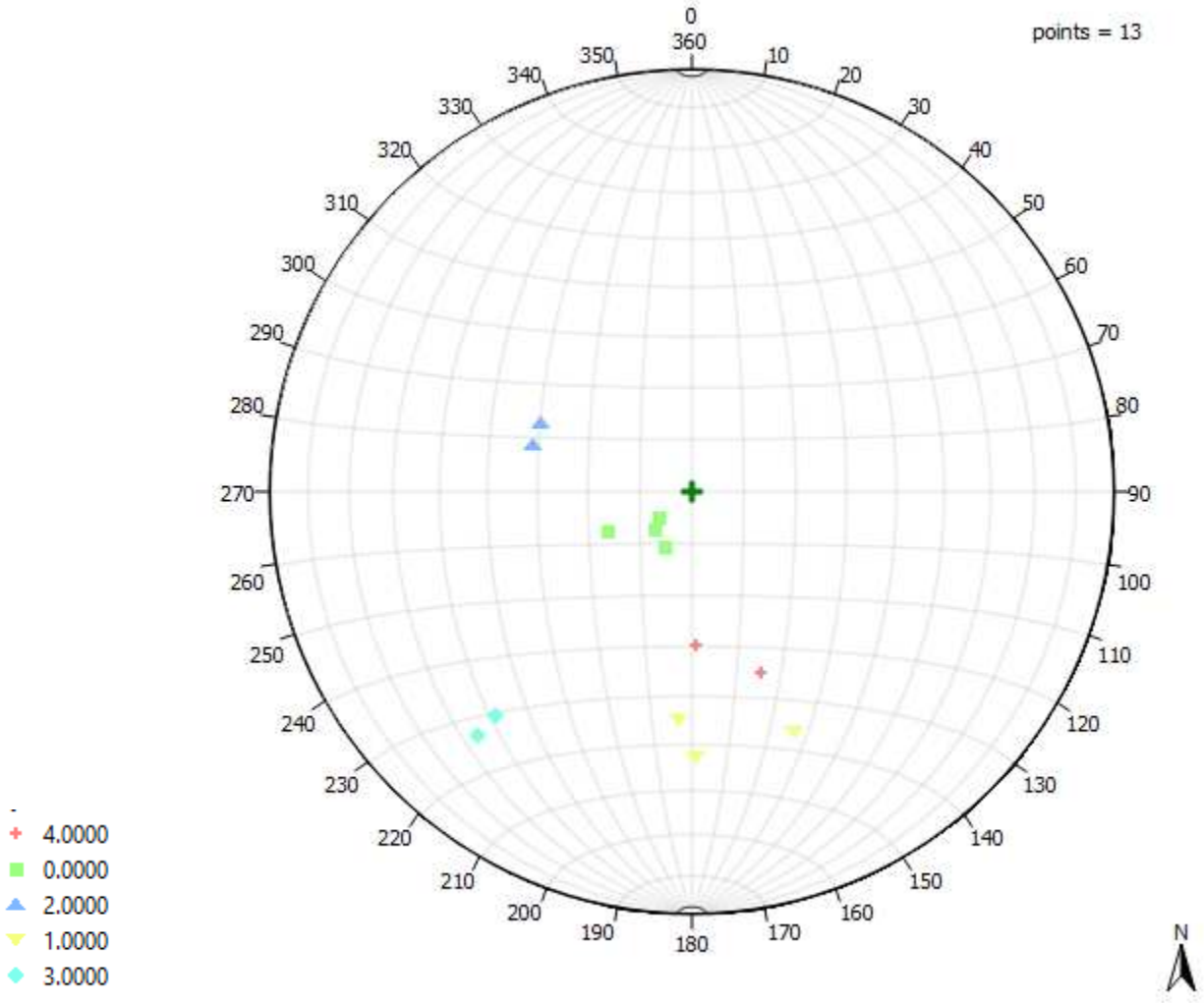

FRATT8

Cluster	Spacing (cm)	Length (m)	Opening (mm)	Fisher's K	Mean dip angle (°)	Mean dip azimuth (°)
0	50	40	10	39.8	11.96	311.68
1	40	30	5	118.5	75.3	204.53
2	50	20	5	-	22	225
3	100	20	10	289.3	76.64	169.66

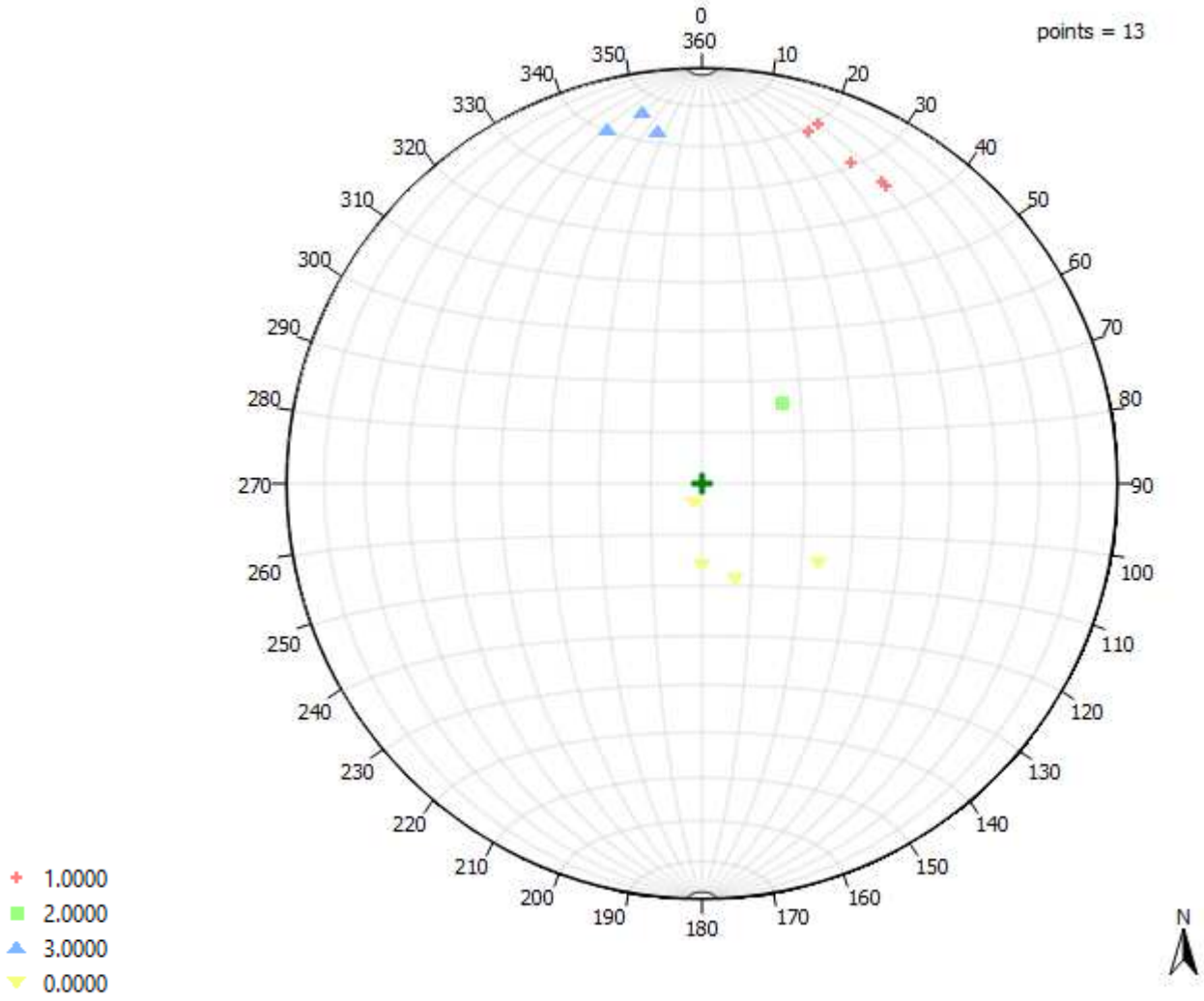

VENT1

Cluster	Spacing (cm)	Length (m)	Opening (mm)	Fisher's K	Mean dip angle (°)	Mean dip azimuth (°)
1	100	5	20	12.98	64.94	337.26
2	300	10	5	32.06	23.09	152.72
0	3000	1	0.1	47.95	40.44	61.43

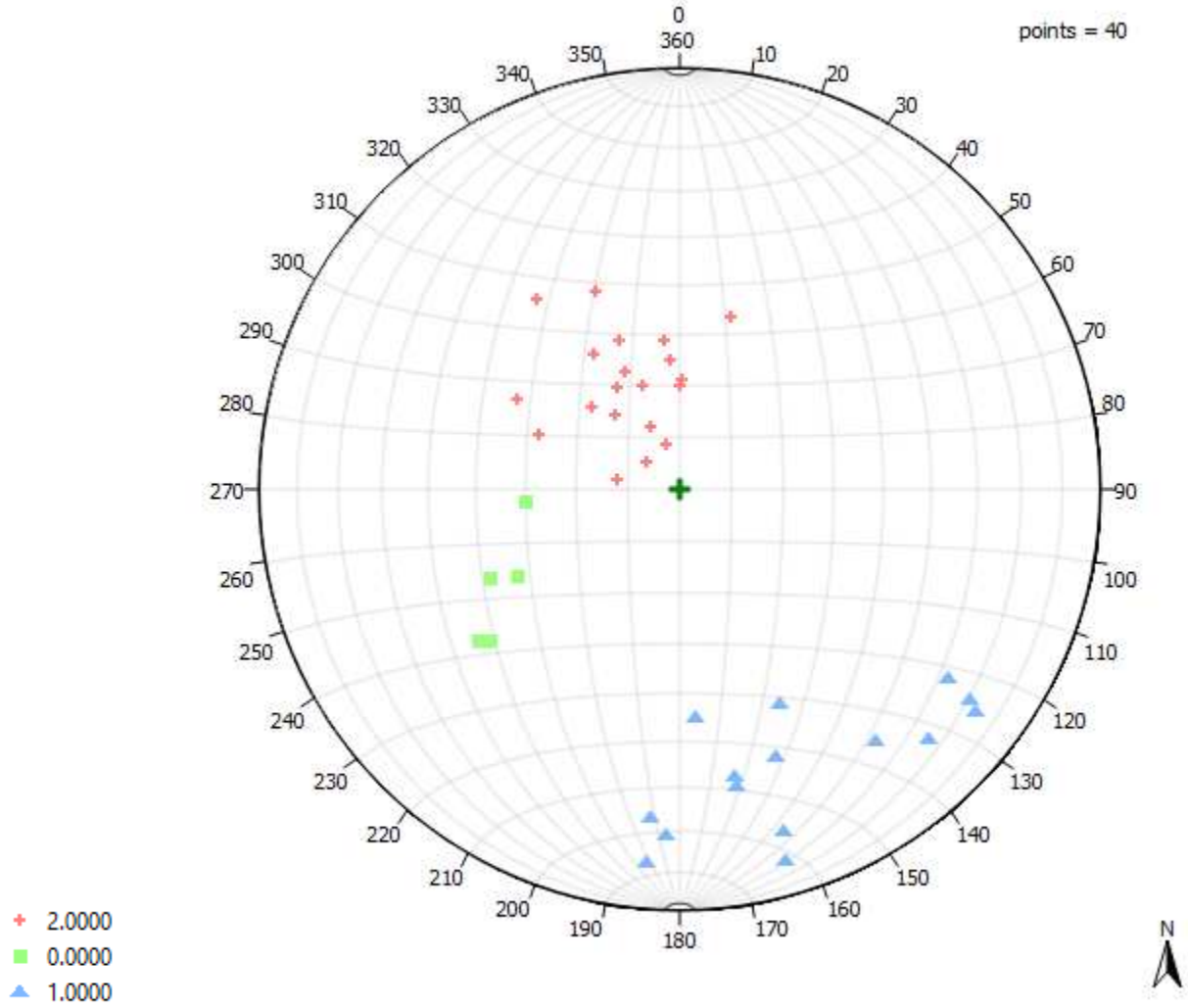

VENT2

Cluster	Spacing (cm)	Length (m)	Opening (mm)	Fisher K	Mean dip angle (°)	Mean dip azimuth (°)
0	500	15	10	18.68	56.68	148.54
2	150	10	10	48.28	45.99	344.4
1		15	0.1	21.58	54.28	288.67

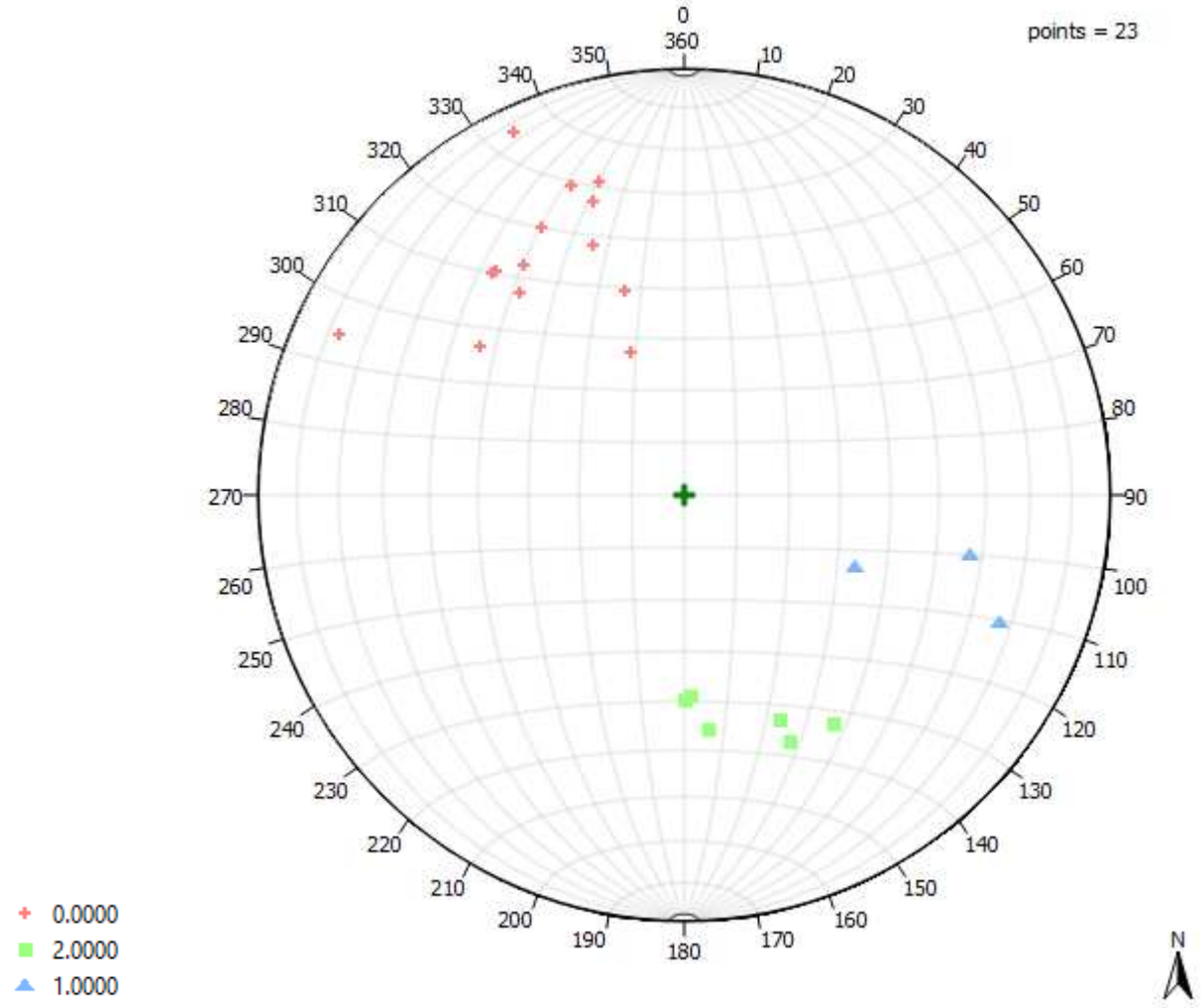

VENT3

Cluster	Spacing (cm)	Length (m)	Opening (mm)	Fisher's K	Mean dip angle (°)	Mean dip azimuth (°)
0	1	25	10	33.86	45.43	74.65
1	1	20	10	14.51	36.41	267.27
2	2	2	10	23.98	61.32	150.91

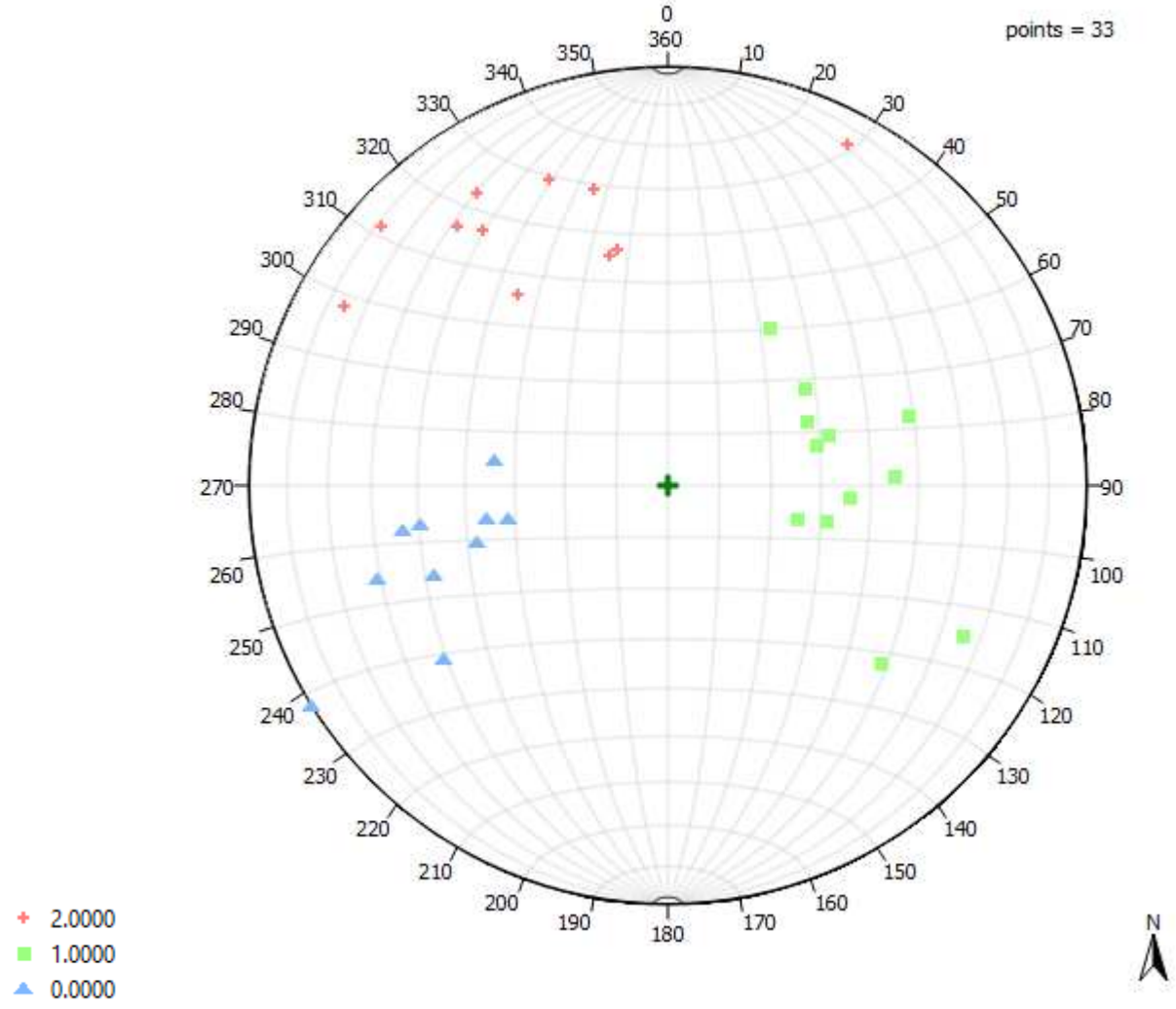

VENT4

Cluster	Spacing (cm)	Length (m)	Opening (mm)	Fisher's K	Mean dip angle (°)	Mean dip azimuth (°)
0	200	20	10	6.12	41.62	274.35
2	200	20	10	19.77	55.07	152.51
1		10	1	12.72	53.28	67.97

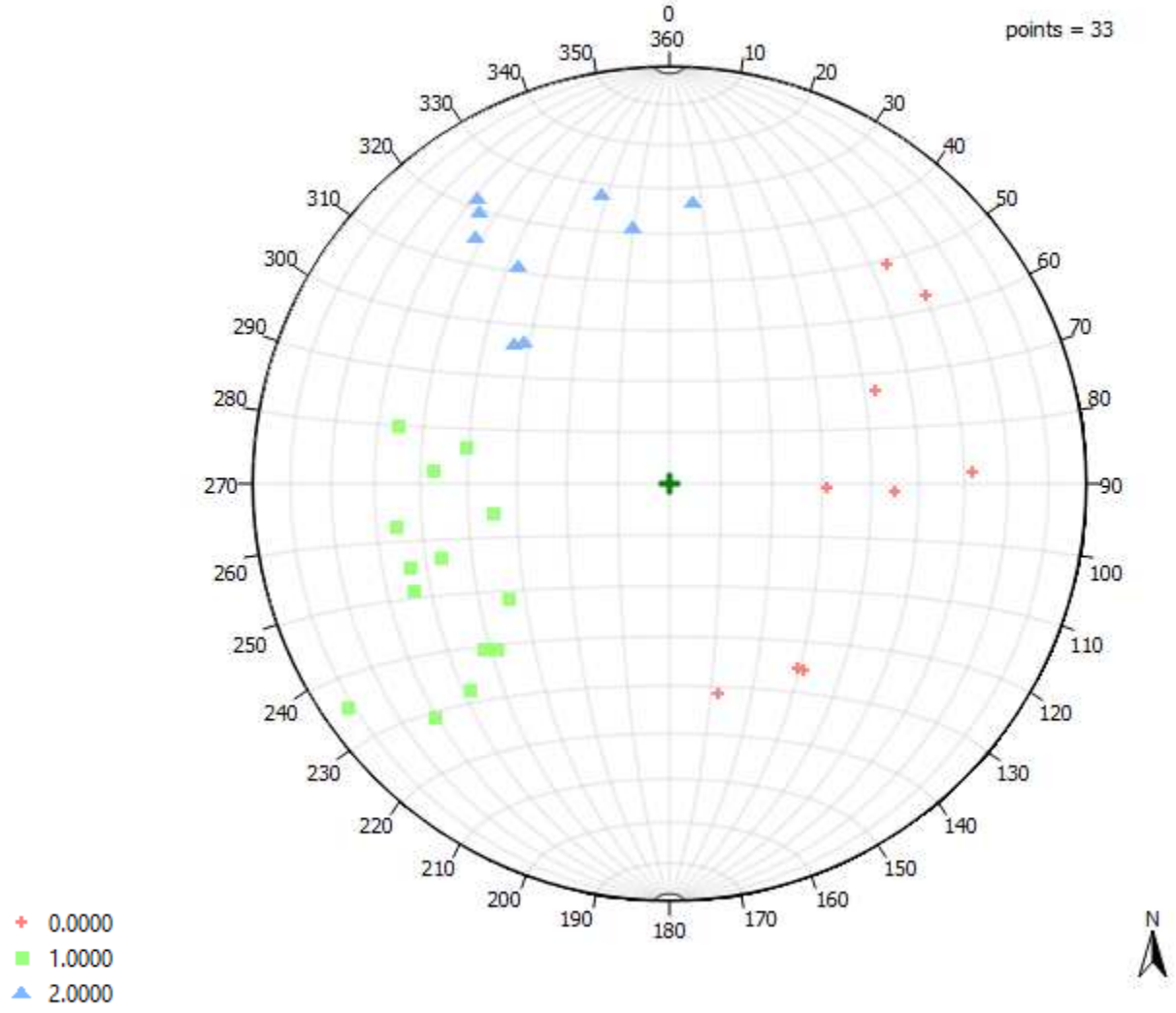

VENT5

Cluster	Spacing (cm)	Length (m)	Opening (mm)	Fisher's K	Mean dip angle (°)	Mean dip azimuth (°)
1	500	30	10	10.44	16.79	213.33
0	250	5	10	26.88	60.04	316.13
2	250	5	10	11.12	67.1	70.29

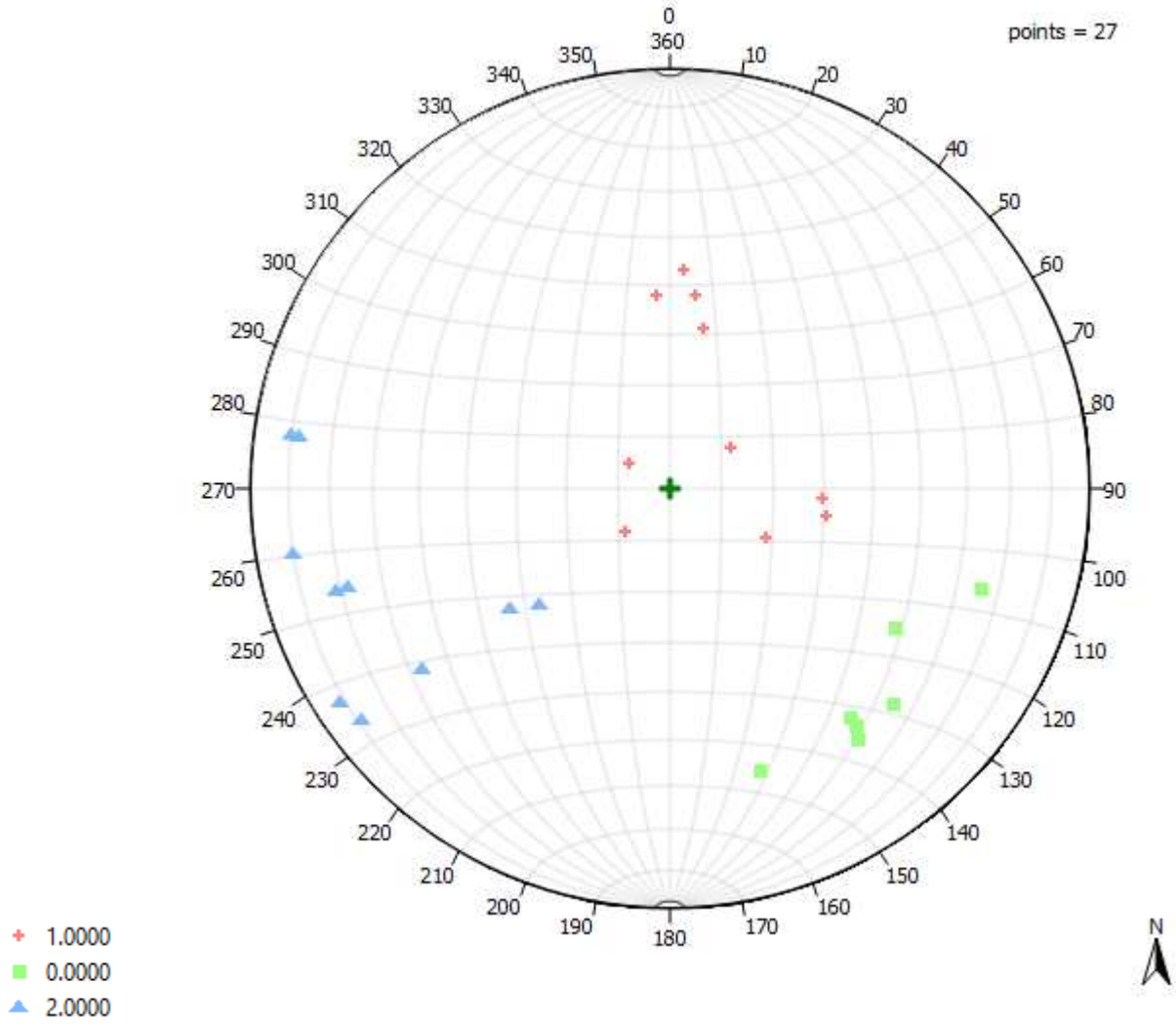

VENT6

Cluster	Spacing (cm)	Length (m)	Opening (mm)	Fisher's K	Mean dip angle (°)	Mean dip azimuth (°)
1	500	30	10	6.01	55.83	273.27
0	3000	2	1	16.71	51.25	95.35

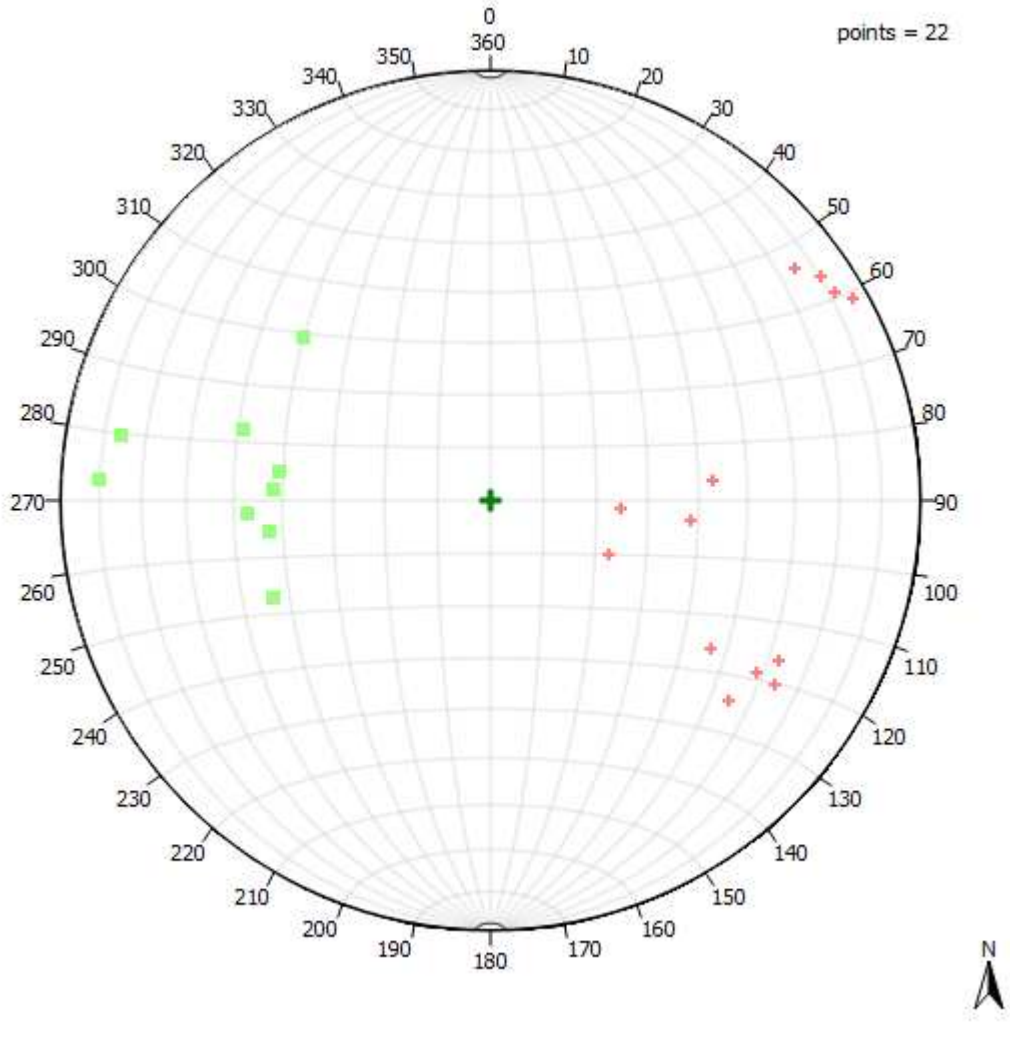

VENTB1

Cluster	Spacing (cm)	Length (m)	Opening (mm)	Fisher's K	Mean dip angle (°)	Mean dip azimuth (°)
0	65	15	5	31.43	71.3	157.72
1	150	15	2.5	9.33	50.73	58.07

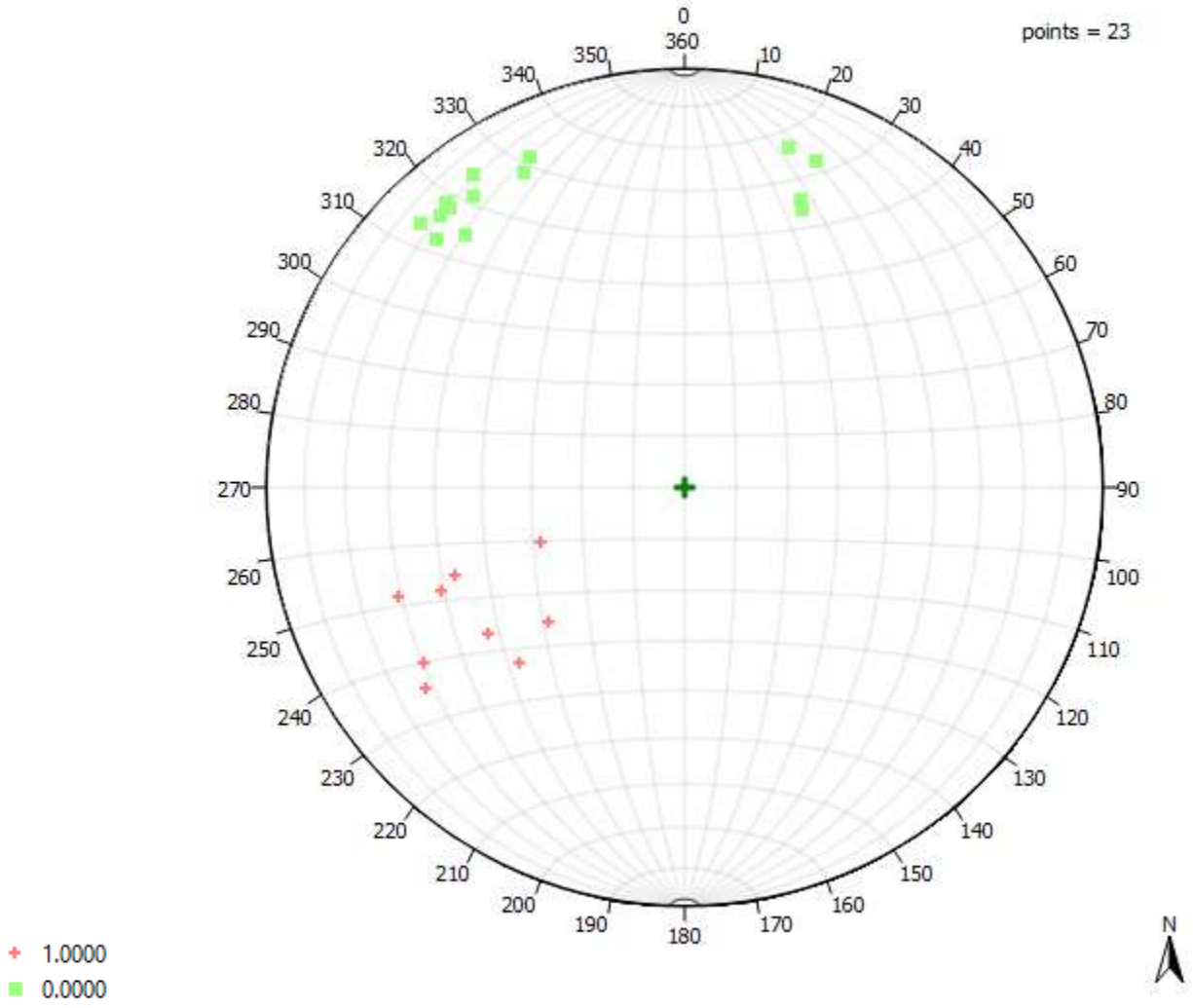

VENTB2

Cluster	Spacing (cm)	Length (m)	Opening (mm)	Fisher's K	Mean dip angle (°)	Mean dip azimuth (°)
0	50	25	5	42.87	6.39	159.55
2	250	5	50	19.47	59.8	297.41
1	100	5	30	23.41	29.23	92.58

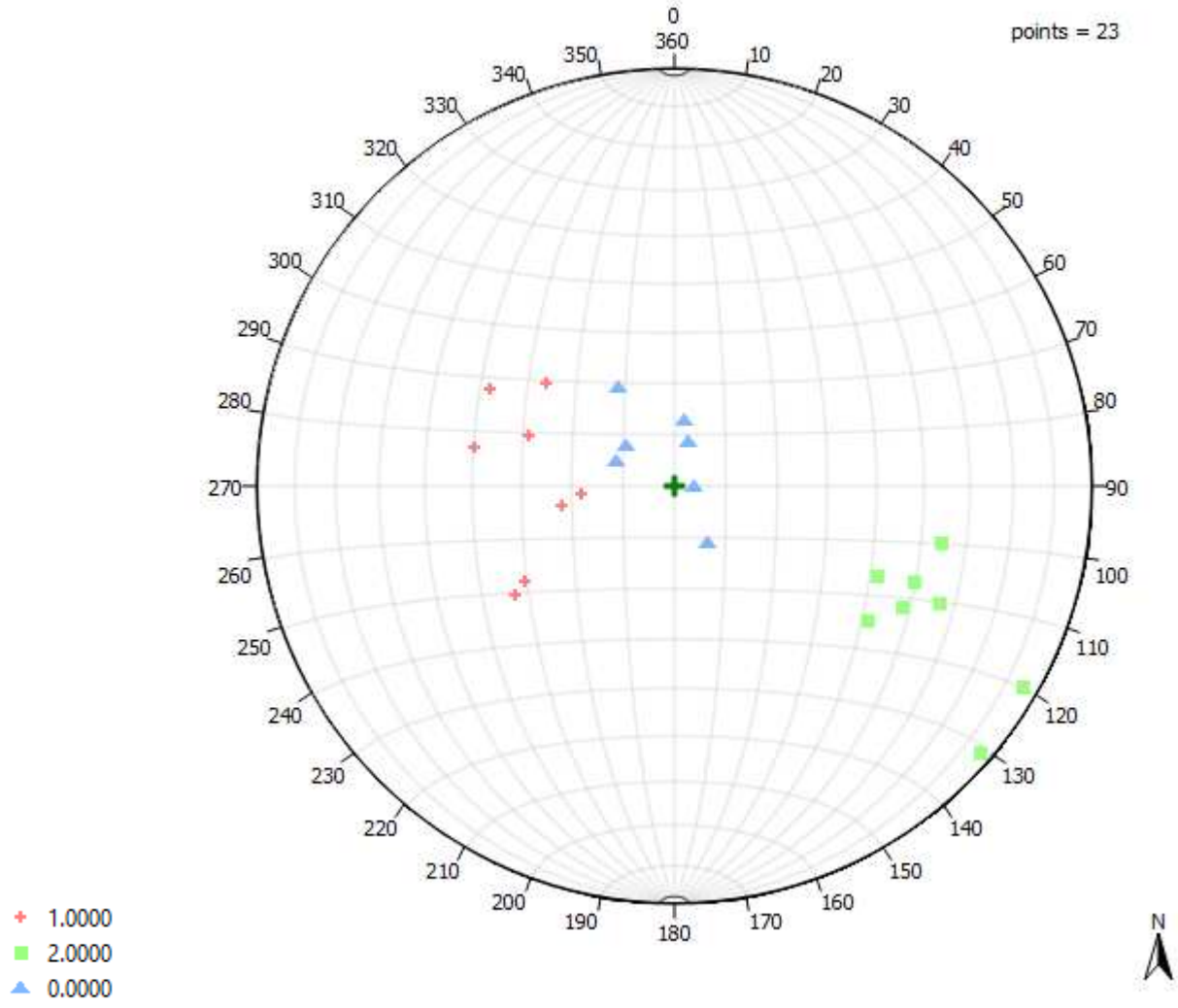

VENTB3

Cluster	Spacing (cm)	Length (m)	Opening (mm)	Fisher's K	Mean dip angle (°)	Mean dip azimuth (°)
2	100	30	30	73.46	51.69	37.5
0	250	30	30	50.05	25.81	102.29
1	75	30	20	9.39	86.31	39.57

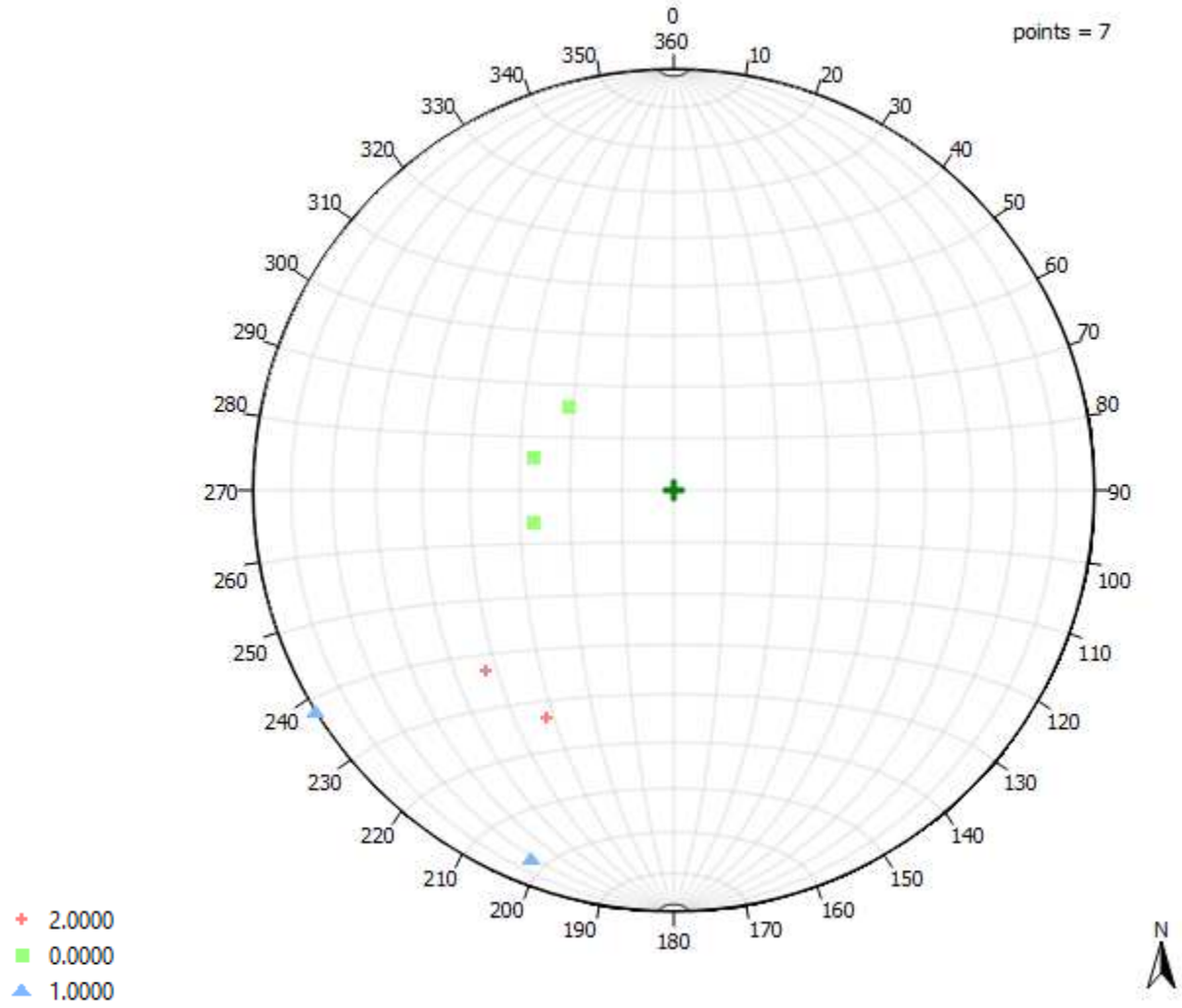

VENTB4

Cluster	Spacing (cm)	Length (m)	Opening (mm)	Fisher's K	Mean dip angle (°)	Mean dip azimuth (°)
2	150	25	30	29.95	29.88	238.74
1	750	35	30	23.83	73.49	14.93
0	750	7.5	5	160	75.97	316.55

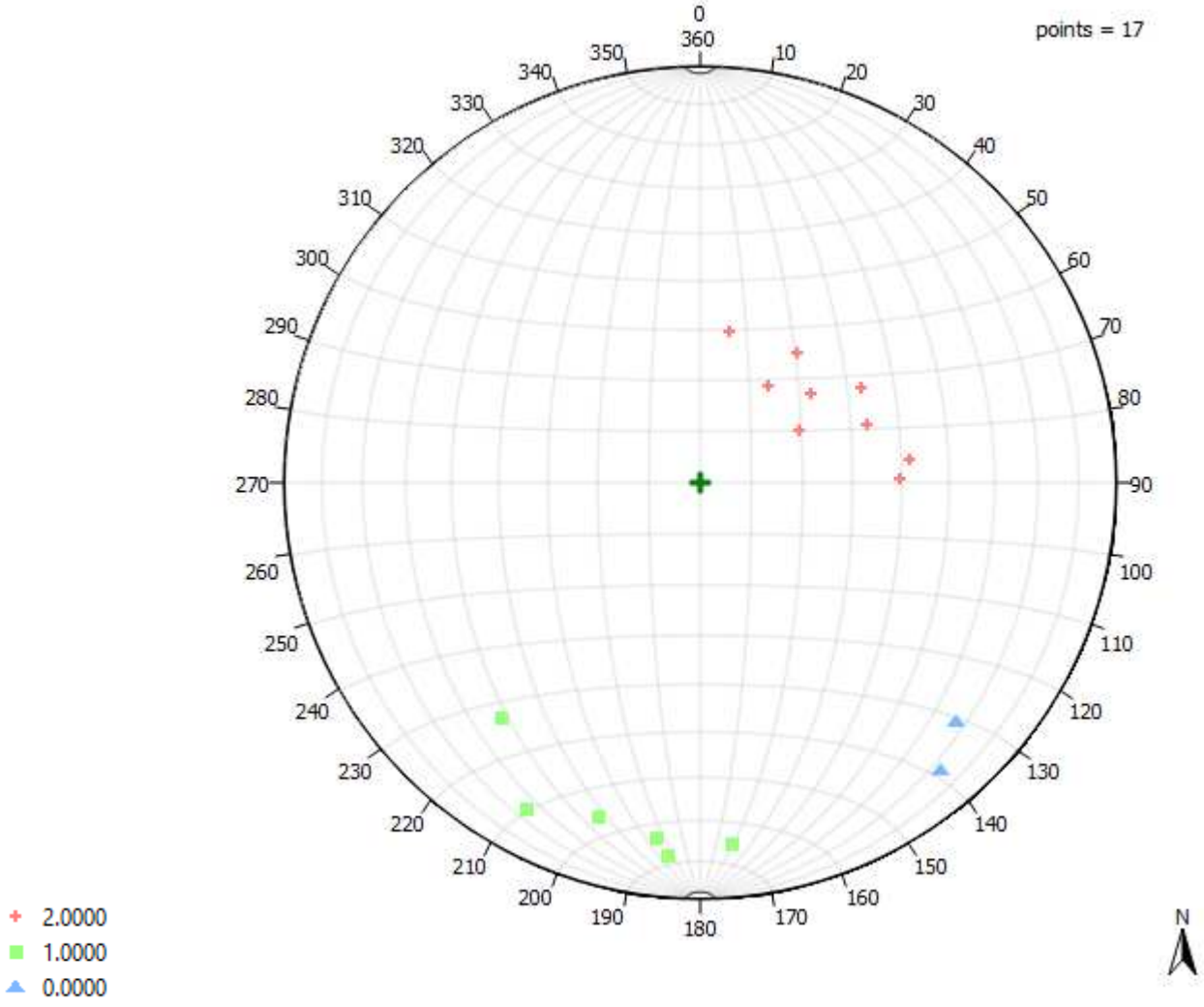

VENTB5

Cluster	Spacing (cm)	Length (m)	Opening (mm)	Fisher's K	Mean dip angle (°)	Mean dip azimuth (°)
2	100	20	25	24.75	67.5	258.92
0	500	10	15	8.07	62.95	348.95
1	500	3.5	5	8.74	52.75	86.78

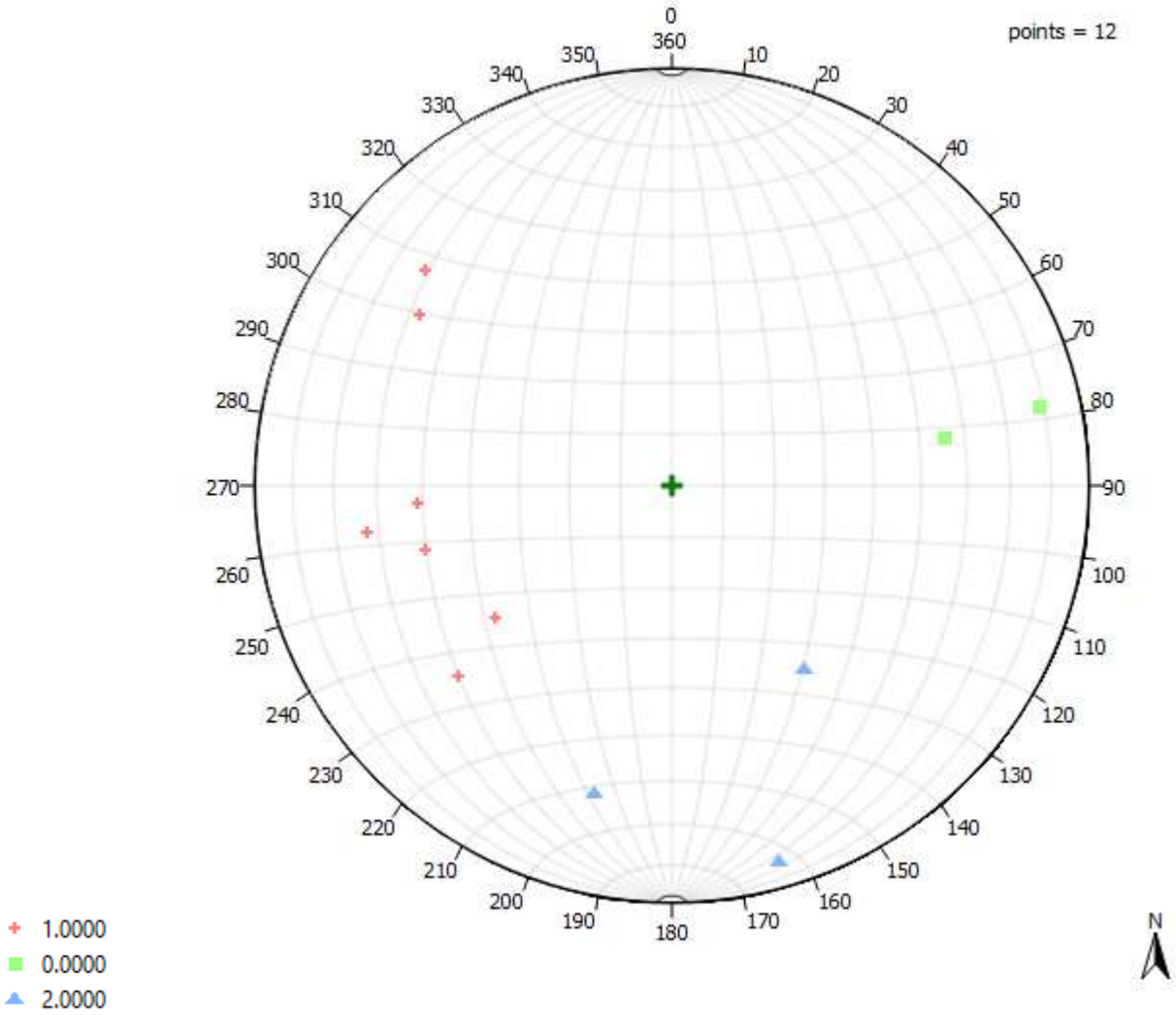

VENTB6

Cluster	Spacing (cm)	Length (m)	Opening (mm)	Fisher K	Mean dip angle (°)	Mean dip azimuth (°)
1	500	20	35	16.52	84.81	121.59
0	100	2	10	3.13	22.84	45.36

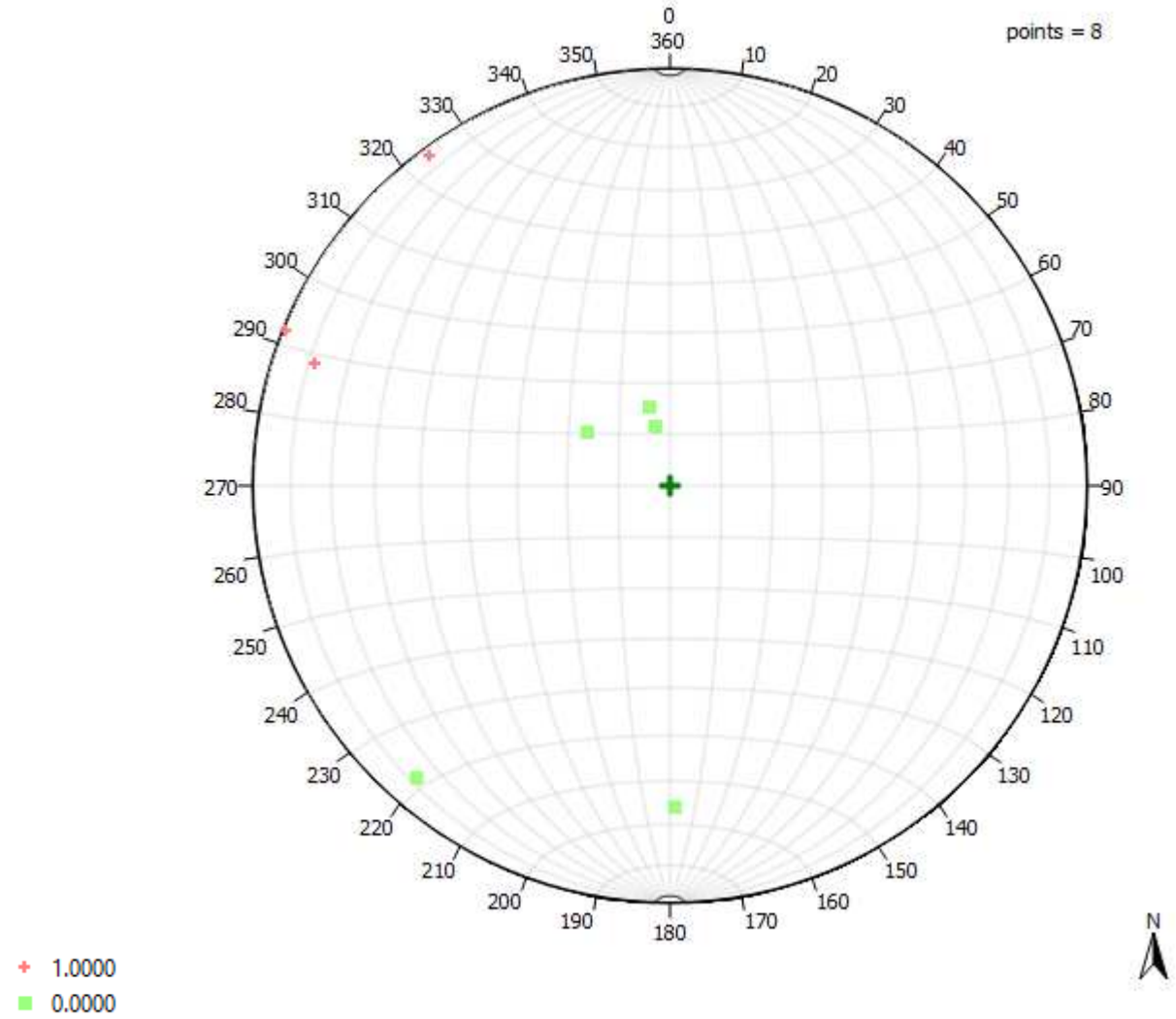

VENTC1

Cluster	Spacing (cm)	Length (m)	Opening (mm)	Fisher's K	Mean dip angle (°)	Mean dip azimuth (°)
3	50	400	0.5	40.58	16.88	227.48
0	100	200	0.2	28.91	61.51	97.16
1	200	250	0.2	11.36	83.38	332.19
2	200	200	0.5	113.19	20.75	88.16

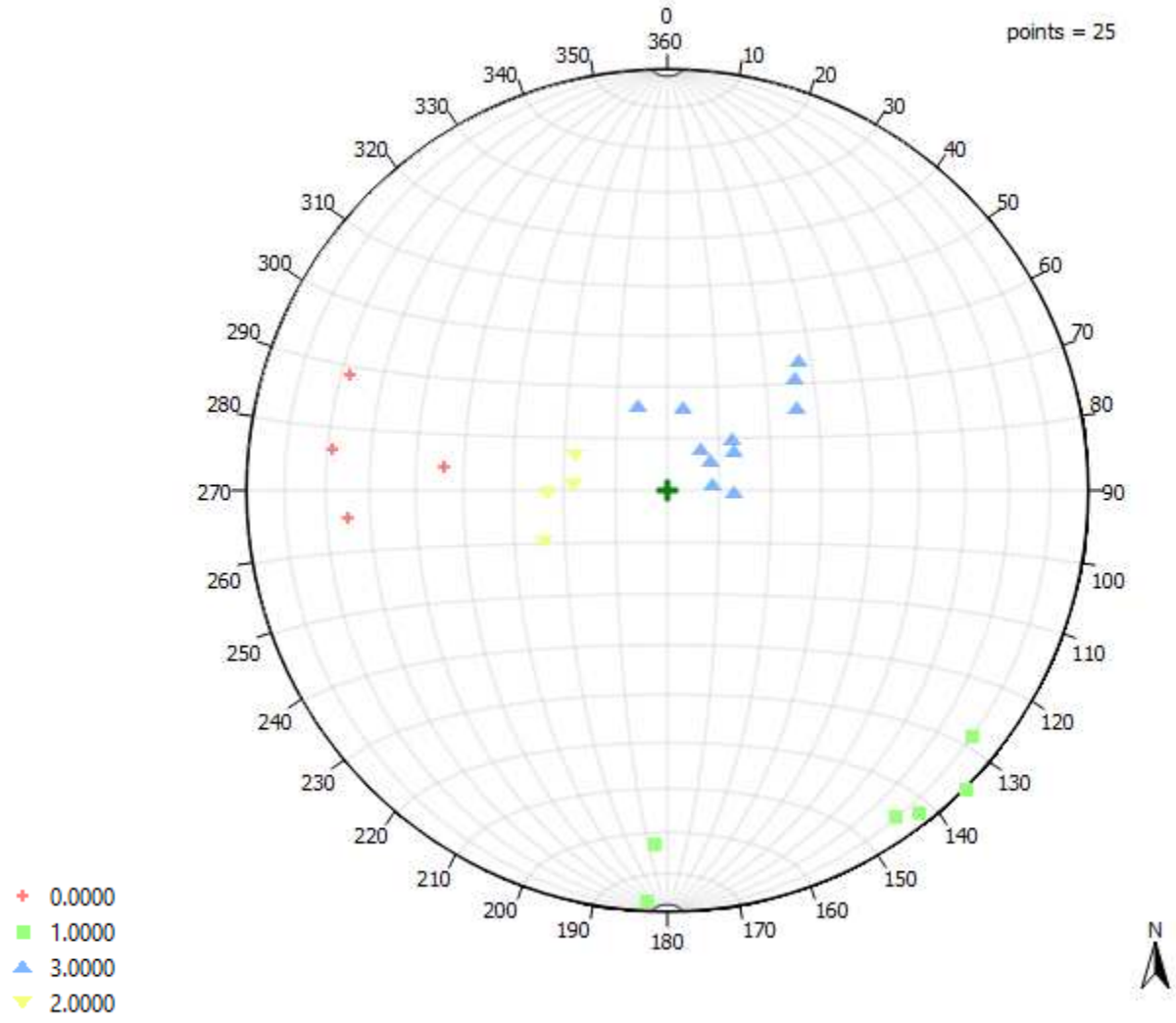

Supplementary_07: Sampling points coordinates (in UTM32N format)

Central Italy water sampling sites

Point	East (m)	North (m)
PES	335664	4692291
SUS	323499	4707753
VIC	324084	4703951
NER	350463	4750115
FP01	357566	4739247
FP02	357565	4738975
FP03	359295	4739548
FP04	358627	4739844
P12	358621	4748368

Ventina valley water and sediments sampling sites

Point	East (m)	North (m)
P01	560393	5128242
P02	560411	5128008
V07	560037	5127007
V09	560170	5126707
V10	560161	5126632
V08	559963	5126879
V06	559858	5127300
P09	561314	5127382
P10	561264	5127403
P11	561229	5127284
P03	561024	5127899
P12	560274	5127333
P08	561396	5127400
V11	560018	5125513
P04	561174	5127892
P05	561461	5127884
P06	561563	5127829
V01	559849	5127553
V02	559869	5127427
V03	559917	5127306
V04	559985	5127170

Ventina valley geological measurements stations

Point	East (m)	North (m)
FRATT3	560669	5128036
FRATT2	560805	5128022
FRATT1	561047	5128006
FRATT7	561182	5127846
FRATT8	561463	5127893
FRATT4	561520	5127741
VENT5	560627	5127840
VENT4	560767	5127750
VENT3	560820	5127660
FRATT6	560848	5127563
VENT6	560655	5127580
FRATT5	561306	5127470
VENTB1	561333	5127460
VENTB2	561224	5127350
VENTB3	561097	5127290
VENTB4	561049	5127180
VENTB5	560977	5127130
VENTB6	560918	5126930
VENTC1	560254	5127300
VENT1	560178	5126650
VENTB2	559938	5127280